



HAL
open science

Investigating Stability of Driver-Vehicle System under Aperiodic Sampling Measurements

Ayush Kumar Jain

► **To cite this version:**

Ayush Kumar Jain. Investigating Stability of Driver-Vehicle System under Aperiodic Sampling Measurements. Automatic. Université Polytechnique Hauts-de-France, 2021. English. NNT : 2021UPHF0036 . tel-03525967v1

HAL Id: tel-03525967

<https://theses.hal.science/tel-03525967v1>

Submitted on 14 Jan 2022 (v1), last revised 7 Apr 2022 (v2)

HAL is a multi-disciplinary open access archive for the deposit and dissemination of scientific research documents, whether they are published or not. The documents may come from teaching and research institutions in France or abroad, or from public or private research centers.

L'archive ouverte pluridisciplinaire **HAL**, est destinée au dépôt et à la diffusion de documents scientifiques de niveau recherche, publiés ou non, émanant des établissements d'enseignement et de recherche français ou étrangers, des laboratoires publics ou privés.



UNIVERSITÉ POLYTECHNIQUE HAUTS-DE-FRANCE

THÈSE

présentée en vue d'obtenir le grade de

DOCTEUR

Spécialité : Automatique, Génie Informatique

par

Ayush Kumar Jain

Ingénieur diplômé de l'École Centrale de Nantes

Doctorat délivré par l'Université Polytechnique Hauts-de-France
et l'INSA Hauts-de-France

Étude de la Stabilité du Système Conducteur-Véhicule sous des Mesures d'échantillonnage apériodiques

Soutenue le 11 Oct 2021, en ligne, devant le jury composé de:

| | | |
|-------------------------------|---------------------|--------------------------------------|
| Président: | Mme. Sihem Tebbani | Professor à Centrale Supélec, Paris |
| Rapporteur: | M. Olivier Sename | Professor à Université de Grenoble |
| Rapporteur: | M. Dalil Ichalal | Professor à Université d'Evry, Paris |
| Directeur de thèse: | M. Philippe Polet | MCF HDR à l'UPHF, Valenciennes |
| Co-encadrant de thèse: | M. Denis Berdjag | MCF à l'UPHF, Valenciennes |
| Co-encadrant de thèse: | M. Christophe Fiter | MCF à l'Université de Lille, Lille |

Thèse préparée au

Laboratoire d'Automatique, de Mécanique et d'Informatique Industriel et Humain
L.A.M.I.H, UMR CNRS 8201 - Université Polytechnique Hauts-de-France
et Centre de Recherche en Informatique, Signal et Automatique de Lille
C.R.I.S.t.A.L, UMR CNRS 9189 - Université de Lille
L'École Doctorale Polytechnique Hauts-de-France (ED PHF 635)



POLYTECHNIC UNIVERSITY HAUTS-DE-FRANCE

THESIS

presented in view of obtaining the rank of

DOCTOR

Speciality : System and Control Engineering

by

Ayush Kumar Jain

Master of Science graduate of Ecole Centrale Nantes

Doctorate delivered by Polytechnic University Hauts-de-France
and INSA Hauts-de-France

**Investigating Stability of Driver-Vehicle System under
Aperiodic Sampling Measurements**

Defended on 11 Oct 2021, Online, before the jury composed of:

| | | |
|-----------------------|---------------------|---|
| President: | Mme. Sihem Tebbani | Professor at Centrale Supélec, Paris |
| Reviewer: | M. Olivier Sename | Professor at University of Grenoble |
| Reviewer: | M. Dalil Ichalal | Professor at University of Evry, Paris |
| Director: | M. Philippe Polet | Associate Professor at UPHF, Valenciennes |
| Co-supervisor: | M. Denis Berdjag | Assistant Professor at UPHF, Valenciennes |
| Co-supervisor: | M. Christophe Fiter | Assistant Professor at University of Lille, Lille |

Thesis prepared at

Laboratory of Industrial and Human Automation, Mechanics and Computer science
L.A.M.I.H, UMR CNRS 8201 - Polytechnic University Hauts-de-France
and Research center in Computer Science, Signal and Automatic Control of Lille
C.R.I.S.t.A.L, UMR CNRS 9189 - University of Lille
Doctoral School of Polytechnique Hauts-de-France (ED PHF 635)

Acknowledgements

The PhD thesis work presented in this document is conducted at "Laboratoire d'Automatique, de Mécanique et d'Informatique Industriel et Humain" (LAMIH) at Université Polytechnique Hauts-de-France, Valenciennes, France and at "Centre de Recherche en Informatique, Signal et Automatique de Lille" (CRISAL) at Université de Lille, Lille, France from October 2017 to December 2020, under the supervision of Associate Professor Philippe Polet, Assistant Professor Denis Berdjag and Assistant Professor Christophe Fiter. The thesis theme with the title "Investigating Stability of Driver-Vehicle System under Aperiodic Sampling Measurements" was funded by the "Fédération de Recherche Transports Terrestres & Mobilité" (FR TTM) (FR3733), an organisation supported by the "Centre National de la Recherche Scientifique" (CNRS).

I would like to express my sincere gratitude to my advisors Philippe Polet, Denis Berdjag, and Christophe Fiter for everything they did for me in the past three years. First of all, I would like to thank them for giving me the opportunity to work with them as part of this project. I would also like to thank them for the trust they have placed in me and upon my work during these years, for their patience and for their availability. Finally, I would like to thank them for their help and advice, their experience and knowledge they generously shared, and for all the discussions both technical and philosophical that have brought life and meaning to this work.

Likewise, I would like to express my sincere gratitude to each and every member of my PhD committee for having accepted to read and examine the present work, namely Professor Olivier Sename from the "Grenoble Images Parole Signal Automatique" (GIPSA) at "Institut Polytechnique de Grenoble" (Grenoble INP), in Grenoble, Professor Dalil Ichalal from the "Laboratoire Informatique, Biologie Intégrative et Systèmes Complexes" (IBISC) at University of Evry Val d'Essonne, in Evry-Courcouronnes and Professor Sihem Tebbani from the "Laboratoire des Signaux et Systèmes" (L2S) at Centrale Supélec, in Paris.

I would also like to thank all the members of the "Robustness and Complexity" team (Automatic Control group, LAMIH) and "Hybrid Systems Observation and Control" team (Co2 group, CRISAL), for the discussions we had and for the great atmosphere. I would like to specially mention the colleagues and friends, Ahmd Ha, Thibault Cattelain, Naila Mekhaldi, John William Mbuli, Tarik Chargui, Wassim Bouazza, Anirut Kantasa, Bruno Mateus, Walid Merrad, Aymen Lakhela, Maroua Nouiri, Moussa Abderrahim, Petru Scutelnicu, Adnane Guettaf, Gulshan Sihag, Bithal El Aatabi, Marcelino Sanchez, Pipit Angraenni, Anh Tu Nguyen from my LAMIH office, and Deesh Dileep, Xinyong Wang, Youness Braidiz, Jiju Thomas from my CRISAL office.

I would also like to thank Thierry Marie Guerra, past director of LAMIH; Laurent

Dubar, current director of LAMIH; Jimmy Lauber, manager of Automatic Control group; Laurentiu Hetel, manager of Co2 group, CRISAL; as well as secretary of staff, Corinne Aurregi, Marlene Genevieve, Maureen Curve and Isabelle Oliveira, who relieved me of an enormous amount of administration work. Additionally, I would like to thank Marc Duquennoy, director of "École Doctorale Polytechnique Hauts-de-France" and the administrative manager and deputy manager, Marie-Hélène Frappart and Marielle Marechal. Furthermore, my thanks go to Sondes Chaabane, Kathia Oliveira, Smail Niar for their help, their humor, and the great atmosphere they bring to LAMIH laboratory.

Finally, I would like to thank my family for their continuous support, with special thoughts for my mother Sanjana Jain, mother-in-law Swati Jain, father Vijay Kumar Jain, father-in-law Manoj Kumar Jain, brother Nidhish Jain, brother-in-law Prasham Jain and my wife, Vrushali Jain.

Contents

| | |
|--|-------------|
| List of Figures | vii |
| List of Tables | x |
| List of Acronyms | xiii |
| Notations | xvii |
| 1 Introduction | 1 |
| 1.1 Background | 1 |
| 1.2 Challenges for safe railway operations | 1 |
| 1.2.1 Time-delayed driver advisory signals problem | 2 |
| 1.3 Research objectives and challenges | 2 |
| 1.4 Thesis contributions | 3 |
| 1.5 Outline of thesis | 5 |
| 1.6 Publications | 7 |
| 2 Railway transportation system | 9 |
| 2.1 Introduction | 10 |
| 2.2 Railway operation | 11 |
| 2.2.1 Outer control loop: Railway traffic control | 11 |
| 2.2.2 Inner control loop: Train operation | 15 |
| 2.3 Automatic Train Control (ATC) | 16 |
| 2.3.1 Speed profile optimisation | 20 |
| 2.3.2 Train model | 22 |
| 2.3.3 Speed control | 24 |
| 2.4 ATC challenges for long journey trains | 30 |
| 2.5 Driving activity | 31 |
| 2.6 Driving challenges | 35 |
| 2.6.1 Driver attention | 36 |
| 2.6.2 Driver vigilance | 36 |
| 2.6.3 Impact of driver fatigue | 37 |
| 2.7 Driver fatigue detection | 38 |
| 2.7.1 Biological feature based | 38 |
| 2.7.2 Facial feature based | 39 |

| | | |
|----------|--|-----------|
| 2.7.3 | Vehicular feature based | 40 |
| 2.7.4 | Subjective reporting | 40 |
| 2.7.5 | Discussion | 40 |
| 2.8 | Driver advisory system (DAS) | 42 |
| 2.9 | Driver modelling | 44 |
| 2.9.1 | Significant factors for driver modelling | 45 |
| 2.9.2 | Driver modelling: literature review | 46 |
| 2.10 | Unreliable measurements problem | 55 |
| 2.11 | Conclusion | 57 |
| 3 | Overview of Networked Control System (NCS) stability | 59 |
| 3.1 | Introduction | 59 |
| 3.2 | Networked Control System (NCS): an introduction | 60 |
| 3.2.1 | NCS as sampled-data system | 63 |
| 3.2.2 | Sampled-data Linear Time-Invariant (LTI) systems | 64 |
| 3.3 | Stability of sampled-data LTI systems under time-varying sampling | 66 |
| 3.3.1 | Preliminaries | 66 |
| 3.3.2 | Time-delay approach with Lyapunov techniques | 68 |
| 3.3.3 | Convex-embedding approach | 72 |
| 3.3.4 | Delay-dependent analysis of sampled-data LTI systems | 73 |
| 3.3.5 | Linearly approximated sampled-data system | 83 |
| 3.4 | Conclusion | 84 |
| 4 | Stability of sampled-data systems with time-varying sampling | 87 |
| 4.1 | Introduction | 87 |
| 4.2 | Stability of perturbed sampled-data LTI system with a state-feedback control | 91 |
| 4.2.1 | Problem formulation | 91 |
| 4.2.2 | L_2 -stability results | 93 |
| 4.2.3 | Discussions | 100 |
| 4.3 | Stability of perturbed sampled-data LTI system with a neural-network control | 101 |
| 4.3.1 | Problem formulation | 101 |
| 4.3.2 | L_2 -stability results | 104 |
| 4.3.3 | Discussions | 110 |
| 4.4 | Stability of non-linear sampled-data system with neural-network control . | 111 |
| 4.4.1 | Problem formulation | 111 |
| 4.4.2 | Exponential stability results | 114 |
| 4.4.3 | Discussion | 120 |

| | | |
|----------|---|------------|
| 4.5 | Algorithm to find maximum sampling period | 121 |
| 4.6 | Conclusion | 122 |
| 5 | Application to stability analysis of driver-in-the-loop train control | 125 |
| 5.1 | Introduction | 125 |
| 5.2 | Simulation protocol | 126 |
| 5.3 | 1st abstraction: Stability of perturbed linear Driver-Train system with a state-feedback based ADAS | 131 |
| 5.3.1 | System description | 131 |
| 5.3.2 | Simulation studies | 132 |
| 5.4 | 2nd abstraction: Stability of perturbed linear Driver-Train system with a neural-network based ADAS | 136 |
| 5.4.1 | System description | 136 |
| 5.4.2 | Simulation studies | 138 |
| 5.5 | 3rd abstraction: Stability of non-linear Driver-Train system with neural-network based ADAS | 141 |
| 5.5.1 | System description | 141 |
| 5.5.2 | Simulation studies | 142 |
| 5.6 | Conclusion | 147 |
| 6 | General Conclusion | 149 |
| 6.1 | Perspectives | 151 |
| | Appendices | 153 |
| A | Some useful matrix properties | 155 |
| B | Stability of sampled-data LTI systems | 157 |
| B.1 | Basic stability concepts | 157 |
| B.1.1 | Stability definition | 157 |
| B.1.2 | Lyapunov method | 158 |
| B.1.3 | Properties of LTI systems with sampled-data control | 160 |
| B.2 | Stability analysis under constant sampling | 160 |
| B.3 | Stability analysis under time-varying sampling | 161 |
| B.3.1 | Difficulties and challenges | 161 |
| C | Numerical example: Stability of non-linear sampled-data system with neural-network control | 165 |

Bibliography

169

List of Figures

| | | |
|------|--|----|
| 1.1 | Driver-in-the-loop train control scheme | 2 |
| 1.2 | Driver-in-the-loop train control with delays | 4 |
| 2.1 | Inner and outer control loop | 12 |
| 2.2 | Signals from outer to inner control loop | 13 |
| 2.3 | a) Signalling tools, b) Track-side signals | 13 |
| 2.4 | ETCS a) Level 1 b) Level 2 c) Level 3 | 14 |
| 2.5 | a) Train operation in a simulated environment b) In-cabin dashboard | 15 |
| 2.6 | A typical speed-distance trajectory | 16 |
| 2.7 | Automatic Train Control (ATC) system in railways | 17 |
| 2.8 | Grades of Automation | 19 |
| 2.9 | Train operation | 19 |
| 2.10 | Single-point train model | 22 |
| 2.11 | Multi-point train model | 24 |
| 2.12 | Train speed control using Proportional Integral Derivative (PID) | 25 |
| 2.13 | Train speed control using data-driven approaches | 27 |
| 2.14 | Methods of driver fatigue detection | 38 |
| 2.15 | Output of driver fatigue detection system | 42 |
| 2.16 | a) Human machine interface, b) Advisory signals | 44 |
| 2.17 | Factors influencing driver behaviour modelling | 45 |
| 2.18 | Principle internal signals of the driver with adaptation and learning blocks | 48 |
| 2.19 | Cybernetic driver model | 49 |
| 2.20 | a) Petri net model b) Finite state automaton for driver-vehicle system | 51 |
| 2.21 | Driver-in-the-loop train control | 56 |
| 2.22 | Driver-in-the-loop train control with delays | 57 |
| 3.1 | A typical NCS setup and information flow | 61 |
| 3.2 | A Driver-Train NCS setup and information flow | 61 |
| 3.3 | Challenges to study stability of NCS system | 62 |
| 3.4 | Sampled-data system | 63 |
| 3.5 | Sampling seen as piece-wise continuous time-delay | 68 |
| 3.6 | Discontinuous in time Lyapunov functional | 79 |
| 4.1 | Linearised system with state-feedback control | 88 |

| | | |
|------|---|-----|
| 4.2 | Linearised system with Neural Network (NN) control | 89 |
| 4.3 | Closed-loop system schematic | 92 |
| 4.4 | Closed-loop system schematic | 102 |
| 4.5 | 3 Layer Full-Connected Feed-Forward Neural Network (TLFCFFNN)-based controller | 102 |
| 4.6 | Non-linear parameter varying system with NN control | 111 |
| 4.7 | Closed-loop system schematic | 112 |
| 5.1 | Simulation scenario: Railway traffic control of Train 1 | 126 |
| 5.2 | Typical train speed-distance trajectory | 126 |
| 5.3 | Reference speed | 127 |
| 5.4 | Varying reference speed | 127 |
| 5.5 | Driver-in-the-loop advisory control scheme | 128 |
| 5.6 | The nominal $K(d(t)) = K_{nom}$ and varying $K(d(t))$ driver gain | 128 |
| 5.7 | The estimated driver state $\hat{d}(t_k)$ | 129 |
| 5.8 | Closed-loop system schematic with non-functional ADAS | 130 |
| 5.9 | Closed-loop system schematic with partially functional ADAS | 130 |
| 5.10 | Closed-loop system schematic with Fully functional ADAS | 130 |
| 5.11 | ADAS-Driver control schematic | 132 |
| 5.12 | The response of $v(t)$, $\eta(t)$ and $d(t)$ without Advanced Driver Assistance System (ADAS) assistance to nominal (blue) and varying driver behaviour (red) | 133 |
| 5.13 | The response of $v(t)$, $\eta(t)$ and $d(t)$ with static-feedback based ADAS assis- tance to varying driver behaviour for only train speed measurements . . . | 134 |
| 5.14 | a) The response of $v(t)$, $\eta(t)$ and $d(t)$ with static-feedback based ADAS assistance to varying driver behaviour for both train speed and driver state measurements b) Comparison of the response of $v(t)$, $\eta(t)$ and $d(t)$ with static-feedback based ADAS assistance to varying driver behaviour for only train speed measurements (blue) and for both train speed and driver state measurements (red) | 135 |
| 5.15 | NN-based ADAS-Driver control schematic | 136 |
| 5.16 | Activation functions and their derivatives | 137 |
| 5.17 | a) The response of $v(t)$, $\eta(t)$ and $d(t)$ with NN-based ADAS assistance to varying driver behaviour for only train speed measurements, b) Comparison of the the response of $v(t)$, $\eta(t)$ and $d(t)$ with state-feedback based (red) and NN-based (blue) ADAS assistance to varying driver behaviour for only train speed measurements | 139 |

| | |
|--|-----|
| 5.18 a) The response of $v(t)$, $\eta(t)$ and $d(t)$ with NN-based ADAS assistance to varying driver behaviour for both train speed and driver state measurements | |
| b) Comparison of the response of $v(t)$, $\eta(t)$ and $d(t)$ with state-feedback based (red) and NN-based (blue) ADAS assistance to varying driver behaviour for both train speed and driver state measurements | 140 |
| 5.19 a) The response of $v(t)$, $\eta(t)$ and $d(t)$ with NN-based ADAS assistance to varying driver behaviour for only train speed measurements, b) Comparison of the response of $v(t)$, $\eta(t)$ and $d(t)$ with Abs3 NN-based (red) and Abs2 NN-based (blue) ADAS assistance to varying driver behaviour for only train speed measurements | 143 |
| 5.20 a) The response of $v(t)$, $\eta(t)$ and $d(t)$ with NN-based ADAS assistance to varying driver behaviour and varying speed reference, for only train speed measurements, b) Comparison of the response of $v(t)$, $\eta(t)$ and $d(t)$ with Abs3 NN-based (red) and Abs2 NN-based (blue) ADAS assistance to varying driver behaviour and varying speed reference for train speed measurements only | 144 |
| 5.21 a) The response of $v(t)$, $\eta(t)$ and $d(t)$ with NN-based ADAS assistance to varying driver behaviour for both train speed and driver state measurements | |
| b) Comparison of the response of $v(t)$, $\eta(t)$ and $d(t)$ with Abs3 NN-based ADAS assistance to varying driver behaviour and varying speed reference for only train speed measurements (blue) and for both train speed and driver state measurements (red) | 145 |
| 5.22 Closed-loop system schematic with $step(t)$ disturbance | 146 |
| 5.23 Comparison of the response of $v(t)$, $\eta(t)$ and $d(t)$ with Abs3 NN-based ADAS assistance to varying driver behaviour in the presence of only train state measurements (blue, yellow) and both train speed and driver state measurements (red, magenta) in the presence of a $step(t)$ disturbance (yellow, magenta) | 146 |
| B.1 Sampled-data system with constant sampling rate | 161 |
| B.2 Sampled-data system with time-varying sampling rate | 162 |
| B.3 Constant sampling rate with $T_1 = 0.18s$ and $T_2 = 0.54s$ - Stable | 162 |
| B.4 Variable sampling $T_1 = 0.18s \rightarrow T_2 = 0.54s \rightarrow T_1 \rightarrow T_2 \rightarrow \dots$ - unstable . | 163 |
| B.5 Variable sampling $T_1 = 2.126s \rightarrow T_2 = 3.950s \rightarrow T_1 \rightarrow T_2 \rightarrow \dots$ - stable . | 164 |
| C.1 Schematic of an inverted pendulum | 165 |
| C.2 $x(t)$, $h(t)$, $V(t)$ variation | 168 |

List of Tables

| | | |
|-----|--|-----|
| 2.1 | Publications on train speed profile optimisation | 21 |
| 5.1 | Parameters of the train. | 131 |
| C.1 | Maximum upper bound \bar{h} V/S decay-rate λ | 167 |

List of Acronyms

| | |
|---|------|
| ACO Ant Colony Optimisation..... | 22 |
| ACT-R Adaptive Component of Rational Thought..... | 52 |
| ADAS Advanced Driver Assistance System..... | viii |
| ARX Auto-regressive Exogenous..... | 51 |
| ATC Automatic Train Control..... | vii |
| ATO Automatic Train Operation..... | 16 |
| ATP Automatic Train Protection..... | 16 |
| ATS Automatic Train Supervision..... | 16 |
| AWS Automatic Warning System..... | 32 |
| C-DAS Connected Driver Advisory System..... | 42 |
| CATO Computer Aided Train Operation..... | 42 |
| CEDRICS Cooperative Eco-Driving Rail Control System..... | 43 |
| COSMO Cognitive Simulation Model of the Driver..... | 52 |
| DAS Driver Advisory Systems..... | 41 |
| DBN Dynamic Bayesian Networks..... | 39 |
| DNN Deep Neural Network..... | 27 |
| DIL Driver-in-the-Loop..... | 4 |
| DP Dynamic Programming..... | 20 |
| DTO Driverless Train Operation..... | 18 |
| ECG Electrocardiography..... | 38 |
| EEG Electroencephalography..... | 38 |
| EoG Electro-oculography..... | 38 |
| ERTMS European Rail Traffic Management System..... | 14 |
| ETCS European Train Control System..... | 14 |
| FIR Finite Impulse Response..... | 89 |
| GA Genetic Algorithm..... | 22 |
| GMM Gaussian Mixture Models..... | 40 |
| GoA Grades of Automation..... | 18 |
| GOMS Goals, Operators, Methods and Selection of Rules..... | 52 |
| GSM-R Global System for Mobile Communications – Railway..... | 14 |
| GPS Global Positioning System..... | 43 |
| HMM Hidden Markov Models..... | 40 |
| HR Heart Rate..... | 38 |

| | |
|--|------|
| HRV Heart Rate Variability..... | 38 |
| HIL Hardware-in-the-Loop..... | 4 |
| iDAS Intelligent Driver Advisory System..... | 43 |
| ILC Iterative Learning Control..... | 27 |
| KNN K Nearest Neighbour..... | 27 |
| KSS Karolinska Sleepiness Scale..... | 40 |
| LKF Lyapunov-Krasovskii Functional..... | 5 |
| LM Lagrange Multiplier..... | 20 |
| LMI Linear Matrix Inequality..... | 6 |
| LPV Linear Parameter Varying..... | 65 |
| LQR Linear Quadratic Regulator..... | 29 |
| LRF Lyapunov-Razumikhin Function..... | 70 |
| LTI Linear Time-Invariant..... | iv |
| MILP Mixed Integer Linear Programming Method..... | 20 |
| MPC Model Predictive Control..... | 26 |
| NCS Networked Control System..... | iv |
| NN Neural Network..... | viii |
| PERCLOS Percent of time the eyes are Closed..... | 39 |
| PID Proportional Integral Derivative..... | vii |
| PMP Pontryagin Maximum Principle..... | 20 |
| PRARX Probability Weighted Auto-regressive Exogenous..... | 51 |
| PS Pseudo Spectral..... | 20 |
| RBF-NN Radial Basis Function Neural Network..... | 28 |
| RNN Recurrent Neural Network..... | 55 |
| RSSB Rail Safety and Standards Board..... | 34 |
| S-DAS Stand-alone Driver Advisory System..... | 42 |
| SA Simulated Annealing..... | 22 |
| SCG Scheduling and Control Group..... | 43 |
| sEMG Surface Electromyography..... | 38 |
| SPaD Signals Passed at Danger..... | 53 |
| SQP Sequential Quadratic Programming..... | 20 |
| STO Semi-Automatic Train Operation..... | 18 |
| SVM Support Vector Machines..... | 39 |
| T-S Takagi–Sugeno..... | 4 |
| TRL Technology Readiness Level..... | 4 |
| TPWS Train Protection and Warning System..... | 33 |

TS Tabu Search 22
TTG Transportation Technology Group 43
UTO Unattended Train Operation 18
TLFCFFNN 3 Layer Full-Connected Feed-Forward Neural Network.....viii

Notations

Notations concerning sets:

- \mathbb{N} is the set of natural numbers $\{\lambda > 0\}$.
- \mathbb{R}^+ is the set $\{\lambda \in \mathbb{R}, \lambda \geq 0\}$.
- \mathbb{R}^* is the set $\{\lambda \in \mathbb{R}, \lambda \neq 0\}$.
- $\mathcal{M}_{n_x, n_u}(\mathbb{R})$ denotes the set of real $n_x \times n_u$ matrices.
- $\mathcal{M}_{n_x}(\mathbb{R})$ denotes the set of real $n_x \times n_x$ matrices.
- S_{n_x} denotes the set of symmetric matrices in $\mathcal{M}_{n_x}(\mathbb{R})$.
- $S_{n_x}^+$ (resp. $S_{n_x}^{+*}$) denotes the set of positive (resp. positive definite) symmetric matrices in $\mathcal{M}_{n_x}(\mathbb{R})$.
- $\text{Co}\{F_i\}_{i \in \mathcal{I}}$, for given matrices $F_i \in \mathcal{M}_{n_x, n_u}(\mathbb{R})$ and a finite set of indexes \mathcal{I} , denotes the convex polytope in $\mathcal{M}_{n_x, n_u}(\mathbb{R})$ formed by vertices F_i , $i \in \mathcal{I}$.
- $\mathcal{C}^0(X \rightarrow Y)$, for two metric spaces X and Y , is the set of continuous functions from X to Y .

- $\mathcal{L}_p(a, b)$, $p \in \mathbb{N}$ denotes the space of square-integrable functions $\phi : (a, b) \rightarrow \mathbb{R}^{n_x}$ with the norm $\|\phi\|_{\mathcal{L}_p} = \left[\int_a^b \|\phi(s)\|^p ds \right]^{1/p}$.
- $\mathcal{W}[a, b]$ denotes the space of functions $\phi : [a, b] \rightarrow \mathbb{R}^{n_x}$, which are absolutely continuous on $[a, b]$, and have square-integrable first order derivatives, with the norm $\mathcal{W} = \max_{\theta \in [a, b]} \|\phi(\theta)\| + \left[\int_a^b \|\dot{\phi}(s)\|^2 ds \right]^{1/2}$.

Notations concerning matrices:

- M^T stands for the transpose of $M \in \mathcal{M}_{n_x \times n_u}(\mathbb{R})$.
- $\mathbf{He}\{M\}$ stands for $M + M^T$ with $M \in \mathcal{M}_{n_x}$.
- $A \succeq B$ (resp. $A \succ B$) for matrices $A, B \in \mathcal{M}_{n_x}(\mathbb{R})$ means that $A - B$ is a positive (resp. positive definite) matrix.
- I is the identity matrix of appropriate dimension.
- $*$, in a matrix, denotes the symmetric elements of a symmetric matrix.
- $\text{rank}(M)$ is the rank of matrix $M \in \mathcal{M}_{n_x \times n_u}(\mathbb{R})$.
- $\lambda_{\max}(M)$ (resp. $\lambda_{\min}(M)$) denotes the largest (resp. lowest) eigenvalue of a symmetric matrix $M \in \mathcal{M}_{n_x}(\mathbb{R})$.
- $\text{diag}\{\dots\}$ denote a block-diagonal matrix.

Notations concerning vectors:

- x^T stands for the transpose of $x \in \mathbb{R}^{n_x}$.
- $\|\cdot\|_2$ stands for the Euclidean norm on \mathbb{R}^{n_x} : for a vector $x \in \mathbb{R}^{n_x}$, $\|x\|_2 = \sqrt{x^T x}$.
- $\|\cdot\|_{\mathcal{C}}$ is the associate norm on $\mathcal{C}^0([-h, 0] \rightarrow \mathbb{R}^{n_x})$, defined by $\|\phi\|_{\mathcal{C}} = \max_{\theta \in [-h, 0]} \|\phi(\theta)\|$.

- $col\{\dots\}$ denote a block-column vector.

Notations concerning functions:

- x_t (resp. \dot{x}_t) denotes the function in $\mathcal{C}^0([-\bar{h}, 0] \rightarrow \mathbb{R}^{n_x})$, for a given maximum delay \bar{h} such that $x_t(\theta) = x(t + \theta)$, $\forall \theta \in [-\bar{h}, 0]$ (resp. $\dot{x}_t(\theta) = \dot{x}(t + \theta)$, $\forall \theta \in [-\bar{h}, 0]$).

- A class \mathcal{K} function is a function $\varphi : [0, a) \rightarrow [0, +\infty)$ that is strictly increasing, and such that $\varphi(0) = 0$.

- A class \mathcal{K}_∞ function is a class \mathcal{K} function such that $a = +\infty$ and $\lim_{t \rightarrow +\infty} \varphi(t) = \infty$.

Introduction

Contents

| | | |
|------------|---|----------|
| 1.1 | Background | 1 |
| 1.2 | Challenges for safe railway operations | 1 |
| 1.2.1 | Time-delayed driver advisory signals problem | 2 |
| 1.3 | Research objectives and challenges | 2 |
| 1.4 | Thesis contributions | 3 |
| 1.5 | Outline of thesis | 5 |
| 1.6 | Publications | 7 |

1.1 Background

Rail-based transportation has a long history dating back to 6th century BC. It was one of the most revolutionary inventions since the wheel. Over the centuries, the technology has drastically improved. Today, all over the world, governments are investing heavily in developing urban-rail/main-line/high-speed railway infrastructure. Particularly, the high-speed railways line lengths have already reached 60,000 km and have also started operating with a maximum speed of 350 km/h, which is bound to increase in the near future.

Under the premise of improving carrying capacity, energy efficiency, and maximum speed limit, how to guarantee safety has become an important issue in the railway transportation. The three main factors that affect the safety of railway travel is the driver, the train and the environment. Wherein, the performance of driver plays a significant role.

1.2 Challenges for safe railway operations

During a train journey, drivers are required to be attentive and vigilant continuously for long hours. Such requirements of long working hours with irregular shift schedules, demands high psychological and cognitive awareness. Due to monotony of the job, train

drivers are susceptible to lack of awareness and fatigue. In efforts to improve transportation safety and to optimise railway operation, railways use **ADAS**, which allows information exchange between railway system and the train driver via signals of the dashboard screens. The train driving advises are generated by considering information not only from the railway control center but also from the driver fatigue detection systems.

1.2.1 Time-delayed driver advisory signals problem

ADAS obtains information about the driver, the train and the environment from various sensors. However, it is possible that the sensors may miss to collect the driver, the train or the environment state data. The information about the state may arrive with a time-delay to the control computing systems. Further it may happen that the **ADAS** algorithms induce time-delay while processing the sensory information to generate driving advise. Thus, in this thesis, considering the aperiodic sensor data availability problem, we are addressing train dynamics stability challenge during varying driver behaviour.

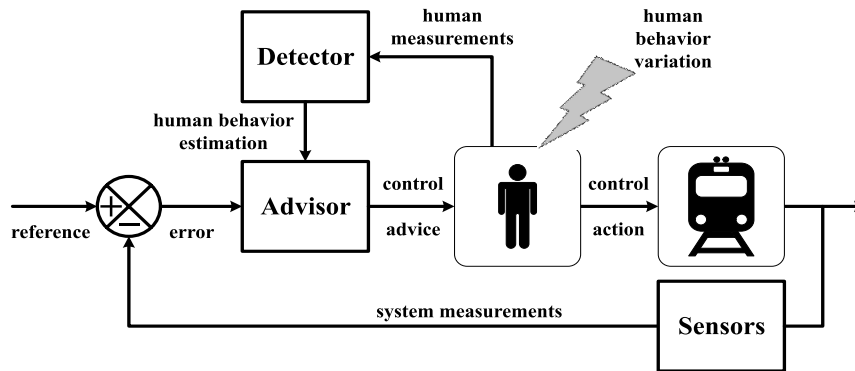


Figure 1.1: Driver-in-the-loop train control scheme

1.3 Research objectives and challenges

The ultimate goal of train dynamics stability is to have it "in spite of external factors", so that railway travel safety and ride comfort can be guaranteed. Due to involvement of human-machine interaction, a combined knowledge of psychology, mechanical engineering, computer science, control theory, etc. is needed to reach the goal. Similar to many other research papers available in the literature, the stability analysis of the error dynamics is the main focus of this thesis. From control theory stand point, the difficulty of train dynamics stability analysis is rooted in three main problems.

1. The non-linear dynamics of the train motion makes accurate modelling and analysis of the train control problem difficult. Several issues arise while considering non-linear modelling of the train. The train model can be single-point or multi-point model, i.e. it can be either considered as a lumped mass or as many masses interacting via connected links. Similarly, the choice to consider a dynamic or a static model, i.e. the choice to consider (or not) the rail-wheel contact dynamics, the aerodynamic drag on all the train compartments and the track gradient, is another point of discussion. Ignoring the non-linearity in train dynamics modelling may lead to imprecise models, which can eventually result in stability issues and uncertainties.
2. Train driving is considered as an structured process. It broadly involves interaction of a professional driver with the train and the environment via [ADAS](#). Further, it also depends on driver's habits and interpretation of [ADAS](#) signals. It is clear that the stability of train dynamics, when a driver acts as an active element will be different compared to an autonomous train. The driver prompts the train to follow the desired path with a desired speed trajectory by manipulating main inputs: brake/accelerator handles. Hence, it is necessary to consider an interacting system architecture with an appropriate driver model for the stability study.
3. The driver's actions are observable but the process of the decision making is unknown and is also difficult to model. The actions depend both on the internal and the external conditions to the driver, such as driver mental state and also on advisory signals information from [ADAS](#). Thus, it is imperative to include an appropriate [ADAS](#) model interacting with driver model for the closed-loop system stability study.

1.4 Thesis contributions

Technological:

One of the principle impediments to deploy large scale [ADAS](#) assistance for public railway transportation is the industrial demand to provide strong guarantees of stability and performance of the [ADAS](#) for the long journeys. There are two ways to address this issue:

1. Either by performing field experimentation of all possible situations, and further adaptation of the [ADAS](#) for each case or,
2. Theoretical stability guarantees based on a detailed [ADAS](#)-Driver-Train model while considering degraded environment and perturbations.

This PhD aims to achieve the latter by using the concept of "approximate computing". Through this approach we first approximate existing [ADAS](#) and other auxiliary systems using deterministic or machine-learning based grey box models and then consider some

realistic degraded situations to derive stability conditions for the driver-in-the-loop ADAS-Driver-Train architecture.

As a technological contribution, the thesis work aims to provide proper stability assessment framework for low to mid Technology Readiness Level (TRL) ADAS-centred Hardware-in-the-Loop (HIL) and Driver-in-the-Loop (DIL) research projects to improve the time to market of such innovative devices.

Scientific:

In the control theoretic context, the stability of ADAS-Driver-Train system given delay in the driver and the train state sensor measurements and a varying driver behaviour, can be addressed as a perturbed sampled-data system stability problem in the presence of time-varying sampling. The objective then is to propose abstract models that approximate the train as a controlled system and ADAS-Driver as the controller to enforce the driver-in-the-loop system stability.

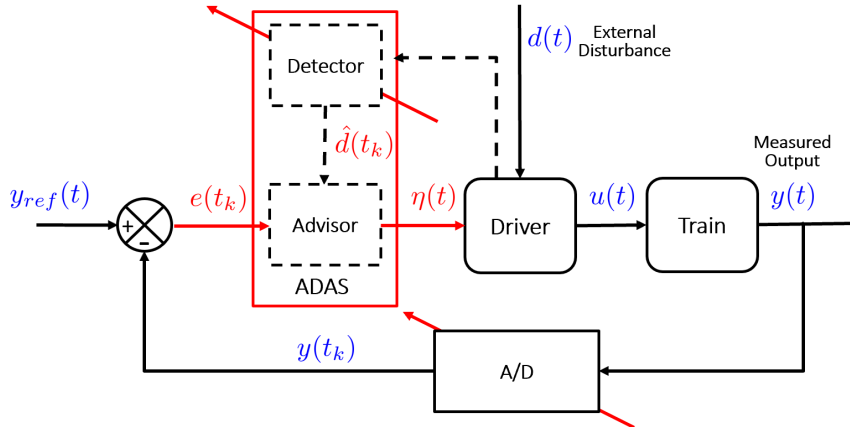


Figure 1.2: Driver-in-the-loop train control with delays

For this purpose, we proposed three modelling abstractions. Considering low complexity levels, the first two abstraction are proposed for a cruise driving context. The abstraction considers a sampled-data LTI system to model the train cruise dynamics, a time-varying gain to model driver dynamics and a state-feedback controller to model the ADAS dynamics. Then, for the second abstraction, we improved over ADAS representation by considering it as a feed-forward NN controller. Further, for the third abstraction, we improved upon the Driver-Train interaction model by a Takagi–Sugeno (T-S) non-linear system model, a NN controller for ADAS and a more advanced driving context.

In order to derive closed-loop stability conditions for a time-varying sampled ADAS-Driver-Train system, the sampled-data system is transformed to a time-delay system to benefit from delay-dependent stability tools of time-delay systems theory. The delay-

dependent tools were essential because they allow to estimate maximum delay in the sensor measurements before which closed-loop system stability is guaranteed. Next, we summarise the scientific contribution of the thesis.

1. The choice of [ADAS-Driver-Train](#) model in the three abstractions has a trend of growing from being simple to complex representation. As per our literature survey, modelling them together has never been addressed before.
2. For each of the three abstractions, a novel time-dependent Lyapunov-Krasovskii Functional ([LKF](#)) is proposed to derive delay-dependent closed-loop stability condition. Namely, the three time-dependent [LKF](#)'s have Wirtinger inequality-based, augmented [LKF](#)-based and derivative of Wirtinger inequality-based novel terms.
3. Further, in order to upper bound the integral terms of the three [LKF](#) derivative of the three abstractions, some recent developments of the field have been utilised i.e. Jensen, affine Bessel-Legendre and again Jensen inequality respectively.
4. The first two abstractions propose \mathcal{L}_2 -stability conditions, while the third propose exponential stability condition. The \mathcal{L}_2 -stability conditions help to understand the impact of driver behaviour variation on train cruise dynamics stability, while the exponential stability conditions goes a bit further to understand the rate at which train dynamics stability is affected.

Societal:

Considering the [ADAS](#) design approach presented in this thesis, driver working conditions will be improved by automating low value repetitive tasks and letting drivers focus on high value operations. Moreover it will also help increase [ADAS](#) acceptability and ease in large scale [ADAS](#) deployment.

Given an estimate of permissible maximum delay in the driver and the train state measurement, the stability of a train dynamics can be guaranteed. Thus it will help improve safety and performance of railway transport and in general of public transportation systems. Particularly, it will help provide safe, comfortable, punctual and energy efficient train journey for the benefit of the society.

All in all, the framework investigated in this PhD bridges control theoretical stability assessment analysis with safety analysis for industrial transportation systems.

1.5 Outline of thesis

Given that, the train dynamics stability study without the driver-in-the-loop is incomplete. Thus an appropriate stability paradigm is required to introduce driver in the train control

loop. This calls for assuming the availability of a driver model in the analysis that enables us to close the [ADAS-Driver-Train](#) loop.

Hence, the focus of this thesis is two fold: firstly, to consider the effects of the driver behaviour variation on the train dynamics, and secondly, to provide stability margins for the [ADAS-Driver-Train](#) system stability. The rest of the thesis is organised as follows:

Chapter2:

The second chapter begins by presenting a literature survey of the most important existing methods in train modelling and control. Some relevant publications with a focus on reference trajectory optimisation are also presented. It then elaborates upon train driving challenges, railway measures to aid driver and the publications on advisory train control with driver-in-the-loop. Next, the chapter presents a review of the most important driver modelling methods and a discussion on the choice of an appropriate driver model. Finally, in the last portion, it discusses the problems surrounding [ADAS](#) design, i.e. delayed and specially unreliable sensor measurements.

Chapter3:

In the third chapter, we argued that the stability problem of driver-in-the-loop train dynamics can be addressed as stability problem of a time-varying sampled [LTI](#) system represented as time-delay system. Next, we presented a literature survey of various tools to study time-delay system stability. We emphasised upon the choice of [LKF](#) approach, the effective over-approximation of integral terms of [LKF](#) derivative and the application of convex-embedding to derive less conservative delay-dependent stability conditions. Further, we identified that affine Bessel-Legendre inequality based over-approximation of derivative of time-dependent augmented [LKF](#) can provide least conservative delay-dependent conditions. Thus we explored stability conditions in that direction.

Chapter4:

In the fourth chapter, we presented main contribution of the thesis, i.e. three modelling abstractions and their corresponding stability theorems to address the problem of stability of driver-in-the-loop train system with varying driver behaviour and unreliable sensor measurements. The three abstractions are presented in three sections. Each section begins with presenting the system description and then presents choice of [LKF](#), positive and negative definiteness of [LKF](#) and [LKF](#) derivative, derivation of the delay-dependent stability conditions in the form of Linear Matrix Inequality ([LMI](#)) and finally concludes by presenting the Theorem. In the last section, an algorithm is presented to obtain the maximum delay utilising the three Theorems.

Chapter5:

In the fifth chapter, we implemented the proposed approaches in the ADAS-Driver-Train system context. For simulation purposes, we studied three scenarios. Namely, interaction of a driver and train without an ADAS, i.e. no driver advisory signals; interaction via an ADAS, however, driver advisory signals are only based on delayed train state measurements and finally interaction via an ADAS, however, driver advisory signals are based on both delayed driver and train state measurements. We tested each abstraction with the three scenarios and estimated the maximum allowable delay in driver and train state measurements. Further, we compared the results of each abstraction and presented concluding remarks. Particularly, we ascertained the ability of NN over state-feedback based ADAS to handle the delayed measurements and provide smoother train dynamics.

Chapter6:

In the sixth and last chapter, we presented concluding remarks and further proposed a few directions for future research.

1.6 Publications

The research exposed in this thesis can be found in the following publications:

International conferences

1. **A.K. Jain**, D. Berdjag, C. Fiter and P. Polet, "Stability of Neural-network based Train Cruise Advisory Control with Aperiodical Measurements", IFAC Conference on Embedded Systems, Computational Intelligence and Telematics in Control (CESCIT), Valenciennes, France, June 2021.
2. **A.K. Jain**, C. Fiter, D. Berdjag and P. Polet. "Investigating Stability for Driver Advisory Train Cruise Control System with Aperiodically Sampled Measurements", 23rd IEEE International Conference on Intelligent Transportation Systems (ITSC), Rhodes, Greece, September 2020.
3. **A.K. Jain**, C. Fiter, D. Berdjag and P. Polet, "Exponential Stability Criteria for Neural Network based Control of Non-linear Systems", IEEE American Control Conference (ACC), Denver, United states of America, June 2020.

National Conferences

1. **A.K. Jain**, D. Berdjag, P. Polet, and C. Fiter, "Approximate Computing Control Approaches using Neural Networks", in National Conference on Modelling, Analysis and Control of Dynamical Systems (JN GDR-MACS), Bordeaux, France, June 2019.

Railway transportation system

Contents

| | | |
|-------------|---|-----------|
| 2.1 | Introduction | 10 |
| 2.2 | Railway operation | 11 |
| 2.2.1 | Outer control loop: Railway traffic control | 11 |
| 2.2.2 | Inner control loop: Train operation | 15 |
| 2.3 | Automatic Train Control (ATC) | 16 |
| 2.3.1 | Speed profile optimisation | 20 |
| 2.3.2 | Train model | 22 |
| 2.3.3 | Speed control | 24 |
| 2.4 | ATC challenges for long journey trains | 30 |
| 2.5 | Driving activity | 31 |
| 2.6 | Driving challenges | 35 |
| 2.6.1 | Driver attention | 36 |
| 2.6.2 | Driver vigilance | 36 |
| 2.6.3 | Impact of driver fatigue | 37 |
| 2.7 | Driver fatigue detection | 38 |
| 2.7.1 | Biological feature based | 38 |
| 2.7.2 | Facial feature based | 39 |
| 2.7.3 | Vehicular feature based | 40 |
| 2.7.4 | Subjective reporting | 40 |
| 2.7.5 | Discussion | 40 |
| 2.8 | Driver advisory system (DAS) | 42 |
| 2.9 | Driver modelling | 44 |
| 2.9.1 | Significant factors for driver modelling | 45 |
| 2.9.2 | Driver modelling: literature review | 46 |
| 2.10 | Unreliable measurements problem | 55 |
| 2.11 | Conclusion | 57 |

2.1 Introduction

In this chapter, we will introduce the problem of "delay in driver advisory signal generation by [ADAS](#) due to delay in driver and train state measurement", a challenge to safety of long journey rail-based transportation. In order to address the problem, we propose a solution to assess closed-loop stability of Driver-Train system, while considering delayed driver and train state measurements.

In an effort to legitimise our problem statement, we first present different modes of railway transportation, i.e. main-line/high-speed/heavy-haul/urban-rail trains. Next, we present two important entities to regulate railway traffic operation, i.e. railway traffic control center and train operation. Then, we delve deeper into train operation and present different automation levels. We particularly emphasise the importance of speed profile optimisation and speed control for train automation.

Irrespective of the automation level both speed profile optimisation and speed control are important to achieve real-time objective of safety, punctuality and energy efficiency. Although, this objective can be achieved either by a driver or by [ATC](#), we argue that [ATC](#) as a train controller is relatively easy to implement for urban-rail (usually operate at higher automation level) but is not easily implementable in main-line/high-speed/heavy-haul train. Thus, we argue that the presence of driver is indispensable in long journey rail-based transportation.

Having reasoned indispensability of driver presence during long train journeys, we then present driving activity and driving challenges during a train operation. We particularly highlight attention and vigilance issues due to driver fatigue. We then present a literature review on traditional and modern techniques to address these issues. We further present literature review on [ADAS](#) based optimal driver advisory signal generation by utilising information about driver and train state. As a driver-in-the-loop train control stability study will require driver models for simulation, we then present a detailed literature review of driver models and further argue about our choice of driver model.

Given the presence of such [ADAS](#) system, we present the problem of unreliable driver and train state measurements during driver fatigue detection that eventually affect driver advisory signal generation. Having presented the problem, we then propose our approach to ascertain the safety of rail-based transportation system, i.e. by assessing closed-loop stability of Driver-Train system, while considering delay in driver and train state measurements. In conclusion, we reiterate the purpose of this chapter, i.e. to provide sufficient arguments to bring the unreliable sensor measurement problem faced in driver advisory signal generation to control theory framework and provide inputs for [ATC](#) or [ADAS](#) design.

2.2 Railway operation

Over the last century, the rise in popularity of rail-based transportation over other modes of transportation such as road or aviation-based is because, rail-based transport offers a cost-effective goods transportation as well as comfortable passenger travel over long journeys. Owing to cost-effectiveness, today, in many countries, rail-based transportation is playing an important role in driving sustainable economic growth.

Until recently, the rail-based transportation broadly involved the main-line and the urban-rails (tram, metro, subway, etc). The main-line railways addressed the demand to commute and to transport goods between the cities cost-effectively, while the demand to commute faster within the city was conveniently fulfilled by the urban-rails. Owing to increasing demand to commute faster between the cities, the new high-speed railways were invented. Since the Japanese Shinkansen (1964), there has been considerable advancement of the high-speed train technology, and the demand to commute faster and cost-effectively between the cities has been made possible and attractive.

Considering the number of humans opting for the services, safety requirements become stringent in main-line/high-speed/heavy-haul railways, since any accident can result in many casualties and loss of time/money. How to ensure safe and efficient operation for a rail-based transportation is an issue of utmost importance in rail-based transportation system management. In order to better understand safety issues, let us first understand how rail-based transportation system operates.

The railway operation management generally involves an extensive planning stage, which broadly consists of planning of timetable, allocation of rolling stock and assigning of crew duties. These plans are usually carried out a long time before the real-time operations, so that the real-time objectives of cost-effective, safe, and on-schedule movement is conveniently achieved. The timetable usually specifies the time and cost optimal conflict-free trips of all the trains. In particular, for each train, the timetable specifies the arrival, departure and wait time at each station in the trip.

With the given timetable, the plan has to be executed for each single train. In order to achieve the real-time objectives, railway operation management involves two fundamental entities, the railway traffic control center and the train operator. The two entities can be described explicitly by using the concept of two control loops, an outer and an inner control loop as shown in Fig. 2.1 ([Yin *et al.* 2017]).

2.2.1 Outer control loop: Railway traffic control

In daily operations, the timetable is usually disrupted by various kind of perturbations (e.g., equipment failure, extreme weather). These perturbations may cause delays or even

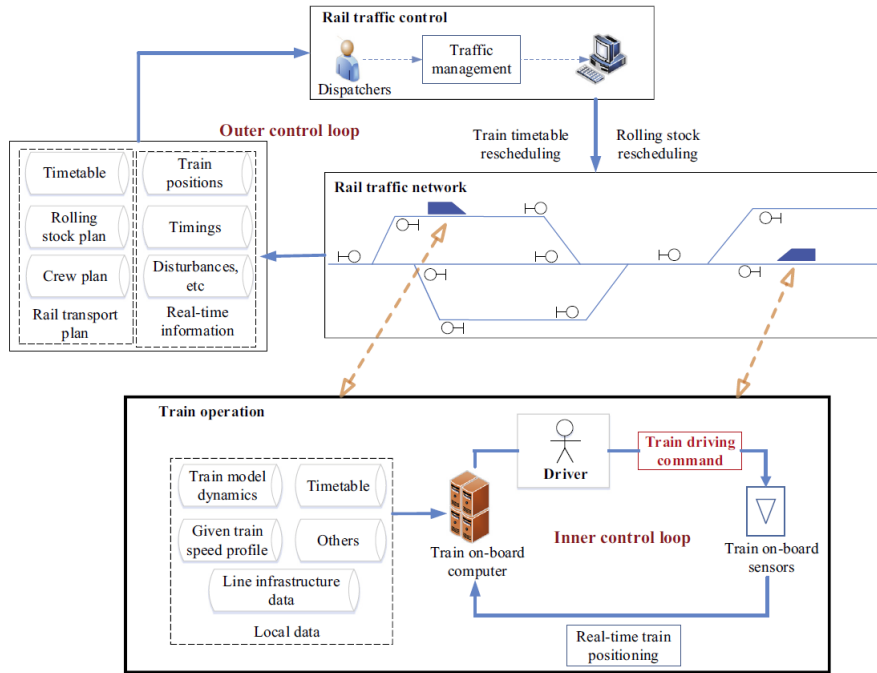


Figure 2.1: Inner and outer control loop

in-feasibility of the original timetable. Therefore, one basic task in daily railway operation management is to reschedule/adjust the timetable with real-time train information and perturbation time estimations. The objective is to minimise the negative effects of unexpected disturbances. This activity is performed in the outer control loop i.e. at railway traffic control center by personals called dispatchers.

Dispatchers supervise the status of traffic and infrastructures, detect deviations and conflicts, and develop a conflict-free rescheduled plan in real-time to make support decisions to train operators to achieve real-time objectives. As shown in Fig. 2.1, the inputs needed by the outer control loop consist of the original railway transport plan (i.e., a timetable, rolling stock plans, crew duties) and the real-time information about trains (i.e. position/speed) and potential disturbances/disruptions. The output of the outer loop is the rescheduled plan that is typically related to the choices of new arrival and departure time at each station or in an extreme case, rerouting of the trains. In particular, this task involves estimating and communicating allowable maximum speed during the trip, for each train, to adhere to the scheduled arriving/departure time.

In order to better understand the outputs of outer loop, let us consider a scenario: the railway traffic control of two trains, as shown in Fig. 2.2. In this scenario, the two trains are running at a distance on the rail track from station A to station B. During this movement, the train operator (either a driver or automatic controller) is assisted

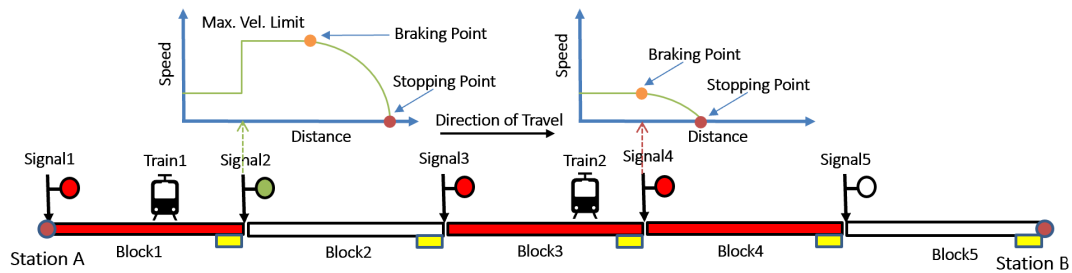


Figure 2.2: Signals from outer to inner control loop

by the dispatcher through the signalling system. For a rail-based transportation system utilising fixed-block technology, a rail track is divided into several blocks. When a train approaches a new block, the train position is detected and sent to the dispatcher by track-side signalling or by in-cabin signalling (depending on the grade of signalling). In return, depending on the rescheduled plan, dispatcher sends the route specificity back to the train.



Figure 2.3: a) Signalling tools, b) Track-side signals

With the development of railways, the method of this information exchange has been evolving. But the basic idea is: if the block is occupied (as in the case of Train 2 in Fig. 2.2), a braking point and a braking curve signal information is sent to stop the train at a safe stopping point. On the contrary, if the block is clear (as in the case of Train 1 in Fig. 2.2) a green signal, i.e. authority to enter the block is given. In addition to moving authority signal, a new travel distance, a new maximum velocity and a new braking curve information is provided for the current block. During the train travel period, the dispatcher/block manager is required to insure that only a single train is travelling in a block, while the train operator (either a human or automatic controller) is required to respond to these signals instantly.

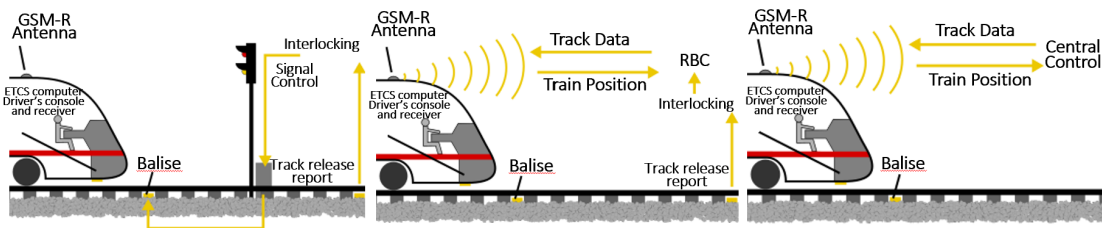


Figure 2.4: ETCS a) Level 1 b) Level 2 c) Level 3

Conventionally for the main-line railways, dispatchers send signals with track-side signalling system. The moving authority for a block is communicated to the train drivers through track-side signals (Fig. 2.3b) using the signalling tools (Fig. 2.3a). However, for a high-speed train, the track-side signals are not usable at speeds more than 200km/h. Because the track-side signals may not be observed in time. For this reason, in-cabin signalling is used for high-speed train operation. In Europe, European Train Control System (ETCS) as part of European Rail Traffic Management System (ERTMS) is implemented to fulfil the purpose of signalling. Such a system is partly installed beside the track and partly installed on-board trains. It has three operation levels, depending on the up-gradation of the track and the on-board equipment status, as shown in Fig. 2.4.

- Level 1 involves continuous supervision of train movement while a non-continuous communication between train and track-side (normally by means of balise). Track-side signalling is necessary and train detection is performed by the track-side equipment such as track circuits or axle counters.
- Level 2 involves continuous supervision of train movement with continuous communication, which is provided by Global System for Mobile Communications – Railway (GSM-R), between both the train and track-side. Track-side signalling is optional in this case, and train detection is performed by the track-side equipment, which is not in the scope of ERTMS.
- Level 3 signalling system also provides continuous train supervision with continuous communication between the train and track-side but with the main difference from Level 2 is that, the train location and integrity is managed within the scope of the ERTMS system, i.e. there is no need for track-side signalling or train detection systems on the track-side other than balises.

Today, most of the high-speed trains in Europe use Level 2 or Level 3 ETCS signalling system to make train and track state information available to the driver inside the cabin.

2.2.2 Inner control loop: Train operation

The inner control loop is where, signals from the outer control loop are considered and executed. The signalling system is an important link to communicate the scheduled plan from the railway traffic control center with the dynamic train. With the scheduled/rescheduled plan, the train operator focuses on following the signals to achieve cost-effective, safe and time-optimal train movement on each block. The train operator does that by determining the appropriate train control commands, i.e. accelerating, cruising, coasting or braking.

The inputs to the inner control loop are the scheduled/rescheduled plan and the real-time information about the train as shown in Fig. 2.1. In particular, the in-cabin dashboard show current train speed, maximum speed-limit for the current block, allowable travel distance, tentative arrival time to the next stop, train dynamics, track information, etc. An in-cabin dashboard proposed by authors [Zhu *et al.* 2016] is as shown in Fig. 2.5.



Figure 2.5: a) Train operation in a simulated environment b) In-cabin dashboard

The outputs of the inner loop are the traction/braking commands, which accelerate, cruise, brake or coast the train. The train operator has to adjust the speed considering factors such as track visibility, adhesion to track (to avoid slip), occupancy of the next block etc, in order to achieve the real-time objective. A typical speed-distance trajectory of a train is shown in Fig. 2.6. The red curve indicate the speed-limit signals from railway traffic control center and the black curve is the actual train operation speed during the journey from station A to station B. The four phases in a train journey, i.e. accelerating, cruising, braking and finally coasting can be seen.

It is worth mentioning that an active participation from both these control loops is necessary for achieving comfortable (i.e. minimising jerk, train vibration or abnormal train motion), cost-effective (influenced by train operation strategies), safe (i.e. respecting speed-limits) and time-optimal operation (i.e. respecting arrival/departure times). The railway traffic control center has to actively supervise status of all the trains in a rail network, and orchestrate the real-time train movements, by providing speed-limit signals,

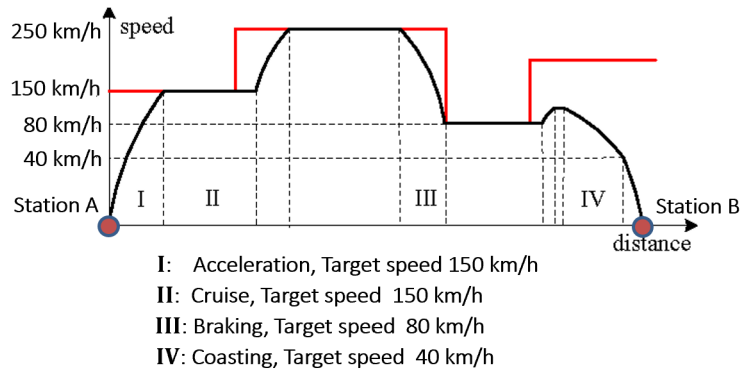


Figure 2.6: A typical speed-distance trajectory

while the train operators have to actively make the speed control commands respecting the speed-limit signals about restricted or free block movement and other environmental factors. Assuming that the railway traffic control center is actively updating the speed-limit signals information, then the responsibility to achieve the real-time objectives lie solely on the train operator. A nominal train operator will achieve the real-time objectives otherwise it will succumb to achieve degraded objectives. Thus the train operator's actions are central for the safe operation of the entire railway traffic.

2.3 Automatic Train Control (ATC)

Conventionally main-line railways are driven by drivers with the help of dispatchers of railway traffic control. The dispatchers/block managers are needed to be aware of which circuit the train is running on, and eventually prevent other trains from entering the same track circuits. Since, this process required strict supervision by the train drivers and the dispatchers for prolonged period, it was impossible to optimise the infrastructure occupation, increase in transport capacity or reduce the headway time, which were the requirements in the urban-rail context. As a possible solution, communication based train control system were developed for urban-rail systems.

With the development of communication, control and computation technologies in the last several decades, **ATC** is considered as a viable solution to help in train operation in urban-rail systems. **ATC** aims at automating train control, supervision and traffic management with the help of an integrated signalling system (similar to **ERTMS** for main-line/high-speed railway system). **ATC** mainly include three subsystems, Automatic Train Protection (**ATP**), Automatic Train Operation (**ATO**) and Automatic Train Supervision (**ATS**), partly installed on-board and partly on the track-side as illustrated in Fig. 2.7

([Yin *et al.* 2017]). The functions of these subsystems are the following:

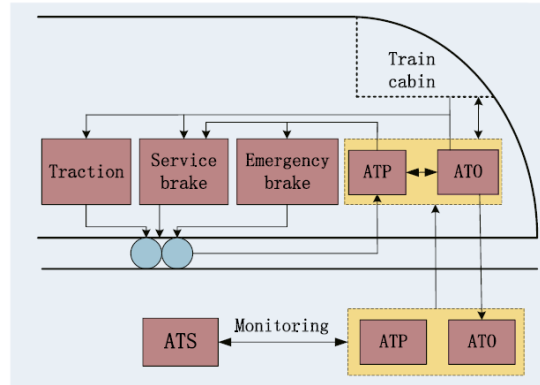


Figure 2.7: ATC system in railways

- **ATS** system is responsible for monitoring the train movement to ensure that the trains conform to an intended schedule and traffic pattern. The aim is to avoid/reduce time loss resulting from system abnormalities/equipment malfunctions by performing the tasks such as train status monitoring, train operations logging and generating train statistics report automatically. In events of disturbance, **ATS** also does reschedule creation and subsequent route selection automatically.
- **ATP** system is a fail-safe system, responsible for the safe movement of individual trains. **ATP** imposes speed-limits on the movement of trains to comply with safety requirements. In particular, it maintains a safe operating distance between the trains and also guarantees a maximum braking distance. If a train exceeds the speed-limits, **ATP** is programmed to execute emergency braking automatically.
- **ATO** system considers inputs from other subsystems, and computes a speed profile with appropriate traction/braking strategy to ensure smooth acceleration to the running speed, speed regulation and precise train stopping at the destination platform. **ATO** does so, by automatically manipulating the train traction and braking commands. Thus, **ATO** is key to the train operational efficiency, i.e. for safety, comfort, time and energy-efficiency.

The three subsystems of **ATC** work together to ensure the cost-effective, safe and time-optimal running of urban-rail system. At the start station, according to the train schedule, **ATS** gives train state, route and schedule information to **ATO**. In particular, **ATO** will get information such as, departure and arrival time, train speed profile, and dwell time at next station. Considering this information, **ATO** generates speed profile and

tracking/braking strategy to accelerate the train to the cruise speed, then later allow the train to coast until it receives brake signal from track-side system (e.g. parking beacon). Finally, under station stopping mode, *ATO* applies brakes dynamically, until the next station is reached. *ATO* ensure that the train's final position at the platform enables the door to open automatically. During this entire trip *ATP* monitors the real-time train running status to ensure a safe distance between trains by providing warnings.

Owing to the automatic generation of real-time decision of optimised accelerating, cruising, coasting and braking commands, *ATC* improve the efficiency of urban-rails operation. A significant reduction in energy consumption, lowered carbon emissions, increased transport capacity, improved quality of services (safety, riding comfort and punctuality) and reduction of manual labour has been made possible with urban-rail automation using *ATC*. Nevertheless, most of the main-line/high-speed/heavy-haul trains run at a lower automation level. The International standard, [IEC62290-1 2014] defines five Grades of Automation (*GoA*) levels of *ATC*, i.e. from *GoA0* to *GoA4*, with *GoA0* as non-automated. The level arise from apportioning responsibility for given basic functions of train operation between the driving staff and the *ATC* system.

- *GoA1* is essentially manual train operation level that need the drivers to operate the trains manually and rely on the track-side signalling system. At this level of automation, the trains are certainly equipped with *ATP* system. Although, actual *ATO* technology can run as a *GoA2* automation level on urban-rail network or even on *ERTMS* equipped tracks but will run as *GoA1* automation level on the rest of the network. The *ATO* in *GoA1* can be considered as an *ADAS* providing speed advice to help drivers drive efficiently. Most of the urban-rail/main-line/high-speed trains run under *GoA1*. *GoA1* is the focal point interest for the present research.
- At *GoA2* level, i.e. Semi-Automatic Train Operation (*STO*), acceleration/braking commands are automated with the help of *ATO*. The driver is responsible only for door control and for any emergency situations. In Europe, some of the main-line railways are running at *GoA2* level using the *ERTMS* [IRJ 2018], [EU 2018].
- *GoA3* level is termed as Driverless Train Operation (*DTO*), i.e. there is no driver in the cabin of the train. Instead, there is only a member of operation staff for the safe departure of train. Most of existing *ATO* systems in urban-rail generally achieve *GoA2* or *GoA3* automation level [UITP 2018].
- The highest level of train operation automation is the Unattended Train Operation (*UTO*), i.e. *GoA4*, in which there is completely no driver or operation staff, and the trains are operated fully automatically. As of 2018 there are more than 1000 km of urban-rail running at *GoA4* automation level worldwide [UITP 2018] and recently

world's first driver-less bullet train, went into service in China, [Wilson 2020].

| Grade of Automation | Type of train operation | Setting train in motion | Stopping train | Door closure | Operation in event of disruption |
|--|--------------------------|-------------------------|----------------|-----------------|----------------------------------|
| GoA1  | ATP* with driver | Driver | Driver | Driver | Driver |
| GoA2  | ATP and ATO* with driver | Automatic | Automatic | Driver | Driver |
| GoA3  | Driverless | Automatic | Automatic | Train attendant | Train attendant |
| GoA4  | UTO | Automatic | Automatic | Automatic | Automatic |

*ATP - Automatic Train Protection; ATO - Automatic Train Operation

Figure 2.8: Grades of Automation

Irrespective of the **GoA**, when the train is at the start station, the on-board computer receive the confirmation messages involving status of train doors, status of on-board & track-side **ATP** equipment and the relevant travel information of the next segment, to generate a recommended speed profile. For trains at **GoA1** level, the recommended speed is shown to a driver through a screen, while for automation levels **GoA2** or higher, the recommended speed is used by control algorithms programmed in on-board **ATO** computers. In both these scenarios the recommended speed profile is updated using real-time information about train position and speed data by on-board (odometers), track-side sensors (balises, if **ERTMS** tracks) and track-side signals (sent by dispatchers).

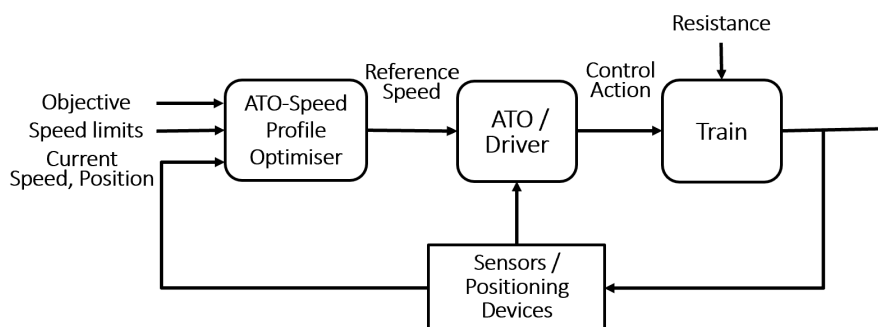


Figure 2.9: Train operation

The driver/**ATO** compares the real-time train speed information with the recommended speed at the current position to determine the control command, so that the

train precisely track the recommended speed profile. The driver additionally uses knowledge from tables/graphics to determine the appropriate control action so that the low level control loops (that dispatch the command through different actuators) work effectively. Thus, speed profile optimisation and speed control are two complementary and necessary actions needed to achieve train operation efficiency. A schematic, illustrating both these actions, is shown in Fig. 2.9. Several researchers have contributed to development of speed profile optimisation and speed control algorithms. In the next sections, we will present a literature review on both these topics.

2.3.1 Speed profile optimisation

The optimisation of speed profile is a problem with multiple objectives and constraints. The speed profile optimisation should not only consider the speed-limits but a series of other factors including track gradient, track curvature, traction efficiency and regenerative energy for meeting the needs of practical operation environments. The optimised speed trajectories basically defer by the accelerating, cruising, coasting and braking distance. In literature several authors have proposed methods to obtain optimised train speed profiles. Based on mathematical formulation, [Yang *et al.* 2016] classified the methods into three categories, i.e., analytical, numerical and evolutionary algorithm.

2.3.1.1 Analytical algorithms

The analytical algorithms are typically based on the optimal control theory and solved by Pontryagin Maximum Principle (PMP). The problem can be formulated either as continuous/discrete input to the train optimal control models, i.e. braking/traction forces can be varied either continuously or discretely. The solution obtained is optimal and exact in nature, in spite of a relatively complicated process. Commonly, these algorithms deal with two objectives, i.e. minimising energy consumption and adhering to punctuality, nevertheless, under simplified environmental condition. The simplification of environmental condition for modelling is a requirement, as these algorithms usually require good properties of the objective function. For example, the objective of comfort is usually left behind as these methods cannot handle complex train dynamic models, variable speed-limits or variable external conditions such as variable track gradients or track curvature.

2.3.1.2 Numerical algorithms

Numerical algorithms, involves Dynamic Programming (DP), Sequential Quadratic Programming (SQP), Lagrange Multiplier (LM) method, Pseudo Spectral (PS) method and also Mixed Integer Linear Programming Method (MILP). These methods have relatively

less requirements for simplified objective function i.e. they can also consider constraints for comfort and can even make a trade-off between optimisation performance and computational time. Generally the computation speed of these algorithms is slow. They are even prone to find a local optimal solution. Nevertheless, the accuracy of the solution can be guaranteed by using numerical solvers ([Atamturk & Savelsbergh 2005], [Linderoth & Ralphs 2005]) for sufficient computation time. In practice, a method with less computation time is preferred, so as to provide quick real-time energy-efficient speed updates to the driver.

| Type | Publication | Algorithm |
|------------------------|---|--|
| Analytical Algorithm | [Howlett <i>et al.</i> 1994] [Howlett 2000] [Khmelnitsky 2000] [Liu & Golovitcher 2003] [Su <i>et al.</i> 2013] [Albrecht <i>et al.</i> 2016] | PMP |
| Numerical Algorithm | [Ko <i>et al.</i> 2004] [Howlett <i>et al.</i> 2009] [Miyatake & Matsuda 2009] [Miyatake & Ko 2010] [Dominguez <i>et al.</i> 2012] [Rodrigo <i>et al.</i> 2013] [Wang <i>et al.</i> 2013b] [Calderaro <i>et al.</i> 2014] [Wang & Goverde 2016] | DP NA SQP SQP NA LM PS DP PS |
| Evolutionary Algorithm | [Chang & Sim 1997] [Wong & Ho 2004] [Ke <i>et al.</i> 2011] [Kim & Chien 2011] [Sicre <i>et al.</i> 2012] [Lu <i>et al.</i> 2013] [Li & Lo 2014] [Liu <i>et al.</i> 2015] | GA GA ACO SA GA GA, ACO, DP GA TS |

Table 2.1: Publications on train speed profile optimisation

2.3.1.3 Evolutionary algorithms

Compared with the former two kinds of methods, evolutionary algorithms, such as Genetic Algorithm (GA), Ant Colony Optimisation (ACO), Tabu Search (TS), or Simulated Annealing (SA) have least requirements for train models for speed profile optimisation. Nevertheless, most of these algorithms can not guarantee the optimality and convergence of the solutions. Even the methods cannot provide theoretical benchmarks for evaluating the solutions. Therefore, most of these evolutionary algorithms use practical case studies or real-world train trajectory as benchmarks for evaluating the performance of the solutions.

Some of the recent literature related to these three categories is listed in Table 2.1. For further information, reader can refer to [Mcclanachan & Cole 2012], where authors gave a detailed review of current train speed optimisation methods for heavy-haul trains.

2.3.2 Train model

In order to develop train speed control strategies, the first essential requirement is to have an approximate train dynamics model. Train dynamics approximation may vary based on the problem statement. For example, in this thesis, we address only longitudinal dynamics of the train without considering rail-wheel dynamics. We preferred this context as we want to develop preliminary results of train longitudinal dynamics stability for unreliable driver and train state measurements. For this context, the existing literature on train dynamics modelling for ATO development considers a train to be modelled either as single-point or as multi-point system. In the next subsection we will present the two train operation models and continue with a review of train control strategies from the literature.

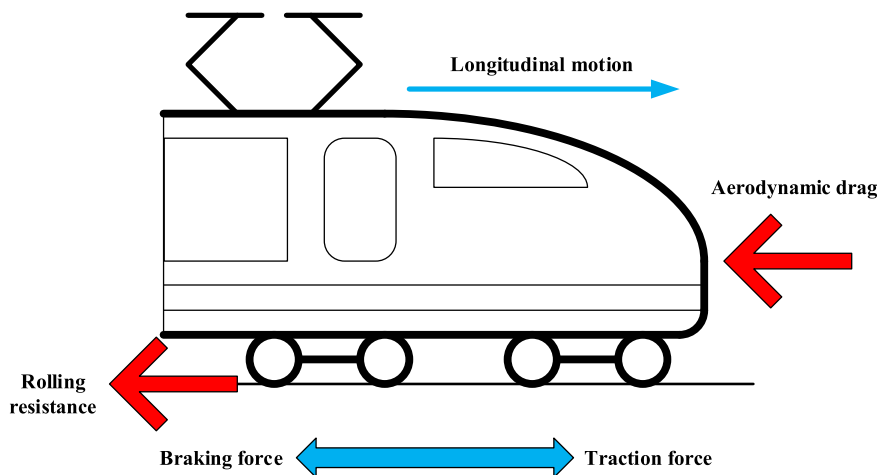


Figure 2.10: Single-point train model

2.3.2.1 Single-point model

The single-point model is the most commonly used model in solving train operation problems. For this modelling approach, a train consisting of multiple carriages and locomotives is simplified as a single-point mass. The train force diagram is as shown in Fig. 2.10. The longitudinal motion of single-point modelled train with a continuous control rate and continuous output can be characterised by Newton equation as:

$$\begin{aligned} m\dot{v}(t) &= u(t) - f(v(t)) - g(p(t)), \\ \dot{p}(t) &= v(t), \end{aligned} \quad (2.1)$$

where m is the mass of the train, $p(t)$ and $v(t)$ represent the train position and speed at time t respectively, $u(t)$ denotes the traction/braking force applied on the train either by ATO or by a driver, $f(v(t)) = m(k_0 + k_1v(t) + k_2v(t)^2)$ represents aerodynamic drag and rolling mechanical resistances given by the Davis formula [Rochard & Schmid 2000], and $g(p(t))$ represents the track gradient/track curvature type resistances with respect to train position $p(t)$. Through this model, the multiple carriages that make up a train are represented by a single-point with identical position and speed.

2.3.2.2 Multi-point model

A single-point train model can achieve good result in developing ATO methods for urban-rail transit systems. However, such simplified model lacks to represent complexity and non-linear dynamics arising in other types of trains. For instance, in the heavy-haul context, in which trains are long and consists of many carriages and locomotives, have larger and different running resistances on each carriage. In such scenario, the positions and speeds of the different carriages cannot be considered same.

In addition, due to long length of the train, there exist delay for a braking signal to reach the last carriage (around 3 secs). Such a delay was easily neglected while modelling of short trains using single-point model. But it cannot be considered negligible while modelling long trains. On the other hand, since the couplers that connect adjacent carriages are not perfectly rigid, the in-train forces among the connected carriages become an important factor to be considered. This helps researchers to study coupler failure issue in heavy-haul trains.

In [Gruber & Bayoumi 1982], the author's considered the in-train forces and also the different position/speed for each carriage to study the coupler failure issue in heavy-haul trains (Fig. 2.11). The authors proposed that if we consider a train that consists of n carriages with $n - 1$ couplers connecting the adjacent carriages, a multi-point train model

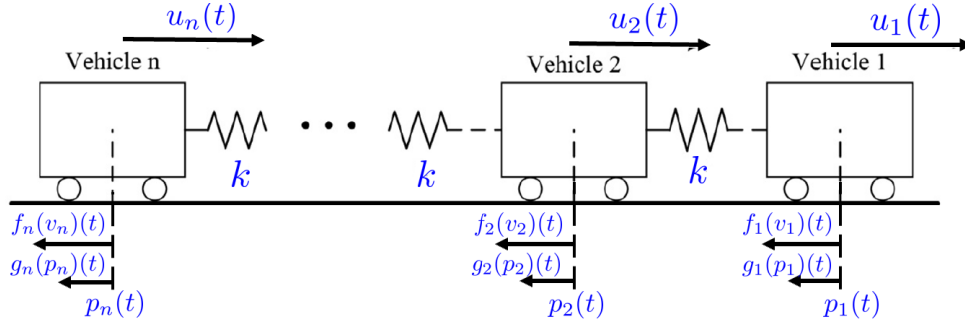


Figure 2.11: Multi-point train model

can be formulated as a non-linear multi-input multi-output model given as,

$$\begin{cases} m_1 \dot{v}_1 = u_1(t) - k\Delta p_{1,2} - f_1(v_1(t)) - g_1(p_1(t)) \\ m_i \dot{v}_i = u_i(t) - k(\Delta p_{i,i+1} - \Delta p_{i-1,i}) - f_i(v_i(t)) - g_i(p_i(t)), \quad i = 2, \dots, n-1 \\ m_n \dot{v}_n = u_n(t) + k\Delta p_{n-1,n} - f_n(v_n(t)) - g_n(p_n(t)) \end{cases} \quad (2.2)$$

where, p_i, v_i, m_i, u_i , denote position, velocity, weight, traction/braking force of the i^{th} carriage, respectively; $\Delta p_{i,i+1}$ represents the relative spring displacement between the neighbouring carriage i and $i+1$; $f_i(v_i(t)) = m_i(k_0 + k_1 v_i(t) + k_2 v_i^2(t))$ denotes the aerodynamic & rolling mechanical resistances and $g_i(p_i(t))$ represents the additional resistances with respect to train position, i.e. due to track gradient/curvature etc.

We can observe, in this model, the behaviour of couplers between two adjacent carriages is approximately described by a linear spring with stiffness coefficient k , and each carriage's speed and position are modelled specifically. In [Chou *et al.* 2007], such a multi-point train model is validated against experimental data collected on a heavy-haul trains with 200 carriages. Having presented the two models, in the next section, we present a literature review on train speed control based on these models.

2.3.3 Speed control

In literature several train speed control strategies are proposed for ATO improvement. The train control strategy depend on the type of the train, the mission and also on the external environmental conditions. For example speed control strategy for main-line, urban-rail and high-speed trains are different. Also, ideally, depending on the running conditions such as track curvature, track gradients, drag resistance, weather condition, mechanical wear, the control strategy for speed tracking should change.

2.3.3.1 PID based speed control

Irrespective of type of train or the running condition, the most widely and commonly used train speed control method of ATO is the PID controller with multiple degree of freedom (cascade PID). In an ATO, PID is used as a high level control (running at 5Hz) to continuously calculate the error between the measured train speed and recommended speed. PID controller adjusts the control command for the low level control, actuators (running at 10Hz), to minimise the speed tracking error over time.

In literature, we find several papers such as [Bing *et al.* 2009], [Xiangxian *et al.* 2010], [Guo & Ahn 2020], utilising PID control strategy because it provides relatively good tracking performance in wide variety of implementations. However, during catching/maintaining the reference speed using low level traction/braking channels in a changing environment, two major issues arise with the use of PID controller: how to get the best PID coefficients, and how to reduce the frequent switching of PID control commands.

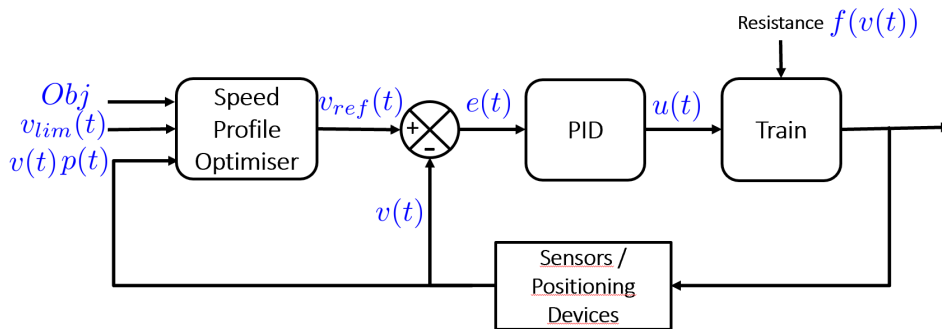


Figure 2.12: Train speed control using PID

- The first issue of PID coefficient estimation is addressed either by empirical tuning methods, such as [Wu *et al.* 2014a] or based on judgement gained through repeated field tests. The classical methods usually require a train model to tune the coefficients. However, during daily operations, the parameters of the models are often affected by external factors (e.g. mechanical wear, varying resistance), that inevitably reduce the performance of PID controller with fixed coefficients.
- The second issue of frequent control command switches raises concern over increased energy consumption for train operation. In order to tackle this issue, the speed error threshold is used to separate activity-/dead- zone at high level control, which does not allow the train to accelerate sharply during accelerating phase.

In recent years, a lot of researchers developed methods to solve these problems. A comprehensive review of train control methods is presented in [Scheepmaker *et al.* 2017].

Apart from the aforementioned classical control method, the other train speed control methods are classified into three categories, model-free, data-based, and model-based control. In the next subsection, we present a literature review of these methods.

2.3.3.2 Model-free speed control

The model-free speed control methods take advantage of empirical knowledge and professional experience of drivers. The idea is to represent the knowledge and experience of drivers in mathematical form as a series of rules. During 1960s, Fuzzy set theory was originally introduced by [Zadeh 1965], which was later used to develop fuzzy logic control based expert system, as a model-free control approach. The method has been widely accepted for ATO development.

In [Yasunobu *et al.* 1983], authors, first used fuzzy set to represent driver skills and challenged use of linearised control for a relatively non-linear automatic train operation system. In [Oshima *et al.* 1988], authors improved the results by utilising predictive fuzzy control for subway ATO development. In [Ke *et al.* 2011], authors proposed to optimise train speed trajectory using MAX-MIN ant system while considering track gradient, speed/acceleration/jerk limits and did the train acceleration regulation by using a fuzzy-PID gain scheduler to meet the speed reference signals for mass rapid transit systems.

In literature, we can also find references that consider fuzzy control for heavy-haul or high-speed railways. In [Dong *et al.* 2013], authors proposed extended fuzzy logic controller for high-speed train. [Wang & Tang 2017] proposed fuzzy Model Predictive Control (MPC) for optimal high-speed train operation. In contrast to above studies that used single-point model, in this work authors used multi-point model for control design and provided sufficiency conditions for existence of controller by set of LMI. Further, [Cao *et al.* 2019] presented real application of fuzzy predictive control technology for ATO.

2.3.3.3 Data-based speed control

Data-based methods are those that rely solely on historical train operation data to develop train speed control models. Unlike the model-free approach such as fuzzy logic or other model-based control approaches (presented in next subsection), data-driven approaches do not need to develop mathematical model of the driver experience or develop sophisticated train model from the mechanical analysis of train motors and wheel-rail frictions, for developing train speed control algorithms. However, these approaches need a lot of I/O data to learn from, which implies a lot of history data and acquisition trial runs. A detailed review of data-driven approaches for train control is presented in [Yin *et al.* 2019]. The authors used historical I/O train control data to develop model such as linear regression,

non-linear regression and Deep Neural Network (DNN) models, as shown in Fig. 2.13.

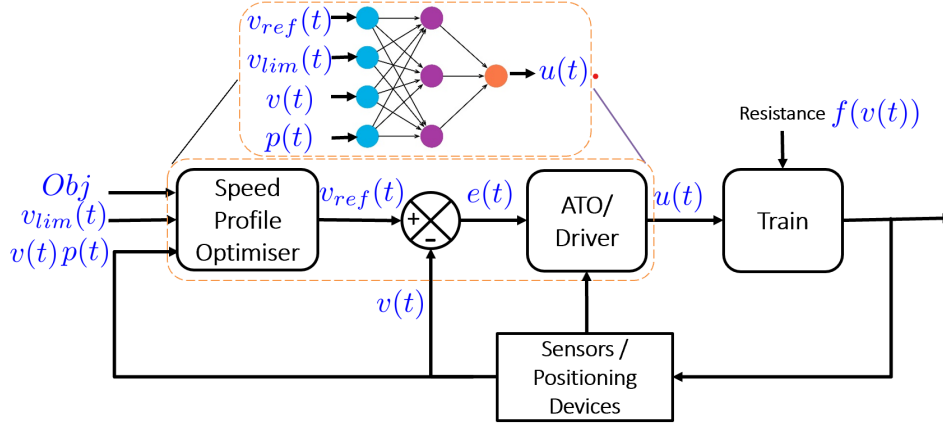


Figure 2.13: Train speed control using data-driven approaches

Some other works in data-driven approaches include [Yin *et al.* 2014], where author proposed an expert system in conjunction with reinforcement learning for both online speed profile optimisation and train speed control. In [Yin *et al.* 2016], same authors proposed smart train operation algorithm based on expert knowledge, but with a classification and regression algorithm for heavy-haul train. In [Wang *et al.* 2019c], authors proposed an automatic operation of heavy-haul train to address the safety and efficiency issue arising due to imprecise train dynamics and pneumatic brake model during steep gradient journey using K Nearest Neighbour (KNN).

In [Song & Song 2011], author proposed a neuro-adaptive fault-tolerant control algorithm to account for various factors such as input non-linearities, actuator failures, and uncertain impacts of in-train forces in the system.

Iterative Learning Control (ILC) is another data-based method used for design of adaptive ATO controllers. The trains are required to run frequently on the same track as per their schedule. In the journey, they usually encounter similar external conditions such as tunnels (signalling), slopes (track gradient) and bridges (track curvature). ILC method en-cashes this information for designing the tracking controller to improve train operation performance, iteratively. In [Chen *et al.* 2019], authors proposed such an ILC controller for a linear time-varying train model with external perturbations, for discrete automatic train operation. In [Huang *et al.* 2019], authors proposed design of adaptive ILC while using multi agent modelling approach for high-speed trains, to handle the unknown time-varying parameters and lumped uncertainties caused by varying resistive and coupler forces.

2.3.3.4 Model-based speed control

The model-based train speed control methods involve design of optimal/robust speed controller using train models. These methods try to deal with problems such as non-linearity of train dynamics (due to unknown/variable in-train/resistance forces) while considering uncertainty in train model parameter to guarantee speed tracking accuracy. However, these approaches need high cost field trials to validate train model parameters.

Single-point model:

In literature, several train speed control strategies are developed in this category. The authors have frequently considered both single-point and multi-point train model to design the strategies. We, at first, cite some works involving use of single-point model. In [Howlett 1996], author proposed an optimal control strategy to minimise the fuel consumption considering non-constant track gradient, a given trip time and assuming that only certain discrete throttle settings are allowed. [Khmelnitsky 2000] also considered variable grade profile but subject to arbitrary speed-limits thus focusing on comfort factor. The maximum principle is first applied to obtain the optimal operation sequences analytically and then a numerical algorithm is employed to find the optimal velocity profile.

In [Liu & Golovitcher 2003], authors provided analytical solution to problem of finding energy optimal control for a train moving along a route with given track profile, traction/braking characteristics, speed-limits and required trip time using maximum principle. [Dong *et al.* 2010] presented in detail, the development and simulation of train control system for high-speed trains using numerical modelling. [Su *et al.* 2015] considered optimising control strategy of the accelerating train by utilising the regenerative energy of braking train (on the opposite track) using numerical algorithm to reduce the energy consumption and even to adjust the departure time of the accelerating train.

The aerodynamic and mechanical resistance parameters of a train model may not be exactly determined or may also change with varying external circumstances in real-world application. In this context, [Gao *et al.* 2013], considered the resistance parameters $k_0, k_1, k_2, g(\cdot)$ as uncertain values and designed an adaptive controller using Radial Basis Function Neural Network (RBF-NN), which could estimate the unknown system parameters on-line and generate control while considering actuator saturation. [Yao *et al.* 2019] developed robust adaptive non-singular terminal sliding mode control methodology for ATO, to solve the position and the velocity tracking control problem considering model uncertainty due to unknown resistance parameters and external resistances.

Multi-point model:

Several authors have also considered multi-point model to develop train control strategies. In [Gruber & Bayoumi 1982], author considered a heavy-haul train as a non-linear

spring connected system and developed sub-optimal train control strategy (piece-wise linear switching control) to minimise a quadratic criterion consisting of coupler forces and velocity deviations from reference values. In [Zhuan & Xia 2008], authors considered a multi-point model for a heavy-haul train and proposed an output regulation with measurement feed-back and optimal scheduling, in order to deal with the problem of unavailability/immeasurable property of the train state.

In [Zhang & Zhuan 2014], author considered a multi-point model of a heavy-haul train and proposed a MPC for overall optimisation (i.e. energy consumption, velocity tracking, and operation safety) over long horizon. In [Zhang & Zhuan 2015], same authors tried to improve the MPC approach, by modifying the cost function by adding two penalty factors, i.e. brake force and coupler damping. The improved cost function helped reduce the energy waste incurred by braking and also alleviated the cyclic vibration of couplers.

In [Song *et al.* 2011b], authors considered a multi-point high-speed train model with uncertain resistive forces from friction and aerodynamic drag, input non-linearities and saturation limitation in traction/braking notches, and proposed a computationally inexpensive robust adaptive controller design for speed and position tracking. In [Song *et al.* 2011a], by considering the uncertain resistive forces and the traction/braking non-linear dynamics for a high-speed train, an integrated adaptive and back stepping control was designed for the speed and position tracking of high-speed trains.

Cruise control:

In high-speed/heavy-haul railways, the travel distances are usually long and the trains are mostly running at the cruise speed. Thus several authors researched particularly about cruise control of trains during train operation.

In [Yang & Sun 2001], authors designed a H_2/H_∞ cruise controller to satisfy a mixed design objective of speed command tracking and perturbation attenuation. In [Chou & Xia 2007], a closed-loop cruise controller was developed using Linear Quadratic Regulator (LQR) technique and a fencing concept is used to improve the velocity tracking, energy usage and in-train force management of the heavy-haul train. In [Zhuan & Xia 2006], authors designed an optimal cruising controller off-line to minimise the in-train forces and used electronic pneumatic braking systems to minimise time-delays in control commands. In [Marino *et al.* 2013], a fault-tolerant control scheme was proposed to address motor speed sensor faults problem for train cruise control.

Further, [Faieghi *et al.* 2014] dealt with the robust cruise control problem of high-speed trains with unknown train model parameters and in the presence of external disturbances by Lyapunov-based controller to achieve asymptotic error tracking. In [Li *et al.* 2015], sufficient condition for the existence of the robust output feed-back cruise control law is given

in terms of LMIs for a multi-point modelled high-speed train, to track the desired speed, to stabilise the spring displacement between adjacent carriages and finally to guarantee a prescribed H_∞ disturbance attenuation level.

In [Li *et al.* 2014], authors designed robust controller for a time-varying measured high-speed train to guarantee reference tracking, to maintain equilibrium spring displacement and to attenuate wind gust disturbance, by providing sufficient LMI stability conditions. In [Li *et al.* 2016], author proposed optimal guaranteed cost control for speed tracking with an adequate level of train performance over admissible uncertain resistance coefficients and control constraints. Further in [Wang *et al.* 2019b], author considered the data loss phenomenon in the wireless communication channels between the heavy-haul train and the railway control center and designed a Lyapunov stability theory based robust optimal MPC controller to ensure velocity tracking ability, energy-efficiency and operational safety with a prescribed H_∞ disturbance attenuation level under the control constraints.

2.4 ATC challenges for long journey trains

In the Section 2.3, we saw that, in literature various methods are proposed to make urban-rail/main-line/high-speed/heavy-haul train operation automatic with the help of ATO. However, compared to urban-rails, implementation of these strategies to real-time operation of main-line/high-speed/heavy-haul trains face challenges. In the following, we present the challenges with ATC implementation in long journey trains.

1. Compared with urban-rail transit networks, in which each line is a relatively enclosed system, i.e. independent from each other and each train moves like a "shuttle" on the fixed tracks, the long journey railway networks are relatively open systems with heterogeneous trains. The trains usually have inter mingled circulation plans, i.e a train may travel on different railway tracks according to its circulation plan. Therefore, the ATC framework design for these open systems would be definitely more constrained than that of urban-rail systems.
2. The large and complex track layout for these trains brings operational constraints such as signalling or interlocking of routes. In Europe, many high-speed trains cross more than one region or nation, thus will require synchronisation of multiple installed signalling systems along the track-side from ERTMS of different countries.
3. The new generation of ATC for high-speed railways is needed to respect the scalability and interpret-ability of the train control systems [Bienfait *et al.* 2012]. Different from urban-rails, in which the main functions of ATC are clearly defined by city specific operating companies, there is currently no uniform standard to clarify

the essential functions of ATO in main-line/high-speed/heavy-haul railways (usually travel among different countries) to achieve the operational goals.

4. An automatic country-wide train network can facilitate time-efficient mobility, green transportation and cost-effective travelling similar to urban-rail network but the required investment in the rolling stocks and infrastructures are huge.
5. For main-line/high-speed/heavy-haul trains, speed tracking is difficult since the train dynamics involve extremely high-speeds and different external environment. The aforementioned survey also indicate that for such complex high-speed train dynamics novel control methods have to be researched.

In consideration of above arguments, it is highly likely that drivers will be the train operators for main-line/high-speed/heavy-haul railway transportation for some time to come. Under this premise, we study train operation safety issues in the railway transportation while considering the driver-in-the-loop. In the coming sections, we present the activities that the driver has to perform and understand the possible reasons of failure to deliver the real-time objectives and ensure safety of the railway transportation.

2.5 Driving activity

Train driving is principally a cognition activity. The driver needs to observe, process and memorise the information coming from the in-cabin dashboard and the environment, in order to anticipate the events, and plan a sequence of train control actions. In order to understand driving activity in-depth, we present various in-cabin equipment, in-cabin signals, driver's information acquisition modalities, driving aids and driving requirements.

In-cabin equipments:

In the cabin, the driver has access to a number of monitoring and control functions such as power/brake lever, emergency brakes, screen for monitoring/signalling/troubleshooting train status, selecting the driving mode, "dead man" functions such as a push button or a pedal under his foot (used to monitor driver state of consciousness in real-time throughout the trip), radio (for communicating with the railway control centre), microphone (for communicating with the passengers), horn, and other functions such as air conditioning control, control board for opening the doors or activating the lights.

Signal types:

While utilising the monitoring and control function of the train, the driver also has to pay attention to the signals coming from railway traffic control. This particular activity is necessary to ensure travel safety and traffic regulation, by maintaining sufficient headway

separation between trains. In practice, drivers are communicated by visual signals (combined with audible alerts) to slow down or to stop. The visual signals can have up to four different states, [McLeod *et al.* 2005]:

- green (meaning it is safe to proceed to the next signal),
- double yellow (expect to stop at the signal after the next one),
- single yellow (expect to stop at the next signal),
- red (stop at this signal).

These coloured light signals are used to provide earlier warning of the state of upcoming signals for drivers. Further, the in-cabin visual signals (of the state of the upcoming signal) are supported with an audible alert from the Automatic Warning System (AWS). The modern AWS system issues two audible warning to discriminate between the signal states:

- ‘clear’ (indicated by a bell or simulated chime at around 1200Hz) sounds, if the driver is approaching a green signal and
- ‘warning’ (indicated by a steady alarm or horn sound at around 800Hz) sounds, if the signal is showing any other aspect apart from green.

Once the visual signal is acknowledged (by pressing a button), a visual reminder of the state of the upcoming signal is kept displaying inside the cabin. If the driver fails to acknowledge the visual signal with the audible warning, a ‘full service’ brake application is made automatically. Thus, during the trip, in order to achieve the real-time objective, driver needs to manage his attention among all these multiple source of information.

Information acquisition modalities:

Driver receives the information through several modes, i.e. visual, audio, vestibular and haptic [Rachedi 2015].

- The visual mode, evidently, the most important mode, gives precise information of in-cabin dash board indicators.
- The audio mode draws driver attention to the system malfunction alerts and also informs about the physical interaction of the train and the environment.
- The vestibular mode informs about the train dynamics. Through this mode, driver feels the information about the linear and the angular acceleration of the train through the otolithic receptors and the internal canals of the ears respectively.
- The haptic mode informs through tactile information (skin deformation) or kinaesthetically (muscle, tendon and joint activities), the train control strategy or other system malfunction alerts.

With several source of information, train control becomes quite a challenging task.

Driving activity analysis:

From the perspective of ecological perception, the train driver is in a relatively unique and paradoxical situation. Seated at the front of a fast moving train, the driver is enclosed in an extremely powerful and compelling optic flow [Gibson 1979]. A phenomenon, in which, information from environment is directly (i.e. without requiring cognition) available from pattern/motion perception and actions are taken without the need for thought/calculation/conscious decision-making to control the timing and co-ordination of train movement.

However, apart from a very few situations (such as approaching signals), the information that their senses would normally draw on for train control, is of no relevance to their driving task. In addition, the driver has no control over directional movement and thus the control of speed is entirely mediated by cognitive processes such as perception of signs, and route knowledge. Thus the driver is required to balance the cognitive use of the speedometer and the direct use of the optic flow in estimating train speed.

Further, in order to manage the tasks, driver needs to develop strategy on the go. It is because strategy helps during very high/low workload or when subject to other influences. In order to have a strategy, driver needs to have situation awareness. Loss of situation awareness may lead to surprises [Sarter & Woods 1998], i.e. a red visual signal with AWS warnings has to be acknowledged and appropriate braking strategy has to be initiated.

Therefore, at a given time, according to the context and the situation, the driver has to execute the tasks efficiently while considering the organisational and technological constraints posed by the complex socio-technical system [Rasmussen *et al.* 1994].

Driving aids:

Recognising the critical role that situation and the environment play in cognitive performance, many artefacts are used in order to properly distribute/direct driver cognition [Hutchins 1995]. For example, in order to avoid crossing red visual signal with AWS warning, the placement of a prominent AWS magnet in the middle of the track is used, to cue the driver in advance of a warning sounding. Other environmental cues include use of Train Protection and Warning System (TPWS) antennas, hot axle box detectors, other incidental AWS sounds (relays clicking) and a myriad of other track-side artefacts.

The knowledge and experience of a route that drivers develop over time also supports anticipation and future-orientated behaviour [Hollnagel 1998]. Route knowledge allows the driver to think ahead, and helps control the allocation of cognitive and perceptual resources based on expectations about the future. It also helps the driver in spotting and interpreting cues and other information. A driver with the route knowledge has more subjectively available time and a greater cognitive control over his performance.

Driving requirements:

The study conducted by the Rail Safety and Standards Board (RSSB) emphasise on the importance of the state of driver cognition at a specific time ('Now') in a specific situation and a specific context for a nominal train operation, [McLeod *et al.* 2005]. That means, a driver is required to be "attentive" and "vigilant" during the train operation.

- The attentiveness is also referred to 'dynamic selective attention'. In real situations, particularly in the case of vision (though also in hearing), attention needs to be directed to one source of information at a time. To some extent attention can be shared between two or more tasks, although performance will usually be degraded.
- On the other hand, vigilance is typical used for 'watch-keeping' tasks, where an observer tries to detect signals that arrive at infrequent intervals during which nothing much happens. Often to promote vigilance, driver is supported by an occasional message, that requires an answer. The experimental Pro-Active AWS system [Dore 1998], provided a means to achieve this, by requiring an 'answer' to the signal ahead, from the driver.

The attention and vigilance requirements are necessary, not just for better environmental perception and information processing, but also to take decisions and execute actions.

- The AWS, which is used to support visual signals to draw the driver's attention, is also sometimes used for a number of non-signal related events such as emergency, temporary or permanent speed-limits, and certain level crossings. The driver has to correctly interpret which of more than one possible condition the audible alert refers to, and therefore what behaviour is appropriate.
- In situations where the in-cabin visual reminder can refer not to the immediate past signal, but to a signal some time prior to that. The driver need to be cautious and need to have an active memory to judge the visual reminders correctly.
- Sometimes it also happens that the time period over which any AWS indication is 'active' in conveying information about the track ahead, can vary from a few seconds to possibly many minutes. The driver need to display patience and gather enough information to develop expectation of the coming situation.

In the high-speed driving scenario, trains normally do not stop at the intermediate stations until it reaches a specific station. During the long term handling drivers choose a driving method to not only reduces in-train forces acted on the coupling systems between neighbouring carriages, but also makes the actual travelling time stick to the nominal scheduled considering various track condition and in-cabin dashboard signals. The handling strategy

primarily relies on their own experience and judgement. Due to long train operating time (>8h), the driving task usually becomes stressful and laborious.

From the actual observations of manual driving, it is noticed that the sophisticated drivers tend to exert control commands intermittently when adjusting the train speed to get rid of sliding and slipping [Wang *et al.* 2019a]. Once the train enters into the cruise stage, it is relatively easy to maintain the target speed due to the large inertia. Under this situation, experienced drivers only apply the tracking/braking force occasionally to avoid the waste of energy. Such situation may give rise to driver fatigue and eventually loss of driver attention/vigilance, which is unsafe for railway operations.

2.6 Driving challenges

The issue with driving is that, despite extremely powerful and compelling attention-getting devices combined with a highly visible visual reminders and signalling cues, experienced train drivers might pass signal at danger (SPaD) [Yan *et al.* 2018]. A SPaD is said to occur, when a train passes the headway limit or a stop sign and moves into a section of track where it has no authority. The driver miss to allocate it's attention resource to determine the immediate priority and expectations, which eventually affects the driving strategy. Although, the chosen strategy will depend, to a large extent on the drivers training, experience and confidence, but it will certainly affect train operation performance.

Several factors can potentially influence the driver's understanding/belief about the current state of the world and therefore how an AWS alarm is interpreted. These include:

- expectations about the current location,
- the nature of the alarm (bell or horn),
- the driver's interpretation of the nature of the preceding alarm,
- visibility of signals and magnets on the track ahead,
- by what time or by what location the train speed to be achieved.

Changes in any of these factors can potentially lead to a change in the driver's interpretation of a particular AWS alarm. In combination or when put into the wider context including factors such as the driver's level of fatigue, emotional state, values and belief system, they have the potential to cause the driver to misinterpret what an AWS alarm refers to and what action to take. In the next subsection, we present various factors that influence degradation of driver "attention" and "vigilance".

2.6.1 Driver attention

Broadly, loss in driver attention is divided into two general categories: (1) insufficient attention and (2) misdirected attention, relating to the activation and selective aspects of attention respectively, [Engstrm & Monk 2013].

Insufficient attention occurs when the cognitive resources allocated by the driver fails to match that demanded by tasks critical for safe driving. While misdirected attention occurs when the demands of task's currently critical for safe driving are not matched due to the allocation of cognitive resources to other safety-/non- critical tasks.

The taxonomy of the inattention states that, insufficient attention usually occur due to internal factors, while misdirected attention occur due to external factors.

- The internal factors are most often linked to mental fatigue. Sleepiness due to lack of sleep quality/quantity, disrupted sleep patterns, sleep disorders due to shift working, lack of sleep recovery time between high work shift lengths lead to compressed work periods and contributes to driver insufficient attention [Filtness & Naweed 2017]. Severe sleepiness are typically accompanied by behavioural impairment, which impact driver's reaction time.
- On the other hand, external factors, such as physical fatigue, which occur while operating the socio-technical system induce misdirected attention. For example, sometimes, driver may focus on non-safety critical activities, i.e. by being distracted due to in-cabin or environmental factors.

In a growing body of research, such as [Raats *et al.* 2020], has shown that trust and confidence in technology also plays an important role in influencing the way driver interact with technology-based systems. If the system is regarded as untrustworthy, it will tend to be used incorrectly or is not paid enough attention.

2.6.2 Driver vigilance

The factors that affect driver vigilance are also categorised into factors internal and external to the driver, [Fletcher *et al.* 2005].

- The internal factors comprise driver personality traits such as humour, introversion or extroversion, sensitivity, time of the day (circadian rhythm), the stimulants etc.

Long train driving hours require high levels of mind concentration on highly monotonous sections of track with minimal input requirements. Such task feature represents high risk of mental/physical fatigue as the monotonous section require sustained vigilance. Moreover, drivers need to control dynamics of relatively long

(upto 10 km), heavy carriages for long distance without the liberty to take regular breaks for recovery, thereby lowering vigilance and reducing the ability to react.

- The external factors comprise, complexity or monotone nature of the task and the environment (such as noise, vibrations or temperature) of the cabin [Cabon *et al.* 1993]. The monotonous nature of task promotes track/task hypnosis, i.e. an uneventful driving, where a lack of novelty promotes automatic responses, while the complexity of the task increases the cognitive load.

In modern multi-aspect signalling there is a tendency to shorten the block sections. When train traffic is dense on a track, a train will often come upon a quick succession of double or single yellow aspects. At every signal, the driver will get an AWS warning, which he has to cancel. In such conditions, the risk of frequent cancelling action degenerate into a reflex action and promote a behaviour of "looking without seeing". Thus, driver can and most often do avoid being vigilant to these signals.

The degree of impact of internal and external factor on driver vigilance are different. The impact even change for different driver. In general, the noise, the vibration or the rhythm circadian have little impact on driver vigilance compared to the mental/physical fatigue, monotony or complexity of task.

2.6.3 Impact of driver fatigue

In the previous subsection, we saw various factors that affect driver attention and vigilance levels. The effect is usually visible through changes in driver behaviour, driver physiology and also through driver performance.

- Owing to driver fatigue, the driver is observed to have some characteristic behaviour sequence for different duration. Some observed symptoms related to driver behaviour include, repeated yawning [Zyla & Skotniczny 1996], nodding of head, reduction in head movement, slow reaction to external stimuli [Kosinski 2008], frequent change of position, frequent touches of face and eyes, frequent blinking of eyes [Schleicher *et al.* 2008].
- Among physiological changes, it has been observed that the activity of certain part of the brain increases. The sympathetic activity in the brain, which characterises wakefulness/vigilant behaviour, increases, while there is decrease in parasympathetic activity in the brain. Other symptoms include increase in cardiac rhythm, loss of memory, loss of concentration.
- It is also reported that fatigue induced loss of attention and vigilance, directly impacts driving performance. Some observable events include jerky increase/decrease

of the train speed, decrease in capacity to follow the in-cabin signals, the increase in time to perform a task, the increase in reaction speed/time to in-cabin signals.

In order to tackle the issue arising due to driver fatigue, driver fatigue detection systems are installed. In the next section, we will present methods used for driver fatigue detection.

2.7 Driver fatigue detection

Driver attention monitoring is important for safe driving. Although, the primary purpose to detect driver fatigue, is to generate alert signals but driver monitoring also helps in, driver workload estimation [Xing *et al.* 2018a], driver activity identification [Xing *et al.* 2018b], secondary task identification [Zhao *et al.* 2017] and driving style recognition [Martinez *et al.* 2018]. Many techniques are presented in literature to detect driver fatigue. Based on the type of data used, [Sikander & Anwar 2019] categorise the techniques into four groups as shown in Fig. 2.14.

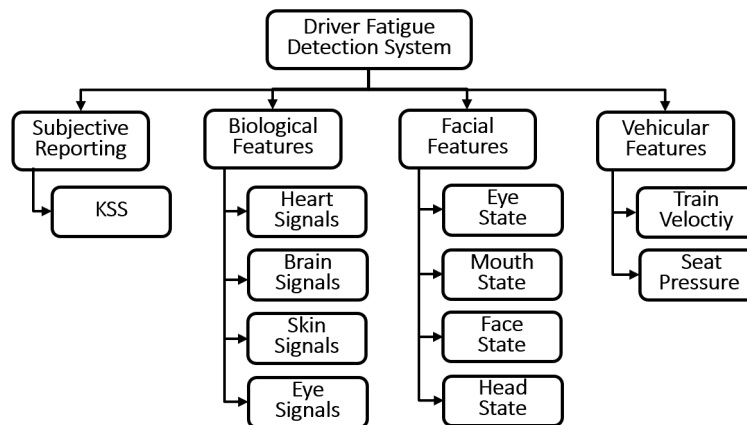


Figure 2.14: Methods of driver fatigue detection

2.7.1 Biological feature based

Biological signs offer good indication of early onset of fatigue and can be utilised to alert driver well on time. Biological signals are categorised into heart, brain, eyes and skin based signals. Changes in biological signals such as Electrocardiography (ECG), Electroencephalography (EEG), Electro-oculography (EoG), and Surface Electromyography (sEMG) are detected to ascertain driver fatigue.

- ECG signals are detected by sensors embedded in the steering wheel or the seat belt or even in the driver seat, to measure variation in parameters such as Heart Rate (HR) and Heart Rate Variability (HRV), [Hu *et al.* 2009].

- EEG signals, which comprise either Gamma (30-42Hz), Beta (13-30Hz), Alpha (8-13Hz), Theta (4-8Hz) or Delta (0.5-4Hz) waves, depending on the driver state, are recorded using flat electrodes attached to the scalp of the driver, ([Lin *et al.* 2006b], [Chouvarda *et al.* 2007]).
- EoG signal, which is actually corneo-retinal potential difference between the back and front of the eye, is used to measure the movement of the eye using electrodes attached to left and right side of the eye, [Zhu *et al.* 2014].
- sEMG signal sensors such as electrodes are placed on the neck, back, shoulders and wrists to record electric potential generated by muscle cells to predict muscular fatigue ([Critchley *et al.* 2000], [Katsis *et al.* 2004], [Balasubramanian & Adalarasu 2007]).

These signals are processed using different techniques, such as model-based techniques, [Lin *et al.* 2008] or data-based techniques such as NNs, [Akin *et al.* 2008], Support Vector Machines (SVM) [Shen *et al.* 2008], [Yeo *et al.* 2009]. Although, biological sensors are highly accurate to observe minute changes of the state of the driver, but owing to intrusive nature of these sensors, fatigue detection is susceptible to driver natural movements.

2.7.2 Facial feature based

Features exhibited on the drivers face and through head movements show some of the most obvious symptoms of fatigue. Facial feature based fatigue detection systems are broadly divided into eyes, mouth and face/head based systems. Facial features such as eye blink frequency/closure rate/closure duration, Percent of time the eyes are Closed (PERCLOS) [Orazio *et al.* 2007], gaze direction [Friedrichs & Yang 2010], yawn count [Wang *et al.* 2004], face/head position [Vural *et al.* 2007] and nodding frequency are observed to assess driver fatigue. The non-intrusive sensors such as camera is used to extract features from eye, mouth and face images to detect driver state.

Several authors have contributed to this field of research. [Bergasa *et al.* 2006], [Senaratne *et al.* 2007], [Damousis & Tzovaras 2008], used rule-based methods such as fuzzy logic inference system, while data-based techniques such as NN were used by [Suzuki *et al.* 2006], Dynamic Bayesian Networks (DBN) by [Sun *et al.* 2007], SVM by [Hu & Zheng 2009] and image filtering techniques such as Gabor Wavelets by [Fan *et al.* 2007], [Fan *et al.* 2010], to detect the anomaly. Although these methods use a non-intrusive sensor, the results from these methods depend on the resolution of images, require complex computation and require high illumination for accuracy of detection.

2.7.3 Vehicular feature based

Fatigue reduces driver's ability of situational awareness, which ultimately reflects in driving performance. Particularly, for road-based transportation, the deviation in features such as lane crossing and steering wheel angle are considered as indicators of deteriorating driving ability [Takei & Furukawa 2005]. These features are popularly used by various automobile companies to design fatigue detection systems. For rail-based transportation, unusual activities such as pressure changes on brake and accelerator [Ersal *et al.* 2010], load distribution on the driver's seat [Furugori *et al.* 2005] and train speed are considered for fatigued driver indications [Rachedi 2015]. The purpose to measure these signals is to assess time-delay in reaction of the driver.

In literature, various techniques are used to process these signals. Some authors use model-based methods, [Zhong *et al.* 2007]; others used data-based methods such as NN, [Sayed & Eskandarian 2001], [Eskandarian & Mortazavi 2007], random forest algorithm [Torkkola *et al.* 2004], Gaussian Mixture Models (GMM) [Wakita *et al.* 2005], Hidden Markov Models (HMM) [Farid *et al.* 2006], DBN [Yang *et al.* 2009], KNN algorithm [Krajewski *et al.* 2017]. Commonly, the methods use real-time signal data about brake pressure and train speed/acceleration signal over a time horizon to compute features for detection of driver reaction time-delay. Compared with facial feature, such as PERCLOS, vehicular feature metrics are more robust for fatigue detection.

2.7.4 Subjective reporting

As a subjective reporting tool, Karolinska Sleepiness Scale (KSS), [Svensson 2004], is used as a self assessment questionnaire to record the fatigue levels of drivers. KSS is a nine point assessment list, where 1 represents highest level of vigilance while 9 represents lowest level of vigilance (high level of sleepiness). The driver is asked to report fatigue level and also the factors responsible for his loss of attention and vigilance after the driving. Authors, [Bekiaris & Amditis 2001] and [Ingre *et al.* 2006] found that there is definite correlation between driver loss of attention and vigilance during driving and KSS results. Further, in order to scientifically prove it, authors, [Craig *et al.* 2006], and [Kaida *et al.* 2006] showed that the results even correlate with the results of previous methods. Since the questionnaire data was recorded after long driving hours, therefore, the technique is less suitable for real-time detection and prevention.

2.7.5 Discussion

In order to mitigate driving fatigue, railways take several measures such as, work rosters or shift/sleep/fatigue management systems. However, fatigue during long driving hours such

as, cruise periods, is natural and unavoidable. In this view, a considerable amount of effort is put to implement above methods in developing fatigue detection systems. The built systems may also be required to fulfil additional purpose of assessing driver's expected actions or evaluate variability in driver's execution.

Currently, a number of commercial driver attention/vigilance monitoring systems exist. These systems are mostly based on a combination of facial and vehicular feature based system. It is because, many researchers such as [Eskandarian & Mortazavi 2007], [Lee & Chung 2012], [Sultan *et al.* 2013], have affirmed that a combination of features can drastically increase the accuracy of fatigue detection. The authors argue that, in the events of noisy driver facial feature signals, the vehicle feature data helps in detecting driver state. The information redundancy makes it possible to compensate for the loss of one of the sensors used. Several other authors have also contributed to this research by processing the combined signals using data-based methods such as NN [Cabon *et al.* 1993], DBN [Yang *et al.* 2010], [Cheng *et al.* 2012] or by using rule-based methods such as fuzzy logic [Khushaba *et al.* 2011], [Picot *et al.* 2012], [Abichou *et al.* 2015].

In general these systems collect facial image and train state data for some minutes (usually 3-4 min), then compute the facial and vehicular features to decide the state of the driver, [Friedrichs & Yang 2010]. In one such recent study, using the collected data, [Sun *et al.* 2015] computed facial features such as PERCLOS, eye blink frequency, mean of eye-opened level & yawning frequency and also the vehicular features such as non-steering percentage, percentage of on center driving, standard deviation of steering wheel angle/vehicle speed and frequency of abnormal lane deviation. Then, a multi source data fusion model based on Takagi-Sugeno fuzzy NN was developed to combine information from both the driver and the train to provide the probability of loss of attention. The prediction accuracy during field experiments was observed to be 93 %. Fig. 2.15 shows the PERCLOS and EEG signals. Both the signals are definitely correlated. However, PERCLOS, which computes a moving average on 2-5min of data has less noise than EEG, which is a bit fast and accurate to detect driver state.

Inspite of high detection accuracy, the applicability of these combined approaches is contextual. It is because they require appropriate environmental conditions such as, proper in-cabin lighting or ambient temperature. The detection robustness also change with inter-individual variation, as each driver has different driving style. Moreover, the real-time data collection and processing methods demand time, which induce time-delays in driver state detection. The aim of driver fatigue detection is to help driver to be vigilant, but the delays in detection will in turn affect generation of alarms/advises by Driver Advisory Systems (DAS).

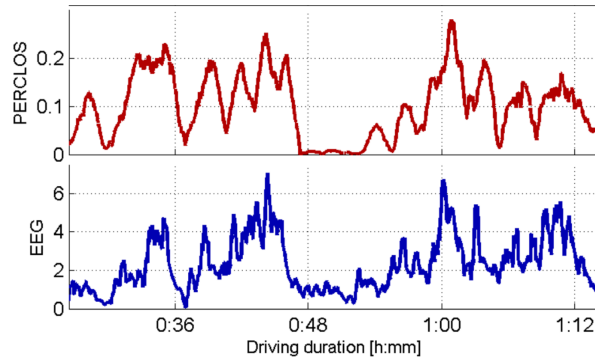


Figure 2.15: Output of driver fatigue detection system

2.8 Driver advisory system (DAS)

In Section 2.7 we presented, a monitoring subsystem of ADAS, i.e. driver fatigue detection system. In this section we will present DAS, which is used to enable safe and eco-driving. The monitoring device detects/predicts the driver state, while DAS generates driver alerts/advises to support the driver, [Filtness & Naweed 2017].

During the journey, a train driver is not only required to ensure safety margins (a minimum braking distance) and guarantee punctuality, but is also required to achieve energy-efficiency and minimise wear by eco-driving. One approach to fulfil this requirement is by the use of DAS. DAS assist train driver by delivering optimised energy-efficient speed advisory signals for train operation based on static or real-time railway operation information. The driver is required to be attentive and follow the recommended speed from DAS. DAS systems are broadly distinguished between two types, Stand-alone Driver Advisory System (S-DAS) and Connected Driver Advisory System (C-DAS) [Yang *et al.* 2013].

S-DAS:

S-DAS calculates driver advise predominantly based on static time table and track profile data. Particularly, S-DAS requires data such as track profile and time left to the next station from the static time table. S-DAS does not need to establish a real-time interface with the global time management system by the railway traffic controller. Today, most of the DAS systems in operation are S-DAS type. For example, Computer Aided Train Operation (CATO), a state of the art DAS, developed by Trans-rail in association with Swedish transportation for mining enterprise, [Leander *et al.* 2013].

In literature, several authors have contributed in development of S-DAS systems. Notably, in [Dong *et al.* 2018], authors proposed a traction-distance-based algorithm for optimising train trajectory and advisory information, which was further evaluated on

an experimental platform including train driving simulation and prototype S-DAS. In [Li *et al.* 2018], proposed dynamic speed trajectory optimisation design for developing S-DAS. The authors first proposed an offline trajectory optimisation using the GA to optimise the energy-efficient trajectory, then constructed an online optimisation to dynamically adjust the trajectory when a driving deviation occurs. In [Zhu *et al.* 2018], authors proposed Intelligent Driver Advisory System (iDAS) to assist train drivers improve driving performance under disturbance situations. iDAS used online optimisation techniques, which considered on-the-way train status information.

C-DAS:

On the contrary, C-DAS has the capability to accommodate current traffic condition. C-DAS provides a medium upon which dispatchers decisions from the railway traffic controller can be communicated to the drivers, dynamically during the journey. Particularly, the dispatchers send speed-limits in real-time for C-DAS to define the optimum driving style and for train to adhere to the schedule. Further, the information about train location and speed regulation is communicated back to the railway traffic control to enhance the quality of traffic regulation decisions by the dispatchers. It is this enabler function of C-DAS that delivers the flexibility to change the timetable according to railway traffic control needs, i.e. enabling both communication and active correction to the driver.

There are several commercially available C-DAS products. One such product is the Energy-miser DAS system, invented by Scheduling and Control Group (SCG) at the University of South Australia and Transportation Technology Group (TTG). While considering static-data such as, track profile (speed-limits, gradients, curves), train characteristics (weight, length, motoring/braking performance etc.) & train scheduled and the real-time measurement such as, train speed & location using Global Positioning System (GPS), it can calculate instantaneous optimal train driving profiles for driver recommendation.

Several authors proposed the development of C-DAS systems. In [Yang *et al.* 2013], authors shared experience of developing and deploying CATO C-DAS in Sweden. In [Zhu *et al.* 2016], authors proposed design methodology for developing C-DAS using smart phone. C-DAS has unlocked a number of opportunities for optimising operational efficiency by integrating DAS with railway traffic control. However, some researchers such as [Wang *et al.* 2013a], and [Xiang *et al.* 2015], have proposed that C-DAS with a driver behaviour adaptive speed advisory model can be a successful tool to understand/enhance driver's ability to read/respond to the generated advises and facilitate eco-driving.

In a recent study at our lab, authors, [Ladelfa *et al.* 2019], designed Cooperative Eco-Driving Rail Control System (CEDRICS). CEDRICS generate speed advises on-line, while also considering real-time driver behaviour information. In order to generate speed recom-

mendation, CEDRICS solves an optimal control problem that minimises the energy consumption under constraints such as speed/acceleration/jerk limitation, travel time since last advice, distance to destination, varying track gradient etc. The optimal control problem considers both the model of the train and the driver. In order to consider real-time driver performance to generate driving advises, the parameters of the driver model were updated recursively, using the information about applied traction force. The developed system was also tested on a full scale train driving simulator [UPHF 2014]. The human-machine interface of CEDRICS system is as shown in Fig. 2.16. A visual transmission mode in the form of head-up-display system can be seen on the windshield. The strategic placement of the transmission mode is to reduce the driver's head movements, to avoid additional workload, and also to increase the driver behaviour detection.

A C-DAS with a driver adaptive speed advisory functionality is beneficial for eco-driving, however, a delay in driver/train state measurements or a delay in signals from the railway control center will jeopardise it's intended benefits. Such delays in detection and transmission may promote false alarms/advises generation by ADAS and will induce driver distraction or even increase cognitive load. Moreover false alarms/advises may hinder ADAS acceptance by the drivers, which raise rail-based transportation safety issues.

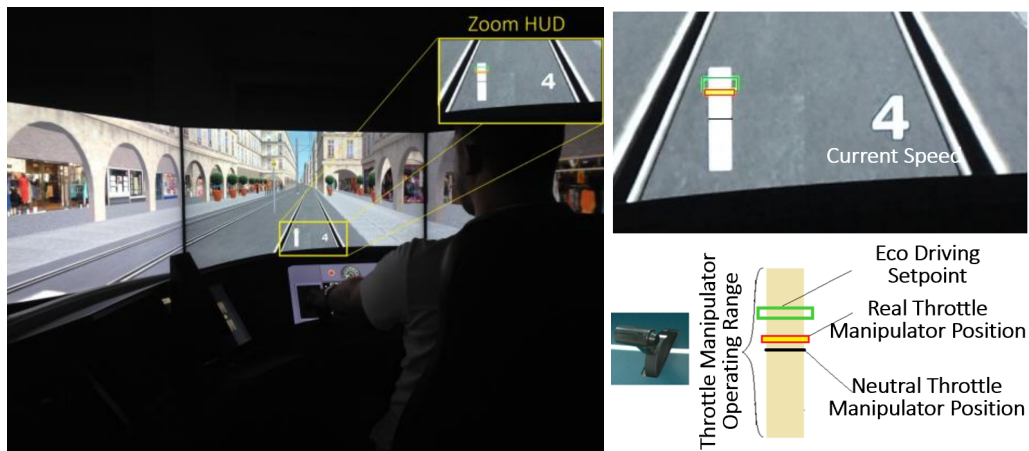


Figure 2.16: a) Human machine interface, b) Advisory signals

2.9 Driver modelling

In the previous section, we highlighted the problem of unreliable driver and train state measurements in generating driver advisory signals. In order to facilitate the study of train dynamics stability in presence of varying driving behaviour and the aforementioned time-delayed measurements, models for driver and train are necessary. The train models

were presented in the Section 2.3.2. In this section, we will present different driver models.

In the context of automatic control, the driver model should give a formal representation of the driver that can conveniently describe the observed driving process and also could be used for simulation of Driver-Train interaction. It would be beneficial if the representation is also usable to predict driver actions or to verify the stability of Driver-Train interacting system or to develop shared control for the Driver-Train systems.

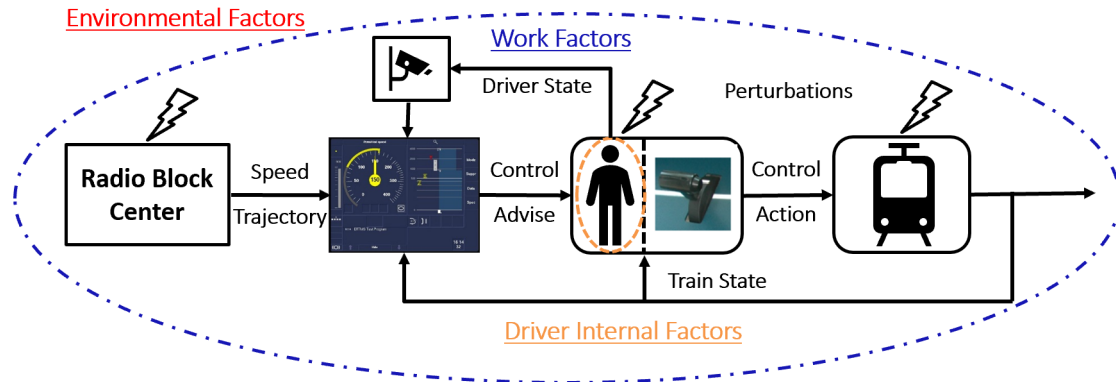


Figure 2.17: Factors influencing driver behaviour modelling

2.9.1 Significant factors for driver modelling

Since early 1950s, several researchers, from different disciplines ranging from psychology, ergonomics to automatic control, have tried to better understand driving behaviour and attempted to describe it in the form of a model. Early research, such as [McRuer & Jex 1967], mainly focused on modelling air-pilots. They broadly categorised, factors influencing driving and subsequently driver modelling into 3 types, namely, task, environment and internal to driver related factors.

2.9.1.1 Task related factors

The task related factors include the type of information coming from the radio block center, the display modality of the information and the control elements available for the driver to act on the information, as shown in Fig. 2.17. These factors have a direct and explicit link with the task, and have a major effect on the dynamics of driver behaviour. For example, the information coming from radio block center can be about speed-limit, which can be communicated either via visual or audio or both interface. Further, considering speed-limit and other sensory information, C-DAS computes speed advisory signals, that can either be shown as a set point or an increase/decrease arrow. The driver can then

either use a physical device, such as a speed control knob or accelerator pedal to control a variable of the train state (either speed or direction). The influence of task related factors in driver modelling is evident from this example. With the change in human-machine interface, there is change in nature of the information obtained and subsequent change in time needed to process this information, which will ultimately change the execution time and the corresponding model representing the process.

2.9.1.2 Environment related factors

The environment related factors include, factors internal to train cabin, such as the humidity, atmospheric conditions, luminosity, sound and vibrations in the driver's cabin, or factors external to train such as the rail track condition, weather. These factors influence the driver in carrying out the task and should ideally be considered in driver modelling.

2.9.1.3 Factors internal to driver

The factors internal to driver that affect driver behaviour include, psychological state (mental fatigue, motivation), experience (anticipating and predicting element) and physical state (physical fatigue due to workload). Drivers are also found to have a non-linear behaviour [Tustin 1947] and to have a reaction time-delay to external stimulus. For example, a driver usually acquire information to a certain threshold before reacting (reaction threshold of the human eye is 50 micrometer). This information acquiring, processing and transmitting time by the driver leads to visual reaction time-delay between 180-200 ms and auditory reaction time-delay of 140-160 ms in ideal conditions [Woodworth & Shlosberg 1954]. Although, the impact of these factors change from one driver to another and also from one situation to another. Ideally such factors should also be considered in modelling, to represent inter-individual variability and intra-individual unpredictability.

Modelling of the driver is usually strategic, i.e. objective driven. Although, all the above mentioned factors contribute to driver modelling, the relative relevance of these factors change with the context of application. The contextual objectives lead to simplified driver models with limited area of validity. For example, in this thesis, the objective is to stabilise only a single degree of freedom of the train motion. In the next subsection, we present methods proposed in the literature to model a driver.

2.9.2 Driver modelling: literature review

The literature on driver models can be classified into three groups, behaviour, cognitive and data-based models [Abuali & Abouzeid 2016]. The classification also represent the progression of driver model development (in that order).

- The behavioural models subgroup is sensory-motor level or low-level modelling. This subgroup try to present the driver control of train aspect analytically, i.e. by using continuous-time or discrete-event control theory.
- The cognitive models subgroup include qualitative models to represent the mental activities of the driver, i.e. possible driving errors or possible risks taken.
- The data-driven models subgroup represent the driver's activity based on past driver and train state measurements. This subgroup use statistical techniques or artificial intelligence on past qualitative or quantitative driving data.

Next, we detail the three subgroups with some example models.

2.9.2.1 Behaviour models

Behaviour models are further classified into three categories, cybernetic, event and hybrid models. Cybernetic models represent the continuous dynamics of driver behaviour in the form of linear/non-linear/quasi-linear analytical models. The parameters of the models are adapted to the task variables in the classical control form such as PID or in the modern control form such as robust/optimal form. Event models allow the driver behaviour to be represented discretely/qualitatively/sequentially in the form of finite state machines such as finite state automata or petri nets. Hybrid models, on the other hand, allow for integration of continuous and discrete description of driver behaviour.

a. Cybernetic models

Cybernetic models are best known and most used in the literature. These models are derived using analytical tools of control theory and form one or several control loops to represent driver behaviour dynamics. They may be expressed as a transfer function or as a differential equation. The model parameters can even be adjusted/adapted to design a satisfactory closed-loop control. Such driver representation are either used to design haptic feed-back controller or to close the Driver-Train control loop for simulation purposes.

Over the past 70 years, several authors have contributed to development of cybernetic driver models. The key developments include [Tustin 1947]'s linear model, [Mcruer & Krendel 1962]'s crossover or feed-back model to represent driver compensation and prediction behaviours, [McRuer & Jex 1967]'s second order delayed transfer function to represent neuro-muscular delay and [Donges 1978], [Mcruer 1980] & [Macadam 2003]'s feed-forward model to represent driver anticipation by perception organs.

Recently more descriptive models were proposed by authors such as by [Sentouh *et al.* 2009] and [Saleh *et al.* 2013], to model automobile drivers, for various ADAS applications such as shared steering control, lane keeping and even detection of

distraction. Considering this model, in [Gordon 2009], author even presented analytic stability results, providing specific relationships between minimum preview, speed and driver reaction time-delay for a straight line path following case in automobile driving. For a recent literature review please refer [Mulder *et al.* 2018].

As an integral part of Driver-Train system, driver is like a black box, that posses a limited information processing bandwidth. In the closed-loop, driver acquires information from the environment using different sense organs, which is used to either compensate, anticipate or pursuit the speed by manipulating the control handle. A simplistic view of driver could be: the inputs to the black box are the state of the train and speed-limits, while the outputs are the necessary corrective actions of acceleration/braking to change the dynamics of the train. A state of the art cybernetic model, considering all essential elements, i.e. neuro-muscular/proprioceptive and sensory perception to characterise different driver behaviours in a manual control is as shown in Fig. 2.18 ([Mulder *et al.* 2018]).

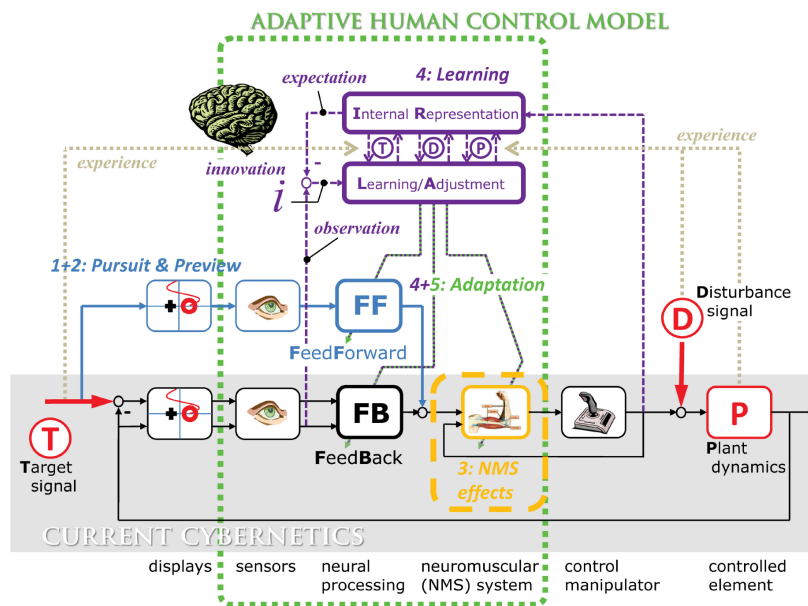


Figure 2.18: Principle internal signals of the driver with adaptation and learning blocks

Driver essential elements:

- The neuro-muscular system captures the interplay between the driver and the train. This level is in itself a complex control system which can operate in open or in closed loop combination, as can be seen in Fig. 2.18. The neuro-muscular system comprises on one side the limb (lower or upper) muscles & the dynamics of the manipulator as the feed-forward of the control loop. On the other side the neuro-muscular spindle & the organ tendons also act as neuro-muscular feed-back.

- The eyes represents the sensory perception system of the operator. They are considered both in feed-forward as well as in feed-back control loop. The vision system helps to identify the position of the limbs of the driver as well as provide information of external environment. Thus, the perception helps in three types of driver inputs to the system; i.e. compensation (feed-back), pursuit and preview/prediction/anticipation (feed-forward) behaviour.

A sample cybernetic driver model for lane keeping application is as shown in Fig. 2.19 ([Mars & Chevrel 2017]). The parameters K_p , K_c , T_I , τ_p , K_r , K_t , T_n and v are the visual anticipation gain, the visual compensation gain, the visual compensation time constant, the processing delay, the gain of the internal model of steering compliance, the gain of the stretch reflex, the neuro-muscular time constant and the vehicle speed respectively.

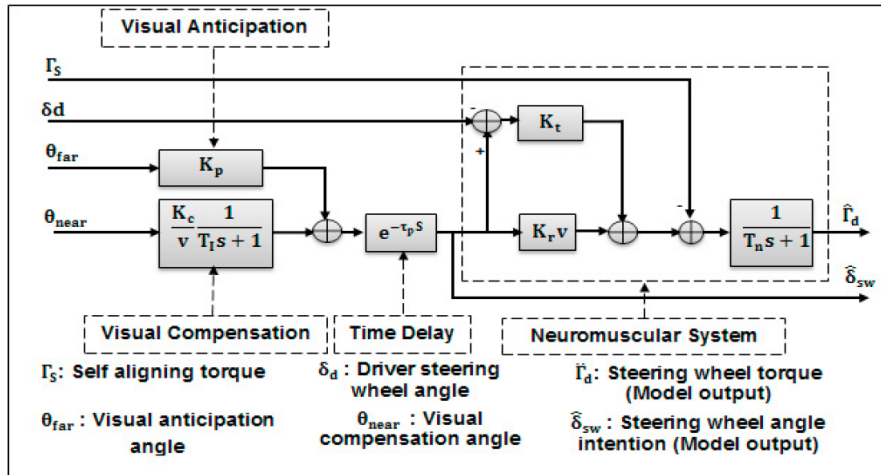


Figure 2.19: Cybernetic driver model

Driver essential behaviour: ([Rachedi 2015])

- The compensation behaviour signifies that the driver either reacts in response to the train state or in response to error between the target signal and the train state. In this behaviour, the control is in a closed-loop and is exercised continuously in order to minimise errors in the presence of disturbances. The driver intervenes only when the random disturbances appear or when the tracking errors or the train outputs are displayed to the driver.
- The pursuit behaviour is added to that of compensation, when the command inputs can be distinguished from the train outputs on the display or when the environment is displayed (for example in the case of following a trajectory). This behaviour adds

open-loop control to the closed-loop error compensating action. The performance of the control is clearly improved compared to a pure compensation behaviour.

- The preview behaviour considers the experience and knowledge of train driving, the working environment and the external environment. The driver can predict variations in the objective and variations in the result, which is also called as anticipation behaviour. With this skill, the driver can therefore produce skilful, discreet, correctly timed, measured and ordered neuro-muscular commands in order to have train states exactly as desired. The driver is trained for a type of action and acts by reflex to obtain the final result. Responses/control commands are somehow learned, conditioned and triggered in relation to situations. This behaviour acts in open-loop, and it adds to the compensation behaviour.

The combination of compensation, pursuit and preview/anticipation/prediction allows the driver to have additional information to flexibly control the train dynamics, while countering his own physiological limitations (such as sensory and neuro-muscular delays). The driver estimates/predicts a low train speed command by foreseeing the route, for example, speed adjustment before start of uphill/downhill. The driver even adapts his behaviour according to the dynamics of the technological system and to the changes of the environment. This characteristic is represented by learning block in the Fig. 2.18.

b. Event models

Event models are based on the theory of discrete-event systems proposed by [Ramadge & Wonham 1989]. The most widely used tools to model driver behaviour as a discrete dynamics are Petri nets and Finite state machines (automatons).

Petri nets:

The work of [Aigner & McCarraghar 1996], is one the earliest attempt to model human activity as an event model. The author stated that by choosing discrete-event formalism, complex process such as, supervising a partially autonomous system, can be modelled in an efficient and systematic manner. In [Thiruvengada & Rothrock 2007], author proposed an affordance based colour petri net model to represent driver behaviours for driving task on highway system. In [Wu *et al.* 2011], authors also proposed a deadlock-free and conflict-free colour petri net model to describe the cooperative behaviour of driver and vehicle co-pilot, while developing an ADAS system.

Finite state machines:

In [Lauferburger 2002], authors proposed an automaton to build a sequential representation of turn negotiation driving task as a function of the vehicle speed. In [Kim *et al.* 2010],

authors again used automata to describe the driver actions in a freeway exit situation based on affordance theory. In [Rachedi *et al.* 2013], authors proposed a model to detect human errors during unexpected tramway departure situations. Some other work include [Berdjag *et al.* 2014] and [Berdjag *et al.* 2015] that focus on detecting human errors during train driving. A sample petri net model [Wu *et al.* 2011] and finite state automaton model ([Kim *et al.* 2010]) is as shown in Fig. 2.20.

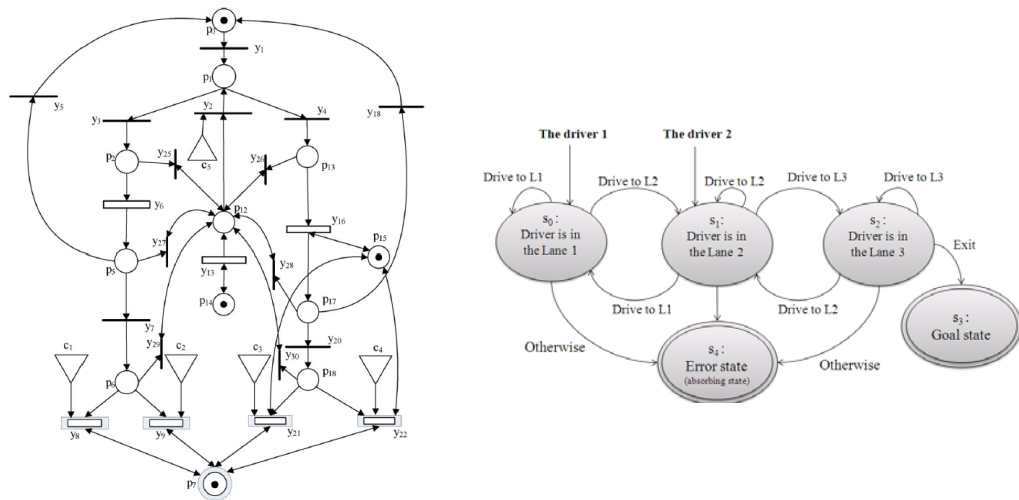


Figure 2.20: a) Petri net model b) Finite state automaton for driver-vehicle system

c. Hybrid model

During a journey, driving behaviour is often found to be a switching control law instead of a complex continuous control law. In this view, hybrid models try to capture both continuous and discrete dynamics of driver behaviour, [Kiencke *et al.* 1999]. In [Kim *et al.* 2005], authors developed a piece-wise linear driver behaviour model, to express the relationship between the driver's sensory information and the braking operation during stopping manoeuvre. In [Sekizawa *et al.* 2007], authors proposed a stochastic switched Auto-regressive Exogenous (ARX) model, for modelling and identification of other vehicle driving behaviours for obstacle avoidance application. In [Mikami *et al.* 2010], authors proposed Probability Weighted Auto-regressive Exogenous (PRARX), to develop an intersection safety system. The model was used to track other driver intentions, to eventually predict other vehicle behaviours and potential outcomes of the situation.

In [Buntins *et al.* 2013], authors first proposed to use hybrid automata formalism to model driver behaviour to capture driver behaviour on a highway. While applying the model, authors were successful in qualitatively predicting vehicle lane change and overtak-

ing actions of the driver. In another such work, [Schwarze *et al.* 2013], described driving behaviour as a result of an optimisation process within the formal framework of hybrid automata, with a focus on highway driving.

2.9.2.2 Cognitive model

Cognitive modelling represents driving activity as a problem-solving approach. The approach incorporates information perception, situation analysis and final decision making. This model family include information processing models, error models and risk models.

a. Information processing models

The most famous cognitive modelling of human-machine interaction is proposed by [Rasmussen 1983]. In this model, author divides complexity of information processing into three hierarchical levels: the knowledge-based, the rule-based, and the skill-based. In driving context, an equivalent classification is proposed by [Michon 1985], showing that the most suitable structure for driver modelling is the hierarchy of tasks. The proposed model has three levels: tactical, operational and strategic corresponding to the knowledge, rules and skills of Rasmussen model.

b. Error models

Error modelling makes it possible to understand the judgement used by the driver in the choice of actions and their execution. It also makes it possible to integrate the anticipation aspect. Among several error models, we cite:

- The Goals, Operators, Methods and Selection of Rules (GOMS) model provides a modelling framework to analyse human-machine interaction. It allows to represent the cognitive, perceptual and neuro-muscular tasks of the operator, [Degani 1996].
- The Cognitive Simulation Model of the Driver (COSMO) allows the computer simulation of the cognitive processes involved in car driving, [Bornard 2012].
- The Adaptive Component of Rational Thought (ACT-R) is a unified theory of human behaviour based on data from cognitive psychology, which provides models that think and act like humans, [Liu & Wu 2006].

The scenarios in which such models may be useful include: suppose at a distance on the front-right side of the car/train a pedestrian appear to be walking across the road. Thus in this urgent situation, the sequence of event or the total reaction time can be divided into perception time, response selection time and device response time. Each time has various different choices available with some probability. The experimental results will highlight the probabilities of the choices and will thus provide a model.

c. Risk models

Risk models are the cognitive models with good information processing capability and performance. They are frequently proposed for the railway sector. In, [Hamilton & Clarke 2005], the model identifies the integration of different sources of information as the main function of the railway driver to achieve the objective and the sub-objectives of driving. A driver performance model interacting with an automatic alert system has been developed by [McLeod *et al.* 2005]. This model describes the understanding of the pilot's state of knowledge at a precise moment and a specific situation/context. The utility of such model is demonstrated by application to the following studies:

- Research on the effect of train speed on driver interaction with signals and signs.
- Calculation of minimum reading times for signals.
- Development of a human factors Signals Passed at Danger (SPaD) hazard checklist, and a method to resolve conflicts between signal sighting solutions.
- Research on the demands imposed on drivers by ETCS driving.

Following above presentation, we can conclude that cognitive models are more useful in human centred ADAS analysis and design than in the management of critical/risky situations. This analysis is necessary for understanding driving difficulties, possible human errors and also for the study of the level of interaction between the ADAS and the driver. This family of models is thus used to help design ADAS adaptable to the driver's needs.

2.9.2.3 Data-based model

Data-based models are constructed using the driver or the machine state measurement data from actual driving scenarios. Artificial intelligence or statistical techniques are commonly used to build this type of model. These models provide the formal and quantitative representation, not only for describing driver behaviour, but also for qualifying them and predicting future actions. In order to qualify any driver behaviour as normal/abnormal from measurements/observations, two modelling solutions are proposed in the literature, [Ali & Abouzeid 2016].

- The first is to either define a model for the abnormal behaviours and show that the observed behaviours are similar to this known model of behaviour or,
- The second is to define a model for normal behaviours and show that the observations are different from this known model of behaviour, [Singh *et al.* 2009].

The first option is not always possible, because it is difficult to generate a list of abnormal behaviours in systems characterised by a large number of degrees of freedom such

as Driver-Train system. For the construction of this type of models, [Boussemart 2013] proposes four paradigms.

1. The first being the use of categorised qualitative data, i.e. the behaviour of a driver is recorded as a set, containing several types of actions to categorise the actions.
2. The second being the interpret-ability of the results, i.e. the models which offer a good recognition and prediction rate are not sufficient. They must also have a descriptive capacity to interpret driver behaviour.
3. The third being, the use of temporal information because they provide exploitable training data to construct these models. This is especially important in system types where life is critical, where time is of the essence. However, taking into account time is sometimes not necessary, because it adds an additional constraint to the modelling.
4. The fourth is the unsupervised learning. In the majority of cases, not all driver behaviour is always known. The behaviour vary from one operator to another and also according to the situation, which means that apriori information is sometimes neither available nor representative.

Next, we present methods from literature to construct these models for drivers.

a. Fuzzy logic

In [Badamchizadeh *et al.* 2010], authors presented a hierarchical fuzzy system for takeover manoeuvre to represent different driver's way of speed and steering angle control. The fuzzy rules are created by means of expert questionnaire data of effects of parameters such as climate, road and vehicle conditions on driving capabilities. In [Shaw 1993], authors proposed a fuzzy logic based model of the driver to perform target compensation and tracking tasks. The model is obtained by using I/O data of vehicle dynamics control by the driver and is later experimentally tested for different driving scenarios. In [Oza 1999], authors used DBN to predict the actions of the ego-vehicle and other-vehicle driver behaviour. In [Gindele *et al.* 2010], authors proposed a DBN to estimate other vehicle behaviours and anticipate their future trajectories for safe decision making/motion planning behaviour of ego-vehicle.

b. Neural network

In literature, several authors used NN to model human actions, [Delice & Ertugrul 2007]. In [Gingrich *et al.* 1992], authors used NN to capture the knowledge of process operators to improve lack of efficiency arising due to different operators. Similar studies have been conducted for drivers, such as in [Zhang *et al.* 2006], where authors addressed the problem of uncertainty in subjective judgements of driver by considering a NN based model to predict driver behaviour. In [Olabiyi *et al.* 2017], authors proposed a driver action/anomaly

prediction solution to find patterns that consistently precede an anomaly. For this purpose, authors trained a Recurrent Neural Network (RNN) using features extracted across multi-modal sensory inputs to mitigate the effects of unsafe driving behaviours, by predicting driver actions at least 5 sec ahead. In [Okamoto & Tsiotras 2019], authors proposed a machine learning based driver model to develop haptic-shared ADAS system while using a new unknown input estimation algorithm, a necessary requirement for low-cost driving simulators that are not equipped with torque sensors. In [Qian *et al.* 2010], authors used SVM to detect whether the driver is a legitimate owner of the vehicle or not from the driver behaviour models.

c. Hidden markov models

In [Pentland & Liu 1999], authors used HMMs for classifying and accurately predicting driving tasks based on the driver's preparatory movements. Further, in [Sathyanarayana *et al.* 2008], authors proposed a hierarchical framework for the modelling of driver behaviour and also two different and complementary approaches based on HMMs have been developed. Some authors even combined above approaches and proposed so called hybrid methods. In [George 2008], authors proposed driver behaviour models for manual tracking tasks based on fuzzy neuro inference systems. Similar work has been identified in [Ertugrul 2008].

2.10 Unreliable measurements problem

To summarise, in the previous sections we reasoned that unlike ATC for urban-rail transport, main-line/high-speed/heavy-haul trains will need a driver and simultaneously a ADAS based train control. We also concluded that while driver-in-the-loop is beneficial, the driver fatigue can induce safety issues during cruising period. In practice, several methods are used to detect driver fatigue using fatigue detection systems and to generate speed advisory signals using C-DAS system. However the advise generated by C-DAS system may not be reliable, due to delay in driver and train state detection. Such delays in detection may promote false alarms/advises by C-DAS, which may hinder ADAS acceptance by the drivers or may induce driver distraction or even increase their cognitive load, which raise rail-based transportation safety issues.

Considering above arguments, in this thesis, we want to address the ADAS-Driver-Train closed-loop stability issue. We propose a C-DAS assisted train control schematic as shown in Fig. 2.21. The driver-in-the-loop train control stability is investigated in the presence of varying driver behaviour and with delayed driver and train state measurements. The delay in driver state measurement and communication to the advisor is primarily due

to unreliability of the collected data and secondly due to data processing time required by the camera images processing algorithms (often considered as primary sensor to capture driver state details). The delay in train state measurement (usually speed) may arise due to faulty carriage speed sensors.

We recall the data flow of driver-in-the-loop system. At first, the speed-limit commands sent by the radio block center are compared with the current train speed and the difference is given to the C-DAS system. In addition to this, the state of the driver, as detected by the driver fatigue detection system (camera as detector in the schematic), is also sent to the C-DAS system (advisor in the schematic). The C-DAS system considers both this signal, i.e. the speed difference, the driver state and other train-track related information to optimise the speed trajectory and generate the recommended speed advises. The driver then considers this recommended speed advise to correct the train speed. Considering this scenario, how to assess driver-in-the-loop train control stability is what we study.

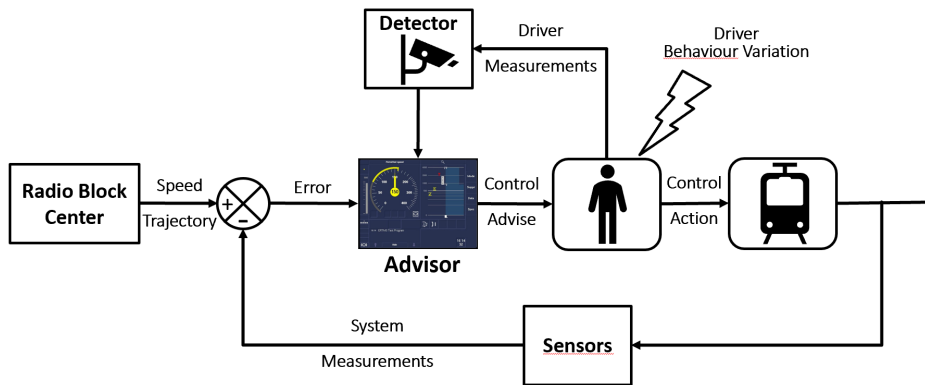


Figure 2.21: Driver-in-the-loop train control

In the previous section, we presented various methods to represent driver behaviour. Broadly, we discussed behavioural, cognitive and data-based models. Particularly in behavioural models we presented cybernetic models (compensation, pursuit & preview modelling), event models (petri nets & finite state machines) and hybrid models; in cognitive models we presented information processing models, error models & risk models and in data-based models we presented fuzzy-logic, neural-network & hidden markov models. Since, in this thesis, we want to study impact of driver and train state measurement delays on the driver-in-the-loop train control stability, we identified cybernetic driver models to be the most suitable. Ideally, we should consider a complete cybernetic driver model, that incorporate all three elements of driver behaviour, namely, compensation, pursuit and preview. But considering the complexity of the problem being studied, we preferred

to consider only the simplest elements, i.e. compensation behaviour of the driver.

Thus, in this thesis, we propose to study the stability of the driver-in-the-loop train control by considering control theoretic modelling approach for ADAS-Driver-Train system and explore the design of driver's state aware ATC.

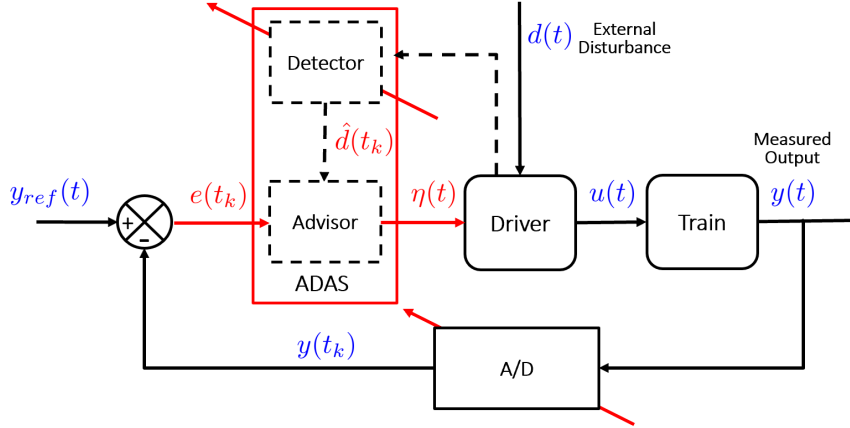


Figure 2.22: Driver-in-the-loop train control with delays

The closed-loop system with the driver-in-the-loop is as shown in Fig. 2.22. Here we consider that some external disturbance $d(t)$ is affecting the driver behaviour and $y(t)$ as the train state measurement. The red arrow represent that both the driver and the train state are measured with a time-delay. We want to study the stability of the train speed, given that their is variation in the driver state.

2.11 Conclusion

This chapter has exposed the operation of railways by describing individual function of railway traffic control and train operation. Emphasising the importance of train operation for rail-based transportation safety, we described in detail about train speed profile optimisation and train speed control for different mode of railways, i.e. urban-rail/main-line/high-speed/heavy-haul and also for train operation at different level of automation. We argued that although ATC is easier to implement for urban-rails, it is quite challenging to implement it on other type of railways. Thus, ascertaining the importance of driver in a main-line/high-speed/heavy-haul railways, we delved deeper into activity of driver, to understand challenges of train driving. We further discussed how issue of driver fatigue is addressed using ADAS subsystems such as driver fatigue detection system and DAS. We further emphasised shortcoming of ADAS based driver advise generation.

Under this premise, we formulated stability of driver-in-the-loop train cruise control

problem with delayed driver and train state measurement. We proposed to choose a sampled-data control theoretic problem formulation method, owing to the resemblance of Driver-Train system as a time-varying sampled NCS. Further, we also stressed on choice of cybernetic driver model for simulation purposes. In the following chapter, we intend to present overview of recent research direction about stability of sampled-data modelled NCS system. In the process we will be presenting the tools available to study stability of time-varying sampled systems.

Overview of Networked Control System (NCS) stability

Contents

| | | |
|------------|--|-----------|
| 3.1 | Introduction | 59 |
| 3.2 | NCS: an introduction | 60 |
| 3.2.1 | NCS as sampled-data system | 63 |
| 3.2.2 | Sampled-data LTI systems | 64 |
| 3.3 | Stability of sampled-data LTI systems under time-varying sampling | 66 |
| 3.3.1 | Preliminaries | 66 |
| 3.3.2 | Time-delay approach with Lyapunov techniques | 68 |
| 3.3.3 | Convex-embedding approach | 72 |
| 3.3.4 | Delay-dependent analysis of sampled-data LTI systems | 73 |
| 3.3.5 | Linearly approximated sampled-data system | 83 |
| 3.4 | Conclusion | 84 |

3.1 Introduction

In this chapter, we first introduce NCSs and the main network-induced imperfections and constraints and then emphasis upon the issue of our concern, i.e. variable sampling/-transmission interval. In order to study the stability of NCS, we consider a sampled-data LTI system based representation. Thus, we then introduce sampled-data LTI system with main mathematical definition.

Next we recall general concept of stability of a system in Appendix B. We then formulate the stability of sampled-data LTI system, which is further elaborated according to sampling type: constant and time-varying sampling. Because of relevance of time-varying sampling to our context, we then present a literature review of approaches to study stability of time-varying sampled systems.

Having reasoned the choice of time-delay system based representation for time-varying sampled LTI system stability study, we then present time-delay approach with Lyapunov techniques. We emphasis upon the choice of LKF and convex-embedding based approach to estimate maximum time-delay in system state measurement.

Next we present the steps involved to design a LKF functional and further present a literature review to obtain delay-dependent LMI-based stability conditions. Particularly, we present model transformation and integral inequality based approach to over-approximate the derivative of the LKF.

In literature, integral inequality approaches were shown to accurately upper-bound LKF derivative. Thus, considering this advantage, we present and compare approximation capability of various integral inequality approaches, such as Jensen, Wirtinger and Bessel-Legendre inequality.

Finally, we argue the choice of our research direction about time-dependent LKF with augmented terms in addition to an affine Bessel-Legendre inequality to accurately approximate LKF derivative for a best estimate of maximum time-delay in system measurements. Moreover, since ADAS-Driver-Train is likely be a non-linear sampled-data system type, thus, a theorem for linearized model around the equilibrium is presented.

Please note that the sections presented in this chapter are inspired from various literature reviews such as [Fiter 2012], [Zhang *et al.* 2016c], [Hetel *et al.* 2017] and [Liu *et al.* 2019].

3.2 NCS: an introduction

In the last chapter we presented how driver advises are generated based on speed profile optimisation algorithms using driver and train state measurements. We also highlighted the fact that data from several sensors may not be available periodically/synchronously and may lead to unreliable driver advise generation, which may eventually hamper safety, energy efficiency and punctuality of the railway operation.

In literature, such similar feed-back control systems wherein the control loops are closed through a real-time network are called NCSs [Zhang *et al.* 2001]. The defining feature of an NCS is that, information such as reference trajectory, control input, system output etc., is exchanged using a shared communication network among different components of the control system, i.e. sensors, controller, actuators, etc., which in usual scenario, are distributed at physically different locations. Fig. 3.1 ([Zhang *et al.* 2001]) illustrates a typical setup and the information flows of a NCS.

The idea that we are pursuing, i.e. to study the stability of the Driver-Train system with driver-in-the-loop, is consistent to a NCS. Fig. 3.2 illustrates a Driver-Train system

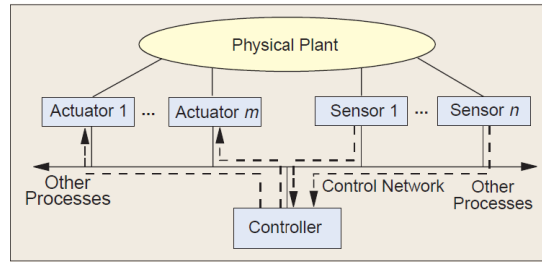


Figure 3.1: A typical NCS setup and information flow

setup and its corresponding information flow. In contrast to the traditional point-to-point architecture, the presence of a communication network in the feedback control loop makes the stability analysis of a Driver-Train system challenging. The main network-induced imperfections and constraints can be categorised in the following five types, variable sampling/transmission intervals; communication/network induced delays; communication scheduling; multiple-packet transmissions and packet loss/dropout [Heemels *et al.* 2010], [Zhang *et al.* 2016c].

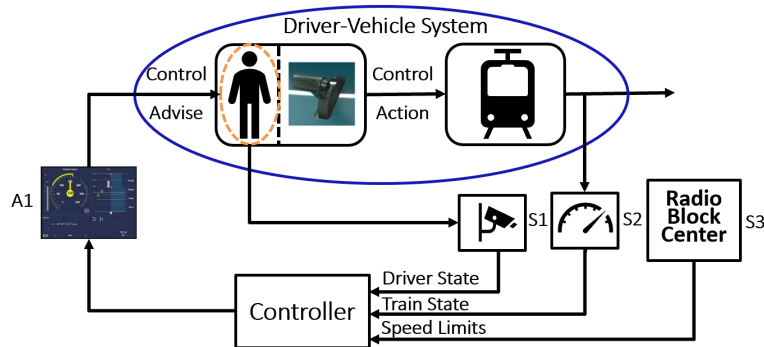


Figure 3.2: A Driver-Train NCS setup and information flow

Variable sampling: The point-to-point architecture is the traditional communication architecture for control systems. Conventionally, for such digitally/computer controlled system, it is assumed that the output are sampled at equal-distance, i.e. the samples are taken periodically in time. However, when a continuous-time signal has to be transmitted over a network, the signal must be first sampled, encoded in a digital format, transmitted over the network, and finally the data must be decoded at the receiver side. This process is significantly different from the usual constant/periodic sampling in digital control and may induce variable sampling/transmission intervals. Thus, the assumption of equal-distance sampling may not be appropriate in NCS analysis.

Network-induced delay: This issue caters to sensor-to-controller delay or controller-

to-actuator delay, that occurs while exchanging data among devices connected to the shared medium. The delay may be constant/time-varying/random and can degrade the performance or can even destabilise the control systems (if designed without considering the delay). The delay depends on the network characteristics such as network load, typologies, routing schemes, etc.

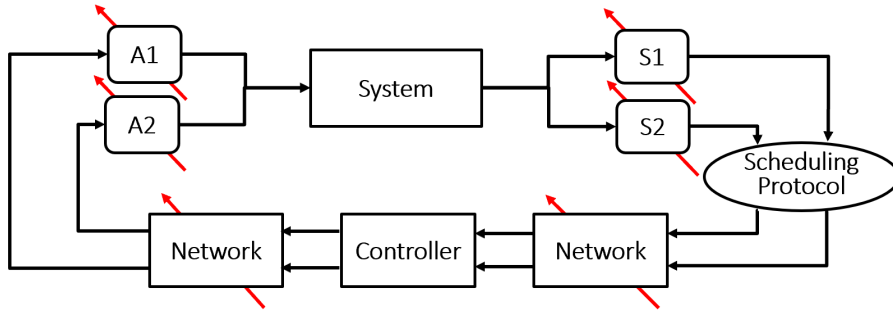


Figure 3.3: Challenges to study stability of NCS system

Communication scheduling: In NCSs, the performance of control loops not only depend on the design of the control algorithms, but also rely on the real-time scheduling of the shared network resource. The communication constraint impose that, per transmission, only one node can access the network and send its information. Hence, how often the system should be scheduled to transmit the data by the system and with what priority the packet should be sent out, is also needed to be considered.

Quantization: Due to limited transmission capacity of the network, data transmitted in practical NCS should be quantized before they are sent to the next network node. The multiple-packet transmission of the system output helps to consider bandwidth and packet size constraints of the network. Nevertheless such signal transmission methods impose challenges, because, while arbitration of the network medium with other nodes on the network, there are chances, that all/part/none of the packets miss to arrive at the time of control calculation, thus generating unreliable control advise.

Packet dropouts: In comparison to standard digital control, NCSs also suffer from unreliable transmission path problem, i.e. in addition to transmission delay, some data packets can even be lost during transmission.

To summarise, the unreliable and time-dependent levels of jitter, delays, losses or network-induced imperfections can jeopardise the stability, safety and performance of the units in a physical environment. Thus, the development of robust stability theory to study the effect of these issues on the performance of a NCS has been an active interest of control engineering researcher's community.

In [Zhang *et al.* 2001], author states that there are two main approaches for accommo-

dating all of these issues in NCS stability study. One way is to design the control system without regards to the aforementioned issues, i.e. no sensor/actuator or transmission delay, no data loss/quantisation, and no scheduling issues, but, design a communication protocol that minimises the likelihood of these events. The other approach is to treat the network protocol and network traffic as given conditions and study stability that explicitly take the above-mentioned issues into account.

In this thesis, we develop stability analysis strategies by the second approach, but only considering the first issues, i.e. variable sampling/transmission interval. We assume that the other four issues are non-existent while formulating the control system in the form of delay-differential equations. The assumption is justifiable since the driver and the train state are available to the ADAS with a variable time-delay. In the following section, we present the sampled-data representation of a simplified NCS and further elaborate upon the intricacies involved in finding stability of the NCS system.

3.2.1 NCS as sampled-data system

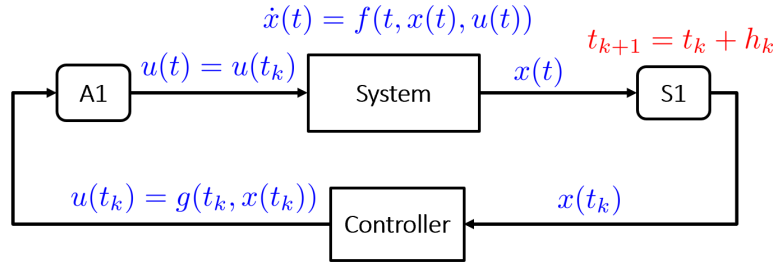


Figure 3.4: Sampled-data system

A simplified NCS can be represented as a sampled-data system, i.e. with a continuous-time system dynamics and a discrete-time controller, connected by a single sensor/actuator combination, as represented by the block diagram in Fig. 3.4. Here, the blocks S1 and A1 can correspond to a sensor/sampler/analog-to-digital converter and a actuator/zero-order-hold/digital-to-analog converter respectively.

Definition 3.1: A general sampled-data system can be written in the form,

$$\begin{aligned} \dot{x}(t) &= f(t, x(t), u(t)), \quad \forall t \geq 0, \\ u(t) &= g(t_k, x(t_k)), \quad \forall t \in [t_k, t_{k+1}), \quad k \in \mathbb{N}, \end{aligned} \quad (3.1)$$

where t is the time-variable, $x : \mathbb{R}^+ \rightarrow \mathbb{R}^{n_x}$ is a measured system "state-trajectory", $u : \mathbb{R}^+ \rightarrow \mathbb{R}^{n_u}$ the "input" or "control signal", and the scalars t_k , for $k \in \mathbb{N}$, monotonically increasing sequence of positive real numbers that satisfy, $0 = t_0 < t_1 < \dots < t_k < \dots$ and

$\lim_{k \rightarrow \infty} t_k = \infty$, and the sampling law is defined as

$$t_{k+1} = t_k + h_k \quad (3.2)$$

where h_k represents the k^{th} sampling interval. In the Section 3.2, we discussed that there can be two source of network transmission delays: sensor-to-controller and controller-to-actuator. We consider that such delays are negligible, but assume that the sensor acts in a time-driven fashion (i.e., sampling occurs at the times $(t_k$ for $k \in \mathbb{N})$ and that both the controller and the actuator act in an event-driven fashion (i.e., they respond instantaneously to the k^{th} system state sample $x(t_k)$, to effectively calculate and implement $u(t_k)$ at the system input). Under these assumptions, the delay in sampling is captured by a single delay h_k and the input signal $u(t)$ becomes a piece-wise constant signal.

The sensor/sampler/analog-to-digital converter, ideally should follow a clock, as in the classical periodic sampling paradigm, or can have a more complex scheduling protocol which may take into account the memory of the last sampled sensor signal. Nevertheless, as we are considering the first issue, they do not perform as desired and produce variation in sampling time. The digital controller operates with a sampled version of the system state signal, x_k , $k \in \mathbb{N}$, obtained at discrete sampling instants t_k using a sensor/sampler/analog-to-digital converter. Note that, here we do not explicitly consider controller induced delay.

It is important to note that with these systems, the discrete-time dynamics introduced by the (digital) controller implies that during the time between two sampling instants, the system is controlled in open-loop (i.e. without updating the feed-back information). Therefore, the sampling time plays an important role in the stability of the system, and appropriate tools have to be used. The study of stability of such sampled-data systems has been addressed in several areas of research in control theory. While significant advances on this subject have been presented in the literature review, [Hetel *et al.* 2017], the problems related to both the fundamentals of such systems and the derivation of constructive methods for stability analysis remain open, even for the case of linear system.

3.2.2 Sampled-data LTI systems

The model of sampled-data systems for NCS provided in Definition 3.1 is very general. In this thesis, rather than dealing with non-linear train dynamics, we will be focusing on a linearised time-invariant train dynamics. Thus, let us first understand stability of linear time-invariant sampled-data systems with a simple state-feedback in closed-loop.

Definition 3.2: A sampled-data LTI system can be written in the form,

$$\begin{aligned} \dot{x}(t) &= Ax(t) + Bu(t), \quad \forall t \geq 0, \\ u(t) &= -Kx(t_k), \quad \forall t \in [t_k, t_{k+1}), \quad k \in \mathbb{N}, \end{aligned} \quad (3.3)$$

where, t is the time-variable, $x : \mathbb{R}^+ \rightarrow \mathbb{R}^{n_x}$ the measured system "state-trajectory", $u : \mathbb{R}^+ \rightarrow \mathbb{R}^{n_u}$ the "input", or "control signal", the scalars t_k , for $k \in \mathbb{N}$, are the sampling instants which satisfy $0 = t_0 < t_1 < \dots < t_k < \dots$ and $\lim_{k \rightarrow \infty} t_k = \infty$. $A \in \mathcal{M}_{n_x}(\mathbb{R})$ is the "state matrix", $B \in \mathcal{M}_{n_x, n_u}(\mathbb{R})$ is the "input gain matrix", and $K \in \mathcal{M}_{n_u, n_x}(\mathbb{R})$ is the "control gain matrix". The sampling law is defined as

$$t_{k+1} = t_k + h_k \quad (3.4)$$

where h_k represents the k^{th} sampling interval. The definition 3.2 presents the case of an "ideal" sampled-data LTI systems. However, throughout this thesis, additional phenomenon such as exogenous perturbations will also be considered. In such case, the associated system equations will be provided. In the absence of perturbations, the evolution of the system's state between two consecutive sampling instants t_k and t_{k+1} is given by

$$\begin{aligned} x(t) &= e^{A(t-t_k)}x(t_k) + \int_0^{t-t_k} e^{As}dsBu(t_k) \\ &= A_d(t-t_k)x(t_k) + B_d(t-t_k)u(t_k) \\ &= [A_d(t-t_k) - B_d(t-t_k)K]x(t_k) \\ &= \Lambda(t-t_k)x(t_k), \quad \forall t \in [t_k, t_{k+1}), \quad k \in \mathbb{N}, \end{aligned} \quad (3.5)$$

with the matrix functions A_d , B_d , and λ defined on \mathbb{R}^+ as $A_d(\sigma) = e^{A\sigma}$, $B_d(\sigma) = \int_0^\sigma e^{As}dsB$, and $\Lambda(\sigma) = A_d(\sigma) - B_d(\sigma)K = e^{A\sigma} - \int_0^\sigma e^{As}dsBK$. Thus, using this notation and the notation h_k in equation (3.4) for the sampling intervals, the discrete-time model of the sampled-data LTI system at instants t_k can be obtained as,

$$x_{k+1} = A_d(h_k)x_k + B_d(h_k)u_k = \Lambda(h_k)x_k, \quad \forall k \in \mathbb{N}, \quad (3.6)$$

where, $x_k \equiv x(t_k)$, $u_k \equiv u(t_k)$. $A_d(h_k)$, $B_d(h_k)$ and $\Lambda(h_k)$ are the "state matrix", the "input matrix", and discrete-time "transition matrix" of the discrete-time model respectively. Such a model belongs to the class of discrete-time Linear Parameter Varying (LPV) systems [Kamen & Khargonekar 1984] and captures the behaviour of (3.3) system only at sampling times, without consideration of the inter-sample behaviour.

Earlier in this section, we discussed about the problems arising due to delays in sensor measurement. In the control theoretic context, the same challenges can be said to be arising due to existence of both a continuous and a discrete dynamics in sampled-data LTI system. Thus the problem of delayed sensor measurements can be rewritten as: determine if the sampled-data LTI system is stable for any time-varying sampling interval h_k with values in a bounded subset $\Omega \subseteq \mathbb{R}^+$.

Remark 3.3: In this thesis, we intend to find solutions which maximise the stable time-varying sampling interval h_k . The solutions will help us quantitatively ascertain

driver-in-the-loop closed loop stability upto a maximum sampling interval \bar{h} of the time-varying/random measurements from the faulty sensors. As we are only considering the deterministic aspects of the sampling problem for sampled-data LTI systems, the case when sampling intervals are random variables, i.e., given by a probability distribution, will not be discussed here.

Remark 3.4: In the Driver-Train system stability context, we want to find: up to what sensor measurement delay limit, or colloquially speaking maximum of time-varying sampling interval, \bar{h} , the stability of the closed-loop system can be ascertained. During this study, some stability performances will be taken into account, such as speed of convergence of the system's state, or the robustness with respect to possible exogenous perturbations (varying driver behaviour). We will even adapt the proposed tools for different controllers, such as, linear (state-feedback) and non-linear (NN), to derive solution for time-varying sampling stability problem.

3.3 Stability of sampled-data LTI systems under time-varying sampling

3.3.1 Preliminaries

In order to study the stability of an NCS represented as a sampled-data LTI system, it is imperative to understand what is stability of a system. Thus, in order to aid the reader we recalled some fundamental concepts for system stability and the classical tools such as Lyapunov stability approach, for both continuous-time and discrete-time system representation in Appendix B.

The first and easiest way to study sampled-data LTI systems is to consider the case when the sampling interval is constant or colloquially speaking, periodic sampling, i.e. $h_k = T$. Stability of sampled-data LTI systems with constant sampling period was extensively studied using discrete-time approach, [Zhang *et al.* 2001], [Ahmadi & Parrilo 2008], [Skaf & Boyd 2009], [Hetel *et al.* 2011].

However, some problems still remain open, since the proposed solutions remain conservative regarding the continuous-time analysis of such systems, or regarding the robustness with respect to exogenous perturbations. For more results regarding robust stability and optimal control of sampled-data LTI systems both with continuous as well as discrete-time approach, please refer [Chen & Francis 1991] and [Åström & Wittenmark 1996].

While in the last fifty years an intensive research has been dedicated to the analysis and design of sampled-data LTI systems under periodic sampling, the study of systems

with time-varying sampling intervals is quite underdeveloped. During the real-time control of a physical systems, it is impossible to maintain a constant sampling rate. In the case of embedded and networked systems, as discussed in Section 3.2, the problem is evident, as delays naturally appear during the measurement/transmission of the information, during the computation of the control, or because of scheduling issues.

From control theoretic point of view, the variations in the sampling interval bring up new challenges. To aid the reader in understanding the challenges, we briefly presented the time-varying sampling stability problem in Appendix B. Succinctly, time-varying sampling can destabilise the closed-loop system, [Wittenmark *et al.* 1995], [Li *et al.* 2010]. Considering the difficulty of the problem, several works in the last two decades have been concerned with the stability analysis of sampled-data LTI systems with time-varying samplings with bounded-values, ($h_k \in [\underline{h}, \bar{h}]$).

In literature, different approaches are used to model such aperiodically sampled systems, namely discrete-time approach, time-delay approach, hybrid modelling approach, Input/Output modelling approach.

- In the Section 3.2.2 we presented the sampled-data LTI system integration over constant sampling interval for discrete-time approach. With time-varying sampling, the same system can be modelled as a discrete-time uncertain system (uncertainty due to time-varying sampling and preferably small network-delays, if present), [Nilsson 1998], [Zhang *et al.* 2001], [Robert *et al.* 2010], [Simon *et al.* 2017].
- The sampled-data LTI system can also be modelled as a time-delay system, where continuous-time system is controlled by delayed control input. This approach allows to study both slow and fast-varying sampling [Mikheev *et al.* 1988].
- Hybrid systems modelling is another approach, widely studied in literature, for simultaneous modelling of both continuous and discrete dynamics present in sampled-data LTI system, [Sivashankar & Khargonekar 1994], [Naghshtabrizi *et al.* 2007].
- Input/Output connection based modelling is another technique, which is inspired from the stability study from a robust control point of view, i.e. the sampling error is considered as a perturbation with respect to a nominal continuous-time control loop, [Zames 1966], [Zhou *et al.* 1996] etc.

A detailed review of stability study of sampled-data system using these approaches can be found at [Hetel *et al.* 2017] and of NCS systems can be found at [Liu *et al.* 2019]. The purpose of the driver-in-the-loop train system stability studies is to estimate the acceptable maximum delay in sensor measurement updates without the closed-loop system goes unstable. Contrary to only qualitative results provided by the emulation approach about existence of sufficiently small periodic/aperiodic sampling stability properties of

sampled-data LTI systems [Karafyllis & Kravaris 2009], the above approaches do give the opportunity to estimate the set of sampling intervals for which the stability properties are still guaranteed.

Among these approaches, for sampled-data LTI systems, discrete-time approach are known to lead to less conservative results in terms of estimating maximum delay in sampling (either periodic/apperiodic) [Donkers *et al.* 2011]. Nevertheless, compared to time-delay systems based modelling, it fail to consider properties of sampling, i.e. slow or even fast-varying delays. Thus, considering this advantage, we preferred to represent our problem using time-delay approach. In the following, we will provide a structural overview of the progress made on the stability analysis problem from time-delay system's point of view. Without being exhaustive, which would be neither possible nor useful, we bring together results from diverse communities and present them in a unified manner.

3.3.2 Time-delay approach with Lyapunov techniques

Time-delay based modelling of sampled-data system was initiated by [Mikheev *et al.* 1988]. In this approach, the discrete-time dynamics induced by a digital controller is considered as a piece-wise continuous time-delay,

$$t_k = t - (t - t_k) = t - h(t), \quad \forall t \in [t_k, t_{k+1}), \quad k \in \mathbb{N},$$

where, $h(t) \equiv t - t_k$ is the induced delay. The LTI system with sampled-data (3.3) is then re-modelled as an LTI system with time-varying delay,

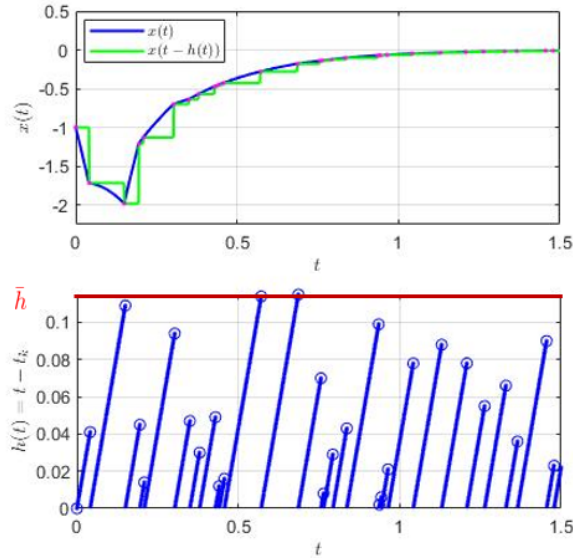


Figure 3.5: Sampling seen as piece-wise continuous time-delay

$$\begin{aligned} \dot{x}(t) &= Ax(t) + Bu(t), \quad \forall t > 0, \\ u(t) &= -Kx(t - h(t)), \quad \forall t > 0, \end{aligned} \tag{3.7}$$

where the delay $h(t)$ is piece-wise linear, satisfying for $t \neq t_k$, and $h(t_k) = 0$. The delay indicates the time that has passed since the last sampling instant. For time-delay systems, the future evolution of the state depends not only to the current state $x(t)$ but is actually a function of the past states of the system until, $x(t - h(t))$. Because of this property time-delay systems are also called as infinite dimensional systems.

An illustration of a typical system state, $x(t)$, the piece-wise linear time-delay, $h(t)$ and the sampled-state representative, $x(t - h(t))$ evolution is shown in Fig. 3.5. Such representation permits to analyse not only systems with known sampling induced delay-derivative, i.e. slow-varying delay ($\dot{h}(t) \leq 1$), but also for systems with fast-varying delay ($\dot{h}(t) > 1$), by using the classical tools ([Richard 2003], [Fridman & Shaked 2003b], [Mounier & Rudolph 2003], [Zhong 2006]).

Stability of such time-delay modelled systems is a fundamental issue from both theoretical and practical points of view. Indeed, as it can be seen in Appendix B, the presence of time-delays can be detrimental to the stability of the practical system. In order to better understand tools used to study stability of time-delay systems and determine the maximum delay interval \bar{h} , let us first understand general time-delay systems.

Definition 3.5: A time-delay system can be defined as the following retarded functional differential equation:

$$\begin{aligned} \dot{x}(t) &= f(t, x_t), \quad \forall t \geq 0, \\ x_{t_0}(\theta) &= \phi(t_0 + \theta), \quad \forall \theta \in [-\bar{h}, 0], \end{aligned} \tag{3.8}$$

where, $f : \mathbb{R}^+ \times \mathcal{C}^0([-\bar{h}, 0] \rightarrow \mathbb{R}^{n_x}) \rightarrow \mathbb{R}^{n_x}$ (continuous in both arguments and locally Lipschitz in the second argument), $\phi \in \mathcal{C}^0([-\bar{h}, 0] \rightarrow \mathbb{R}^{n_x})$ (\mathcal{C}^0 is the set of continuous functions mapping the interval $[-\bar{h}, 0] \rightarrow \mathbb{R}^{n_x}$, with $\bar{h} > 0$, the maximal delay), and $x_t \in \mathcal{C}^0([-\bar{h}, 0] \rightarrow \mathbb{R}^{n_x})$, which represents the state function and is defined by:

$$x_t(\theta) = x(t + \theta), \quad \forall \theta \in [-\bar{h}, 0]. \tag{3.9}$$

It is assumed that there exists a unique solution to the above differential equation and there is a unique equilibrium point : $x_e = 0$. In [Gu *et al.* 2003], authors even provided some Lipschitz conditions for the existence and unicity of solutions. Under existence and unicity of the solution, [Dambrine 1995] shown that the equilibrium state defined by $\dot{x}(t) = 0$ is a constant function $x_t(\theta) \equiv x_e$, thus the expression "equilibrium point" is justified. Moreover, if the equilibrium point is not 0, we can come down to it by using a simple change of coordinates as in the delay-free case.

In the general case of time-delay systems, it is difficult to apply classical Lyapunov stability theory from Theorem B.3 (Appendix B), because the derivative $\frac{dV(x)}{dt}$ will depend on the past values of the state: x_t . We can also ascertain this fact by considering the sampled-data LTI system equation in (3.7). The closed-loop system $\dot{x}(t) = Ax(t) - BKx(t - h(t))$, $\forall t > 0$, is an infinite-dimensional delay-differential equation, i.e. system dynamics is not only dependent on current state but also on former states.

To overcome this issue, two different stability approaches, better suited to time-delay systems, have been developed. Both of them make use of a wider class of functions or functionals as Lyapunov candidates.

1. The first approach is called Lyapunov-Razumikhin [Razumikhin 1956], which uses vector $x(t)$ and time-dependent "energy" function $V \equiv V(t, x(t))$, to approach the "infinite-dimensional" problem using a "finite-dimensional" tool.
2. The second approach is called Lyapunov-Krasovskii [Krasovskii 1963], a most popular generalisation of the direct Lyapunov method for time-delay system. This approach uses $V \equiv V(t, x_t)$ functionals, which depend on x_t . Thus the functional differential equation is seen as evolving in an Euclidean space.

The introduction of Lyapunov-Razumikhin approach in stability theory was advantageous as it reduced the conservatism with respect to the classic Lyapunov stability theory, and made possible to work with simple Lyapunov-Razumikhin Function (LRF)s. Initially, the derived stability conditions were delay-independent, (i.e. stability property was robust and holds for all positive and finite values of the delays). Later, checkable delay was explicitly introduced in the equations to get delay-dependent stability conditions [Briat 2015].

In spite of the advantages, the use of Lyapunov-Razumikhin functions is very often considered as leading to conservative stability conditions. In order to overcome this drawback, Lyapunov-Krasovskii techniques were proposed. At the cost of more sophisticated structure, this technique could provide less conservative delay-dependent conditions. Thus, as an effect the conditions can estimate a less conservative maximum delay \bar{h} , beyond which, the system becomes unstable. For this reason, we choose to use LKF approach to develop delay-dependent conditions to study stability of Driver-Train system in the presence of sensor-delays. In the next subsection, let us understand the LKF approach.

3.3.2.1 Lyapunov-Krasovskii approach

The Lyapunov-Krasovskii approach is an extension of the Lyapunov theory to functional differential equations. Here, we are searching for positive functionals $V \equiv V(t, x_t)$ which are decreasing along the trajectories of (3.8).

Theorem 3.6: (Lyapunov-Krasovskii (from [Gu et al. 2003])) Consider three continuous non-decreasing functions $\alpha, \beta, \gamma : \mathbb{R}^+ \rightarrow \mathbb{R}^+$, such that $\alpha(\theta)$ and $\beta(\theta)$ are strictly positive for all $\theta > 0$, and $\alpha(0) = \beta(0) = 0$. Assume that the vector field f from (3.8) is bounded for bounded values of its arguments. Further, if there exists a continuously differentiable function $V : \mathbb{R}^+ \times \mathcal{C}^0([-\bar{h}, 0] \rightarrow \mathbb{R}^{n_x}) \rightarrow \mathbb{R}^+$ such that:

$$\alpha(\|\phi(0)\|) \leq V(t, \phi) \leq \beta(\|\phi\|_c), \quad (3.10)$$

with $\|\cdot\|$ any norm of \mathbb{R}^{n_x} , and $\|\cdot\|_c$ is associate norm on $\mathcal{C}^0([-\bar{h}, 0] \rightarrow \mathbb{R}^{n_x})$, defined by $\|\phi\|_c = \max_{\theta \in [-\bar{h}, 0]} \|\phi(\theta)\|$, and if

$$\dot{V}(t, \phi) \leq -\gamma(\|\phi(0)\|), \quad (3.11)$$

then the origin of the system (3.8) is uniformly stable. If, in addition, $\gamma(\theta) > 0$ for all $\theta > 0$, then the functional V is called the LKF, and the origin of the system (3.8) is uniformly asymptotically stable. If in addition $\lim_{s \rightarrow \infty} \alpha(s) = +\infty$, then the origin of the system (3.8) is globally uniformly asymptotically stable. The functionals that are usually considered, have the following form [Kolmanovskii & Shaikhet 1996]:

$$\begin{aligned} V(t, \phi) = & \phi^T(0)P(t)\phi(0) + \phi^T(0) \left(\int_{-\bar{h}}^0 Q(t, s)\phi(s)ds \right) + \left(\int_{-\bar{h}}^0 Q(t, s)\phi(s)ds \right)^T \phi(0) \\ & + \int_{-\bar{h}}^0 \int_{-\bar{h}}^0 \phi^T(s)R(t, s, p)\phi(p)dsdp + \int_{-\bar{h}}^0 \phi^T(s)S(s)\phi(s)ds, \end{aligned} \quad (3.12)$$

where, P, Q, R , and $S \in \mathcal{M}_{n_x}(\mathbb{R})$. $P(t)$ and $S(s) \in S_{n_x}^{+*}$, and R satisfies $R(t, s, p) = R^T(t, s, p)$. It was proved in [Kolmanovskii & Shaikhet 1996] that the existence of such a LKF is necessary and sufficient condition to ensure the system's stability in the case of LTI systems with time-varying delay (i.e. when the system (3.8) is considered with $f(t, x_t) = Ax(t) + A_d x(t - h(t))$). An analytical description of fitting matrices functions Q, R and S has also been presented in [Kharitonov & Zhabko 2003]. In practice ([Niculescu 2001a]), these matrices terms are considered constant, and we search functional of the type:

$$\begin{aligned} V(t, \phi) = & \phi^T(0)P\phi(0) + 2\phi^T(0) \left(\int_{-\bar{h}}^0 Q\phi(s)ds \right) \\ & + \int_{-\bar{h}}^0 \int_{-\bar{h}}^0 \phi^T(s)R\phi(p)dsdp + \int_{-\bar{h}}^0 \phi^T(s)S\phi(s)ds, \end{aligned} \quad (3.13)$$

Although more conservative, this form of LKFs with constant matrices allow to derive LMI stability conditions, which make it easier to look for solutions. In recent works concerning time-delay systems, the conservatism has been reduced by considering P, Q, R and S matrices as piece-wise constant functions [Gu 1997], [Gu et al. 2003], [Fridman & Shaked 2005], [Fridman 2006].

The advantage of the Lyapunov-Krasovskii approach is that it essentially enlarges the class of Lyapunov candidates. It was shown in [Driver 1977] for the constant delay and in [Kolmanovskii & Myshkis 1999] for the general time-varying delay, that the existence of LRF implies the existence of a LKF. For general time-delay systems, Lyapunov-Krasovskii approach introduce delay, $h(t)$ and often unknown delay-derivative, $\dot{h}(t)$, in the derivative of $\frac{dV(t,x_t)}{dt}$. However, in the context of sampled-data LTI system, $\dot{h}(t) = 1$. The introduction of delay $h(t)$ in the equations eases derivation of delay-dependent/sampling interval dependent stability conditions. The approach may also be extended to control design and to the case of systems with parameter uncertainties and perturbations. In the Section 3.3.4, we will present LKF functionals for time-delay modelled sampled-data LTI systems.

3.3.3 Convex-embedding approach

An appropriate choice of LKF may lead to a less conservative delay-dependent condition. However, it may not provide an estimate of the system's performance in between sampling instants. For this purpose, in this subsection, we will introduce an approach called "convex-embedding", a technique based on convexification of the transition matrix between sampling times in order to derive stability conditions, [Hetel *et al.* 2006], [Fujioka 2009a], [Cloosterman *et al.* 2010], [Gielen *et al.* 2010]. Particularly, this approach is based on the property of describing the evolution of system's state $x(t)$ with respect to the sampled-state $x(t_k)$ and the time $t - t_k$:

$$x(t) = \Lambda(t - t_k)x(t_k), \quad \forall t \in [t_k, t_{k+1}), \quad k \in \mathbb{N},$$

and on the study of the transition matrix operator Λ defined in (3.5). In the case of sampled-data LTI system (3.3) with time-varying sampling intervals with values in $[\underline{h}, \bar{h}]$ with $\underline{h} > 0$, the classic Lyapunov theory in discrete-time can be used with a simple quadratic Lyapunov function $V(x) = x^T P x$, so as to obtain sufficient stability conditions under the form of parameter-dependent LMIs:

$$\Lambda(\theta)^T P \Lambda(\theta) - P \prec 0, \quad \forall \theta \in [\underline{h}, \bar{h}]. \quad (3.14)$$

These stability conditions involve infinite number of LMIs, since they depend on parameter θ that takes value in the line segment $[\underline{h}, \bar{h}]$. The idea of convex-embedding approach is to reduce these conditions down to a finite number, by designing a polytopic approximation of the operator Λ . Thus, the set of matrices:

$$\Lambda \equiv \{\Lambda(h) | h \in [\underline{h}, \bar{h}]\}, \quad (3.15)$$

can be over-approximated as follows:

$$\Lambda \subseteq \text{Co}\{F_i\}_{i \in \{1, \dots, N\}} = \left\{ \sum_{i=1}^N \alpha_i F_i \mid \alpha = \begin{bmatrix} \alpha_1 \\ \vdots \\ \alpha_N \end{bmatrix} \in \mathcal{A} \right\}, \quad (3.16)$$

where, $F_i \in \mathcal{M}_{n_x, n_u}$, $\forall \{1, \dots, N\}$ are suitably constructed matrices, N is the number of vertices in the polytopic over-approximation, and:

$$\mathcal{A} = \left\{ \alpha \in \mathbb{R}^N \mid \alpha_i \geq 0, \forall i \in \{1, \dots, N\}, \text{ and } \sum_{i=1}^N \alpha_i = 1 \right\}. \quad (3.17)$$

The properties of the over-approximating convex set $\text{Co}\{F_i\}_{i \in \{1, \dots, N\}}$ makes it possible to derive a finite number of sufficient stability conditions from (3.14), by writing simple LMIs over the polytope vertices:

$$F_i^T P F_i - P \prec 0, \forall \{1, \dots, N\}. \quad (3.18)$$

Moreover, a continuous-time approach to the stability analysis of sampled-data LTI systems based on convexification arguments has been proposed in [Hetel *et al.* 2011]. It is based on the parameter-dependent LMI:

$$\begin{bmatrix} \Lambda(\theta) \\ I \end{bmatrix}^T \begin{bmatrix} A^T P + AP - PBK \\ * & 0 \end{bmatrix} \begin{bmatrix} \Lambda(\theta) \\ I \end{bmatrix} \prec 0, \forall \theta \in [\underline{h}, \bar{h}], \quad (3.19)$$

and the same convexification tools. Several over-approximation methods to design the polytope vertices F_i from (3.16) are used in the literature. For example, gridding and norm bounding in [Skaf & Boyd 2009], [Donkers *et al.* 2011], Taylor series expansion in [Hetel *et al.* 2006], [Hetel *et al.* 2007a], [Hetel *et al.* 2011] Real-Jordan form decomposition in [Olaru & Niculescu 2008], [Wouw *et al.* 2010], [Cloosterman *et al.* 2010], or the Cayley-Hamilton theorem in [Gielen *et al.* 2010], [Goebel *et al.* 2012].

The main advantage of the convex-embedding approach for the stability analysis of sampled-data LTI systems is that it is intuitive, tractable and provides less conservative conditions. Also, it was proved using various numerical benchmarks [Fiter *et al.* 2012], that convex-embedding allow for approaching the stability condition (3.14) as close as desired, by increasing N of the over-approximation algorithm [Fiter *et al.* 2015]. The main drawback of the method is that with increase in numerical precision the computational complexity and computational time increases.

3.3.4 Delay-dependent analysis of sampled-data LTI systems

In the Subsection 3.3.2 we presented different approaches for stability of general time-delay systems. In this subsection, we want to focus particularly on LKF approach so as to obtain

delay-dependent conditions for sampled-data LTI system. In the case of sampled-data systems [Fridman *et al.* 2004], [Naghshabrizi *et al.* 2008], [Seuret 2009], [Fridman 2010], [Seuret 2012], the induced delay has a known derivative $\dot{h}(t) = 1$, $\forall t \in [t_k, t_{k+1})$, $k \in \mathbb{N}$. This property enables to simplify the LKFs to derive less conservative stability conditions. However, the choice of LKF is crucial for deriving stability criteria [Fridman 2014b].

The derivation of stability conditions using LKFs needs quite elaborate developments. The process usually involve 4 basic steps as following.

- Step 1 is to propose a LKF candidate.
- Step 2 is to compute LKF derivative and identify integral terms.
- Step 3 is to over-approximate the integral terms (using inequalities), to replace them by simpler expressions and obtain delay-dependent sufficiency conditions of stability.
- Finally, Step 4 is to over-approximate the delay-dependent terms (using convex-embedding) by simpler expressions which are either constant or \bar{h} dependent.

In order to give a glimpse of the procedure, we present the history of development for the derivation of LMI stability conditions for the case of sampled-data LTI systems (3.3) with the associated time-delay model (3.7). In order to derive a less conservative stability criteria both Step 1 and Step 3 are crucial. In this view, we can find various LKF proposition and various approaches to approximate the integral terms.

3.3.4.1 Model transformation approach

The early development used model transformation approach to facilitate approximation of the integrals of the LKF derivative. This approach employs Leibniz-Newton formula,

$$x(t - h(t)) = x(t) - \int_{t-h(t)}^t \dot{x}(s) ds. \quad (3.20)$$

to transform system (3.7) (while substituting $\dot{x}(s)$ by the right-hand side of (3.7)) to,

$$\dot{x}(t) = (A - BK)x(t) + BK \int_{t-h(t)}^t [Ax(s) - BKx(s - h(s))] ds, \quad (3.21)$$

which facilitate generation of the cross-terms in the derivative of the LKF.

In order to obtain first delay-dependent conditions in terms of LMI, the cross-terms are bounded using Young's inequality, [Li & Souza 1997], [Kolmanovskii & Richard 1999], [Park 1999]. Note that this transformation is valid for $t - h(t) \geq t_0$. The stability of the transformed system (3.21) guarantees the stability of the original system, but not vice versa. It is because the later system is not equivalent to original system, as it possess some addition dynamics, [Gu *et al.* 2003], [Kharitonov & Niculescu 2003].

In literature, various model transformation approaches are proposed, namely, 'parameterised first-order transformation', [Kolmanovskii *et al.* 1998], 'second-order transformation', [Kolmanovskii & Richard 1999], 'neutral transformation', [Niculescu 2001b], and 'descriptor model transformation', [Fridman 2001], [Fridman & Shaked 2002].

The first delay-dependent conditions treated only the slow-varying delays ($\dot{h}(t) \leq 1$), whereas the fast-varying delay ($\dot{h}(t) > 1$) were analysed via LRFs. The authors, [Fridman & Shaked 2003a], for the first time, analysed systems with fast-varying delays by using LKF via the descriptor model transformation introduced in [Fridman 2001]:

$$0 = -\dot{x}(t) + (A - BK)x(t) + BK \int_{t-h(t)}^t \dot{x}(s)ds. \quad (3.22)$$

The descriptor system (3.22) is equivalent to (3.7) in the sense of stability. In the descriptor approach, $\dot{x}(t)$ is not substituted by the right-hand side of the differential equation. Instead, it is considered as an additional state variable of the resulting descriptor system (3.22). Therefore, the novelty of the descriptor approach is not in $V(x(t)) = x^T(t)Px(t) + \dots$ ($P > 0$), but in \dot{V} ,

$$\begin{aligned} \frac{d}{dt} [x^T(t)Px(t)] &= 2x^T(t)P\dot{x}(t) + 2 [x^T(t)P_2^T + \dot{x}^T(t)P_3^T] \times \\ &\quad \left[-\dot{x}(t) + (A - BK)x(t) + BK \int_{t-h(t)}^t \dot{x}(s)ds \right], \end{aligned} \quad (3.23)$$

where $P_2 \in \mathbb{R}^{n_x \times n_x}$ and $P_3 \in \mathbb{R}^{n_x \times n_x}$ are "slack variables". This leads to $\dot{V} \leq -\gamma(\|x(t)\|^2 + \|\dot{x}(t)\|^2)$, $\gamma > 0$. The descriptor method is beneficial as it brought free-weighting matrices P_2 and P_3 into the Lyapunov-based analysis. Later, [Suplin *et al.* 2005] and [Gouaisbaut & Peaucelle 2006a] shown that Finsler's lemma leads to the same slack matrices. The descriptor method is advantageous because it helps to obtain less conservative conditions (even for systems without delay) for uncertain systems. It even provides "unifying" LMIs for the discrete-time and the continuous-time systems, i.e. they have almost the same form and the same advantages ([Fridman & Shaked 2006]). The design can even be obtained for systems with either state, input or output delays by choosing $P_3 = \varepsilon P_2$ with a tuning scalar parameter ε ([Suplin *et al.* 2007]).

3.3.4.2 Integral inequality approach:

In spite of benefits of model transformation and cross-term bounding, most of the recent LKF based results rather use application of Jensen's inequality.

1) Jensen inequality for time-independent LKF:

The choice of Jensen's inequality owes to it's accuracy, i.e. it provides strict upper bound to the integrals. Thus, compared to over-approximation of integral terms using

model transformation and cross-term bounding, the over-approximation using integral inequality was shown to reduce conservatism [Gouaisbaut & Peaucelle 2006b], [Briat 2011], [Seuret & Gouaisbaut 2013]. Let us see.

Lemma 3.7: (Jensen's Inequality from [Gu *et al.* 2003]) Given $R > 0$, $\theta \geq 0$, and a differentiable function $x : [t - \theta, t] \rightarrow \mathbb{R}^{n_x}$, the following inequality holds:

$$J(\dot{x}_t, \theta) = - \int_{t-\theta}^t \dot{x}(s) R \dot{x}(s) ds \leq -\frac{1}{\theta} (x(t) - x(t-\theta))^T R (x(t) - x(t-\theta)) \quad (3.24)$$

The first LKFs based LMI conditions for systems with fast-varying delays ($\dot{h}(t) > 1$) were derived in [Fridman & Shaked 2003a] via the descriptor method. The authors differentiated $x^T(t) P x(t)$ as in (3.23) along system (3.7) with maximum sampling period, \bar{h} . To “compensate” $\int_{t-h(t)}^t \dot{x}(s) ds$ in (3.23), authors considered the double integral term, $V_R(\dot{x}_t)$ ([Fridman & Shaked 2003a]) in the LKF, as $V(x(t), \dot{x}_t) = x^T(t) P x(t) + V_R(\dot{x}_t)$.

$$V(x(t), \dot{x}_t) = x^T(t) P x(t) + \int_{-\bar{h}}^0 \int_{t+\theta}^t \dot{x}^T(s) R \dot{x}(s) ds d\theta, R > 0 \quad (3.25)$$

During the differentiation of LKF $V(x(t), \dot{x}_t)$, the authors first advantageously converted the term $V_R(\dot{x}_t)$ to $\int_{t-\bar{h}}^t (\bar{h} + s - t) \dot{x}^T(s) R \dot{x}(s) ds$ and then computed an approximate derivative as $-\int_{t-h(t)}^t \dot{x}^T(s) R \dot{x}(s) ds + \bar{h} \dot{x}^T(t) R \dot{x}(t)$, while ignoring $-\int_{t-\bar{h}}^{t-h(t)} \dot{x}^T(s) R \dot{x}(s) ds$. Further using Jensen's inequality as $-\int_{t-h(t)}^t \dot{x}^T(s) R \dot{x}(s) ds \leq -\frac{1}{h} \int_{t-h(t)}^t \dot{x}^T(s) R \int_{t-h(t)}^t \dot{x}(s) ds$ and descriptor approach authors obtain,

$$\begin{aligned} \frac{d}{dt} V(x(t), \dot{x}_t) &\leq 2x^T(t) P \dot{x}(t) + \bar{h} \dot{x}^T(t) R \dot{x}(t) - \frac{1}{h} \int_{t-h(t)}^t \dot{x}^T(s) R \int_{t-h(t)}^t \dot{x}(s) ds \\ &\quad + 2 \left[x^T(t) P_2^T + \dot{x}^T(t) P_3^T \right] \left[-\dot{x}(t) + (A - BK)x(t) + BK \int_{t-h(t)}^t \dot{x}(s) ds \right] \\ &\leq \eta^T(t) \Psi \eta(t) \\ &\leq -\varepsilon (\|x(t)\|^2 + \|\dot{x}(t)\|^2), \quad \varepsilon > 0, \end{aligned} \quad (3.26)$$

where, $\eta(t) = \text{col}\{x(t), \dot{x}(t), \frac{1}{h} \int_{t-h(t)}^t \dot{x}(s) ds\}$, if

$$\begin{aligned} \Psi &= \begin{bmatrix} \Phi & P - P_2^T + (A - BK)^T P_3 & \bar{h} P_2^T BK \\ * & -P_3 - P_3^T + \bar{h} R & \bar{h} P_3^T BK \\ * & * & -\bar{h} R \end{bmatrix} \prec 0, \\ \Phi &= P_2^T (A - BK) + (A - BK)^T P_2. \end{aligned} \quad (3.27)$$

Note that $\Psi < 0$ yields that the eigenvalues of $-\bar{h}BK$ are inside of the unit circle. Nevertheless, in the example $\dot{x} = -x(t - h(t))$ with $-BK = -1$, the simple delay-dependent conditions, presented above, cannot guarantee the stability for $\bar{h} \geq 1$, which is far from the analytical bound 1.5. This shows the conservatism of the simple conditions.

In [He *et al.* 2007], author further improved upon these simple delay-dependent condition and proposed improved delay-dependent conditions, by utilising relation not only between the time-varying delayed/exact delayed state $x(t - h(t))$ and the current state $x(t)$ but also the relation between $x(t - h(t))$ and the delay upper-bounded/marginally delayed state $x(t - \bar{h})$. With these developments, the widely used state-derivative dependent LKF for delay-dependent stability of the form,

$$\begin{aligned} V(x(t), \dot{x}_t) = & x^T(t)Px(t) + \bar{h} \int_{-\bar{h}}^0 \int_{t+\theta}^t \dot{x}^T(s)R\dot{x}(s)dsd\theta \\ & + \int_{t-\bar{h}}^t x^T(s)Sx(s)ds + \int_{t-h(t)}^t x^T(s)Qx(s)ds, \end{aligned} \quad (3.28)$$

where $P > 0$, $R \geq 0$, $S \geq 0$, $Q \geq 0$, was constructed.

This functional with $Q = 0$ leads to delay-dependent conditions for systems with fast-varying delays ($\dot{h}(t) > 1$), whereas for $R = S = 0$ it leads to delay-independent conditions (for systems with slow-varying delays, $\dot{h}(t) \leq 1$). The above $V(x(t), \dot{x}_t)$ with $S = 0$ was introduced in [Fridman & Shaked 2003a], whereas the S-dependent term was added in [He *et al.* 2007]. Contrary to the simple delay-dependent conditions, which ignored the term $\int_{t-\bar{h}}^{t-h(t)} \dot{x}^T(s)R\dot{x}(s)ds$, the author here, while differentiating $V(x(t), \dot{x}_t)$ given by (3.28), employed the representation,

$$-\bar{h} \int_{t-\bar{h}}^t \dot{x}^T(s)R\dot{x}(s)ds = -\bar{h} \int_{t-\bar{h}}^{t-h(t)} \dot{x}^T(s)R\dot{x}(s)ds - \bar{h} \int_{t-h(t)}^t \dot{x}^T(s)R\dot{x}(s)ds, \quad (3.29)$$

and applied Jensen's inequality to both the terms on the right hand side to obtain,

$$-\bar{h} \int_{t-\bar{h}}^t \dot{x}^T(s)R\dot{x}(s)ds \leq -\frac{\bar{h}}{h(t)}e_1^T Re_1 - \frac{\bar{h}}{\bar{h} - h(t)}e_2^T Re_2, \quad (3.30)$$

where, $e_1 = x(t) - x(t - h(t))$, $e_2 = x(t - h(t)) - x(t - \bar{h})$.

Here, for $h(t) = 0$ and $h(t) = \bar{h}$, the following limits are satisfied:

$$\begin{aligned} \lim_{h(t) \rightarrow 0} -\frac{\bar{h}}{h(t)}e_1^T Re_1 &= -\bar{h} \lim_{h(t) \rightarrow 0} h(t)\dot{x}^T(t)R\dot{x}(t) = 0 \\ \lim_{h(t) \rightarrow \bar{h}} -\frac{\bar{h}}{\bar{h} - h(t)}e_2^T Re_2 &= 0. \end{aligned} \quad (3.31)$$

In [He *et al.* 2007], the right-hand side of (3.30) was upper-bounded by $-e_1^T Re_1 - e_2^T Re_2$, which is conservative. The convex analysis of [Park *et al.* 2011b] allowed to avoid

this restrictive bounding. The novelty of this method consists in merging the non-convex terms into a single expression to derive an accurate convex inequality. Several others methods are proposed to upper-bound the right-hand side, such as reciprocally convex combination lemma ([Park *et al.* 2011b]), Moon's inequality ([Lee & Kwon 2002]), relaxed reciprocally convex combination lemma ([Zhang *et al.* 2016a]) and its extension ([Zhang *et al.* 2017b]). More insights on the relationship between these inequalities can be found in [Seuret *et al.* 2018].

Note that the existing methods in the framework of time-delay approach are based on some Lyapunov-based analysis of systems with uncertain and bounded fast-varying delays. Therefore, these methods cannot guarantee the stability, if the delay is not smaller than the analytical upper-bound on the constant delay that preserves the stability. However, it is well-known that in many systems the upper-bound on the sampling that preserves the stability may be higher than the one for the constant delay, see examples in [Louisell 1999].

2) Jensen inequality for time-dependent LKF:

Consider for example the sampled-data LTI system ([Papachristodoulou *et al.* 2007]),

$$\dot{x}(t) = -x(t_k), \quad t \in [t_k, t_{k+1}), \quad k \in \mathbb{N}.$$

It is well-known that the equation $\dot{x} = -x(t-T)$, with constant delay T is asymptotically stable for $T \leq \pi/2$ and unstable for $T > \pi/2$. Although, for fast-varying delay, it is stable for $\bar{h} < 1.5$ and there exists a destabilising delay with an upper-bound greater than 1.5. This means that all the existing methods via time-independent Lyapunov functionals cannot guarantee the stability of this system for sampling intervals greater than $\pi/2$.

It is easy to check, that in the case of pure (uniform) sampling, the system remains stable for all constant samplings less than 2 and becomes unstable for samplings greater than 2. Therefore, it was felt necessary to develop new Lyapunov functional-based techniques for sampled-data control to improve the results. Inspired by the construction of discontinuous Lyapunov functions in [Naghshabrizi *et al.* 2008] for the impulsive systems, time-dependent Lyapunov functionals were introduced in [Fridman 2010] for the analysis of sampled-data systems in the framework of time-delay approach.

The main idea is that, compared to the classical fast-varying delay approach, where the delay-derivative is assumed to be unknown and arbitrary varying, the proposed LKFs allow to take into account the particular saw-tooth evolution of the sampling induced delay, $\dot{h}(t) = 1, \forall t \in [t_k, t_{k+1})$. Thus, for the stability analysis of sampled-data LTI systems (3.7), the time-independent term $\int_{-\bar{h}}^0 \int_{t+\theta}^t \dot{x}^T(s) R \dot{x}(s) ds d\theta$ used in [Fridman *et al.* 2004], [Park & Ko 2007] is advantageously replaced by the time-dependent term $(t_{k+1} - t) \int_{t_k}^t \dot{x}^T(s) R \dot{x}(s) ds$, which provide time-dependent LKF $\bar{V}(t) = V(t, x_t, \dot{x}_t)$.

The function $\bar{V}(t)$ may be discontinuous at sampling time, but it is not allowed to grow in the jumps as shown in Fig. 3.6. The proposed time-dependent Lyapunov functional reduces conservatism and provide a fair compromise between accuracy and complexity, to finally lead to qualitatively new results for time-delay systems, allowing a superior performance under the time-varying sampling, when compared with the constant delay. The stability of system (3.7) with time-varying sampling is thus based on the following:

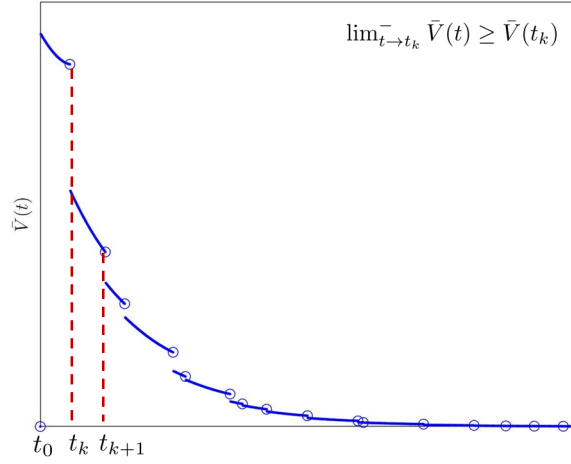


Figure 3.6: Discontinuous in time Lyapunov functional

Theorem 3.8: (Lyapunov-Krasovskii (from [Kolmanovskii & Myshkis 1992]))

Consider three continuous non-decreasing functions, $\alpha, \beta, \gamma : \mathbb{R}^+ \rightarrow \mathbb{R}^+$, such that, $\alpha(\theta)$ and $\beta(\theta)$ are strictly positive for all $\theta > 0$, $\alpha(0) = \beta(0) = 0$. Assume that the vector field f from (3.8) follows $f(t, 0) = 0$ for all $t \in \mathbb{R}^+$ and that f maps $\mathbb{R} \times$ (bounded sets in $\mathcal{C}^0[-\bar{h}, 0]$) into bounded sets of \mathbb{R}^{n_x} , i.e. the vector field is bounded for bounded values of its arguments. Further, if there exists a continuous positive-definite functional $V : \mathbb{R}^+ \times \mathcal{W}[-\bar{h}, 0] \times \mathcal{L}_2(-\bar{h}, 0) \rightarrow \mathbb{R}^+$, such that:

$$\alpha(\|\phi(0)\|) \leq V(t, \phi, \dot{\phi}) \leq \beta(\|\phi\|_{\mathcal{W}}), \quad (3.32)$$

for all $\phi \in \mathcal{W}[-\bar{h}, 0]$, $t \in \mathbb{R}^+$, where $\|\cdot\|$ is any norm of \mathbb{R}^{n_x} , the symbol $\mathcal{L}_p(a, b)$, $p \in \mathbb{N}$ denotes a space of functions $\phi : (a, b) \rightarrow \mathbb{R}^{n_x}$ with the norm $\|\phi\|_{\mathcal{L}_p} = \left[\int_a^b \|\phi(\theta)\|^p d\theta \right]^{1/p}$ and the symbol $\mathcal{W}[a, b]$ denote the space of functions $\phi : [a, b] \rightarrow \mathbb{R}^{n_x}$, which are absolutely continuous on $[a, b]$, and have square integrable first order derivatives, with the norm $\|\phi\|_{\mathcal{W}} = \max_{\theta \in [a, b]} \|\phi(\theta)\| + \left[\int_a^b \|\dot{\phi}(\theta)\|^2 d\theta \right]^{1/2}$. Then, if the derivative along (3.8) system's solutions is non-positive as,

$$\dot{V}(t, x_t, \dot{x}_t) \leq -\gamma(\|x_t(0)\|), \quad (3.33)$$

that trivial solution is said to be uniformly stable. If, in addition, $\gamma(\theta) > 0$ for all $\theta > 0$, then the origin of the system is uniformly asymptotically stable. If, in addition $\lim_{s \rightarrow \infty} \alpha(s) = \infty$, then the origin of the system is globally uniformly asymptotically stable. Further, if there exist three positive numbers $\bar{\alpha}$, $\bar{\beta}$, $\bar{\gamma}$ such that:

$$\bar{\alpha}\|x_t(0)\|^2 \leq V(t, x_t, \dot{x}_t) \leq \bar{\beta}\|x_t\|_{\mathcal{W}}^2. \quad (3.34)$$

Let the function $\bar{V}(t) = V(t, x_t, \dot{x}_t)$ be continuous from the right for $x(t)$ satisfying (3.7), absolutely continuous for $t \neq t_k$ and satisfy $\lim_{t \rightarrow t_k^-} \bar{V}(t) \geq \bar{V}(t_k)$, then, the origin $x = 0$ of the system (3.7) is,

- asymptotically stable, if

$$\bar{V}(t) \leq -\tilde{\gamma}\|x(t)\|^2,$$

holds for $t \neq t_k$ and for some scalar $\tilde{\gamma} > 0$;

- exponential stable, if

$$\bar{V}(t) + 2\gamma\bar{V}(t) \leq 0,$$

for $t \neq t_k$, and then $\bar{V}(t) \leq e^{-2\gamma t}\bar{V}(0)$, which implies that $\|x(t)\|^2 \leq e^{-2\gamma t\frac{\beta}{\alpha}}\|x_0\|_{\mathcal{W}}^2$.

In such a case, the equilibrium point x_e of system (3.7) allows a decay rate γ .

Remark 3.9: In the case of sampled-data LTI systems, in [Fridman *et al.* 2004] the Theorem 3.8 is even extended to linear systems with a discontinuous saw-tooth delay by use of the Barbalat lemma ([Barbalat 1959]).

3) Wirtinger inequality ([Hardy *et al.* 1934]):

In literature, alternative to the use of Jensen's inequality, the integral terms are also over-approximated using Wirtinger's inequality ([Liu *et al.* 2010], [Seuret & Gouaisbaut 2013], [Gyurkovics 2015]). This is because, the use of Wirtinger inequality could provide a larger lower bound to over-approximate the non-negative integral term.

Lemma 3.10: (Wirtinger Inequality (from [Liu *et al.* 2010])) Let $z : [a, b] \rightarrow \mathbb{R}^{n_x}$ be an absolutely continuous function with $\dot{z} \in \mathcal{L}_2(a, b)$ and with $z(a) = 0$. Then, for any $n_x \times n_x$ - matrix $R > 0$, the following inequality holds:

$$\int_a^b z(t)^T R z(t) d\xi \leq \frac{4(b-a)^2}{\pi^2} \int_a^b \dot{z}(t)^T R \dot{z}(t) d\xi \quad (3.35)$$

In [Liu & Fridman 2012], author proposed a novel discontinuous in time LKF based on the extension of the Wirtinger inequality to the vector case. Further refinements with additional free-weighted matrices were also developed in [Lee *et al.* 2014], where the authors considered a discretized version of Wirtinger inequality, [Zeng *et al.* 2015].

In [Selivanov & Fridman 2016], an extension of Wirtinger inequality of Lemma 3.10 for Lyapunov-based exponential stability analysis was presented. Based on this extended Wirtinger inequality, a novel discontinuous LKF with a Wirtinger-based discontinuous term was constructed, $\bar{V}(t) = x^T(t)Px(t) + \bar{V}_R(t, x_t, \dot{x}_t)$, $P > 0$, $R > 0$, $\forall t \in [t_k, t_{k+1})$:

$$\bar{V}_R = \bar{h}^2 e^{2\alpha\bar{h}} \int_{t_k}^t e^{2\alpha(s-t)} \dot{x}(s)^T R \dot{x}(s) ds - \frac{\pi^2}{4} \int_{t_k}^t e^{2\alpha(s-t)} (x(s) - x(t_k))^T R (x(s) - x(t_k)) ds. \quad (3.36)$$

Since $[x(s) - x(t_k)]_{s=t_k} = 0$, by Lemma 3.10, we have $\bar{V}_R \geq 0$. Moreover, \bar{V}_R vanishes at $t = t_k$. Hence, the condition $\lim_{t \rightarrow t_k} \bar{V}(t) \geq \bar{V}(t_k)$ holds. This new method leads to numerically simplified LMI condition for the stability analysis, and can be also applied to performance analysis such as exponential stability [Selivanov & Fridman 2016], input-to-state stability and \mathcal{L}_2 -gain analysis, [Liu & Fridman 2012]. The application of the Wirtinger-based inequality to the case of triple integral-type of LKFs is also considered in [Park *et al.* 2015a].

4) Bessel-Legendre inequality:

In order to avoid the over-approximation of the derivative of LKF, improvements based on Bessel's inequality and Legendre polynomials were introduced in [Seuret & Gouaisbaut 2014]. In [Seuret & Gouaisbaut 2015], authors also show that the canonical Bessel-Legendre inequality can produce larger delay upper bound, \bar{h} .

Lemma 3.11: (Bessel-Legendre Inequality (from [Zhang *et al.* 2018b])) Let $z : [a, b] \rightarrow \mathbb{R}^{n_x}$ be an absolutely continuous function. Then, for a non-negative number N and any $n_x \times n_x$ - matrix $R > 0$, the following inequality holds:

$$\begin{aligned} \int_a^b z(s)^T R z(s) ds &\geq \sum_{i=0}^N \frac{2i+1}{b-a} \tilde{\Omega}_i^T R \tilde{\Omega}_i \\ &= \sum_{i=0}^N \frac{2i+1}{b-a} \hat{\Omega}_i^T R \hat{\Omega}_i \end{aligned} \quad (3.37)$$

where,

$$\begin{aligned} \tilde{\Omega} &:= \int_a^b \tilde{L}_i(s) z(s) ds, \quad \hat{\Omega} := \int_a^b \hat{L}_i(s) z(s) ds \\ \tilde{L}_i(s) &:= \sum_{k=0}^i (-1)^k \binom{i}{k} \binom{k+i}{k} \left(\frac{b-s}{b-a}\right)^k, \\ \hat{L}_i(s) &:= \sum_{k=0}^i (-1)^k \binom{i}{k} \binom{k+i}{k} \left(\frac{s-a}{b-a}\right)^k. \end{aligned} \quad (3.38)$$

As a special case, i.e. for $N = 1$ and $N = 2$, the canonical Bessel-Legendre inequality includes both, the Wirtinger-based inequality and its improvement, i.e. the proper auxiliary-function-based inequality ([Park *et al.* 2015b]) respectively. The underlying idea of Bessel-Legendre inequality is to provide a generic and expandable integral inequality which is asymptotically (in the sense that $N \rightarrow \infty$) not conservative. Notice that $\tilde{\Omega}_i$

depends on the Legendre polynomial and $(b - a)$ also appears in the inverse form in the inequality (3.37). To overcome this inconvenience, [Zhang *et al.* 2018a], developed an affine form of the canonical integral inequality, also called free-matrix based integral inequality, for stability analysis of time-delay systems. In [Chen *et al.* 2017a], authors even proved that the integral inequality and its affine version provide an equivalent lower bound for the related integral term.

Lemma 3.12: (Affine Bessel-Legendre Inequality(from [Lee *et al.* 2018])) Let $x(s) \mid s \in [a, b] \rightarrow \mathbb{R}^{n_x}$ be a continuous function. Then, for a non-negative integer N , a positive integer c , an arbitrary vector $\zeta \in \mathbb{R}^{cn_x}$, $R \in \mathbb{S}_+^{n_x}$, and a matrix $F \in \mathbb{R}^{cn_x \times (N+1)n_x}$ with appropriate dimensions, the following inequality holds:

$$-\int_a^b \dot{x}^T(s) R \dot{x}(s) ds \leq (b-a) \zeta^T F R_N^{-1} F^T \zeta + \mathbf{He} \{ \zeta^T F \mathbb{L}(a, b) \}, \quad (3.39)$$

where,

$$\begin{aligned} R_N &= \text{diag} \{ R, 3R, \dots, (2N+1)R \}, \\ \mathbb{L}(a, b) &= \text{col} \{ \mathbb{L}_0(a, b), \dots, \mathbb{L}_N(a, b) \}, \\ \mathbb{L}_k(a, b) &= \begin{cases} x(b) - x(a) & \text{if } k = 0 \\ x(b) - (-1)^k x(a) - \sum_{l=1}^k p_l^k \frac{l!}{(b-a)^l} \mathbb{I}_{l-1}(a, b) & \text{for } k \in \mathbb{N} \end{cases}, \\ p_l^k &= (-1)^{l+k} \binom{k}{l} \binom{k+l}{l}, \\ \mathbb{I}_l(a, b) &= \int_a^b \int_{s_1}^b \dots \int_{s_l}^b x(s_{l+1}) ds_{l+1} \dots ds_1. \end{aligned} \quad (3.40)$$

In the preceding discussion we saw that the estimate of the LKF derivative mainly depends on, how integral terms in the LKF derivative are approximated. However, such an estimate sometimes is not enough for a less conservative stability criterion. In both [Zhang *et al.* 2017c] and [Zhang *et al.* 2017a], it has been proven that Wirtinger-based inequality can produce a tighter estimate on the LKF derivative compared to Jensen, but both of these stability criteria are of the same conservatism if the LKF is not augmented.

The choice of LKF in Step 1 is crucial. The key feature of an augmented Lyapunov functional as introduced in [He *et al.* 2005], [Lin *et al.* 2006a] is that it augments some terms in (3.28) such that more information about the delayed states is exploited to enhance the feasibility of derived LMI stability criterion. For example, in [He *et al.* 2005], the first two terms $x^T(t) P x(t)$ and $\int_{t-h(t)}^t x^T(s) Q x(s) ds$ in (3.28) are augmented, respectively, by

$$\begin{bmatrix} x(t) \\ x(t-\bar{h}) \\ \int_{t-\bar{h}}^t x(s) ds \end{bmatrix}^T P \begin{bmatrix} x(t) \\ x(t-\bar{h}) \\ \int_{t-\bar{h}}^t x(s) ds \end{bmatrix}, \int_{t-h(t)}^t \begin{bmatrix} \dot{x}(s) \\ x(s) \end{bmatrix}^T Q \begin{bmatrix} \dot{x}(s) \\ x(s) \end{bmatrix}. \quad (3.41)$$

Recent research such as [Seuret & Gouaisbaut 2018], [Zhang *et al.* 2018a] shows that using an augmented LKF and the N-order Bessel–Legendre inequality indeed can yield a better stability criteria with less conservatism. Some other forms of LKF are also proposed in literature to reduce the sources of conservatism arising due to the choice of the LKF in Step 1, such as, [Ariba & Gouaisbaut 2009], [Park *et al.* 2011a], [Shao & Han 2012], [Seuret *et al.* 2013] and [Fridman 2014a]. The reduction of the conservatism induced by the over-approximations of delay-dependent terms of Step 4, has also been considered by several authors, such as [He *et al.* 2007], [Shao 2009], with [Park *et al.* 2011b], as the most accurate over-approximation of delay-dependent terms.

The research on LKFs for sampled-data LTI systems is still a wide open domain. Currently, an important effort is dedicated to finding better LKFs and better over approximations of the derivatives. Note that providing improvements (in terms of conservatism reduction) at one step usually requires changes at all the others steps. For this reason, the derivation of constructive stability conditions may be quite an elaborate analytical process. We have even observed above that the design of LKFs may not be intuitive, which makes it difficult to identify the source of conservatism of the approach. The employed upper-bounding techniques can sometimes be the cause to introduce heavy conservatism. Thus there are possibilities to improve upon the upper-bounds, that are introduced when checking the sign of the derivative \dot{V} , so as to properly condition the problem in a tunable and solvable way (e.g. tuning non-linear to linear LMI) and propose better LKFs.

3.3.5 Linearly approximated sampled-data system

The ADAS-Driver-Train interaction is certainly a non-linear type. However, the study of stability/stabilisation of sampled-data system with linear model and controller is often easier to address than the non-linear case. For such non-linear sampled-data system, local stability can be deduced from the property of a linearized model around the equilibrium ([Hou *et al.* 1997], [H. & Michel 2000]). Consider the following non-linear system:

$$\begin{aligned} \dot{x}(t) &= F(t, x(t), u(t)), \quad \forall t \geq 0, \\ y(t) &= H(x(t)) \end{aligned} \tag{3.42}$$

with a discrete-time controller:

$$\begin{aligned} x(t_{k+1})^c &= F_d^c(t_k, x(t_k)^c, y(t_k)), \quad \forall t \in [t_k, t_{k+1}), \quad k \in \mathbb{N}, \\ u(t_k) &= H_d^c(x(t_k)^c, y(t_k)), \end{aligned} \tag{3.43}$$

where t is the time-variable, $x : \mathbb{R}^+ \rightarrow \mathbb{R}^{n_x}$ is a measured system "state-trajectory", $u : \mathbb{R}^+ \rightarrow \mathbb{R}^{n_u}$ the "input" or "control signal", and the scalars t_k , for $k \in \mathbb{N}$, monotonically

increasing sequence of positive real numbers that satisfy, $0 = t_0 < t_1 < \dots < t_k < \dots$ and $\lim_{k \rightarrow \infty} t_k = \infty$, and the sampling law is defined as

$$t_{k+1} = t_k + h_k \quad (3.44)$$

where h_k represents the k^{th} sampling interval. The closed-loop system can be represented as a set of equations:

$$\begin{aligned} \dot{x}(t) &= f(t, x(t), x(t_k), x(t_k)^c), \quad \forall t \in [t_k, t_{k+1}), \\ x(t_{k+1})^c &= g(t_k, x(t_k), x(t_k)^c), \quad k \in \mathbb{N}, \end{aligned} \quad (3.45)$$

where, $f(t, x(t), x(t_k), x(t_k)^c) = F(t, x(t), H_d^c(x(t_k)^c, H(x(t_k))))$ and $g(t_k, x(t_k), x(t_k)^c) = F_d^c(t_k, x(t_k)^c, H(x(t_k)))$. For $f(x, v, w)$ and $g(v, w)$, let $A = \frac{\partial f}{\partial x}|_0$, $A_0 = \frac{\partial f}{\partial v}|_0$, $B = \frac{\partial f}{\partial w}|_0$, $C = \frac{\partial g}{\partial v}|_0$ and $D = \frac{\partial g}{\partial w}|_0$. Thus, the system (3.45), can be represented as the following linearised system,

$$\begin{aligned} \dot{x}(t) &= A_0 x(t) + Ax(t_k) + Bx(t_k)^c, \quad \forall t \in [t_k, t_{k+1}), \\ x(t_{k+1})^c &= Cx(t_k)^c + Dx(t_k), \quad k \in \mathbb{N}. \end{aligned} \quad (3.46)$$

Now, integrating the system over a sampling interval and letting $z(t_k)^T = [x(t_k)^T, x(t_k)^{cT}]$ leads to the following linear time-varying discrete-time system,

$$z_{k+1} = \Omega(h_k)z_k, \quad \forall k \in \mathbb{N}, \quad (3.47)$$

with $\Omega(h_k) = \begin{bmatrix} e^{Ah_k}x(t_k) + \int_0^{h_k} e^{As}dsA_0 & \int_0^{h_k} e^{As}dsB \\ D & C \end{bmatrix}$. The following theorem establishes conditions for the stability of the non-linear system (3.45) under arbitrary variations of the sampling interval.

Theorem 3.13: (Time-varying sampling stability (from [H. & Michel 2000]))

Assume that, for every possible sequence $\sigma = \{t_k\}$, $k \in \mathbb{N}$ defined in (3.44), one has $h_k = t_{k+1} - t_k \leq \bar{h}$, and for any $k \in \mathbb{N}$, $\|\Omega(h_k)\|_2 < q < 1$, where h_k and q are constant scalars. Then the equilibrium point $[x^T x^{cT}] = 0$ of system (3.45) is exponentially stable.

The nature of the result is in the spirit of the Lyapunov's first method ([Khalil 2002]), as it permits to guarantee the stability of the equilibrium of the non-linear system, by studying the stability of its linearisation at the origin. In the same way, it remains qualitative and it does not provide any estimate of the domain of attraction. However, the result does not require the sampling intervals to be small.

3.4 Conclusion

This chapter exposed the problem of finding stability of sampled-data LTI systems with time-varying sampling. We addressed the problem by first presenting an overview of

various sampled-data modelling approaches from the literature. Recognising the ability to handle both slow and fast varying delays, we choose to elaborate time-delay approach. We then recalled various tools to study time-delay system stability, but, emphasised on use of time-dependent LKF to derive delay-dependent stability conditions for time-varying sampled LTI systems.

From the literature review to derive delay-dependent stability conditions, it appeared that, integral inequality based approaches are more accurate than model transformation approach to over-approximate integral terms of LKF derivative. Further, among various integral inequalities, the affine Bessel-Legendre inequality is considered better than Wirtinger-based or Jensen inequality. In addition, to derive further less conservative stability condition for sampled-data LTI system, the design of time-dependent LKF by augmented Lyapunov functional was highly recommended.

Thus, in the following chapter, we will introduce the theoretical contributions of the PhD, which will allow us to solve stability of Driver-Train system with sensor measurement delay problem through time-delay based modelling of sampled-data LTI system with time-varying sampling. We intend to propose novel stability criteria for time-varying sampling using the latest development in the field, i.e. use of both affine Bessel-Legendre inequality and Wirtinger-based inequality with augmented Lyapunov-Krasovskii functionals.

Stability of sampled-data systems with time-varying sampling

Contents

| | | |
|------------|---|------------|
| 4.1 | Introduction | 87 |
| 4.2 | Stability of perturbed sampled-data LTI system with a state-feedback control | 91 |
| 4.2.1 | Problem formulation | 91 |
| 4.2.2 | L_2 -stability results | 93 |
| 4.2.3 | Discussions | 100 |
| 4.3 | Stability of perturbed sampled-data LTI system with a neural-network control | 101 |
| 4.3.1 | Problem formulation | 101 |
| 4.3.2 | L_2 -stability results | 104 |
| 4.3.3 | Discussions | 110 |
| 4.4 | Stability of non-linear sampled-data system with neural-network control | 111 |
| 4.4.1 | Problem formulation | 111 |
| 4.4.2 | Exponential stability results | 114 |
| 4.4.3 | Discussion | 120 |
| 4.5 | Algorithm to find maximum sampling period | 121 |
| 4.6 | Conclusion | 122 |

4.1 Introduction

In the previous chapter, several basic concepts and some research directions pertaining to time-delay modelling approach based stability of sampled-data LTI system were presented. It was reasoned that the problem of finding stability of Driver-Train system with aperiodic

sensor measurement can be formulated as time-delay system to benefit from the LKF based delay-dependent techniques in estimation of maximum sensor measurement delay.

However, in order to do that, an appropriate model should be used to represent ADAS-Driver-Train non-linear system. In order to simplify the problem, we focused our study on driver's interaction with ADAS during cruise phase. ADAS takes into consideration input data from the environment, the driver and the train coming in the form of images, speed or position data at different frequency, to generate driver advises in the form of, either audio, visual or haptic modality.

As a first abstraction, we considered a model-based approach for driver and train modelling and used a state-feedback controller to represent ADAS. The driver was modelled as a time-varying compensating system (no anticipation or delays), while the train as a non-linear system with various dynamical resistive forces. The proposed modelling abstraction is as shown in Fig. 4.1. In order to simplify the problem, we considered cruise control scenario and thus linearised the Driver-Train system. Moreover, we considered variation in the driver model parameters to study robustness of closed-loop system stability.

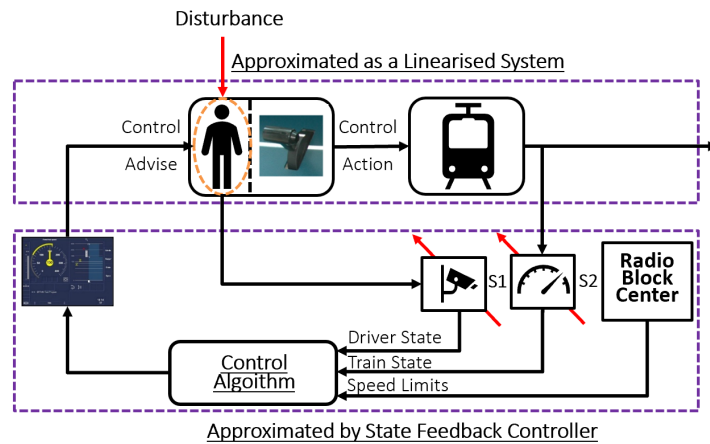


Figure 4.1: Linearised system with state-feedback control

The last few decades have witnessed the use of artificial NN in many real-world applications, [Chiddarwar & Babu 2011]. The literature review also shows a general trend in the study of modelling of driver behaviour, [Gingrich *et al.* 1992], [Zhang *et al.* 2005], [Lin *et al.* 2005], [Khodayari *et al.* 2012], [Wei *et al.* 2013], intelligent train operation, [Yin *et al.* 2014], and even train modelling, [Okamoto & Tsiotras 2019] using application of such artificial intelligence approaches. Recently DNN techniques have also been implemented to predict driver behaviour, [Olabiyi *et al.* 2017], [Kuefler *et al.* 2017], [Phillips *et al.* 2017], [Zyner *et al.* 2018], and to optimise train operation [Wang *et al.* 2019c], and even for train modelling [Li *et al.* 2019], [Yin *et al.* 2019].

In control engineering domain also, NN has found use, both in system identification as non-linear black-box modelling, [Nechyba & Xu 1994] and also in control design, such as classical, [Cong & Liang 2009], optimal [Sahoo & Narayanan 2018], robust [Zhong *et al.* 2013] or even adaptive controller design [Yang *et al.* 2017]. Such a trend is because of the ability of NNs to approximate with some degree of accuracy the non-linear dynamics of systems with unknown governing first principles. Rather NNs address the mathematical modelling problem using only observed I/O data and learning algorithms.

In literature, to meet varying needs of robustness and stability study, several kinds of NN and their corresponding learning algorithms have been proposed [Liu *et al.* 2017]. Particularly, feed-forward, a NN with static I/O mapping schemes that can approximate a continuous function to an arbitrary degree of accuracy, and RNN, a NN with each neuron connected bidirectionally to every other neuron, are popular.

In [Jain *et al.* 2019], these different NN architectures were tested for their efficiency in approximate control computation. Specifically, they were compared with Finite Impulse Response (FIR) filter in generating a jerk-free reference trajectory for a robotic arm. The study suggested that NN outperformed FIR in better complexity/accuracy compromise. Thus, as a second modelling abstraction, for the case of ADAS-Driver-Train system, a NN is considered to generate driving advise depending on driver behaviour dynamics.

The relative easiness of implementation and the accuracy of the obtained results have made feed-forward NN quite popular for both system identification and approximate control computation. Thus, considering the capability of feed-forward NNs to approximate non-linear functions, we proposed the second abstraction as shown in Fig. 4.2, for the closed-loop system stability study.

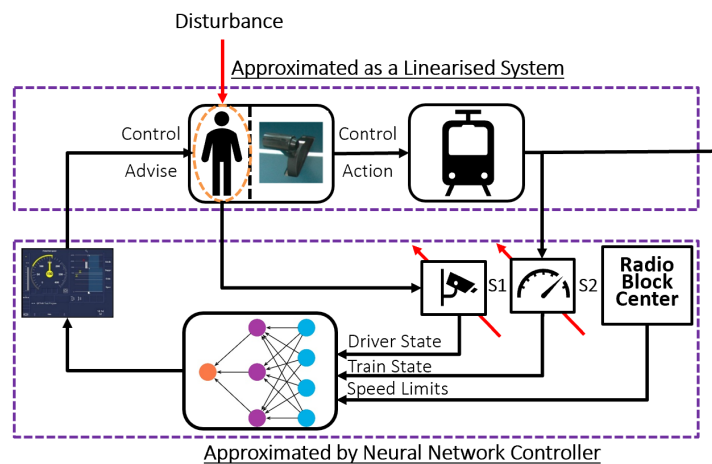


Figure 4.2: Linearised system with NN control

For these two abstractions, we propose to study \mathcal{L}_2 -stability of perturbed sampled-data LTI systems. The \mathcal{L}_2 -stability conditions try to design a ADAS-Driver-Train stable system while limiting the impact of time-delayed measurement of driver behaviour variation. \mathcal{L}_2 -stability is considered over \mathcal{L}_∞ -stability because we are interested in reducing the long-term energy impact rather than the maximum amplitude of the driver behaviour variation. In literature, for \mathcal{L}_2 -stability setting, various techniques have been proposed for stability analysis of both constant and time-varying sampled LTI systems [Kao & Lincoln 2004], [Kao & Rantzer 2007], [Mirkin 2007], [Fujioka 2009b], [Fiter *et al.* 2015].

Although a large amount of works have been presented on stability analysis of time-varying sampled LTI system using convex-embeddings, [Hetel *et al.* 2006], [Hetel *et al.* 2007b], [Fujioka 2009a], [Skaf & Boyd 2009], [Wouw *et al.* 2010], [Donkers *et al.* 2011], [Hetel *et al.* 2011], none of them have included robustness with respect to perturbations while considering a state-feedback or a NN controller in addition to a time-varying gain. In fact, including both the exogenous unknown perturbations and a state-feedback or a NN controller with additional time-varying gain in the stability analysis is not a simple matter.

The chapter is thus organised as follows. In Section 4.2, \mathcal{L}_2 -stability of state-feedback controlled perturbed sampled-data LTI system under time-varying sampling is considered. For this scenario, Section 4.2.1 formulates the problem. Then, Section 4.2.2 provides tools for the robust stability analysis regarding time-varying sampling and presents the \mathcal{L}_2 -stability results. Finally, Section 4.2.3 summarises the contributions in this approach.

Next, in Section 4.3, \mathcal{L}_2 -stability of NN controlled perturbed sampled-data LTI system under time-varying sampling is considered. For this scenario, Section 4.3.1 formulates the problem. Then, Section 4.3.2 provides tools for the robust stability analysis regarding time-varying sampling and presents the \mathcal{L}_2 -stability results. Finally, Section 4.3.3 summarises the contributions in this approach.

The first and second abstractions are simplified approximations of ADAS-Driver-Train system, during a cruise control scenario. However, driver behaviour variation and delay in sensor measurements may happen outside this context. Thus, to better approximate the system, for the third abstraction, we represent Driver-Train dynamics as a T-S time-varying system and ADAS as a NN controller. Then, we studied exponential stability to improve the agility of ADAS-Driver to stabilise the train.

Thus, in Section 4.4, exponential stability of NN controlled non-linear sampled-data systems under time-varying sampling is presented. For this scenario, Section 4.4.1 formulates the problem. Then, Section 4.4.2 provides tools for the exponential stability analysis regarding time-varying sampling and also presents the exponential stability results. Section 4.4.3 summarises the contributions of this approach. In the last Section 4.5, we

present algorithm allowing to find the maximum sampling period \bar{h} offline for the three stability results. Lastly, Section 4.6 presents the chapter's conclusion.

4.2 Stability of perturbed sampled-data LTI system with a state-feedback control

Following the previous discussion, in this section, we consider the first modelling abstraction, i.e. a sampled-data LTI system with a state-feedback controller and a time-varying gain. The gain variation is considered to be bounded by a convex polytope ($K(t) \in Co\{K_1, \dots, K_q\}$). Further, it is considered to vary with an unknown exogenous perturbation, $d(t) \in \mathcal{L}_2$. The stability criteria aims to guarantee robustness with respect to this perturbation. Note that no other assumption is made about the perturbation. In particular, the perturbation is not required to be bounded or state-bounded (i.e. there is no need of a scalar $\delta < 0$ such that $\|d(t)\| \leq \delta$ or $\|d(t)\| \leq \delta\|x(t)\|$). Considering these assumptions, we provide tools to perform robust stability analysis regarding time-varying sampling. For this application, we ensure system's finite-gain \mathcal{L}_2 -stability for given gain γ_1, γ_2 , thanks to Lyapunov-Krasovskii stability conditions and convexification arguments.

4.2.1 Problem formulation

We consider the linear time-invariant system,

$$\left. \begin{aligned} \dot{x}(t) &= Ax(t) + Bu(t) \\ z(t) &= Cx(t) \end{aligned} \right\}, \forall t \geq 0, \quad (4.1)$$

where $x = [x_1, \dots, x_{n_x}]^T \in \mathbb{R}^{n_x}$ is the state vector, $u = [u_1, \dots, u_{n_u}]^T \in \mathbb{R}^{n_u}$ denotes the control input vector, and $z(t) \in \mathbb{R}^{n_z}$ is the controlled output. $A \in \mathbb{R}^{n_x \times n_x}$, $B \in \mathbb{R}^{n_x \times n_u}$, $C \in \mathbb{R}^{n_z \times n_x}$ are known constant system matrices. The control is designed as a piece-wise constant state-feedback multiplied by a time-varying gain (relative to $d(t)$),

$$u(t) = \bar{u}(t) + K(d(t))(G_1x(t_k) + G_2\hat{d}(t_k)), \forall t \in [t_k, t_{k+1}), k \in \mathbb{N}, \quad (4.2)$$

with $d(t), \hat{d}(t_k) \in \mathbb{R}^r$ as the unknown and the estimated exogenous disturbances, $G_1 \in \mathbb{R}^{l \times n_x}$, $G_2 \in \mathbb{R}^{l \times r}$ as state-feedback gains, $K(d(t))$ a time-varying gain (in the next chapter we will use it as a variation in driver behaviour) and with t_k the k^{th} sampling and actuation time. Note that we have considered no delay between the sampling and actuation times. Further, the sequence of sampling times $(t_k)_{k \geq 0}$ is assumed to satisfy $0 = t_0 < t_1 < \dots < t_k < \dots$, $\lim_{k \rightarrow \infty} t_k = \infty$, $0 < t_{k+1} - t_k \leq \bar{h}$, and the sampling law is defined as,

$$t_{k+1} = t_k + h_k, \quad (4.3)$$

with a variable sampling step h_k , that we aim to maximise. Moreover, here we considered the gain $K(d(t))$ to be varying in a convex polytope as,

$$K(d(t)) \in Co\{K_1, \dots, K_q\}, \quad (4.4)$$

with $K_i \in \mathbb{R}^{n_u \times l}$, $\forall i \in \{1, \dots, q\}$. Since $K(d(t))$ varies in a convex polytope, it is represented as,

$$K(d(t)) = \sum_{i=1}^q a_i(d(t))K_i, \quad (4.5)$$

where, $\sum_{i=1}^q a_i(d(t)) = 1$, $a_i(d(t)) \in [0, 1]$, $\forall i \in \{1, \dots, q\}$. We denote S , the closed-loop system $\{(4.1), (4.2), (4.3)\}$ and the corresponding closed-loop schematic as in Fig. 4.3.

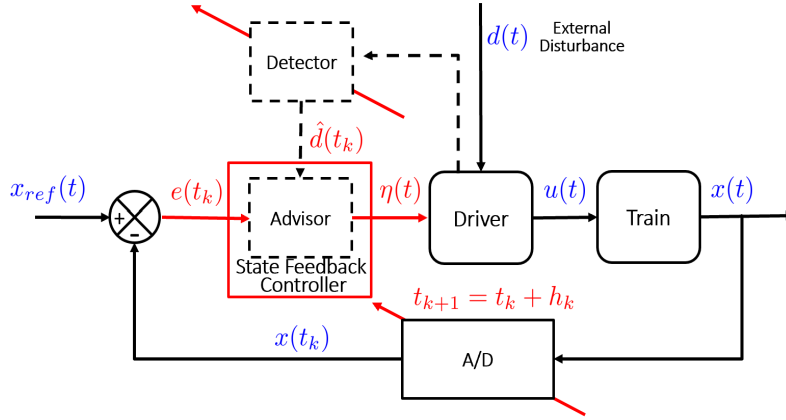


Figure 4.3: Closed-loop system schematic

The closed-loop system can also be rewritten as,

$$\begin{cases} \dot{x}(t) = Ax(t) + BK(d(t))G_1x(t_k) + BK(d(t))G_2w_1(t) + Bw_2(d(t)), \\ z(t) = Cx(t), \end{cases} \quad (4.6)$$

with $t_k \leq t < t_{k+1}$, $k \in \mathbb{N}$, $w_1(t) = \hat{d}(t_k) - d_{nom}$ and $w_2(d(t)) = (K(d(t)) - K_{nom})G_2d_{nom}$ as small perturbations. Note, here d_{nom} and K_{nom} are nominal value of exogenous disturbance and its corresponding nominal gain. In this modelling abstraction, due to the unknown exogenous disturbance $w_1(t)$ and $w_2(d(t))$ (a refinement of $d(t)$), the system S is studied from \mathcal{L}_2 -stability point of view, which is recalled in the following definition.

Definition 4.1: (from [Fridman 2010]) A linear system F is said to be finite-gain \mathcal{L}_2 -stable from w to Fw with an induced gain less than γ , if F is a linear operator from \mathcal{L}_2 to \mathcal{L}_2 and if there exist positive real constants γ and η such that for all $w \in \mathcal{L}_2$,

$$\|Fw\|_{\mathcal{L}_2} \leq \gamma\|w\|_{\mathcal{L}_2} + \eta. \quad (4.7)$$

The work in the present section aims at estimating maximum sampling period, \bar{h} , with $t_{k+1} - t_k \leq \bar{h}$, while ensuring the finite-gain \mathcal{L}_2 -stability of S from $w_1(t) \rightarrow z(t)$ and $w_2(d(t)) \rightarrow z(t)$, with a gain less than a fixed $\gamma_1 \geq 0$ and $\gamma_2 \geq 0$ respectively. To this aim, we will use the following lemma:

Lemma 4.2: (Adapted from [Fridman 2010]) Assume that there exist real constants $\gamma_1, \gamma_2 \geq 0$ and a positive continuous function $V : t \in \mathbb{R}^+ \rightarrow V(t) \in \mathbb{R}^+$, differentiable for all $t \neq t_k, k \in \mathbb{N}$ that satisfy,

$$\dot{V}(t) + z^T(t)z(t) - \gamma_1 w_1^T(t)w_1(t) - \gamma_2 w_2^T(t)w_2(t) \leq 0, \quad (4.8)$$

along S . Then, S is \mathcal{L}_2 -stable from $w_1(t) \rightarrow z(t)$ and $w_2(t) \rightarrow z(t)$ with gain less than γ_1 and γ_2 respectively.

Proof: Let $t \gg 0$ and $k \in \mathbb{N}$ such that $t \in [t_k, t_{k+1})$. Integrating (4.8) over $[0, t]$ gives

$$\begin{aligned} & V(t) - V(t_k) + V(t_k^-) - V(t_{k-1}) + \dots + V(t_0^-) - V(0) \\ & + \int_0^t [z(s)^T z(s) - \gamma_1 w_1(s)^T w_1(s) - \gamma_2 w_2(s)^T w_2(s)] ds \leq 0. \end{aligned}$$

Since $V(t) \geq 0$ and $V(t_k) = V(t_k^-)$ for all $k \in \mathbb{N}$ (V is assumed to be continuous), we get:

$$\int_0^t z(s)^T z(s) ds \leq \gamma_1 \int_0^t w_1(s)^T w_1(s) ds + \gamma_2 \int_0^t w_2(s)^T w_2(s) ds + V(0).$$

Using the positivity of $z(s)^T z(s)$, one can show that $z(s) = Sw_1(s) \in \mathcal{L}_2$, $z(s) = Sw_2(s) \in \mathcal{L}_2$, and by having $t \rightarrow \infty$, one can see that \mathcal{L}_2 -stability conditions (4.7) is satisfied with $\eta = \sqrt{V(0)}$.

Our objective in this section is to compute largest sampling interval \bar{h} while ensuring the expected \mathcal{L}_2 -stability for a fixed $\gamma_1, \gamma_2 \geq 0$. We will thus provide a *stability analysis* of the system for a given state-feedback gain G_1, G_2 , and a convex polytope for time-varying gain $K(d(t))$. All these studies are based on a quite general class of LKF, based on Wirtinger inequality, which take into account the delays (in the case of delayed systems), the perturbations and the sampling (the maximum sampling period \bar{h} dependent terms).

4.2.2 L_2 -stability results

In this subsection, we propose stability analysis of system S with a given state-feedback gain G_1, G_2 , a convex polytope for time-varying gain $K(d(t))$ and a sampling (4.3).

4.2.2.1 Stability analysis of the perturbed sampled-data LTI system

We consider the following LKF, which depends on, the actual state $x(t)$, the sampled-state $x(t_k)$, the delayed state x_t and the delayed state derivative \dot{x}_t (defined for a maximum

sampling period \bar{h} as $x_t(\theta) = x(t + \theta)$, $\dot{x}_t(\theta) = \dot{x}(t + \theta)$, $\forall \theta \in [-\bar{h}, 0]$:

$$\begin{aligned} V(t, x(t), x_t, \dot{x}_t, k) = & x(t)^T P x(t) + \int_{t_k}^t x(s)^T Q x(s) ds + (t_{k+1} - t) \int_{t_k}^t \dot{x}(s)^T Z \dot{x}(s) ds \\ & + \bar{h}^2 \int_{t_k}^t \dot{x}(s)^T U \dot{x}(s) ds - \frac{\pi^2}{4} \int_{t_k}^t (x(s) - x(t_k))^T U (x(s) - x(t_k)) ds \\ & + (t_{k+1} - t) \begin{bmatrix} x(t) \\ x(t_k) \end{bmatrix}^T \Omega \begin{bmatrix} x(t) \\ x(t_k) \end{bmatrix}, \end{aligned} \quad (4.9)$$

defined for all $t \in [t_k, t_{k+1})$ and $k \in \mathbb{N}$, with matrix Ω defined as:

$$\Omega = \begin{bmatrix} \frac{X+X^T}{2} & -X + X_1 \\ * & -X_1 - X_1^T + \frac{X+X^T}{2} \end{bmatrix}, \quad (4.10)$$

where, matrices $P, Q, Z, U \in \mathbb{S}_+^{n_x}$ and $X, X_1 \in \mathbb{R}^{n_x \times n_x}$ are of appropriate dimensions.

The new aspect of LKF (4.9) compared to previous works, [Naghshabrizi *et al.* 2008], [Fridman 2010], [Jiang & Seuret 2010], [Jiang *et al.* 2010], [Seuret 2012], on systems with time-varying samplings, is the fact that it involves the application of the Wirtinger inequality [Hardy *et al.* 1934]. The functional V is time-dependent, i.e. continuous over the the sampling interval $t \in [t_k, t_{k+1})$, but it is discontinuous at times t_k as:

$$\begin{aligned} \lim_{t \rightarrow t_k^-} V(t, x(t), x_t, \dot{x}_t, k-1) = & x^T(t_k) P x(t_k) + \int_{t_{k-1}}^{t_k} x(s)^T Q x(s) ds \\ & + \bar{h}^2 \int_{t_{k-1}}^{t_k} \dot{x}(s)^T U \dot{x}(s) ds - \frac{\pi^2}{4} \int_{t_{k-1}}^{t_k} (x(s) - x(t_k))^T U (x(s) - x(t_k)) ds \end{aligned}, \quad (4.11)$$

$$\text{and} \quad \lim_{t \rightarrow t_k^+} V(t_k, x(t_k), x_{t_k}, \dot{x}_{t_k}, k) = x^T(t_k) P x(t_k). \quad (4.12)$$

Note that, this is because \bar{V} has two discontinuous term $\int_{t_k}^t x(s)^T Q x(s) ds$ and $\bar{h}^2 \int_{t_k}^t \dot{x}(s)^T U \dot{x}(s) ds - \frac{\pi^2}{4} \int_{t_k}^t (x(s) - x(t_k))^T U (x(s) - x(t_k)) ds$. These terms do not increase along the jumps at t_k , but actually vanish. Thus inequality $\lim_{t \rightarrow t_k^-} V(t, x(t), x_t, \dot{x}_t, k) \geq V(t_k, x(t_k), x_{t_k}, \dot{x}_{t_k}, k)$ holds. This new LKF is well adapted to the stability analysis of systems with time-varying sampling. In the following, as in [Fridman 2010], we denote

$$\bar{V}(t) = V(t, x(t), x_t, \dot{x}_t, k) \text{ for all } t \in [t_k, t_{k+1}), k \in \mathbb{N}. \quad (4.13)$$

The \mathcal{L}_2 -stability analysis is based on Lemma 4.2 and is divided into two main steps.

- First, we prove that \bar{V} is continuous over $\mathbb{R}^+ \setminus \{t_k, k \in \mathbb{N}\}$ and differentiable for all $t \in [t_k, t_{k+1})$, and provide conditions for its positive definiteness.
- Then, we differentiate \bar{V} , upper-bound the obtained result and derive the \mathcal{L}_2 -stability conditions.

4.2.2.2 LKF's required properties

To begin with, we propose the following lemma, which ensures LKF functional's continuity, piece-wise differentiability, and positivity conditions.

Lemma 4.3: The function \bar{V} defined in (4.13) is continuous over $\mathbb{R}^+ \setminus \{t_k, k \in \mathbb{N}\}$ and differentiable for all $t \neq t_k, k \in \mathbb{N}$. If its matrix parameters satisfy $P, Q, Z, U \in \mathbb{S}_+^{n_x}$, $X, X_1 \in \mathbb{R}^{n_x \times n_x}$ and

$$\left[\begin{array}{c} \left[\begin{array}{cc} P & 0 \\ 0 & 0 \end{array} \right] + \bar{h}\Omega \end{array} \right] \succ 0, \quad (4.14)$$

then \bar{V} is also positive definite, and there exists scalar $\beta > 0$ such that $\bar{V} \geq \beta \|x(t)\|^2$ for all $t \geq 0$.

Proof: \bar{V} is defined on \mathbb{R}^+ , differentiable over each time interval $[t_k, t_{k+1})$, and is designed to satisfy,

$$\begin{aligned} \bar{V}(t_k^-) = \lim_{t \rightarrow t_k^-} \bar{V}(t) = & x(t_k)^T P x(t_k) + \int_{t_{k-1}}^{t_k} x(s)^T Q x(s) ds \\ & + \bar{h}^2 \int_{t_{k-1}}^{t_k} \dot{x}(s)^T U \dot{x}(s) ds \\ & - \frac{\pi^2}{4} \int_{t_{k-1}}^{t_k} (x(s) - x(t_k))^T U (x(s) - x(t_k)) ds \end{aligned} \quad (4.15)$$

and $\bar{V}(t_k^+) = \lim_{t \rightarrow t_k^+} \bar{V}(t) = x(t_k)^T P x(t_k)$ for all $k \in \mathbb{N}$. It is therefore continuous and differentiable over $\mathbb{R}^+ \setminus \{t_k, k \in \mathbb{N}\}$. Now, we can say that \bar{V} is positive definite if, and only if, for all $k \in \mathbb{N}, t \in [t_k, t_{k+1})$:

$$\begin{bmatrix} x(t) \\ x(t_k) \end{bmatrix}^T \left[\begin{array}{c} \left[\begin{array}{cc} P & 0 \\ 0 & 0 \end{array} \right] + (t_{k+1} - t)\Omega \end{array} \right] \begin{bmatrix} x(t) \\ x(t_k) \end{bmatrix} \geq 0, \quad (4.16)$$

with equality if and only if $x(t) = x(t_k) = 0$,

$$\int_{t_k}^t x(s)^T Q x(s) ds + (t_{k+1} - t) \int_{t_k}^t \dot{x}(s)^T Z \dot{x}(s) ds \geq 0, \quad (4.17)$$

$$\text{and} \quad \bar{h}^2 \int_{t_k}^t \dot{x}(s)^T U \dot{x}(s) ds - \frac{\pi^2}{4} \int_{t_k}^t (x(s) - x(t_k))^T U (x(s) - x(t_k)) ds \geq 0. \quad (4.18)$$

Note that equation (4.18) can be shown to be the extension of the vector case of Wirtinger inequality [Liu *et al.* 2010] (see Theorem A.2 in Appendix A). Further as, $0 \leq t_{k+1} - t \leq \bar{h}$, remarking that the right part of (4.17) and the middle matrix term in the right part of (4.16) is linear with respect to $\rho = t_{k+1} - t$, one can use Theorem A.3 (in the Appendix A) and show that a sufficient condition for \bar{V} to be positive definite is that, for all $k \in \mathbb{N}, t \in [t_k, t_{k+1})$:

$$x(t)^T P x(t) > 0, \text{ for all } x(t) \neq 0 \quad (4.19)$$

and
$$\begin{bmatrix} x(t) \\ x(t_k) \end{bmatrix}^T \left[\begin{bmatrix} P & 0 \\ 0 & 0 \end{bmatrix} + \bar{h}\Omega \right] \begin{bmatrix} x(t) \\ x(t_k) \end{bmatrix} \geq 0, \text{ for all } \begin{bmatrix} x(t) \\ x(t_k) \end{bmatrix} \neq 0. \quad (4.20)$$

The condition (4.20) is ensured by assuming that P is positive definite. Furthermore, if $P \succ 0$, then there exists scalar $\beta > 0$, such that for all $k \in \mathbb{N}$ and $t \in [t_k, t_{k+1})$, $\left[\begin{bmatrix} P & 0 \\ 0 & 0 \end{bmatrix} + \bar{h}\Omega \right] \succ \beta \begin{bmatrix} I & 0 \\ 0 & 0 \end{bmatrix}$. Thus, $\bar{V}(t) \geq \beta \|x(t)\|^2$, for all $t \in [t_k, t_{k+1})$, $\forall k \in \mathbb{N}$. Therefore, there exists a scalar β , such that $\bar{V}(t) \geq \beta \|x(t)\|^2$ for all $t \geq 0$, which ends the proof. \square

4.2.2.3 L_2 -stability conditions

Having proposed conditions to ensure \bar{V} 's continuity, differentiability, and positivity, now, in order to analyse the \mathcal{L}_2 -stability of system S , we will refer to Lemma 4.2. The lemma is needed to provide conditions to satisfy

$$\dot{\bar{V}}(t) + z^T(t)z(t) - \gamma_1 w_1^T(t)w_1(t) - \gamma_2 w_2^T(d(t))w_2(d(t)) \leq 0, \forall t \neq t_k, \forall k \in \mathbb{N}. \quad (4.21)$$

In order to analyse this \mathcal{L}_2 -stability condition, we study the restriction of $\dot{\bar{V}}$ on any interval $[t_k, t_{k+1})$, $k \in \mathbb{N}$. We compute

$$\begin{aligned} \dot{\bar{V}}(t) = & \mathbf{He} \{x(t)^T P \dot{x}(t)\} + x(t)^T Q x(t) + (t_{k+1} - t) \dot{x}(t)^T Z \dot{x}(t) \\ & - \int_{t_k}^t \dot{x}(s)^T Z \dot{x}(s) ds + \bar{h}^2 \dot{x}(t)^T U \dot{x}(t) - \frac{\pi^2}{4} \begin{bmatrix} x(t) \\ x(t_k) \end{bmatrix}^T \begin{bmatrix} U & -U \\ * & U \end{bmatrix} \begin{bmatrix} x(t) \\ x(t_k) \end{bmatrix} \\ & - \begin{bmatrix} x(t) \\ x(t_k) \end{bmatrix}^T \Omega \begin{bmatrix} x(t) \\ x(t_k) \end{bmatrix} + (t_{k+1} - t) \mathbf{He} \left\{ \begin{bmatrix} x(t) \\ x(t_k) \end{bmatrix}^T \Omega \begin{bmatrix} \dot{x}(t) \\ 0 \end{bmatrix} \right\}. \end{aligned} \quad (4.22)$$

Using the Jensen inequality [Gu *et al.* 2003] (see Theorem A.1 in Appendix A), we compute an upper-bound of the integral term:

$$- \int_{t_k}^t \dot{x}(s)^T Z \dot{x}(s) ds \leq -(t - t_k) v_1(t)^T Z v_1(t), \quad (4.23)$$

with,
$$v_1(t) = \frac{1}{(t - t_k)} \int_{t_k}^t \dot{x}(s)^T ds = \frac{x(t) - x(t_k)}{t - t_k}. \quad (4.24)$$

Here, $v_1(t)$ is well defined by continuity in $t = t_k$, as when $t \rightarrow t_k$, $v_1(t) \rightarrow \dot{x}(t_k)$.

Using majoration (4.23) in $\dot{V}(t)$, equation (4.22) leads to,

$$\begin{aligned}
 & \dot{V}(t) + z^T(t)z(t) - \gamma_1 w_1^T(t)w_1(t) - \gamma_2 w_2^T(d(t))w_2(d(t)) \leq \mathbf{He} \{x(t)^T P \dot{x}(t)\} \\
 & + x(t)^T Q x(t) + z^T(t)z(t) - \gamma_1 w_1^T(t)w_1(t) - \gamma_2 w_2^T(d(t))w_2(d(t)) + (t_{k+1} - t)\dot{x}(t)^T Z \dot{x}(t) \\
 & - (t - t_k)v_1(t)^T Z v_1(t) + \bar{h}^2 \dot{x}(t)^T U \dot{x}(t) - \frac{\pi^2}{4} \begin{bmatrix} x(t) \\ x(t_k) \end{bmatrix}^T \begin{bmatrix} U - U \\ * \quad U \end{bmatrix} \begin{bmatrix} x(t) \\ x(t_k) \end{bmatrix} \\
 & - \begin{bmatrix} x(t) \\ x(t_k) \end{bmatrix}^T \Omega \begin{bmatrix} x(t) \\ x(t_k) \end{bmatrix} + (t_{k+1} - t) \mathbf{He} \left\{ \begin{bmatrix} x(t) \\ x(t_k) \end{bmatrix}^T \Omega \begin{bmatrix} \dot{x}(t) \\ 0 \end{bmatrix} \right\}.
 \end{aligned} \tag{4.25}$$

Further we apply the descriptor method from [Fridman 2010]. In order to do so, we consider equalities (4.26) and (4.27),

$$0 = \mathbf{He} \{ [x(t)^T Y_1^T + \dot{x}^T(t) Y_2^T + x(t_k)^T T^T] [-x(t) + x(t_k) + (t - t_k)v_1(t)] \}, \tag{4.26}$$

$$\begin{aligned}
 0 = \mathbf{He} \{ & [x(t)^T P_2^T + \dot{x}(t)^T P_3^T] \times \\
 & [-\dot{x}(t) + Ax(t) + BK(d(t))G_1 x(t_k) + BK(d(t))G_2 w_1(t) + Bw_2(d(t))] \},
 \end{aligned} \tag{4.27}$$

with some $n_x \times n_x$ arbitrary matrices P_2 , P_3 , Y_1 , Y_2 and T . These equalities are added to the right hand side of equation (4.25). The purpose is to get the system dynamics into the Lyapunov condition and consider $\dot{x}(t)$ in the extended state vector. Thus,

$$\begin{aligned}
 & \dot{V}(t) + z^T(t)z(t) - \gamma_1 w_1^T(t)w_1(t) - \gamma_2 w_2^T(d(t))w_2(d(t)) \leq \mathbf{He} \{x(t)^T P \dot{x}(t)\} \\
 & + x(t)^T Q x(t) + z^T(t)z(t) - \gamma_1 w_1^T(t)w_1(t) - \gamma_2 w_2^T(d(t))w_2(d(t)) + (t_{k+1} - t)\dot{x}(t)^T Z \dot{x}(t) \\
 & - (t - t_k)v_1(t)^T Z v_1(t) + \bar{h}^2 \dot{x}(t)^T U \dot{x}(t) - \frac{\pi^2}{4} \begin{bmatrix} x(t) \\ x(t_k) \end{bmatrix}^T \begin{bmatrix} U - U \\ * \quad U \end{bmatrix} \begin{bmatrix} x(t) \\ x(t_k) \end{bmatrix} \\
 & - \begin{bmatrix} x(t) \\ x(t_k) \end{bmatrix}^T \Omega \begin{bmatrix} x(t) \\ x(t_k) \end{bmatrix} + (t_{k+1} - t) \mathbf{He} \left\{ \begin{bmatrix} x(t) \\ x(t_k) \end{bmatrix}^T \Omega \begin{bmatrix} \dot{x}(t) \\ 0 \end{bmatrix} \right\} \\
 & + \mathbf{He} \{ [x(t)^T Y_1^T + \dot{x}^T(t) Y_2^T + x(t_k)^T T^T] [-x(t) + x(t_k) + (t - t_k)v_1(t)] \} \\
 & + \mathbf{He} \{ [x(t)^T P_2^T + \dot{x}(t)^T P_3^T] \times \\
 & [-\dot{x}(t) + Ax(t) + BK(d(t))G_1 x(t_k) + BK(d(t))G_2 w_1(t) + Bw_2(d(t))] \}.
 \end{aligned} \tag{4.28}$$

Let us now introduce the augmented state vector $\zeta(t) \in \mathbb{R}^{4n_x + n_{w_1} + n_{w_2}}$:

$$\zeta(t) = [x^T(t), x^T(t_k), v_1^T(t), \dot{x}^T(t), w_1^T(t), w_2^T(d(t))]. \tag{4.29}$$

Then, by considering $K(d(t))$ to be in the convex polytope as in (4.5), there exist matrices

$M_i^{(0)}$, $M^{(1)}$ and $M^{(2)}$ for all $i \in \{1, \dots, q\}$ such that:

$$M_i^{(0)} = \begin{bmatrix} M_{i,A}^{(0)} & M_{i,B}^{(0)} & 0 & M_{i,C}^{(0)} & M_{i,D}^{(0)} & M_{i,E}^{(0)} \\ * & M_{i,F}^{(0)} & 0 & M_{i,G}^{(0)} & 0 & 0 \\ * & * & 0 & 0 & 0 & 0 \\ * & * & * & M_{i,H}^{(0)} & M_{i,I}^{(0)} & M_{i,J}^{(0)} \\ * & * & * & * & -\gamma_1 I & 0 \\ * & * & * & * & * & -\gamma_2 I \end{bmatrix}, \quad (4.30)$$

$$M^{(1)} = \begin{bmatrix} 0 & 0 & 0 & M_A^{(1)} & 0 & 0 \\ * & 0 & 0 & M_B^{(1)} & 0 & 0 \\ * & * & 0 & 0 & 0 & 0 \\ * & * & * & Z & 0 & 0 \\ * & * & * & * & 0 & 0 \\ * & * & * & * & * & 0 \end{bmatrix}, \quad (4.31)$$

$$M^{(2)} = \begin{bmatrix} 0 & 0 & Y_1^T & 0 & 0 & 0 \\ * & 0 & T^T & 0 & 0 & 0 \\ * & * & -Z & Y_2 & 0 & 0 \\ * & * & * & 0 & 0 & 0 \\ * & * & * & * & 0 & 0 \\ * & * & * & * & * & 0 \end{bmatrix}, \quad (4.32)$$

with,

$$\begin{aligned} M_{i,A}^{(0)} &= Q - \frac{\pi^2}{4}U - \frac{X+X^T}{2} + P_2^T A + A^T P_2 - Y_1 - Y_1^T + C^T C, \\ M_{i,B}^{(0)} &= \frac{\pi^2}{4}U - (-X + X_1) + P_2^T B K_i G_1 + Y_1^T - T, \\ M_{i,C}^{(0)} &= P - P_2^T - Y_2 + A^T P_3, \\ M_{i,D}^{(0)} &= P_2^T B K_i G_2, \\ M_{i,E}^{(0)} &= P_2^T B, \\ M_{i,F}^{(0)} &= -\frac{\pi^2}{4}U - (-X_1 - X_1^T + \frac{X+X^T}{2}) + T^T + T, \\ M_{i,G}^{(0)} &= Y_2 + G_1^T K_i^T B^T P_3, \\ M_{i,H}^{(0)} &= \bar{h}^2 U - P_3^T - P_3, \\ M_{i,I}^{(0)} &= P_3^T B K_i G_2, \\ M_{i,J}^{(0)} &= P_3^T B, \\ M_A^{(1)} &= \frac{X+X^T}{2}, \\ M_B^{(1)} &= (-X + X_1)^T. \end{aligned}$$

Using these matrix notation, we can rewrite (4.28) as,

$$\begin{aligned} & \dot{V}(t) + z^T(t)z(t) - \gamma_1 w_1^T(t)w_1(t) - \gamma_2 w_2^T(d(t))w_2(d(t)) \\ & \leq \sum_{i=1}^q a_i(d(t))\zeta(t)^T M_i^{(0)} \zeta(t) + (t_{k+1} - t)\zeta(t)^T M^{(1)} \zeta(t) + (t - t_k)\zeta(t)^T M^{(2)} \zeta(t). \end{aligned} \quad (4.33)$$

Since $\sum_{i=1}^q a_i(d(t)) = 1$, $a_i(d(t)) \in [0, 1]$, $\forall i \in \{1, \dots, q\}$, equation (4.33) can be rewritten as:

$$\begin{aligned} & \dot{V}(t) + z^T(t)z(t) - \gamma_1 w_1^T(t)w_1(t) - \gamma_2 w_2^T(d(t))w_2(d(t)) \\ & \leq \sum_{i=1}^q a_i(d(t)) \left[\zeta(t)^T M_i^{(0)} \zeta(t) + (t_{k+1} - t) \zeta(t)^T M^{(1)} \zeta(t) + (t - t_k) \zeta(t)^T M^{(2)} \zeta(t) \right], \\ & \leq \sum_{i=1}^q a_i(d(t)) \left[\zeta(t)^T \left[M_i^{(0)} + (t_{k+1} - t)M^{(1)} + (t - t_k)M^{(2)} \right] \zeta(t) \right]. \end{aligned} \quad (4.34)$$

Since equation (4.34) is linear in the variable t , it is possible to reduce the number of conditions to be checked to a finite number by applying Theorem A.3 (in the Appendix A), with the variable $\rho = t \in [t_k, t_{k+1})$. Then, the two obtained inequalities are both linear in the variable $t_{k+1} - t_k$. Thus we can use once again Theorem A.3 (in the Appendix A) with the variable $\rho = t_{k+1} - t_k \in [0, \bar{h}]$ to prove that if the four inequalities $\zeta(t)^T \Xi_i \zeta(t) \preceq 0$ are satisfied for all $\zeta(t) \in \mathbb{R}^{4n_x + n_{w_1} + n_{w_2}}$ and $i \in \{1, \dots, q\}$, with Ξ_i defined as

$$\Xi_i = \begin{cases} M_i^{(0)}, \\ M_i^{(0)} + \bar{h}M^{(1)}, \\ M_i^{(0)} + \bar{h}M^{(2)}, \\ M_i^{(0)} + \bar{h}M^{(1)} + \bar{h}M^{(2)}, \end{cases} \quad (4.35)$$

then, $\dot{V}(t) + \|z(t)\|^2 - \gamma_1 \|w_1(t)\|^2 - \gamma_2 \|w_2(d(t))\|^2 \leq 0$ for all $t \in [t_k, t_{k+1})$, $k \in \mathbb{N}$. Note that we considered any sampling sequence $h_k = t_{k+1} - t_k \in [0, \bar{h}]$. Therefore, the \mathcal{L}_2 -stability results we obtained will be valid for any sampling sequence satisfying (4.3). Further, since we have shown that $\dot{V}(t) \leq -\|z(t)\|^2 + \gamma_1 \|w_1(t)\|^2 + \gamma_2 \|w_2(d(t))\|^2$ for all $t \in [t_k, t_{k+1})$, $k \in \mathbb{N}$, if we have $V(t_0) = 0$, we find

$$\int_{t_0}^t [z(t)^T z(t) - \gamma_1 w_1(t)^T w_1(t) - \gamma_2 w_2(d(t))^T w_2(d(t))] dt < 0. \quad (4.36)$$

Therefore, we will have the following theorem.

Theorem 4.4: Consider scalars $\gamma_1, \gamma_2 > 0$ with matrices $G_1 \in \mathbb{R}^{l \times n_x}, G_2 \in \mathbb{R}^{l \times r}$, $K_i \in \mathbb{R}^{n_u \times l}$, $i \in \{1, \dots, q\}$ and a maximum sampling interval \bar{h} . Then, the perturbed system S is finite-gain \mathcal{L}_2 -stable from $w_1(t) \rightarrow z(t)$ and $w_2(d(t)) \rightarrow z(t)$ with \mathcal{L}_2 gain less than γ_1 and γ_2 respectively, for any sampling sequence satisfying (4.3), if there exist matrices $P, Q, Z, U \in \mathbb{S}_+^{n_x}$ and arbitrary matrices $X, X_1, Y_1, Y_2, T, P_2, P_3 \in \mathbb{R}^{n_x \times n_x}$ such that (4.20) and (4.35) satisfy, for all $i \in \{1, \dots, q\}$.

Remark 4.5: if w_1 and w_2 satisfies $z^T(t)z(t) - \gamma_1 w_1^T(t)w_1(t) - \gamma_2 w_2^T(d(t))w_2(d(t)) \geq 0$, and if the LMIs (4.35) are strict, the sampled-data system S is asymptotically stable for any sampling sequence satisfying (4.3). Indeed, in such a case, \dot{V} is negative definite and there is a $\beta > 0$ such that $\bar{V}(t) \geq \beta \|x(t)\|^2$ for all $t \geq 0, k \in \mathbb{N}$ and $x(t) \in \mathbb{R}^{n_x}$. In the

unperturbed case, $d(t) = d_{nom} = 0$ and $K(d(t)) = K_{nom}$, thus, we get $w_1(t) = 0$ and $w_2(d(t)) = 0$. In this case, it is sufficient to verify that $\dot{V}(t) < 0$, and thus the term $z^T(t)z(t) = \gamma_1 w_1^T(t)w_1(t) + \gamma_2 w_2^T(d(t))w_2(d(t))$ and the rows/columns corresponding to $w_1(t)$ and $w_2(d(t))$ are removed from the LMIs (4.35).

Remark 4.6: When searching for solutions of LMIs (4.20) and (4.35), one needs to remove the zero rows/columns that may appear in (4.35) since LMI solvers search for strict solutions. Indeed, one can see that $M_i^{(0)}$ and $M^{(1)}$ in Ξ_i are independent of v_1 .

4.2.3 Discussions

In this section we proposed a stability analysis allowing to estimate maximum sampling period, \bar{h} while ensuring \mathcal{L}_2 -stability for perturbed sampled-data LTI with a state-feedback controller. The study was based on a new class of LKF involving application of Wirtinger inequality. The application of Wirtinger inequality was advantageous in over-approximating the integral term and eventually maximising the time-varying sampling interval \bar{h} while ensuring the system \mathcal{L}_2 -stability.

Nevertheless, in the literature review presented in the last chapter, it was positively argued that the application of canonical Bessel-Legendre inequality can provide a better lower bound for the over-approximation of the integral terms and also a larger maximum sampling interval, \bar{h} . This was owing to the fact that the canonical Bessel-Legendre inequality can provide a generic and expandable integral inequality which is asymptotically (in the sense that $N \rightarrow \infty$) not conservative.

In recent years, however, most researchers focused only on its special cases, such as $N = 1$, [Seuret & Gouaisbaut 2013] and $N = 2$ [Park *et al.* 2015b]. It is proven in [Zhang *et al.* 2017a] that a tighter bound of the integral term in the LKF derivative is not the solely responsible, for deriving a less conservative stability criterion. Nevertheless, in recent research such as [Seuret & Gouaisbaut 2018], [Zhang *et al.* 2018a], it was proved that by using an augmented LKF plus the N-order Bessel-Legendre inequality indeed can yield stability criteria with less conservatism and higher maximum sampling period, \bar{h} .

Furthermore, we realised a state-feedback based explicit modelling of ADAS is far from reality. Thus, to better approximate ADAS behaviour and improve upon our ADAS model, we sought use of artificial intelligence based approach. This lead us to propose a NN form of driver advisor. Recognising the ease of implementation, approximate control computation accuracy, ability to model non-deterministic and highly non-linear dynamic systems and robust training methods, we considered feed-forward NN controller.

A NN controlled perturbed sampled-data LTI system gave us the opportunity to improve results from previous modelling abstraction, to maximise sampling period h_k while

maintaining \mathcal{L}_2 -stability of the closed-loop system with respect to exogenous disturbance $d(t)$. Considering the above arguments, in the next section, we will be presenting new \mathcal{L}_2 -stability results for a NN controlled perturbed sampled-data LTI system by considering an augmented LKF with $N = 2$, Bessel-Legendre inequality and convexity arguments.

4.3 Stability of perturbed sampled-data LTI system with a neural-network control

4.3.1 Problem formulation

We again consider a linear time-invariant system,

$$\left. \begin{aligned} \dot{x}(t) &= Ax(t) + Bu(t) \\ z(t) &= Cx(t) \end{aligned} \right\}, \forall t \geq 0, \quad (4.37)$$

where $x = [x_1, \dots, x_{n_x}]^T \in \mathbb{R}^{n_x}$ is the state vector, $u = [u_1, \dots, u_{n_u}]^T \in \mathbb{R}^{n_u}$ denotes the control input vector, and $z(t) \in \mathbb{R}^{n_z}$ is the controlled output. $A \in \mathbb{R}^{n_x \times n_x}$, $B \in \mathbb{R}^{n_x \times n_u}$, $C \in \mathbb{R}^{n_z \times n_x}$ are known constant system matrices. However, the control is designed as a piece-wise constant three layer fully-connected feed-forward neural-network (TLFCFFNN) based controller multiplied by a time-varying gain as follows.

$$u(t) = \bar{u}(t) + K(d(t))\eta(t_k), \quad \forall t \in [t_k, t_{k+1}), \quad k \in \mathbb{N}, \quad (4.38)$$

with $d(t)$, $\hat{d}(t_k) \in \mathbb{R}^r$ as the unknown and the estimated exogenous disturbance, $K(d(t))$ a time-varying gain, $\eta(t_k)$ is the NN control and with t_k the k^{th} sampling and actuation time. Further, the sequence of sampling times $(t_k)_{k \geq 0}$ is assumed to satisfy $0 = t_0 < t_1 < \dots < t_k < \dots$, $\lim_{k \rightarrow \infty} t_k = \infty$, $0 < t_{k+1} - t_k \leq \bar{h}$, and the sampling law is defined as,

$$t_{k+1} = t_k + h_k, \quad (4.39)$$

with a variable sampling step h_k , that we aim to maximise. Here again we considered the gain $K(d(t))$ to be varying in a convex polytope as,

$$K(d(t)) \in Co\{K_1, \dots, K_q\}, \quad (4.40)$$

with $K_i \in \mathbb{R}^{n_u \times l}$, $\forall i \in \{1, \dots, q\}$. Since $K(d(t))$ varies in a convex polytope, it is represented as,

$$K(d(t)) = \sum_{i=1}^q a_i(d(t))K_i, \quad (4.41)$$

where, $\sum_{i=1}^q a_i(d(t)) = 1$, $a_i(d(t)) \in [0, 1]$, $\forall i \in \{1, \dots, q\}$. We denote S as the closed-loop system, $\{(4.37), (4.38), (4.39)\}$ and the corresponding closed-loop schematic as given in Fig. 4.4. Next, we will present NN architecture.

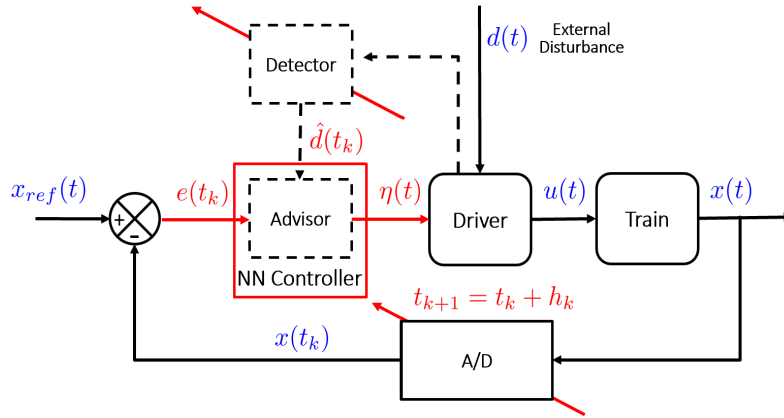


Figure 4.4: Closed-loop system schematic

4.3.1.1 Neural-network control

The input-output based relationship of a discrete-time TLFCFFNN is defined as,

$$Y_d(t_k) = \sum_{j=1}^{n_h} g_{d,j} t_f \left(\sum_{i=1}^{n_x} m_{j,i} X_i(t_k) + b_j \right), \quad d \in \{1, \dots, n_{out}\}, \quad (4.42)$$

where $m_{j,i}$, denotes the connection weight between the j^{th} hidden node and the i^{th} input node, $g_{d,j}$ denotes the connection weight between the d^{th} output node and the j^{th} hidden node, b_j denotes the bias for the j^{th} hidden node, $t_f(\cdot)$ denotes the activation function, n_x , n_{out} and n_h denotes the number of input, output and hidden nodes respectively, $X(t_k) = [X_1(t_k), \dots, X_n(t_k)]^T$ denotes the sampled input vector X at the sampled time t_k . The structure of TLFCFFNN is as shown in Fig. 4.5.

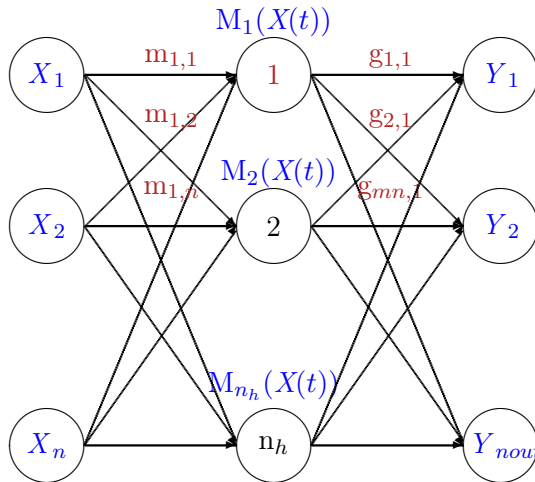


Figure 4.5: TLFCFFNN-based controller

Thus, based on the I/O relationship given in (4.42), a sampled-data TLFCFFNN-based controller with $n_{out} = n_u n_x$ is defined as,

$$\eta(t) = \frac{\begin{bmatrix} Y_1(t_k) & Y_2(t_k) & \cdots & Y_{n_x}(t_k) \\ Y_{n_x+1}(t_k) & Y_{n_x+2}(t_k) & \cdots & Y_{2n_x}(t_k) \\ \vdots & \vdots & \ddots & \vdots \\ Y_{(n_u-1)n_x+1}(t_k) & Y_{(n_u-1)n_x+2}(t_k) & \cdots & Y_{n_u n_x}(t_k) \end{bmatrix} \begin{bmatrix} X_1(t_k) \\ X_2(t_k) \\ \vdots \\ X_{n_x}(t_k) \end{bmatrix}}{\sum_{l=1}^{n_h} t_f(\sum_{i=1}^{n_x} m_{l,i} X_i(t_k) + b_l)}, \quad (4.43)$$

for all $t \in [t_k, t_{k+1})$, which can be further rewritten as,

$$\eta(t) = \frac{\sum_{j=1}^{n_h} t_f(\sum_{i=1}^{n_x} m_{j,i} X_i(t_k) + b_j) \begin{bmatrix} g_{1,j} & g_{2,j} & \cdots & g_{n_x,j} \\ g_{n_x+1,j} & g_{n_x+2,j} & \cdots & g_{2n_x,j} \\ \vdots & \vdots & \ddots & \vdots \\ g_{(n_u-1)n_x+1,j} & g_{(n_u-1)n_x+2,j} & \cdots & g_{n_u n_x,j} \end{bmatrix} \begin{bmatrix} X_1(t_k) \\ X_2(t_k) \\ \vdots \\ X_{n_x}(t_k) \end{bmatrix}}{\sum_{l=1}^{n_h} t_f(\sum_{i=1}^{n_x} m_{l,i} X_i(t_k) + b_l)}, \quad (4.44)$$

or
$$\eta(t) = \sum_{j=1}^{n_h} M_j(X(t_k)) \mathbf{G}_j X(t_k), \quad (4.45)$$

where,
$$\mathbf{G}_j = \begin{bmatrix} g_{1,j} & g_{2,j} & \cdots & g_{n_x,j} \\ g_{n_x+1,j} & g_{n_x+2,j} & \cdots & g_{2n_x,j} \\ \vdots & \vdots & \ddots & \vdots \\ g_{(n_u-1)n_x+1,j} & g_{(n_u-1)n_x+2,j} & \cdots & g_{n_u n_x,j} \end{bmatrix}, \quad (4.46)$$

$$M_j(X(t_k)) = \frac{t_f(\sum_{i=1}^{n_x} m_{j,i} X_i(t_k) + b_j)}{\sum_{l=1}^{n_h} t_f(\sum_{i=1}^{n_x} m_{l,i} X_i(t_k) + b_l)} \in [0, 1], \quad (4.47)$$

with the property $\sum_{j=1}^{n_h} M_j(X(t_k)) = 1$. It is assumed that the activation function $t_f(\cdot)$ is chosen such that $t_f(\sum_{i=1}^{n_x} m_{j,i} X_i(t_k) + b_j) > 0$ and $\sum_{l=1}^{n_h} t_f(\sum_{i=1}^{n_x} m_{l,i} X_i(t_k) + b_l) \neq 0$ at any time to satisfy the property above.

Remark 4.7: Please note, that the expression of NN control given by equation (4.45) has $M_j(X(t_k))$ term, which acts as a scaling factor, due to the assumption $\sum_{j=1}^{n_h} M_j(X(t_k)) = 1$. The assumption also serves the purpose to bound the connection weight between input nodes and the hidden nodes, $m_{j,i}$ and the bias b_j with the help of activation function $t_f(\cdot)$. The choice of activation function ensures that the value of $M_j(X(t_k))$ always lies between $[0, 1]$. Thus, we consider boundedness of weights implicitly, contrary to work such as, [Sahoo *et al.* 2016], where the authors consider the bounds on weights explicitly.

Now, if we consider the input vector for the NN as $X(t_k) = [X_1(t_k) X_2(t_k)]^T = [x(t_k) \hat{d}(t_k)]^T$, then, the control signal can be re written as,

$$u(t) = K(d(t)) \left[\sum_{j=1}^{n_h} M_j(X(t_k)) \left[G_{1,j}x(t_k) + G_{2,j}\hat{d}(t_k) \right] \right] \quad (4.48)$$

where, $K(d(t)) \in Co\{K_1, \dots, K_q\}$ with $K_i \in \mathbb{R}^{n_u \times l}$, $\forall i \in \{1, \dots, q\}$, $x(t_k) \in \mathbb{R}^{n_x}$, $\hat{d}(t_k) \in \mathbb{R}^r$, $G_{1,j} \in \mathbb{R}^{l \times n_x}$ and $G_{2,j} \in \mathbb{R}^{l \times r}$ respectively. Here, $x(t_k)$ is the system state at time t_k and $\hat{d}(t_k)$ is the estimated exogenous disturbance at time t_k . Then, the dynamic behaviour of the closed-loop linear system with the presented TLFCFFNN-based controller and a time-varying gain, $K(d(t))$ can be written as:

$$\begin{cases} \dot{x}(t) = \sum_{j=1}^{n_h} M_j(X(t_k)) \left[Ax(t) + BK(d(t))G_{1,j}x(t_k) \right. \\ \quad \left. + BK(d(t))G_{2,j}w_1(t) + Bw_2(d(t)) \right], \\ z(t) = Cx(t), \end{cases} \quad (4.49)$$

when $t_k \leq t < t_{k+1}$, $k \in \mathbb{N}$, with $w_1(t) = \hat{d}(t_k) - d_{nom}$ and $w_2(d(t)) = (K(d(t)) - K_{nom})G_{2,j}d_{nom}$ as small perturbations. Note, here d_{nom} and K_{nom} are nominal exogenous disturbance and its corresponding nominal gain. Compared to the previous modelling abstraction, we can observe an additional non-linear term, $\sum_{j=1}^{n_h} M_j(X(t_k))$ introduced in the control expression. It serves the purpose to change the weights of the delayed state measurement, $x(t_k)$ and the delayed estimate of the disturbance, $\hat{d}(t_k)$. Next, considering the unknown exogenous disturbance $w_1(t)$ and $w_2(d(t))$, the system S is studied from \mathcal{L}_2 -stability point of view, which was as recalled in the Definition 4.1.

Our objective in this subsection is to compute largest sampling interval \bar{h} which ensures the expected \mathcal{L}_2 -stability for a fixed $\gamma_1, \gamma_2 \geq 0$. We will thus provide a *stability analysis* of the system for a given NN controller gain $G_{1,j}, G_{2,j}$, and a convex polytope for time-varying gain $K(d(t))$. Compared to the Section 4.2, these studies are based on another, quite general class of LKF, based on Bessel-Legendre inequality, while taking into account the delays (in the case of delayed systems), the perturbations and the sampling (the maximum sampling period \bar{h} dependent terms).

4.3.2 L_2 -stability results

In this subsection, we propose stability analysis of system S with a given NN gain $G_{1,j}, G_{2,j}$, a convex polytope for time-varying gain $K(d(t))$ and a sampling (4.39).

4.3.2.1 Stability analysis of the perturbed sampled-data LTI system

We consider the following LKF, which depends on, the actual state $x(t)$, the sampled-state $x(t_k)$, the delayed state x_t and the delayed state derivative \dot{x}_t (defined for a maximum

sampling period \bar{h} as $x_t(\theta) = x(t + \theta)$, $\dot{x}_t(\theta) = \dot{x}(t + \theta)$, $\forall \theta \in [-\bar{h}, 0]$:

$$V(t, x(t), x_t, \dot{x}_t, k) = \eta_1(t)^T P \eta_1(t) + \int_{t_k}^t \eta_2(t, s)^T Q \eta_2(t, s) ds + (t_{k+1} - t) \int_{t_k}^t \dot{x}(s)^T Z \dot{x}(s) ds + (t_{k+1} - t) \begin{bmatrix} x(t) \\ x(t_k) \end{bmatrix}^T \Omega \begin{bmatrix} x(t) \\ x(t_k) \end{bmatrix}, \quad (4.50)$$

defined for all $t \in [t_k, t_{k+1})$ and $k \in \mathbb{N}$, with $\eta_1(t) = \text{col} \left\{ x(t), x(t_k), \int_{t_k}^t x(s) ds, \frac{1}{t-t_k} \int_{t_k}^t \int_s^t x(r) dr ds \right\}$, $\eta_2(t, s) = \text{col} \left\{ \dot{x}(s), x(s), x(t), x(t_k), \int_s^t x(r) dr \right\}$, with matrix Ω defined as:

$$\Omega = \begin{bmatrix} \frac{X+X^T}{2} & -X + X_1 \\ * & -X_1 - X_1^T + \frac{X+X^T}{2} \end{bmatrix}, \quad (4.51)$$

where, matrices $P \in \mathbb{S}_+^{4n_x}$, $Q \in \mathbb{S}_+^{5n_x}$, $Z \in \mathbb{S}_+^{n_x}$ and $X, X_1 \in \mathbb{R}^{n_x \times n_x}$ are of appropriate dimensions. Compared to (4.9), the new aspect of LKF (4.50), is the fact that it involves application of augmented terms $\eta_1(t)$ and $\eta_2(t, s)$, inspired from [Park & Park 2018]. However, similar to (4.9), the functional V is also time-dependent, i.e. it is continuous over the sampling interval $t \in [t_k, t_{k+1})$ and is discontinuous at times t_k as:

$$\lim_{t \rightarrow t_k^-} V(t, x(t), x_t, \dot{x}_t, k-1) = \eta_1^T(t_k) P \eta_1(t_k) + \int_{t_{k-1}}^{t_k} \eta_2(t, s)^T Q \eta_2(t, s) ds, \quad (4.52)$$

and
$$\lim_{t \rightarrow t_k^+} V(t_k, x(t_k), x_{t_k}, \dot{x}_{t_k}, k) = \eta_1^T(t_k) P \eta_1(t_k). \quad (4.53)$$

Note that, this is because \bar{V} has one discontinuous term $\int_{t_k}^t \eta_2(t, s)^T Q \eta_2(t, s) ds$. This term do not increase along the jumps at t_k , but actually vanishes. Thus the inequality $\lim_{t \rightarrow t_k^-} V(t, x(t), x_t, \dot{x}_t, k) \geq V(t_k, x(t_k), x_{t_k}, \dot{x}_{t_k}, k)$ holds. This new LKF is also well adapted to the stability analysis of systems with time-varying sampling. For ease in notation in the following, we denote

$$\bar{V}(t) = V(t, x(t), x_t, \dot{x}_t, k) \text{ for all } t \in [t_k, t_{k+1}), k \in \mathbb{N}. \quad (4.54)$$

Based on \mathcal{L}_2 -stability definition of Lemma 4.2, the analysis will have same two steps.

- First, we prove that \bar{V} is continuous over $\mathbb{R}^+ \setminus \{t_k, k \in \mathbb{N}\}$ and differentiable for all $t \in [t_k, t_{k+1})$, and provide conditions for its positive definiteness.
- Then, we differentiate \bar{V} , upper-bound the obtained result and derive the \mathcal{L}_2 -stability conditions.

4.3.2.2 LKF's required properties

As a necessary first step, we propose the following new lemma, which ensures the LKF functional's continuity, piece-wise differentiability, and positivity conditions.

Lemma 4.8: The function \bar{V} defined in (4.54) is continuous over $\mathbb{R}^+ \setminus \{t_k, k \in \mathbb{N}\}$ and differentiable for all $t \neq t_k, k \in \mathbb{N}$. If its matrix parameters satisfy $P \in \mathbb{S}_+^{4n_x}, Q \in \mathbb{S}_+^{5n_x}, Z \in \mathbb{S}_+^{n_x}, X, X_1 \in \mathbb{R}^{n_x \times n_x}$ and

$$\left[P + \bar{h} \begin{bmatrix} \Omega & 0_{2n_x \times 2n_x} \\ 0_{2n_x \times 2n_x} & 0_{2n_x \times 2n_x} \end{bmatrix} \right] \succ 0, \quad (4.55)$$

then \bar{V} is also positive definite, and there exists scalar $\beta > 0$ such that $\bar{V} \geq \beta \|x(t)\|^2$ for all $t \geq 0$.

Proof: \bar{V} is defined on \mathbb{R}^+ , differentiable over each time interval $[t_k, t_{k+1})$, and is designed to satisfy,

$$\bar{V}(t_k^-) = \lim_{t \rightarrow t_k^-} \bar{V}(t) = \eta_1(t_k)^T P \eta_1(t_k) + \int_{t_{k-1}}^{t_k} \eta_2(t, s)^T Q \eta_2(t, s) ds$$

and $\bar{V}(t_k^+) = \lim_{t \rightarrow t_k^+} \bar{V}(t) = \eta_1(t_k)^T P \eta_1(t_k)$ for all $k \in \mathbb{N}$. It is therefore continuous and differentiable over $\mathbb{R}^+ \setminus \{t_k, k \in \mathbb{N}\}$. Now, we can say that \bar{V} is positive definite if, and only if, for all $k \in \mathbb{N}, t \in [t_k, t_{k+1})$:

$$\eta_1^T(t) \left[P + (t_{k+1} - t) \begin{bmatrix} \Omega & 0_{2n_x \times 2n_x} \\ 0_{2n_x \times 2n_x} & 0_{2n_x \times 2n_x} \end{bmatrix} \right] \eta_1(t) \geq 0, \quad (4.56)$$

with equality if and only if $x(t) = x(t_k) = 0$ and

$$\int_{t_k}^t \eta_2(t, s)^T Q \eta_2(t, s) ds + (t_{k+1} - t) \int_{t_k}^t \dot{x}(s)^T Z \dot{x}(s) ds \geq 0. \quad (4.57)$$

Further as $0 \leq t_{k+1} - t \leq \bar{h}$, remarking that the right part of (4.57) and the middle matrix term in the left part of (4.56) is linear with respect to $\rho = t_{k+1} - t$, one can use Theorem A.3 (in the Appendix A) and show that a sufficient condition for \bar{V} to be positive definite is that, for all $k \in \mathbb{N}, t \in [t_k, t_{k+1})$:

$$\eta_1(t)^T P \eta_1(t) > 0, \text{ for all } \eta_1(t) \neq 0 \quad (4.58)$$

and
$$\eta_1^T(t) \left[P + \bar{h} \begin{bmatrix} \Omega & 0_{2n_x \times 2n_x} \\ 0_{2n_x \times 2n_x} & 0_{2n_x \times 2n_x} \end{bmatrix} \right] \eta_1(t) \geq 0, \text{ for all } \eta_1(t) \neq 0. \quad (4.59)$$

The condition (4.59) is ensured by assuming that P is positive definite. Furthermore, if $P \succ 0$, then there exists a scalar $\beta > 0$, such that for all $k \in \mathbb{N}$ and $t \in [t_k, t_{k+1})$, $\left[P + \bar{h} \begin{bmatrix} \Omega & 0_{2n_x \times 2n_x} \\ 0_{2n_x \times 2n_x} & 0_{2n_x \times 2n_x} \end{bmatrix} \right] \succ \beta I$. Thus, $\bar{V}(t) \geq \beta \|x(t)\|^2$, for all $t \in [t_k, t_{k+1}), \forall k \in \mathbb{N}$. Therefore, there exists a scalar β , such that $\bar{V}(t) \geq \beta \|x(t)\|^2$ for all $t \geq 0$, which ends the proof. \square

4.3.2.3 L_2 -stability conditions

Having proposed conditions to ensure \bar{V} 's continuity, differentiability, and positivity, now, in order to analyse the \mathcal{L}_2 -stability of the system S , we will again refer to Lemma 4.2. The lemma is needed to provide conditions to satisfy,

$$\dot{\bar{V}}(t) + z^T(t)z(t) - \gamma_1 w_1^T(t)w_1(t) - \gamma_2 w_2^T(d(t))w_2(d(t)) \leq 0, \forall t \neq t_k, \forall k \in \mathbb{N}. \quad (4.60)$$

In order to analyse the \mathcal{L}_2 -stability condition, we study the restriction of $\dot{\bar{V}}$ on any interval $[t_k, t_{k+1})$, $k \in \mathbb{N}$. We compute:

$$\begin{aligned} \dot{\bar{V}}(t) = & \mathbf{He} \left\{ \eta_1(t)^T P \dot{\eta}_1(t) \right\} + \eta_2(t, t)^T Q \eta_2(t, t) + \mathbf{He} \left\{ \int_{t_k}^t \eta_2(t, s)^T Q \frac{\partial \eta_2(t, s)}{\partial t} ds \right\} \\ & + (t_{k+1} - t) \dot{x}(t)^T Z \dot{x}(t) - \int_{t_k}^t \dot{x}(s)^T Z \dot{x}(s) ds \\ & - \begin{bmatrix} x(t) \\ x(t_k) \end{bmatrix}^T \Omega \begin{bmatrix} x(t) \\ x(t_k) \end{bmatrix} + (t_{k+1} - t) \mathbf{He} \left\{ \begin{bmatrix} x(t) \\ x(t_k) \end{bmatrix}^T \Omega \begin{bmatrix} \dot{x}(t) \\ 0 \end{bmatrix} \right\}. \end{aligned} \quad (4.61)$$

Using the affine Bessel-Legendre inequality [Lee *et al.* 2018] (see Theorem A.4 in Appendix A), we compute an upper-bound of the integral term:

$$- \int_{t_k}^t \dot{x}^T(s) Z \dot{x}(s) ds \leq (t - t_k) \zeta^T(t) F Z_N^{-1} F^T \zeta(t) + \mathbf{He} \left\{ \zeta^T(t) F \mathbb{L}(t_k, t) \right\}, \quad (4.62)$$

where, we consider $N = 2$, $\mathbb{L}(t_k, t) = \text{col} \{ \mathbb{L}_0(t_k, t), \mathbb{L}_1(t_k, t), \mathbb{L}_2(t_k, t) \}$ and write $\mathbb{L}(t_k, t) = \varrho_f \zeta(t)$ with $\zeta(t) \in \mathbb{R}^{7n_x + n_{w_1} + n_{w_2}}$ as the augmented state vector:

$$\zeta(t) = \text{col} \left\{ x(t), x(t_k), \frac{1}{(t-t_k)} \int_{t_k}^t x(s) ds, \frac{1}{(t-t_k)^2} \int_{t_k}^t \int_{t_k}^s x(r) dr ds, \int_{t_k}^t x(s) ds, \frac{1}{(t-t_k)} \int_{t_k}^t \int_{t_k}^s x(r) dr ds, \dot{x}(t), w_1(t), w_2(d(t)) \right\}. \quad (4.63)$$

Here, $\zeta(t)$ is well defined by continuity in $t = t_k$, as when $t \rightarrow t_k$, $\zeta(t) \rightarrow \zeta(t_k)$. Compared to equation (4.23), the upper-bound of integral term in (4.62) is less conservative, [Zhang *et al.* 2018c]. Using majoration (4.62) in $\dot{\bar{V}}(t)$, equation (4.61) leads to

$$\begin{aligned} \dot{\bar{V}}(t) + z^T(t)z(t) - \gamma_1 w_1^T(t)w_1(t) - \gamma_2 w_2^T(d(t))w_2(d(t)) \leq & \mathbf{He} \left\{ \eta_1(t)^T P \dot{\eta}_1(t) \right\} \\ & + \eta_2(t, t)^T Q \eta_2(t, t) + \mathbf{He} \left\{ \int_{t_k}^t \eta_2(t, s)^T Q \frac{\partial \eta_2(t, s)}{\partial t} ds \right\} + (t_{k+1} - t) \dot{x}(t)^T Z \dot{x}(t) \\ & + (t - t_k) \zeta^T(t) F Z_N^{-1} F^T \zeta(t) + \mathbf{He} \left\{ \zeta^T(t) F \mathbb{L}(t_k, t) \right\} - \begin{bmatrix} x(t) \\ x(t_k) \end{bmatrix}^T \Omega \begin{bmatrix} x(t) \\ x(t_k) \end{bmatrix} \\ & + (t_{k+1} - t) \mathbf{He} \left\{ \begin{bmatrix} x(t) \\ x(t_k) \end{bmatrix}^T \Omega \begin{bmatrix} \dot{x}(t) \\ 0 \end{bmatrix} \right\} + z^T(t)z(t) - \gamma_1 w_1^T(t)w_1(t) - \gamma_2 w_2^T(d(t))w_2(d(t)). \end{aligned} \quad (4.64)$$

Further, we apply the descriptor method from [Fridman 2010]. Here we consider equality (4.65), (4.66) and (4.67). The right hand side expression of the equations,

$$0 = \mathbf{He} \left\{ \zeta(t) Y_1 [((t - t_k) e_3 - e_5] \zeta(t) \right\}, \quad (4.65)$$

$$0 = \mathbf{He} \{ \zeta(t) Y_2 [(t - t_k) e_4 - e_6] \zeta(t) \}, \quad (4.66)$$

$$0 = \mathbf{He} \left\{ \left[x(t)^T P_2^T + \dot{x}(t)^T P_3^T \right] \left[-\dot{x}(t) + \sum_{j=1}^{n_h} M_j(X(t_k)) [Ax(t) + BK(d(t))G_{1,j}x(t_k) + BK(d(t))G_{2,j}w_1(t) + Bw_2(d(t))] \right] \right\}, \quad (4.67)$$

with some arbitrary matrices $P_2, P_3 \in \mathbb{R}^{n_x \times n_x}$ and $Y_1, Y_2 \in \mathbb{R}^{c n_x \times n_x}$ are added into the right hand side of equation (4.64) expression. The purpose is to get system dynamics into the Lyapunov condition and consider $\dot{x}(t)$ in the extended state vector. Thus,

$$\begin{aligned} & \dot{V}(t) + z^T(t)z(t) - \gamma_1 w_1^T(t)w_1(t) - \gamma_2 w_2^T(d(t))w_2(d(t)) \leq \mathbf{He} \{ \eta_1(t)^T P \dot{\eta}_1(t) \} \\ & + \eta_2(t, t)^T Q \eta_2(t, t) + \mathbf{He} \left\{ \int_{t_k}^t \eta_2(t, s)^T Q \frac{\partial \eta_2(t, s)}{\partial t} ds \right\} + (t_{k+1} - t) \dot{x}(t)^T Z \dot{x}(t) \\ & + (t - t_k) \zeta^T(t) F Z_N^{-1} F^T \zeta(t) + \mathbf{He} \{ \zeta^T(t) F \mathbb{L}(t_k, t) \} - \begin{bmatrix} x(t) \\ x(t_k) \end{bmatrix}^T \Omega \begin{bmatrix} x(t) \\ x(t_k) \end{bmatrix} \\ & + (t_{k+1} - t) \mathbf{He} \left\{ \begin{bmatrix} x(t) \\ x(t_k) \end{bmatrix}^T \Omega \begin{bmatrix} \dot{x}(t) \\ 0 \end{bmatrix} \right\} + z^T(t)z(t) - \gamma_1 w_1^T(t)w_1(t) - \gamma_2 w_2^T(d(t))w_2(d(t)) \\ & + \mathbf{He} \{ \zeta(t) Y_1 [(t - t_k) e_3 - e_5] \zeta(t) \} + \mathbf{He} \{ \zeta(t) Y_2 [(t - t_k) e_4 - e_6] \zeta(t) \} \\ & + \mathbf{He} \left\{ \left[x(t)^T P_2^T + \dot{x}(t)^T P_3^T \right] \left[-\dot{x}(t) + \sum_{j=1}^{n_h} M_j(X(t_k)) [Ax(t) + BK(d(t))G_{1,j}x(t_k) \right. \right. \\ & \left. \left. + BK(d(t))G_{2,j}w_1(t) + Bw_2(d(t))] \right] \right\}. \end{aligned} \quad (4.68)$$

Then, by considering $K(d(t))$ to be in the convex polytope as in (4.41), there exist matrix $\Phi_{[t-t_k]}^{ij}$ for all $i \in \{1, \dots, p\}$ and $j \in \{1, \dots, n_h\}$ such that:

$$\begin{aligned} \Phi_{[t-t_k]}^{ij} &= \varrho_{q_0}^T Q \varrho_{q_0} - \varrho_{\psi_0}^T \Omega \varrho_{\psi_0} + e_1^T C^T C e_1 - \gamma_1 e_8^T e_8 - \gamma_2 e_9^T e_9 + \mathbf{He} \{ \varrho_{p_1}^T P \varrho_{p_2} \\ & + \varrho_{q_1}^T Q \varrho_{q_2} + F \varrho_f + Y_1 \varrho_{y_1} + Y_2 \varrho_{y_2} + [e_1^T P_2^T + e_7^T P_3^T] \times [-e_7 + A e_1 \\ & + BK_i G_{1,j} e_2 + BK_i G_{2,j} e_8 + B e_9] \} \\ \varrho_{q_0} &= \text{col} \{ e_7, e_1, e_1, e_2, e_0 \}, \\ \varrho_{\psi_0} &= \text{col} \{ e_1, e_2 \}, \\ \varrho_{\psi_1} &= \text{col} \{ e_7, e_0 \}, \\ \varrho_{p_1} &= \text{col} \{ e_1, e_2, e_5, e_6 \}, \\ \varrho_{p_2} &= \text{col} \{ e_7, e_0, e_1, e_1 - e_4 \}, \\ \varrho_{q_1} &= \text{col} \{ e_1 - e_2, e_5, (t - t_k) e_1, (t - t_k) e_2, (t - t_k) e_6 \}, \\ \varrho_{q_2} &= \text{col} \{ e_0, e_0, e_7, e_0, e_1 \}, \\ \varrho_f &= \text{col} \{ e_1 - e_2, e_1 + e_2 - 2e_3, e_1 - e_2 + 6e_3 - 12e_4 \}, \\ \varrho_{y_1} &= \text{col} \{ (t - t_k) e_3 - e_5 \}, \\ \varrho_{y_2} &= \text{col} \{ (t - t_k) e_4 - e_6 \}, \\ e_i &= [0_{n \times (i-1)n} \ I_n \ 0_{n \times (c-i)n}], \quad i = 1, \dots, c, \\ e_0 &= [0_{n \times cn}]. \end{aligned} \quad (4.69)$$

Using these matrix notation, we can rewrite (4.68) as,

$$\begin{aligned} & \dot{V}(t) + z^T(t)z(t) - \gamma_1 w_1^T(t)w_1(t) - \gamma_2 w_2^T(d(t))w_2(d(t)) \\ & \leq \sum_{j=1}^{n_h} M_j(X(t_k)) \sum_{i=1}^q a_i(d(t)) \zeta(t)^T \Phi_{[t-t_k]}^{ij} \zeta(t) + (t-t_k) \zeta(t)^T F Z_N^{-1} F^T \zeta(t) \\ & + (t_{k+1} - t) \zeta(t)^T \left(e_7^T Z e_7 + \mathbf{He} \left\{ \varrho_{\psi_0}^T \Omega \varrho_{\psi_1} \right\} \right) \zeta(t). \end{aligned} \quad (4.70)$$

Since, $\sum_{i=1}^q \sum_{j=1}^{n_h} M_j(X(t_k)) a_i(d(t)) = \sum_{j=1}^{n_h} M_j(X(t_k)) = \sum_{i=1}^q a_i(d(t)) = 1$, as $M_j(X(t_k)) \in [0, 1]$, $\forall j \in \{1, \dots, n_h\}$, $a_i(d(t)) \in [0, 1]$, $\forall i \in \{1, \dots, q\}$, equation (4.70) can be rewritten as:

$$\begin{aligned} & \dot{V}(t) + z^T(t)z(t) - \gamma_1 w_1^T(t)w_1(t) - \gamma_2 w_2^T(d(t))w_2(d(t)) \\ & \leq \sum_{j=1}^{n_h} \sum_{i=1}^q M_j(X(t_k)) a_i(d(t)) \zeta(t)^T \left[\Phi_{[t-t_k]}^{ij} + (t-t_k) F Z_N^{-1} F^T \right. \\ & \left. + (t_{k+1} - t) \left(e_7^T Z e_7 + \mathbf{He} \left\{ \varrho_{\psi_0}^T \Omega \varrho_{\psi_1} \right\} \right) \right] \zeta(t). \end{aligned} \quad (4.71)$$

Similar to equation (4.34), since equation (4.71) is also linear in the variable t , we follow similar steps to reduce the number of conditions to be checked to a finite number, i.e. by applying Theorem A.3 (in the Appendix A) with the variable $\rho = t \in [t_k, t_{k+1}]$. We thus obtain two inequalities, both linear in the variable $t_{k+1} - t_k$. We, then, use Theorem A.3 (in the Appendix A), with the variable $\rho = t_{k+1} - t_k \in [0, \bar{h}]$ to prove that if the two inequalities $\zeta(t)^T \Xi_{ij} \zeta(t) \preceq 0$ are satisfied for all $\zeta(t) \in \mathbb{R}^{7n_x + n_{w_1} + n_{w_2}}$, $i \in \{1, \dots, q\}$ and $j \in \{1, \dots, n_h\}$, with Ξ_{ij} defined as,

$$\Xi_{ij} = \begin{Bmatrix} \begin{bmatrix} \Phi_{\bar{h}}^{ij} & \sqrt{\bar{h}} F \\ * & -Z_N \end{bmatrix}, \\ \left[\Phi_0^{ij} + \bar{h} e_7^T Z e_7 + \bar{h} \mathbf{He} \left\{ \varrho_{\psi_0}^T \Omega \varrho_{\psi_1} \right\} \right], \end{Bmatrix}, \quad (4.72)$$

then, $\dot{V}(t) + \|z(t)\|^2 - \gamma_1 \|w_1(t)\|^2 - \gamma_2 \|w_2(d(t))\|^2 \leq 0$ for all $t \in [t_k, t_{k+1}]$, $k \in \mathbb{N}$. Note that we considered any sampling sequence $h_k = t_{k+1} - t_k \in [0, \bar{h}]$. Therefore, the \mathcal{L}_2 -stability results we obtained will be valid for any sampling sequence satisfying (4.39). Further, since we have shown that $\dot{V}(t) \leq -\|z(t)\|^2 + \gamma_1 \|w_1(t)\|^2 + \gamma_2 \|w_2(d(t))\|^2$ for all $t \in [t_k, t_{k+1}]$, $k \in \mathbb{N}$, if we have $V(t_0) = 0$, we find

$$\int_{t_0}^t [z(t)^T z(t) - \gamma_1 w_1(t)^T w_1(t) - \gamma_2 w_2(d(t))^T w_2(d(t))] dt < 0. \quad (4.73)$$

Therefore, we will have the following theorem.

Theorem 4.9: Consider scalars $c, N, \gamma_1, \gamma_2 > 0$ with matrices $G_{1,j} \in \mathbb{R}^{l \times n_x}$, $G_{2,j} \in \mathbb{R}^{l \times r}$, $j \in \{1, \dots, n_h\}$, $K_i \in \mathbb{R}^{n_u \times l}$, $i \in \{1, \dots, q\}$ and a maximum sampling interval \bar{h} . Then, the perturbed system S is finite-gain \mathcal{L}_2 -stable from $w_1(t) \rightarrow z(t)$ and $w_2(d(t)) \rightarrow z(t)$ with \mathcal{L}_2 gain less than γ_1 and γ_2 respectively, for any sampling sequence satisfying (4.39), if

there exist matrices $P \in \mathbb{S}_+^{4n_x}$, $Q \in \mathbb{S}_+^{5n_x}$, $Z \in \mathbb{S}_+^{n_x}$ and arbitrary matrices X , X_1 , P_2 , $P_3 \in \mathbb{R}^{n_x \times n_x}$, $F \in \mathbb{R}^{cn_x \times (N+1)n_x}$, Y_1 , $Y_2 \in \mathbb{R}^{cn_x \times n_x}$ such that (4.59) and (4.72) satisfy, for all $i \in \{1, \dots, q\}$ and $j \in \{1, \dots, n_h\}$.

Remark 4.10: It can be seen from Theorem 4.9 that the LMI's for \mathcal{L}_2 -stability depend only on the NN parameters from hidden nodes to outer nodes, i.e. $G_{1,j}$ and $G_{2,j}$ but not on inner nodes to hidden nodes, i.e. $m_{j,i}$, $\forall i \in \{1, \dots, n_x\}$, $\forall j \in \{1, \dots, n_h\}$. Thus we can see that system stability do not depend on the trained NN parameters rather it depends on NN parameter that can be tested by LMI's.

Remark 4.11: Compared to Theorem 4.2, the stability conditions provided by Theorem 4.9 are aimed at the perturbed system S with a given NN gain $G_{1,j}$, $G_{2,j}$, a convex polytope for time-varying gain $K(d(t))$ and a sampling satisfying (4.39). The key difference involve the application of an augmented time-dependent LKF and a better choice of upper-bounding the integral term, i.e. using affine Bessel-Legendre inequality.

4.3.3 Discussions

In this section we proposed a stability analysis allowing to estimate maximum sampling period \bar{h} , while ensuring \mathcal{L}_2 -stability for perturbed sampled-data LTI with a NN controller. The study was based on a new class of LKF involving use of a form of Bessel-Legendre inequality. The application of affine Bessel-Legendre, in addition to augmented Lyapunov functional, was advantageous in over-approximating the integral term and eventually maximising the time-varying sampling interval \bar{h} while ensuring the system \mathcal{L}_2 -stability.

However, we realised there is still room for improvement in the ADAS-Driver-Train modelling. The assumption that a ADAS-Driver-Train model be linear in nature is an over simplification of the problem. Thus, we searched for other modelling methods. In the literature, fuzzy logic theory has been well recognised as a powerful tool to represent the non-linearities in dynamical systems, [Liu *et al.* 2013], [Wang *et al.* 2016], [Chen *et al.* 2017b], [Wang *et al.* 2018], [Niu *et al.* 2018]. In particular, due to features such as structural simplicity and universal function approximation capability, T-S models, [Takagi & Sugeno 1985], have received tremendous research efforts in the past few decades, [Lam *et al.* 2000], [Precup *et al.* 2010], [Vrkalovic *et al.* 2017], [Choi *et al.* 2017].

The aforementioned reason led us to consider T-S model to represent the Train. We particularly considered a fuzzy parameter varying system, [Zhao *et al.* 2014], [Wei *et al.* 2018]. Such system can fruitfully represent non-linear time-varying systems by combining the advantages of both the T-S fuzzy system and the LPV system. This representation not only overcomes the disadvantage of the traditional T-S fuzzy system in

4.4. Stability of non-linear sampled-data system with neural-network control

handling time-varying systems, but also expands the scope of application of LPV system theory, [Zhang *et al.* 2016b].

We propose a third modelling abstraction as shown in Fig. 4.6. In the next section we will present a T-S model with NN controller based modelling abstraction for stability study of ADAS-Driver-Train system in the presence of delayed sensor measurements.

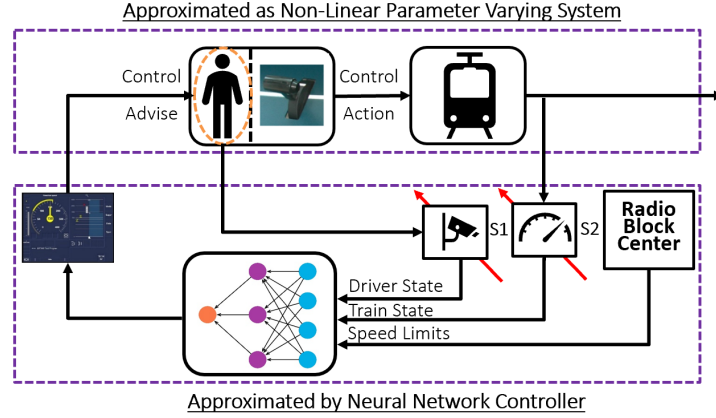


Figure 4.6: Non-linear parameter varying system with NN control

4.4 Stability of non-linear sampled-data system with neural-network control

4.4.1 Problem formulation

In this modelling abstraction, the Driver-Train non-linear system is represented using the T-S model, [Takagi & Sugeno 1985]. These models have the advantage of exactly representing a non-linear system in a certain domain of validity. The domain is a polytope whose vertices are composed of linear subsystems (based on the sector non-linearity approach). Inside this domain, the non-linear system is exactly represented by a combination of several linear subsystems triggered together with non-linear functions called membership functions, $w_i(x(t))$.

4.4.1.1 Takagi-Sugeno system model

This class of non-linear continuous-time system is described by,

$$\dot{x}(t) = \sum_{i=1}^p w_i(x(t))(A_i x(t) + B_i u(t)), \quad (4.74)$$

112 Chapter 4. Stability of sampled-data systems with time-varying sampling

where $x = [x_1, \dots, x_{n_x}]^T \in \mathbb{R}^{n_x}$ is the state vector and $u = [u_1, \dots, u_{n_u}]^T \in \mathbb{R}^{n_u}$ denotes the control input vector. $A_i \in \mathbb{R}^{n_x \times n_x}$ and $B_i \in \mathbb{R}^{n_x \times n_u}$ are known constant system matrices, respectively, p is a non-zero positive integer, and w_i has the following properties:

$$\sum_{i=1}^p w_i(x(t)) = 1, \text{ and } w_i(x(t)) \in [0, 1], \forall i \in \{1, \dots, p\}. \quad (4.75)$$

The control is designed as a piece-wise constant sampled-data controller such that

$$u(t) = u(t_k), \forall t \in [t_k, t_{k+1}), k \in \mathbb{N}, \quad (4.76)$$

with t_k is the k^{th} sampling and actuation time. Note that similar to the modelling abstraction of the previous sections, we have considered no delay between the sampling and actuation times. Further, the sequence of sampling times $(t_k)_{k \geq 0}$ is assumed to satisfy $0 = t_0 < t_1 < \dots < t_k < \dots, \lim_{k \rightarrow \infty} t_k = \infty, 0 < t_{k+1} - t_k \leq \bar{h}$, and the sampling law is defined as,

$$t_{k+1} = t_k + h_k \quad (4.77)$$

with a variable sampling step h_k , that we aim to maximise. In order to fulfil this aim, we consider a NN controller, equation (4.46). Please note, for this stability analysis we consider $X(t_k) = x(t_k)$ and $\eta(t) = u(t)$. We denote S as the closed-loop system, $\{(4.74), (4.77), (4.45)\}$ and the corresponding closed-loop schematic as given in Fig. 4.7.

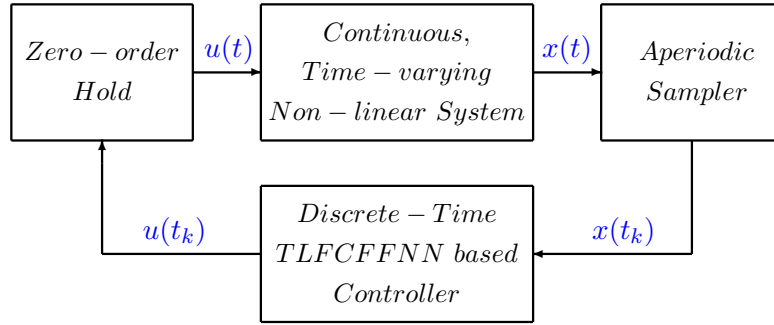


Figure 4.7: Closed-loop system schematic

Then, the dynamic behaviour of the non-linear continuous-time system with the presented NN controller in closed-loop can be written as:

$$\dot{x}(t) = \sum_{i=1}^p \sum_{j=1}^{n_h} w_i(x(t)) M_j(x(t_k)) (A_i x(t) + B_i G_j x(t_k)), \quad (4.78)$$

when $t_k \leq t < t_{k+1}$, $k \in \mathbb{N}$, by utilising the following property,

$$\sum_{i=1}^p w_i(x(t)) = \sum_{j=1}^{n_h} M_j(x(t_k)) = \sum_{i=1}^p \sum_{j=1}^{n_h} w_i(x(t)) M_j(x(t_k)) = 1. \quad (4.79)$$

4.4. Stability of non-linear sampled-data system with neural-network control

In order to have faster convergence rate of the system states to the steady state, the system S is studied from exponential stability point of view, which is recalled in the following definition:

Definition 4.12: (from [Fridman 2010]) Consider a non-linear system $\dot{x}(t) = f(x(t))$, $\forall t \geq t_0$ with $f : \mathbb{R}^{n_x} \rightarrow \mathbb{R}^{n_x}$. Then, an equilibrium point of the system, x_e is said to be exponentially stable, if there exist three scalars $\alpha, \lambda, \delta > 0$ such that,

$$\|x(t_0) - x_e\| < \delta \Rightarrow \|x(t) - x_e\| \leq \alpha \|x(t_0) - x_e\| e^{-2\lambda(t-t_0)}, \quad \forall t \geq t_0. \quad (4.80)$$

The work in the present section aims at estimating the largest sampling interval \bar{h} ,

$$t_{k+1} - t_k \leq \bar{h}, \quad (4.81)$$

while ensuring the exponential stability of S with a decay-rate λ . To this aim, we recall the following lemma:

Lemma 4.13: (from [Fridman 2010]) Assume that there exist real constants $\lambda \geq 0$ and a positive continuous function $V : t \in \mathbb{R}^+ \rightarrow V(t) \in \mathbb{R}^+$, differentiable for all $t \neq t_k, k \in \mathbb{N}$ that satisfy,

$$\dot{V}(t) + 2\lambda V(t) \leq 0, \quad (4.82)$$

along S . Then S is exponential stable with decay-rate λ .

Proof: Let $t \gg 0$ and $k \in \mathbb{N}$ such that $t \in [t_k, t_{k+1})$. Integrating (4.82) over $[0, t]$ gives,

$$\int_{t_k}^t \frac{1}{V(t)} d(V(t)) \leq -2\lambda \int_{t_k}^t dt.$$

Since $V(t) \geq 0$ and $V(t_k) = V(t_k^-)$ for all $k \in \mathbb{N}$ (V is assumed to be continuous), we get $V(t) \leq e^{-2\lambda(t-t_k)} V(t_k)$, for all $t \in [t_k, t_{k+1})$, $k \in \mathbb{N}$. Furthermore, taking into account the fact that $V(t)$ is decreasing during the sampling instants, we further obtain,

$$\begin{aligned} V(t) &\leq e^{-2\lambda(t-t_k)} V(t_k) \leq e^{-2\lambda(t-t_k)} V(t_k^-) \\ &\leq e^{-2\lambda(t-t_{k-1})} V(t_{k-1}) \leq e^{-2\lambda(t-t_{k-1})} V(t_{k-1}^-) \leq \dots \\ &\leq e^{-2\lambda(t-t_0)} V(t_0) \end{aligned}$$

and thus $V(t) \leq e^{-2\lambda(t-t_0)} V(t_0)$. Now, if we have $\exists c_1, c_2 > 0, c_1 \|x(t)\|^2 \leq V(t) \leq c_2 \|x_t\|_{\mathcal{W}}^2$ for all $t \geq 0$, we can conclude that,

$$\|x(t)\| \leq \sqrt{\frac{c_2}{c_1}} e^{-\lambda(t-t_0)} \|x_0\|_{\mathcal{W}}, \quad \forall t \geq 0,$$

which ends the proof. \square

Considering this approach, our objective is to compute largest sampling interval \bar{h} which ensures the expected exponential stability for a fixed decay-rate λ . We will thus

provide a *stability analysis* of the system (4.78) for a given NN controller gain G_j and a given maximum sampling interval \bar{h} . Please note, all these studies are based on a quite general class of LKF, based on derivative of Wirtinger inequality, which take into account the delays (in the case of delayed systems), the perturbations and the sampling (the maximum sampling period \bar{h} dependent terms).

4.4.2 Exponential stability results

In this section, we propose exponential stability analysis of system S for a given NN controller gain G_j and the samplings satisfying (4.77).

4.4.2.1 Stability analysis of non-linear sampled-data systems

We consider the following LKF, which depends on the actual state $x(t)$, the sampled-state $x(t_k)$, the delayed state x_t and the delayed state derivative \dot{x}_t (defined for a maximum sampling period \bar{h} as $x_t(\theta) = x(t + \theta)$, $\dot{x}_t(\theta) = \dot{x}(t + \theta)$, $\forall \theta \in [-\bar{h}, 0]$):

$$\begin{aligned}
 V(t, x(t), x_t, \dot{x}_t, k) = & x(t)^T P x(t) + \int_{t_k}^t e^{2\lambda(s-t)} x(s)^T Q x(s) ds \\
 & + (t_{k+1} - t) \int_{t_k}^t e^{2\lambda(s-t)} \dot{x}(s)^T Z \dot{x}(s) ds \\
 & + \bar{h}^2 \int_{t_k}^t e^{2\lambda(s-t)} \dot{x}(s)^T U \dot{x}(s) ds \\
 & + (\bar{h}^2 \lambda^2 - \frac{\pi^2}{4}) \int_{t_k}^t e^{2\lambda(s-t)} (x(s) - x(t_k))^T U (x(s) - x(t_k)) ds \\
 & + 2\bar{h}^2 \lambda \int_{t_k}^t e^{2\lambda(s-t)} (x(s) - x(t_k))^T U \dot{x}(s) ds \\
 & + (t_{k+1} - t) \begin{bmatrix} x(t) \\ x(t_k) \end{bmatrix}^T \Omega \begin{bmatrix} x(t) \\ x(t_k) \end{bmatrix},
 \end{aligned} \tag{4.83}$$

defined for all $t \in [t_k, t_{k+1})$ and $k \in \mathbb{N}$, with matrix Ω defined as:

$$\Omega = \begin{bmatrix} \frac{X+X^T}{2} & -X + X_1 \\ * & -X_1 - X_1^T + \frac{X+X^T}{2} \end{bmatrix}. \tag{4.84}$$

Matrices $P, Q, Z, U \in \mathbb{S}_+^{n_x}$ and $X, X_1 \in \mathbb{R}^{n_x \times n_x}$ are of appropriate dimensions.

Compared to (4.9) and (4.50), the new aspect of LKF (4.83) is the fact that it involves the application of the derivative of the extended form of the Wirtinger inequality (terms with \bar{h}). The LKF includes classical $e^{2\lambda(s-t)}$ terms to follow the definition of deriving exponential stability conditions. Further, the functional V is continuous over the sampling interval $t \in [t_k, t_{k+1})$, however, it is discontinuous at times t_k as:

$$\begin{aligned}
 \lim_{t \rightarrow t_k^-} V(t, x(t), x_t, \dot{x}_t, k-1) = & x^T(t_k) P x(t_k) \\
 & + \int_{t_{k-1}}^{t_k} e^{2\lambda(s-t)} x(s)^T Q x(s) ds + \bar{h}^2 \int_{t_{k-1}}^{t_k} e^{2\lambda(s-t)} \dot{x}(s)^T U \dot{x}(s) ds \\
 & + (\bar{h}^2 \lambda^2 - \frac{\pi^2}{4}) \int_{t_{k-1}}^{t_k} e^{2\lambda(s-t)} (x(s) - x(t_k))^T U (x(s) - x(t_k)) ds \\
 & + 2\bar{h}^2 \lambda \int_{t_{k-1}}^{t_k} e^{2\lambda(s-t)} (x(s) - x(t_k))^T U \dot{x}(s) ds
 \end{aligned}, \tag{4.85}$$

4.4. Stability of non-linear sampled-data system with neural-network control

and
$$\lim_{t \rightarrow t_k^+} V(t_k, x(t_k), x_{t_k}, \dot{x}_{t_k}, k) = x^T(t_k)Px(t_k). \quad (4.86)$$

Note that this is because V has two discontinuous term $\int_{t_k}^t e^{2\lambda(s-t)}x(s)^TQx(s)ds$ and $\bar{h}^2 \int_{t_k}^t e^{2\lambda(s-t)}\dot{x}(s)^TU\dot{x}(s)ds + (\bar{h}^2\lambda^2 - \frac{\pi^2}{4}) \int_{t_k}^t e^{2\lambda(s-t)}(x(s) - x(t_k))^TU(x(s) - x(t_k))ds + 2\bar{h}^2\lambda \int_{t_k}^t e^{2\lambda(s-t)}(x(s) - x(t_k))^TU\dot{x}(s)ds$. These terms do not increase along the jumps at t_k . In fact they vanish after the jumps. Thus the limit $\lim_{t \rightarrow t_k^-} V(t, x(t), x_t, \dot{x}_t, k) \geq V(t_k, x(t_k), x_{t_k}, \dot{x}_{t_k}, k)$ holds. Thus, the proposed LKF is well adapted for exponential stability analysis of systems with time-varying sampling. In the following, we denote

$$\bar{V}(t) = V(t, x(t), x_t, \dot{x}_t, k) \text{ for all } t \in [t_k, t_{k+1}), k \in \mathbb{N}. \quad (4.87)$$

The exponential stability analysis based on Lemma 4.13 is thus divided into two steps.

- First, we prove that \bar{V} is continuous over $\mathbb{R}^+ \setminus \{t_k, k \in \mathbb{N}\}$ and differentiable for all $t \in [t_k, t_{k+1})$, and provide conditions for its positive definiteness.
- Then, we differentiate \bar{V} , upper-bound the obtained result and derive the exponential stability conditions.

4.4.2.2 Continuity, piece-wise differentiability, and positivity condition

Again, as a necessary first step, we propose Lemma 4.14 to ensure the functional's continuity, piece-wise differentiability, and positivity properties. Please note, Lemma 4.14 and Lemma 4.3 do seem similar, however, because \bar{V} is different, the steps involved to reach \bar{V} positive-definiteness conditions are different.

Lemma 4.14: The function \bar{V} defined in (4.87) is continuous over $\mathbb{R}^+ \setminus \{t_k, k \in \mathbb{N}\}$ and differentiable for all $t \neq t_k, k \in \mathbb{N}$. If its matrix parameters satisfy $P, Q, Z, U \in \mathbb{S}_+^{n_x}$ and $X, X_1 \in \mathbb{R}^{n_x \times n_x}$,

$$\left[\begin{array}{c} \left[\begin{array}{cc} P & 0 \\ 0 & 0 \end{array} \right] + \bar{h}\Omega \end{array} \right] \succ 0, \quad (4.88)$$

then \bar{V} is also positive definite, and there exists a scalar $\beta > 0$ such that $\bar{V} \geq \beta \|x(t)\|^2$ for all $t \geq 0$.

Proof: \bar{V} is defined on \mathbb{R}^+ , differentiable over each time interval $[t_k, t_{k+1})$, and is designed to satisfy,

$$\begin{aligned} \bar{V}(t_k^-) = & x^T(t_k)Px(t_k) + \int_{t_{k-1}}^{t_k} e^{2\lambda(s-t)}x(s)^TQx(s)ds \\ & + \bar{h}^2 \int_{t_{k-1}}^{t_k} e^{2\lambda(s-t)}\dot{x}(s)^TU\dot{x}(s)ds \\ & + (\bar{h}^2\lambda^2 - \frac{\pi^2}{4}) \int_{t_{k-1}}^{t_k} e^{2\lambda(s-t)}(x(s) - x(t_k))^TU(x(s) - x(t_k))ds \\ & + 2\bar{h}^2\lambda \int_{t_{k-1}}^{t_k} e^{2\lambda(s-t)}(x(s) - x(t_k))^TU\dot{x}(s)ds \end{aligned} \quad (4.89)$$

and $\bar{V}(t_k^+) = \lim_{t \rightarrow t_k^+} \bar{V}(t) = x(t_k)^T P x(t_k)$ for all $k \in \mathbb{N}$. It is therefore continuous and differentiable over $\mathbb{R}^+ \setminus \{t_k, k \in \mathbb{N}\}$. Now, we can say, \bar{V} can be positive definite if, and only if, for all $k \in \mathbb{N}$, $t \in [t_k, t_{k+1})$:

$$\begin{bmatrix} x(t) \\ x(t_k) \end{bmatrix}^T \left[\begin{bmatrix} P & 0 \\ 0 & 0 \end{bmatrix} + (t_{k+1} - t)\Omega \right] \begin{bmatrix} x(t) \\ x(t_k) \end{bmatrix} \geq 0, \quad (4.90)$$

with equality if and only if $x(t) = x(t_k) = 0$,

$$\int_{t_k}^t e^{2\lambda(s-t)} x(s)^T Q x(s) ds + (t_{k+1} - t) \int_{t_k}^t e^{2\lambda(s-t)} \dot{x}(s)^T Z \dot{x}(s) ds \geq 0, \quad (4.91)$$

$$\begin{aligned} & \bar{h}^2 \int_{t_k}^t e^{2\lambda(s-t)} \dot{x}(s)^T U \dot{x}(s) ds \\ \text{and,} \quad & + (\bar{h}^2 \lambda^2 - \frac{\pi^2}{4}) \int_{t_k}^t e^{2\lambda(s-t)} (x(s) - x(t_k))^T U (x(s) - x(t_k)) ds \\ & + 2\bar{h}^2 \lambda \int_{t_k}^t e^{2\lambda(s-t)} (x(s) - x(t_k))^T U \dot{x}(s) ds \geq 0. \end{aligned} \quad (4.92)$$

Note that the equation (4.92) is a derivative of the extension of the vector case of Wirtinger inequality [Liu *et al.* 2010] (see Theorem A.2 in Appendix A). i.e.

$$\frac{d}{dt} \left[e^{2\lambda(s-t)} \left(\bar{h}^2 \int_{t_k}^t \dot{x}(s)^T U \dot{x}(s) ds - \frac{\pi^2}{4} \int_{t_k}^t (x(s) - x(t_k))^T U (x(s) - x(t_k)) ds \right) \right] \geq 0. \quad (4.93)$$

Further as, $0 \leq t_{k+1} - t \leq \bar{h}$, remarking that the right part of (4.91) and the middle matrix term in the left part of (4.90) is linear with respect to $\rho = t_{k+1} - t$, one can use Theorem A.3 (in Appendix A) and show that a sufficient condition for \bar{V} to be positive definite is that, for all $k \in \mathbb{N}$, $t \in [t_k, t_{k+1})$:

$$x(t)^T P x(t) > 0, \text{ for all } x(t) \neq 0, \quad (4.94)$$

$$\text{and} \quad \begin{bmatrix} x(t) \\ x(t_k) \end{bmatrix}^T \left[\begin{bmatrix} P & 0 \\ 0 & 0 \end{bmatrix} + \bar{h}\Omega \right] \begin{bmatrix} x(t) \\ x(t_k) \end{bmatrix} \geq 0, \text{ for all } \begin{bmatrix} x(t) \\ x(t_k) \end{bmatrix} \neq 0. \quad (4.95)$$

The condition (4.95) is ensured by assuming that P is positive definite. Furthermore, if $P \succ 0$, then there exists scalar $\beta > 0$, such that for all $k \in \mathbb{N}$, $t \in [t_k, t_{k+1})$, $\left[\begin{bmatrix} P & 0 \\ 0 & 0 \end{bmatrix} + \bar{h}\Omega \right] \succ \beta \begin{bmatrix} I & 0 \\ 0 & 0 \end{bmatrix}$. Thus, $\bar{V}(t) \geq \beta \|x(t)\|^2$ for all $t \in [t_k, t_{k+1})$, $\forall k \in \mathbb{N}$. Therefore, there exists a scalar β , such that $\bar{V}(t) \geq \beta \|x(t)\|^2$ for all $t \geq 0$, which ends the proof. \square

4.4.2.3 Exponential stability conditions

Having proposed the conditions to ensure \bar{V} 's continuity, differentiability, and positivity, now, in order to analyse the exponential stability of system S , we will refer to Lemma

4.4. Stability of non-linear sampled-data system with neural-network control

4.13. The lemma is needed to provide conditions that satisfy,

$$\dot{\bar{V}}(t) + 2\lambda\bar{V}(t) \leq 0, \quad \forall t \neq t_k, \forall k \in \mathbb{N}. \quad (4.96)$$

In order to analyse this exponential stability condition, we study the restriction of $\dot{\bar{V}}$ on any interval $[t_k, t_{k+1})$, $k \in \mathbb{N}$. We compute:

$$\begin{aligned} \dot{\bar{V}}(t) + 2\lambda\bar{V}(t) = & \mathbf{He} \{x(t)^T P \dot{x}(t)\} + 2\lambda x(t)^T P x(t) + x(t)^T Q x(t) \\ & + (t_{k+1} - t) \dot{x}(t)^T Z \dot{x}(t) - \int_{t_k}^t e^{2\lambda(s-t)} \dot{x}(s)^T Z \dot{x}(s) ds \\ & + \bar{h}^2 \dot{x}(t)^T U \dot{x}(t) + 2\bar{h}^2 \lambda (x(t) - x(t_k))^T U \dot{x}(t) \\ & + (\bar{h}^2 \lambda^2 - \frac{\pi^2}{4}) \begin{bmatrix} x(t) \\ x(t_k) \end{bmatrix}^T \begin{bmatrix} U & -U \\ * & U \end{bmatrix} \begin{bmatrix} x(t) \\ x(t_k) \end{bmatrix} - \begin{bmatrix} x(t) \\ x(t_k) \end{bmatrix}^T \Omega \begin{bmatrix} x(t) \\ x(t_k) \end{bmatrix} \\ & + (t_{k+1} - t) \mathbf{He} \left\{ \begin{bmatrix} x(t) \\ x(t_k) \end{bmatrix}^T \Omega \begin{bmatrix} \dot{x}(t) \\ 0 \end{bmatrix} \right\} \\ & + 2\lambda(t_{k+1} - t) \begin{bmatrix} x(t) \\ x(t_k) \end{bmatrix}^T \Omega \begin{bmatrix} x(t) \\ x(t_k) \end{bmatrix}. \end{aligned} \quad (4.97)$$

Notice, because of presence of $e^{2\lambda(s-t)}$, it is not possible to apply Wirtinger and Bessel-Legendre inequality directly. However, since $\max(s-t) = \bar{h}, \forall t \in [t_k, t_{k+1})$, we compute an upper-bound of the integral term:

$$- \int_{t_k}^t e^{2\lambda(s-t)} \dot{x}(s)^T Z \dot{x}(s) ds \leq -e^{2\lambda\bar{h}} \int_{t_k}^t \dot{x}(s)^T Z \dot{x}(s) ds, \quad (4.98)$$

Next, using the Jensen inequality [Gu *et al.* 2003] (see Theorem A.1 in Appendix A), we compute an upper-bound of the right hand side of (4.98):

$$- \int_{t_k}^t \dot{x}(s)^T Z \dot{x}(s) ds \leq -(t - t_k) v_1(t)^T Z v_1(t), \quad (4.99)$$

with,
$$v_1(t) = \frac{1}{(t - t_k)} \int_{t_k}^t \dot{x}(s)^T ds = \frac{x(t) - x(t_k)}{t - t_k}. \quad (4.100)$$

Here, $v_1(t)$ continuity is well defined at $t = t_k$. It is because, when $t \rightarrow t_k$, $v_1(t) \rightarrow \dot{x}(t_k)$. Using majoration (4.98) and (4.99) in $\dot{\bar{V}}(t)$, equation (4.97) leads to

$$\begin{aligned} \dot{\bar{V}}(t) + 2\lambda\bar{V}(t) \leq & \mathbf{He} \{x(t)^T P \dot{x}(t)\} + 2\lambda x(t)^T P x(t) + x(t)^T Q x(t) \\ & + (t_{k+1} - t) \dot{x}(t)^T Z \dot{x}(t) - (t - t_k) e^{2\lambda\bar{h}} v_1(t)^T Z v_1(t) + \bar{h}^2 \dot{x}(t)^T U \dot{x}(t) \\ & + 2\bar{h}^2 \lambda (x(t) - x(t_k))^T U \dot{x}(t) - (\bar{h}^2 \lambda^2 - \frac{\pi^2}{4}) \begin{bmatrix} x(t) \\ x(t_k) \end{bmatrix}^T \begin{bmatrix} U & -U \\ * & U \end{bmatrix} \begin{bmatrix} x(t) \\ x(t_k) \end{bmatrix} \\ & - \begin{bmatrix} x(t) \\ x(t_k) \end{bmatrix}^T \Omega \begin{bmatrix} x(t) \\ x(t_k) \end{bmatrix} + (t_{k+1} - t) \mathbf{He} \left\{ \begin{bmatrix} x(t) \\ x(t_k) \end{bmatrix}^T \Omega \begin{bmatrix} \dot{x}(t) \\ 0 \end{bmatrix} \right\} \\ & + 2\lambda(t_{k+1} - t) \begin{bmatrix} x(t) \\ x(t_k) \end{bmatrix}^T \Omega \begin{bmatrix} x(t) \\ x(t_k) \end{bmatrix}. \end{aligned} \quad (4.101)$$

Further we apply the descriptor method from [Fridman 2010]. In order to do so, we consider equality (4.102) and (4.103),

$$0 = \mathbf{He} \left\{ [x(t)^T Y_1^T + \dot{x}^T(t) Y_2^T + x(t_k)^T T^T] [-x(t) + x(t_k) + (t - t_k)v_1(t)] \right\}, \quad (4.102)$$

$$0 = \mathbf{He} \left\{ [x(t)^T P_2^T + \dot{x}^T(t) P_3^T] \times \left[-\dot{x}(t) + \sum_{i=1}^p \sum_{j=1}^{n_h} w_i(x(t)) M_j(x(t_k)) (A_i x(t) + B_i G_j x(t_k)) \right] \right\}, \quad (4.103)$$

with some $n_x \times n_x$ arbitrary matrices P_2 , P_3 , Y_1 , Y_2 and T . These equalities are added to the right hand side of equation (4.101) expression. The purpose is to get the system dynamics into the Lyapunov condition and consider $\dot{x}(t)$ in extended state vector. Thus,

$$\begin{aligned} \dot{\bar{V}}(t) + 2\lambda \bar{V}(t) &\leq \mathbf{He} \left\{ x(t)^T P \dot{x}(t) \right\} + 2\lambda x(t)^T P x(t) + x(t)^T Q x(t) \\ &+ (t_{k+1} - t) \dot{x}(t)^T Z \dot{x}(t) - (t - t_k) e^{2\lambda \bar{h}} v_1(t)^T Z v_1(t) + \bar{h}^2 \dot{x}(t)^T U \dot{x}(t) \\ &+ 2\bar{h}^2 \lambda (x(t) - x(t_k))^T U \dot{x}(t) - \left(\bar{h}^2 \lambda^2 - \frac{\pi^2}{4} \right) \begin{bmatrix} x(t) \\ x(t_k) \end{bmatrix}^T \begin{bmatrix} U & -U \\ * & U \end{bmatrix} \begin{bmatrix} x(t) \\ x(t_k) \end{bmatrix} \\ &- \begin{bmatrix} x(t) \\ x(t_k) \end{bmatrix}^T \Omega \begin{bmatrix} x(t) \\ x(t_k) \end{bmatrix} + (t_{k+1} - t) \mathbf{He} \left\{ \begin{bmatrix} x(t) \\ x(t_k) \end{bmatrix}^T \Omega \begin{bmatrix} \dot{x}(t) \\ 0 \end{bmatrix} \right\} \\ &+ 2\lambda (t_{k+1} - t) \begin{bmatrix} x(t) \\ x(t_k) \end{bmatrix}^T \Omega \begin{bmatrix} x(t) \\ x(t_k) \end{bmatrix} \\ &+ \mathbf{He} \left\{ [x(t)^T Y_1^T + \dot{x}^T(t) Y_2^T + x(t_k)^T T^T] [-x(t) + x(t_k) + (t - t_k)v_1(t)] \right\} \\ &+ \mathbf{He} \left\{ [x(t)^T P_2^T + \dot{x}^T(t) P_3^T] \times \left[-\dot{x}(t) + \sum_{i=1}^p \sum_{j=1}^{n_h} w_i(x(t)) M_j(x(t_k)) (A_i x(t) + B_i G_j x(t_k)) \right] \right\}. \end{aligned} \quad (4.104)$$

Let us now introduce the augmented state vector $\zeta(t) \in \mathbb{R}^{4n_x}$:

$$\zeta(t) = [x^T(t), x^T(t_k), v_1^T(t), \dot{x}^T(t)]. \quad (4.105)$$

Then, there exist matrices $M_{ij}^{(0)}$, $M^{(1)}$ and $M^{(2)}$ for all $i \in \{1, \dots, p\}$ and $j \in \{1, \dots, n_h\}$ such that:

$$M_{ij}^{(0)} = \begin{bmatrix} M_{ij,A}^{(0)} & M_{ij,B}^{(0)} & 0 & M_{ij,C}^{(0)} \\ * & M_{ij,D}^{(0)} & 0 & M_{ij,E}^{(0)} \\ * & * & 0 & 0 \\ * & * & * & M_{ij,F}^{(0)} \end{bmatrix}, \quad (4.106)$$

$$M^{(1)} = \begin{bmatrix} M_A^{(1)} & M_B^{(1)} & 0 & M_C^{(1)} \\ * & M_D^{(1)} & 0 & M_E^{(1)} \\ * & * & 0 & 0 \\ * & * & * & Z \end{bmatrix}, \quad (4.107)$$

4.4. Stability of non-linear sampled-data system with neural-network control

$$M^{(2)} = \begin{bmatrix} 0 & 0 & Y_1^T & 0 \\ * & 0 & T^T & 0 \\ * & * & -e^{-2\lambda\bar{h}}Z & Y_2 \\ * & * & * & 0 \end{bmatrix}, \quad (4.108)$$

with,

$$\begin{aligned} M_{ij,A}^{(0)} &= \lambda(P + P^T) + Q + (\bar{h}^2\lambda^2 - \frac{\pi^2}{4})U - \frac{X+X^T}{2} + P_2^T A_i + A_i^T P_2 - Y_1 - Y_1^T, \\ M_{ij,B}^{(0)} &= -(\bar{h}^2\lambda^2 - \frac{\pi^2}{4})U - (-X + X_1) + P_2^T B_i G_j + Y_1^T - T, \\ M_{ij,C}^{(0)} &= P + \bar{h}^2\lambda U - P_2^T - Y_2 + A_i^T P_3, \\ M_{ij,D}^{(0)} &= (\bar{h}^2\lambda^2 - \frac{\pi^2}{4})U - (-X_1 - X_1^T + \frac{X+X^T}{2}) + T^T + T, \\ M_{ij,E}^{(0)} &= -\bar{h}^2\lambda U + Y_2 + G_j^T B_i^T P_3, \\ M_{ij,F}^{(0)} &= \bar{h}^2 U - P_3^T - P_3, \\ M_A^{(1)} &= 2\lambda \frac{X+X^T}{2}, \\ M_B^{(1)} &= 2\lambda(-X + X_1), \\ M_C^{(1)} &= \frac{X+X^T}{2}, \\ M_D^{(1)} &= 2\lambda(-X_1 - X_1^T + \frac{X+X^T}{2}), \\ M_E^{(1)} &= (-X + X_1)^T, \end{aligned}$$

Using these matrix notation, we can rewrite (4.104) as

$$\begin{aligned} \dot{\bar{V}}(t) + 2\lambda\bar{V}(t) &\leq \sum_{i=1}^p \sum_{j=1}^{n_h} w_i(x(t)) M_j(x(t_k)) \zeta(t)^T M_{ij}^{(0)} \zeta(t) \\ &\quad + (t_{k+1} - t) \zeta(t)^T M^{(1)} \zeta(t) + (t - t_k) \zeta(t)^T M^{(2)} \zeta(t). \end{aligned} \quad (4.109)$$

Since, $\sum_{i=1}^p \sum_{j=1}^{n_h} w_i(x(t)) M_j(x(t_k)) = 1$, $\forall i \in \{1, \dots, q\}, j \in \{1, \dots, n_h\}$, equation (4.109) can be rewritten as:

$$\begin{aligned} \dot{\bar{V}}(t) + 2\lambda\bar{V}(t) &\leq \\ \sum_{i=1}^p \sum_{j=1}^{n_h} w_i(x(t)) M_j(x(t_k)) &\left[\zeta(t)^T \left[M_{ij}^{(0)} + (t_{k+1} - t) M^{(1)} + (t - t_k) M^{(2)} \right] \zeta(t) \right]. \end{aligned} \quad (4.110)$$

Similar to equation (4.34) and (4.71), since equation (4.110) is also linear in the variable t , we follow similar steps to reduce the number of conditions to be checked to a finite number by applying Theorem A.3 (in the Appendix A), with the variable $\rho = t \in [t_k, t_{k+1})$. We thus obtain two inequalities, both linear in the variable $t_{k+1} - t_k$. Thus we can use once again Theorem A.3 (in the Appendix A) with the variable $\rho = t_{k+1} - t_k \in [0, \bar{h}]$ to prove that if the four inequalities $\zeta(t)^T \Xi_{ij} \zeta(t) \preceq 0$ are satisfied for all $\zeta(t) \in \mathbb{R}^{4n_x}$, $i \in \{1, \dots, q\}$ and $j \in \{1, \dots, n_h\}$, with Ξ_{ij} defined as

$$\Xi_{ij} = \begin{cases} M_{ij}^{(0)}, \\ M_{ij}^{(0)} + \bar{h} M^{(1)}, \\ M_{ij}^{(0)} + \bar{h} M^{(2)}, \\ M_{ij}^{(0)} + \bar{h} M^{(1)} + \bar{h} M^{(2)}, \end{cases} \quad (4.111)$$

then, $\dot{\bar{V}}(t) + 2\lambda\bar{V}(t) \leq 0$ for all $t \in [t_k, t_{k+1})$, $k \in \mathbb{N}$. Again we considered any sampling sequence $h_k = t_{k+1} - t_k \in [0, \bar{h}]$. Therefore, the exponential stability results we obtained will be valid for any sampling sequence satisfying (4.77). Further, since we have shown that $\dot{\bar{V}}(t) \leq -2\lambda\bar{V}(t)$ for all $t \in [t_k, t_{k+1})$, $k \in \mathbb{N}$, we find

$$\bar{V}(t) \leq e^{-2\lambda(t-t_0)}\bar{V}(t_0). \quad (4.112)$$

Therefore, we will have the following theorem.

Theorem 4.15: Consider scalars $\lambda > 0$ with matrices $G_j \in \mathbb{R}^{n_u \times n_x}$, $j \in \{1, \dots, n_h\}$, with maximum sampling interval \bar{h} . Then, the perturbed system S is exponentially stable with decay-rate λ for any sampling sequence satisfying (4.77), if there exist matrices $P, Q, Z, U \in \mathbb{S}_+^{n_x}$ and arbitrary matrices $X, X_1, Y_1, Y_2, T, P_2, P_3 \in \mathbb{R}^{n_x \times n_x}$ such that (4.95) and (4.111) satisfy, for all $i \in \{1, \dots, q\}$ and $j \in \{1, \dots, n_h\}$.

Remark 4.16: Similar to Remark 3 from [Hu *et al.* 2018], It can be seen from Theorem 4.15 that the LMI's for exponential stability depend only on the hidden node to outer node parameter, G_j but not on front node to outer node parameter or the plant parameters $w_i(x(t))$, $\forall i \in \{1, \dots, p\}$. Further, if plant parameter uncertainties are related only to w_i but not to A or B matrices, then the robust exponential stability of the closed-loop system (4.78) with respect to w_i is obtainable.

Remark 4.17: Similar to Remark 4.6, when searching for solutions of LMIs (4.95) and (4.111), one needs to remove the zero rows/columns that may appear in (4.111) since LMI solvers search for strict solutions. Indeed, one can see that $M_{ij}^{(0)}$ and $M^{(1)}$ in Ξ_{ij} are independent of v_1 .

Remark 4.18: The choice of a non-linear time-varying system to represent Driver-Train interaction and a NN controller to represent ADAS did expanded the scope of exponential stability study of ADAS-Driver-Train interaction via system modelling approach. However, while deriving the LMI condition, the choice of Jensen inequality to upper-bound the integral terms added conservativeness to the proof.

4.4.3 Discussion

This section has proposed a stability analysis allowing to estimate maximum time-varying sampling period \bar{h} , while ensuring exponential stability for NN-based control of non-linear systems. The study is based on a new class of LKF involving application of derivative of extension of Wirtinger inequality that reduce the conservatism of time-varying sampling.

However, we would like to highlight that compared to previous abstractions, the approach did not consider the estimated exogenous perturbations. It was assumed that the driver and the train can be represented together by a continuous non-linear time-varying system, while ADAS by a NN controller to study the closed-loop system stability.

The modelling and stability approach was indeed a necessary step to improve system description and stability approach. In the future works, we would like to separate the driver and the train representation, i.e. in addition to the non-linear system representation for the train, we would like to consider the time-varying gain, $K(d(t))$ for the driver, to derive closed-loop stability conditions. We would also like to consider the integral action by the driver and its influence on the time-varying sampled stability context.

Further, while deriving the LMI conditions, the choice of Jensen inequality to upper-bound the integral term can be replaced by either Wirtinger or affine Bessel-Legendre inequality. In addition, to further improve the results, a combination of augmented LKF and affine Bessel-Legendre to study the exponential stability problem may provide a further improved maximum time-varying sampling interval \bar{h} , that will ensure the closed-loop system stability.

4.5 Algorithm to find maximum sampling period

In the previous sections, we presented three methods to stabilise the ADAS-Driver-Train system, in the presence of delayed sensor measurements and a varying driver behaviour. In the following we provide steps of a search algorithm that uses the stability conditions from either of the three approaches, to find the maximum sampling period \bar{h} . The computational steps of the algorithm are as follows:

1. If abstraction 1, then:
 - Fix values of $\gamma_1, \gamma_2; G_1, G_2$ gains of state-feedback controller and $K_i, i \in \{1, \dots, q\}$ gains of the convex polytope of $K(d(t))$,
 - Decide a range $[h_{min}, h_{max}]$ to test \bar{h} ,
 - Test the LMI from (4.35) for the system (4.6) with $\gamma_1, \gamma_2, G_1, G_2, K_i$ and the maximum sampling interval, h_{max} ,
2. If abstraction 2, then:
 - Fix values of $\gamma_1, \gamma_2; G_{1,j}, G_{2,j}, j \in \{1, \dots, n_h\}$ gains of NN controller and $K_i, i \in \{1, \dots, q\}$ gains of the convex polytope of $K(d(t))$,
 - Decide a range $[h_{min}, h_{max}]$ to test \bar{h} ,

- Test the LMI from (4.72) for the system (4.49) with $\gamma_1, \gamma_2, G_{1,j}, G_{2,j}, j \in \{1, \dots, n_h\}, K_i, i \in \{1, \dots, q\}$ and the maximum sampling interval, h_{max} ,
3. If abstraction 3, then:
- Fix values of λ and $G_j, j \in \{1, \dots, n_h\}$ gains of NN controller,
 - Decide a range $[h_{min}, h_{max}]$ to test \bar{h} ,
 - Test the LMI from (4.111) for the system (4.78) with $\lambda, G_j, j \in \{1, \dots, n_h\}$ and maximum sampling interval, h_{max} ,
4. If the LMI are solved, \bar{h} is h_{max} . Now set $h_{min} = h_{max}$ and $h_{max} = \frac{h_{max} + \bar{h}}{2}$ and go to 3rd step of the appropriate abstraction to test the LMI with new h_{max} ,
5. If the LMI are not solved, set $h_{max} = \frac{h_{min} + h_{max}}{2}$ while keeping h_{min} the same and go to 3rd step of the appropriate abstraction to test the LMI with new h_{max} ,
6. Keep solving the LMI until $h_{max} - h_{min} > 0.0001$. Here, 0.0001 decides the desired precision of \bar{h} .

Keep in mind that all the steps in the algorithm are computed off-line, i.e. The maximum sampling interval \bar{h} is computed with the help of a numerical solver such as MOSEK or YALMIP in MATLAB before the controller gains in the three abstraction are implemented.

4.6 Conclusion

In this chapter, we presented three modelling abstractions to deal with ADAS-Driver-Train closed-loop stability problem, in the presence of delays in sensor measurement and driver behaviour variation. The chapter presented progressive evolution of the manner in which the problem is addressed.

The first abstraction presented a stability study of a state-feedback controlled sampled-data LTI system in the presence of time-varying sampling and a time-varying gain. The stability conditions utilised time-dependent LKF based on Wirtinger inequality, used Jensen inequality for upper-bounding integral terms of LKF derivative, and finally used convexity arguments to obtain stability conditions in the form of LMIs.

The second abstraction presented a stability study of a NN controlled sampled-data LTI system in the presence of time-varying sampling and a time-varying gain. The stability conditions utilised augmented time-dependent LKF, used affine Bessel-Legendre inequality for upper-bounding integral terms of LKF derivative, and finally used convexity arguments to obtain stability conditions in the form of LMIs.

Finally, the third abstraction presented a stability study of a NN controlled non-linear sampled system (represented in the form of time-varying T-S system) in the presence of time-varying sampling. The stability conditions again utilised time-dependent LKF based on derivative of Wirtinger inequality, used Jensen inequality for upper-bounding integral terms of LKF derivative, and finally used convexity arguments to obtain stability conditions in the form of LMIs.

The first and second abstraction were intended to address a simple stability scenario, such as cruise control scenario. For this purpose, linear Driver-Train system modelling and two varying complexity ADAS control models were considered. For the third abstraction, both Driver-Train and ADAS models were upgraded and a relatively conservative stability criteria was considered, to fit tight performance requirements, i.e. exponential stability and also to increase the horizon of applicability of the obtained results.

In the next chapter, we will implement the three abstractions on a Driver-Train model and compare the stability results of different approaches.

Application to stability analysis of driver-in-the-loop train control

Contents

| | | |
|------------|--|------------|
| 5.1 | Introduction | 125 |
| 5.2 | Simulation protocol | 126 |
| 5.3 | 1st abstraction: Stability of perturbed linear Driver-Train system with a state-feedback based ADAS | 131 |
| 5.3.1 | System description | 131 |
| 5.3.2 | Simulation studies | 132 |
| 5.4 | 2nd abstraction: Stability of perturbed linear Driver-Train system with a neural-network based ADAS | 136 |
| 5.4.1 | System description | 136 |
| 5.4.2 | Simulation studies | 138 |
| 5.5 | 3rd abstraction: Stability of non-linear Driver-Train system with neural-network based ADAS | 141 |
| 5.5.1 | System description | 141 |
| 5.5.2 | Simulation studies | 142 |
| 5.6 | Conclusion | 147 |

5.1 Introduction

In the previous chapter, we presented time-delay system stability based solutions for the ADAS-Driver-Train system stability in midst of unreliable driver and train state measurements. The estimation of maximum admissible measurement delay was studied for three modelling abstractions, namely, perturbed sampled-data LTI system with a state-feedback, perturbed sampled-data LTI system with NN controller and non-linear sampled-data system with NN controller. In this chapter, we will utilise these frameworks to study the driver-in-the-loop train control stability.

The chapter is organised as follows: First, Section 5.2 presents the driver advisory control simulation context. In the next three sections, i.e. 5.3, 5.4 and 5.5, we consider the three modelling abstractions sequentially. In each section we first present a system description, i.e. train model, driver model, ADAS model and the closed-loop equation. Then, we present simulations for three different scenarios. Lastly, we compare simulation results with other abstractions to illustrate the effectiveness of the proposed approach. Finally, Section 5.6 summarises the results obtained in this chapter.

5.2 Simulation protocol

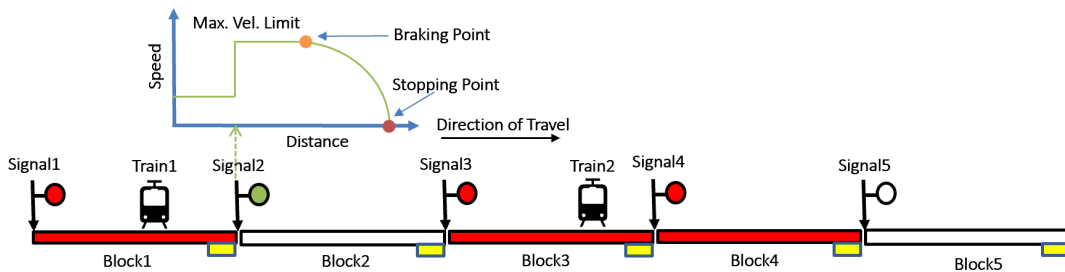


Figure 5.1: Simulation scenario: Railway traffic control of Train 1

For simulation purpose, we considered railway traffic control of a high-speed train travelling through several blocks as shown in Fig. 5.1. When the train approaches a new block, the train position is detected, sent to the dispatcher and in return a new reference speed is sent back to the train via in-cabin signalling system.

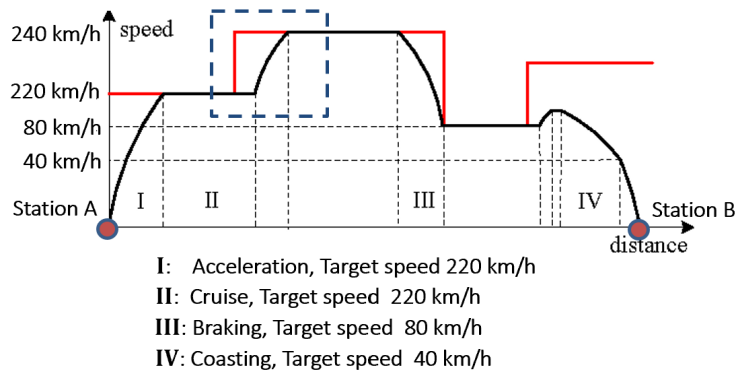


Figure 5.2: Typical train speed-distance trajectory

A typical speed-distance trajectory of the train is shown in Fig. 5.2. The red curve indicates the speed-limit signals from railway traffic control center and the black curve is

the actual train operation speed during the journey from station A to station B. However, we are interested in the journey period, when a dispatcher sends the signal to accelerate the train speed from 220km/h to 240km/h,

$$v_r(t) = \begin{cases} 220 \text{ km/h,} & \text{if } 0s \leq t < 1500s, \\ 240 \text{ km/h,} & \text{if } 1500s \leq t < 12000s, \end{cases} \quad (5.1)$$

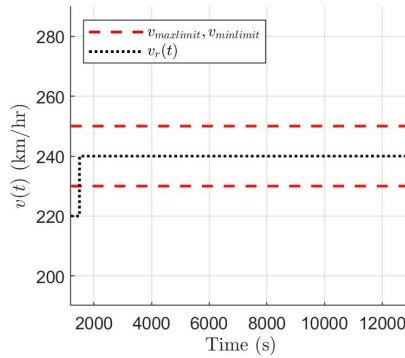


Figure 5.3: Reference speed

Moreover, in later simulations, the assumption of constant reference is relaxed by considering a varying speed reference that gradually increases as follows:

$$v_r(t) = \begin{cases} 220 \text{ km/h,} & \text{if } 0s \leq t < 1500s, \\ 220 + 10\left(\frac{2}{(1+\exp(-7(\frac{t-1500}{300}))+7))}\right) \text{ km/h,} & \text{if } 1500s \leq t < 2100s, \\ 240 \text{ km/h,} & \text{if } 2100s \leq t < 12000s, \end{cases} \quad (5.2)$$

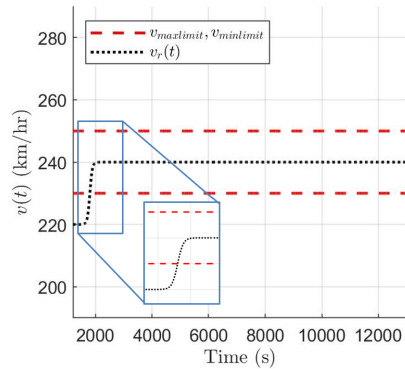


Figure 5.4: Varying reference speed

We recall the driver advisory train control system in Fig. 5.5. Once the reference speed is sent by the railway traffic control, the driving advices are generated using sampled train

speed tracking error and sampled driver state measurements from driver attention level detection system. Particularly, the driver is provided with graphical/text information about the level of acceleration/braking control actions.

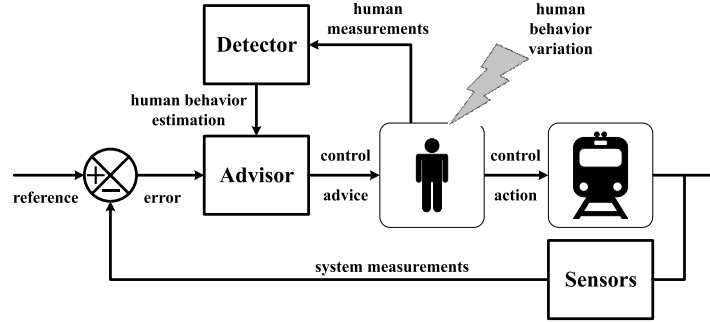


Figure 5.5: Driver-in-the-loop advisory control scheme

Further, we consider that the driver is able to accelerate the train to the new cruise speed. However, while maintaining the new cruise speed, the driver behaviour starts varying according to the equation,

$$K(d(t)) = K_{nom} + \Delta K d(t), \quad (5.3)$$

with $d(t) \in \mathcal{L}_2$ as the unknown exogenous disturbance, and $\Delta K = K_{max} - K_{nom}$ with K_{nom} and K_{max} as the nominal and maximum gains. Considering these parameters, the driver behaviour variation is as shown in Fig. 5.6.

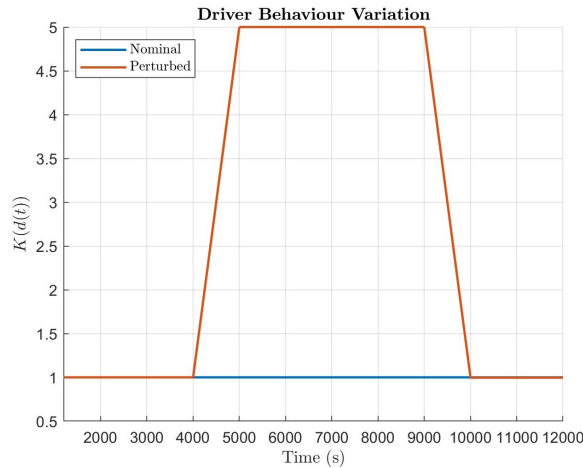


Figure 5.6: The nominal $K(d(t)) = K_{nom}$ and varying $K(d(t))$ driver gain

If $K = K_{nom}$, then the driver interprets the advices correctly. Moreover, it also signify that the driver is contributing positively to the closed-loop stability, i.e. closed-loop poles

are in negative half plane. However, when $K = K_{max}$ then the driver misinterprets/discards the advices. Therefore the driver might be destabilising the closed-loop and the **ADAS** based advice needs to adjust accordingly.

For simulation purposes, the nominal and maximum gains are considered to be $K_{nom} = 1$ and $K_{max} = 5$ respectively. Without loss of generality, the disturbance is considered as $d(t) \in [0, 1]$. The duration of the perturbation is considered to be 6000s, i.e. from $t_{dstart} = 4000s$ to $t_{dend} = 10000s$, with rise and recovery time of 1000s.

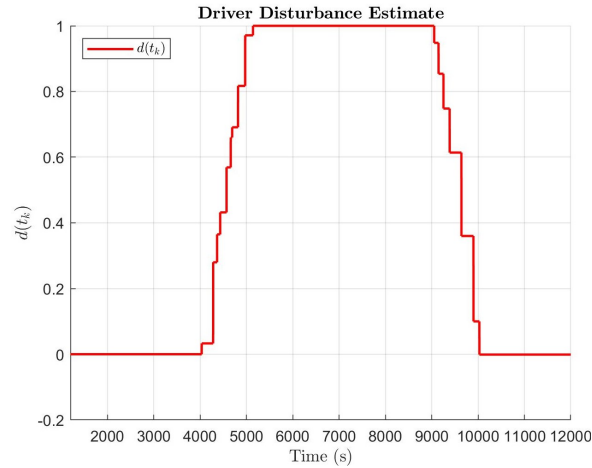


Figure 5.7: The estimated driver state $\hat{d}(t_k)$

The driver attention level is detected based on physical features (eye, mouth, face/head state based) or can also be from train features (current/advised actuator level). However, the estimates are available only at specific times to the driver advisory system. A sample estimate of driver attention, with $\bar{h} \sim 4min$, is shown in Fig. 5.7.

Further, we also consider a wind gust disturbance acting on the train. Here, the wind disturbance is assumed to last during the interval $[t_{dstart}, t_{dend}]$. The start and end time of the disturbance is usually unknown, however, for a realistic scenario we consider it as,

$$w(t) = \begin{cases} 0.002 \sin(0.01t) & \text{if } t_{dstart} < t < t_{dend} \\ 0 & \text{otherwise.} \end{cases} \quad (5.4)$$

Considering this situation, our objective is to assess the maximum admissible delay in driver and train measurements, until which, the driver-in-the-loop train control is stable. For this purpose, we will use Theorems 4.4, 4.9 & 4.15 and corresponding \bar{h} search algorithms, as proposed in the contribution chapter, for the following three scenarios.

1. **Non functional ADAS:** This scenario considers interaction of driver and train without an **ADAS**, i.e. no driver advisory signals as shown in Fig. 5.8.

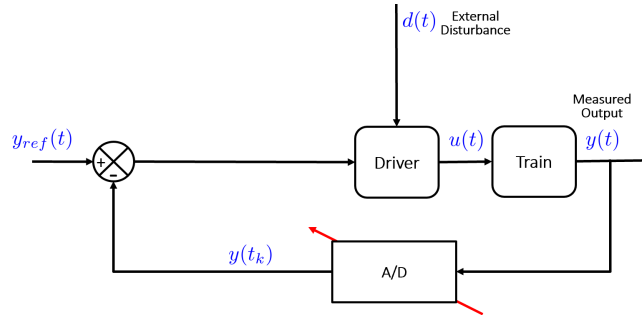


Figure 5.8: Closed-loop system schematic with non-functional ADAS

2. **Partially functional ADAS (with train measurements only):** This scenario considers interaction of driver and train via an ADAS, however, driver advisory signals are based only on train state measurements as shown in Fig. 5.9.

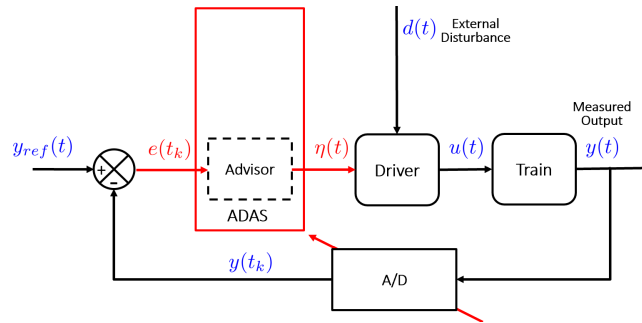


Figure 5.9: Closed-loop system schematic with partially functional ADAS

3. **Fully functional ADAS (with both train and driver measurements):** This scenario considers interaction of driver and train via an ADAS, however, driver advisory signals are based on both driver and train state measurements as shown in Fig. 5.10.

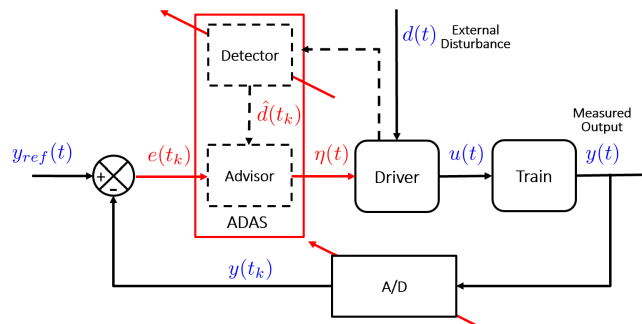


Figure 5.10: Closed-loop system schematic with Fully functional ADAS

In the following sections we will first present each abstraction and then study the three scenarios for each case. In our discussion, we will compare the results of different scenarios for each abstraction and then of different abstractions.

5.3 1st abstraction: Stability of perturbed linear Driver-Train system with a state-feedback based ADAS

In this section, we considered train, driver and ADAS model as a sampled-data LTI system, a time-varying gain and a state-feedback controller respectively.

5.3.1 System description

Train model: We considered a single-point train dynamics model subject to rolling mechanical resistance and aerodynamic drag. Since the train is running at a constant cruise speed, i.e. $v_r(t) \equiv v_r = \text{const}$, we can get the linearised error dynamical equation around the equilibrium state ($\dot{v}_r(t) = 0$) as,

$$\dot{e}(t) = Ae(t) + Bu(t) - k_0 - k_1v_r - k_2v_r^2, \quad (5.5)$$

where, $e(t) = v(t) - v_r(t)$, $A = -k_1 - 2k_2v_r$, $B = 1/m$. The train parameters are chosen from the experimental results of Japan Shinkansen train [Maeda *et al.* 1989], Table 5.1. However we considered only partial knowledge of the drag coefficients, i.e. the values used for calculus are slightly different than those used by the simulated train, by 5-10%.

| Symbol | Value | Unit |
|--------|----------------------|--------------------------------|
| m | 800×10^3 | kg |
| k_0 | 0.01176 | N/kg |
| k_1 | 0.00077616 | $N \text{ s}/m \text{ kg}$ |
| k_2 | 1.6×10^{-5} | $N \text{ s}^2/m^2 \text{ kg}$ |

Table 5.1: Parameters of the train.

Driver model: We choose the following equation for driver control response,

$$\begin{aligned} u(t) &= \hat{u}(t) + \bar{u}(t), \\ \hat{u}(t) &= K(d(t))\eta(t), \end{aligned} \quad (5.6)$$

where, $K(d(t))$ is the ability of the driver to interpret the advised control action $\eta(t)$. Together, $\hat{u}(t)$ and $\bar{u}(t)$ constitute driver control to maintain the cruise speed, with $\bar{u}(t) = B^{-1}(k_0 + k_1v_r + k_2v_r^2) - K_{nom}G_2d_{nom}$ as the reference control and $\hat{u}(t)$ as the stabilizing/robust control.

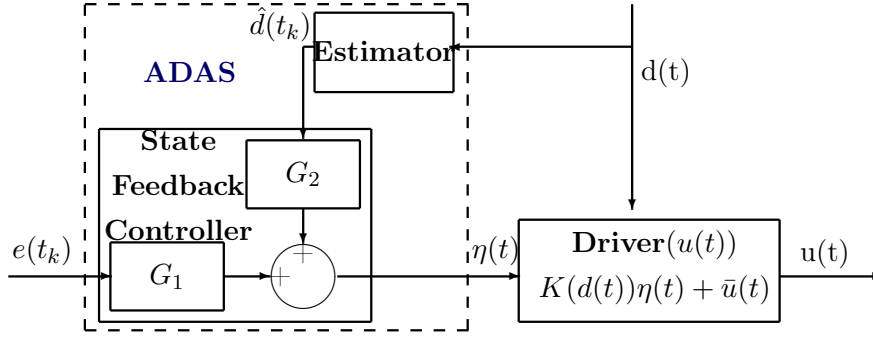


Figure 5.11: ADAS-Driver control schematic

ADAS model: The state-feedback controller based ADAS model is considered as,

$$\eta(t) = G_1 e(t_k) + G_2 \hat{d}(t_k), \quad (5.7)$$

with t_k is the k^{th} sampling instant satisfying $t_k, k \in \mathbb{N}$,

$$t_0 = 0, 0 < t_{k+1} - t_k \leq \bar{h}, \lim_{k \rightarrow \infty} t_k = \infty, \quad (5.8)$$

where, $e(t_k)$ and $\hat{d}(t_k)$ are the speed error and driver state measurement at time t_k , respectively. The advisory control $\eta(t)$ will adjust according to the driver current behaviour using appropriate values of G_1 and G_2 gains. The G_1 can be obtained by pole-placement, while G_2 gain value can be obtained by considering the fact that at nominal driving condition $\hat{d}(t_k) = d_{nom}$ and $K_{nom}G_2\hat{d}(t_k) - B^{-1}(k_0 + k_1v_r + k_2v_r^2) = const$ should satisfy.

Closed-loop system: We obtain the ADAS-Driver-Train closed-loop error dynamics as,

$$\dot{e}(t) = Ae(t) + BK(d(t))G_1e(t_k) + BK(d(t))G_2w_1(t) + Bw_2(d(t)). \quad (5.9)$$

with, $t_k \leq t < t_{k+1}, k \in \mathbb{N}, w_1(t) = \hat{d}(t_k) - d_{nom}$ and $w_2(d(t)) = (K(d(t)) - K_{nom})G_2d_{nom}$ as small perturbations corresponding to the measurement delays and deviation from the nominal performance, varying with an unknown exogenous perturbation, $d(t) \in \mathcal{L}_2$.

The objective is to find an estimate of the largest allowable sampling interval \bar{h} in (5.8) for some given ADAS gains G_1 and G_2 , using Theorem 4.4 while guaranteeing \mathcal{L}_2 -stability of the closed-loop system.

5.3.2 Simulation studies

In this subsection, we test the three scenarios to verify the effectiveness of state-feedback based ADAS to reduce the tracking error in the presence of varying driver behaviour.

5.3.2.1 Non functional ADAS

In this scenario we consider that there is no ADAS installed on the train. Thus, when the driver is inattentive, no driver advisory control signals will be available. In order to simulate this case, we considered $G_1 = 1$ and $G_2 = 0$ and considered $\bar{h} = 1s$. Fig. 5.12 shows the speed $v(t)$ response for two possibilities of this scenario, i.e. driver with a stable/nominal behaviour K_{nom} and a varying/ab-nominal behaviour $K(d(t))$. The following observation can be made from Fig. 5.12.

- When the driver’s state is nominal, he accurately follows the reference train speed even during the wind disturbance.
- However, when the driver’s state is impacted by $d(t)$, the train speed tracking performance decreases even with speed measurement delay of $\bar{h} = 1s$.

Remark 5.1: The speed divergence of the Fig. 5.12 indicate that if the driver is insufficiently attentive, he is unable to apply the required controller level and follow the reference speed advice correctly. However, the divergence is exaggerated by the simulation, because the considered driver’s model is valid for speed tracking. In reality, the driver’s actions are more sophisticated. The tracking performance losses at the security level are compensated by other means than the ADAS.

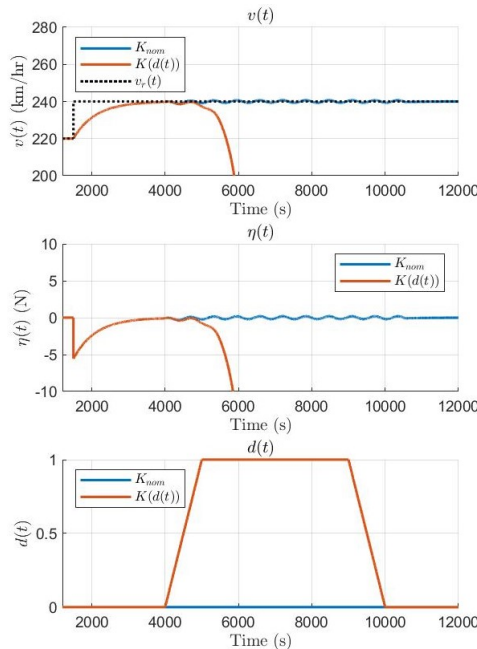


Figure 5.12: The response of $v(t)$, $\eta(t)$ and $d(t)$ without ADAS assistance to nominal (blue) and varying driver behaviour (red)

5.3.2.2 Partially functional ADAS (with train measurements only)

In this scenario we consider a driver advisory system with partial functionality. Thus, the ADAS helps the driver by providing advisory control signal based only on delayed train speed measurements, i.e. $\eta(t) = G_1 e(t_k)$. Fig. 5.13 gives speed $v(t)$ response considering a varying driver behaviour $K(d(t))$. In order to simulate this scenario, we considered the controller gains as $G_1 = -1$ by pole-placement method and $G_2 = 0$ and obtained $\bar{h} \sim 5min$ for $\gamma_1, \gamma_2 = 15$. The following observation can be made from Fig. 5.13.

- If the delay in train speed measurement gradually increases from $0s \rightarrow 180s \rightarrow 285s$, the train cruise control stability will become more and more compromised. Moreover, the speed tracking performance will decrease with bigger values of the delay \bar{h} .
- The train speed of yellow plot with maximum sampling period $\bar{h} \sim 285s$ compared to red plot with maximum sampling period of $\bar{h} \sim 180s$ is unstable because LMIs of Theorem 4.6 are solvable only for $\bar{h} < 285s$.

Remark 5.2: The speed divergence of the Fig. 5.13 models the discrepancy arising due to driver’s inability to follow ADAS advice exactly. In reality, the discordant advises of the ADAS would be rejected by the driver, who will rather drive on sight. This will nullify practical benefits of ADAS and rather reduce ADAS’s acceptability by the drivers.

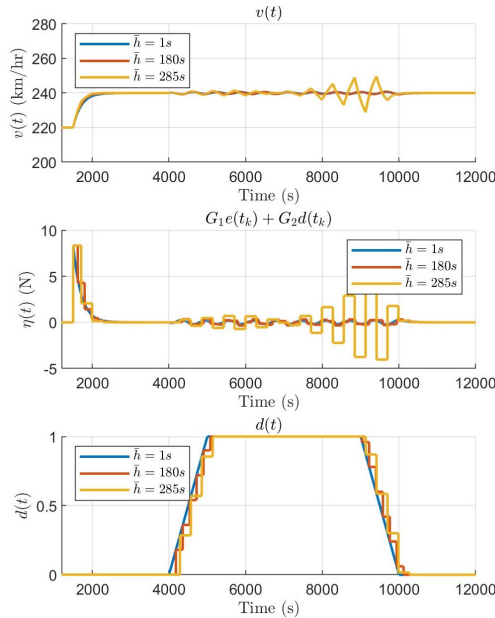


Figure 5.13: The response of $v(t)$, $\eta(t)$ and $d(t)$ with static-feedback based ADAS assistance to varying driver behaviour for only train speed measurements

5.3.2.3 Fully functional ADAS (with both train and driver measurements)

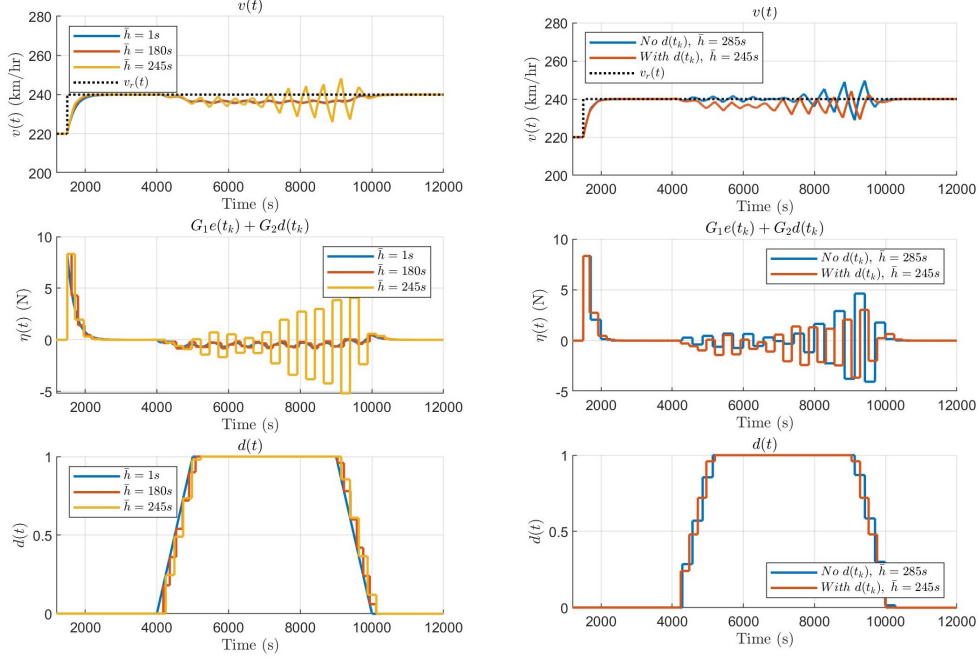


Figure 5.14: a) The response of $v(t)$, $\eta(t)$ and $d(t)$ with static-feedback based ADAS assistance to varying driver behaviour for both train speed and driver state measurements b) Comparison of the response of $v(t)$, $\eta(t)$ and $d(t)$ with static-feedback based ADAS assistance to varying driver behaviour for only train speed measurements (blue) and for both train speed and driver state measurements (red)

In this scenario, we consider that the driver advisory system is present with full functionality. Compared to previous scenarios, ADAS will help the driver by adjusting the advisory control signal $\eta(t)$ based on both the time-delayed train speed $e(t_k)$ and driver state $\hat{d}(t_k)$ measurements. Thus, the advisory control signal $\eta(t)$ given by (5.7), depends on both, $G_1 e(t_k)$ and $G_2 \hat{d}(t_k)$. Fig. 5.14 gives speed $v(t)$ response for this scenario considering a varying driver behaviour $K(d(t))$. In order to simulate this scenario, we considered the controller gains as $G_1 = -1$ by pole-placement method and $G_2 = -2$, and obtained $\bar{h} \sim 4min$ for $\gamma_1, \gamma_2 = 15$. The negative G_1 value will keep the closed-loop poles in negative half plane, whereas, a negative G_2 value will actively correct the ab-nominal driver behaviour. The following observations can be made from Fig. 5.14.

- Similar to previous scenario, if delay in train speed and driver state measurement gradually increases from $0s \rightarrow 180s \rightarrow 245s$, the train cruise control is compromised and the tracking performance is deteriorated.
- However, notice from the yellow plot corresponds to $\bar{h} \sim 245s$, i.e. the maximum

delay until which stability can be guaranteed. This is because the LMIs of Theorem 4.6 are solvable only for $\bar{h} < 245s$.

- Moreover, when the train speed and driver state measurements are within the maximum delay limit, the cruise speed decreases during inattentiveness of the driver. The steady state error depends on G_2 design and signify the impact of delayed driver state on the stability of the ADAS-Driver-Train closed-loop system.
- The smaller value of \bar{h} in this scenario further signify that when ADAS considers time-delayed driver state signals to decide driver advisory signal, the time-delay margin for closed-loop system stability is decreased. This means that injecting two delayed measurements will induce less stability, which is logical.

5.4 2nd abstraction: Stability of perturbed linear Driver-Train system with a neural-network based ADAS

In this section, we consider train, driver and ADAS modelled as a sampled-data LTI system, a time-varying gain and a NN controller respectively.

5.4.1 System description

Compared to the previous modelling abstraction, for this approach, we considered the same train and driver model. However, we considered a NN controller for ADAS representation. Thus, we will only present ADAS-Driver control model.

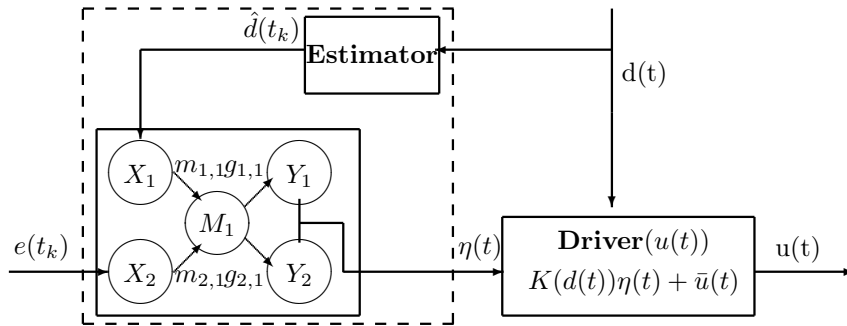


Figure 5.15: NN-based ADAS-Driver control schematic

ADAS model:

The NN controller based ADAS model is considered as,

$$\eta(t) = \sum_{j=1}^{n_h} M_j(X(t_k)) [G_{1,j}e(t_k) + G_{2,j}\hat{d}(t_k)] \tag{5.10}$$

with the sampling instants t_k , $k \in \mathbb{N}$, that satisfy,

$$t_0 = 0, 0 < t_{k+1} - t_k \leq h, \lim_{k \rightarrow \infty} t_k = \infty. \quad (5.11)$$

where $e(t_k)$ and $\hat{d}(t_k)$ are the speed error and estimated driver behaviour measurement at time t_k , respectively. Note, that the input vector of the neural-network are considered as $X(t_k) = [X_1(t_k) \ X_2(t_k)]^T = [e(t_k) \ \hat{d}(t_k)]^T$ and

$$M_j(X(t_k)) = \frac{t_f(\sum_{i=1}^{n_x} m_{j,i} X_i(t_k) + b_j)}{\sum_{l=1}^{n_h} t_f(\sum_{i=1}^{n_x} m_{l,i} X_i(t_k) + b_l)} \in [0, 1], \quad (5.12)$$

with the property $\sum_{j=1}^{n_h} M_j(X(t_k)) = 1$. Further, we assume a *sigmoid* activation function, i.e. $t_f(\sum_{i=1}^{n_x} m_{j,i} X_i(t_k) + b_j) = \frac{1}{1 + \exp(-\sum_{i=1}^{n_x} m_{j,i} X_i(t_k) - b_j)} > 0$ and $\sum_{l=1}^{n_h} t_f(\sum_{i=1}^{n_x} m_{l,i} X_i(t_k) + b_l) \neq 0$. The task of advisory control is to adjust to the driver state change due to $d(t)$ by using appropriate values of $G_{1,j}$ and $G_{2,j}$ gains, obtained by offline training of the NN using I/O data of "to be approximated" embedded device.

Remark 5.3: In literature, several activation functions are proposed for NN-based control, [Nwankpa *et al.* 2018]. In our context, the choice of activation function should ensure that the impact of connection weight $m_{j,i}$ between input nodes and the hidden nodes is bounded and differentiable. Without loss of generality, we choose *sigmoid* over *tanh* activation function to limit $t_f(\cdot) \in [0, 1]$ for any $x(t_k)$ and further considered the $\sum_{j=1}^{n_h} M_j(X(t_k)) = 1$ to normalise the output of various hidden nodes. The tuning of $m_{j,i}$ weights can be done by employing an optimisation criteria [Lam & Leung 2006]. For simplicity, in the following, equal importance is given to each input $X_i(t_k)$.

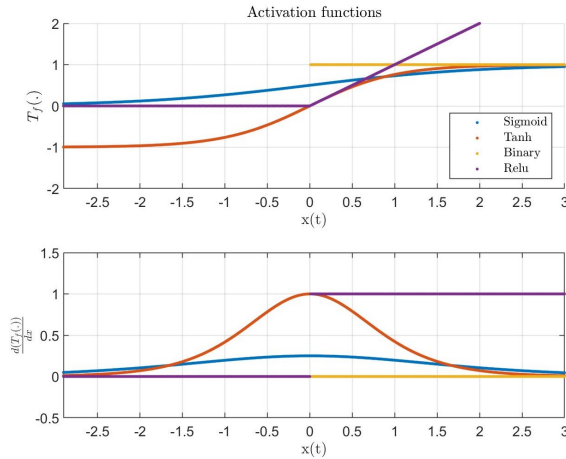


Figure 5.16: Activation functions and their derivatives

Closed-loop system: The ADAS-Driver-Train closed-loop error dynamics becomes,

$$\begin{aligned} \dot{e}(t) = & \sum_{j=1}^{n_h} M_j(X(t_k)) \left[Ae(t) + BK(d(t))G_{1,j}e(t_k) + BK(d(t))G_{2,j}(\hat{d}(t_k) - d_{nom}) \right. \\ & \left. + B(K(d(t)) - K_{nom})G_{2,j}d_{nom} \right]. \end{aligned} \quad (5.13)$$

with $t_k \leq t < t_{k+1}$, $k \in \mathbb{N}$, $\bar{u}(t) = \sum_{j=1}^{n_h} M_j(X(t_k)) \left[B^{-1}(k_0 + k_1v_r + k_2v_r^2) - K_{nom}G_{2,j}d_{nom} \right]$, $w_1(t) = \hat{d}(t_k) - d_{nom}$ and $w_2(d(t)) = (K(d(t)) - K_{nom})G_{2,j}d_{nom}$ as small perturbations, corresponding to the measurement delays and deviation from the nominal performance respectively and the sampling instants t_k , $k \in \mathbb{N}$ satisfy,

$$t_0 = 0, \quad 0 < t_{k+1} - t_k \leq \bar{h}, \quad \lim_{k \rightarrow \infty} t_k = \infty. \quad (5.14)$$

Again, the objective is to find an estimate of the largest allowable sampling interval \bar{h} , (5.18) for some given ADAS gains $G_{1,j}$ and $G_{2,j}$, using Theorem 4.9, while guaranteeing \mathcal{L}_2 stability of the closed-loop system.

5.4.2 Simulation studies

In this subsection, we test the three scenarios to assess the usefulness of NN-based ADAS to reduce tracking error in the presence of varying driver behaviour.

5.4.2.1 Non functional ADAS

In this scenario, since there is no intervention of ADAS, the train speed response is similar to the scenario of last section. Thus, we take liberty to skip presenting these simulations.

5.4.2.2 Partially functional ADAS (with train measurements only)

In this scenario, we consider a driver advisory system is present with partial functionality. Thus the ADAS helps the driver by providing the advisory control signal $\eta(t)$ given by equation (5.10). However, ADAS does not have information about driver's state variation, i.e. $G_{2,j} = 0$, $\forall j \in 1, \dots, n_h$. Thus, the $\eta(t)$ signals are generated based only on train speed measurements, i.e. $\eta(t) = \sum_{j=1}^{n_h} M_j(X(t_k))G_{1,j}e(t_k)$. Fig. 5.17 presents speed $v(t)$ response considering a varying driver behaviour $K(d(t))$. In order to simulate this scenario, we considered NN parameters as $m_{1,1}$, $m_{1,2}$, $m_{2,1}$, $m_{2,2} = 0.5$, and $G_{1,1}$, $G_{1,2} = -0.5$ and $G_{2,1}$, $G_{2,2} = 0$ and obtained higher than $\bar{h} \sim 5min$ for γ_1 , $\gamma_2 = 15$. The gains were considered so that to have a comparison of performance with the state-feedback controller. The following observations can be made from Fig. 5.17.

- When delay in train speed measurement increases, i.e. from $0s \rightarrow 180s \rightarrow 285s$, the train cruise control stability is not compromised and the speed tracking performance is also achievable. Compared to state-feedback, a NN-based ADAS successfully smooth out the speed variations and thus improved the tracking performance.
- Moreover, compared to the previous abstraction and the same scenario, the state-feedback controller was stable for $\bar{h} < 285s$. Nevertheless, NN-based advisory control is stable for even higher delays, i.e. $\bar{h} \sim 300s$. This is noticeable by the comparison of speed $v(t)$ response of the two controllers at $\bar{h} \sim 285s$ in Fig. 5.17. This is because the LMI's of Theorem 4.9 are solvable even for delays higher than $\bar{h} > 285s$.

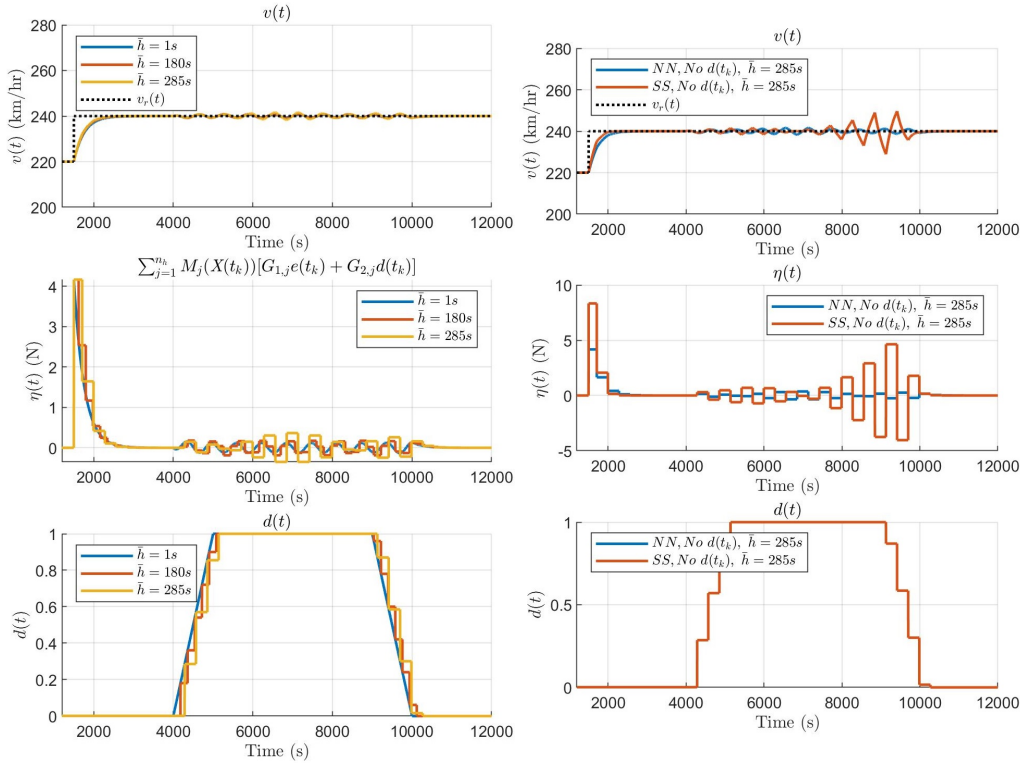


Figure 5.17: a) The response of $v(t)$, $\eta(t)$ and $d(t)$ with NN-based ADAS assistance to varying driver behaviour for only train speed measurements, b) Comparison of the the response of $v(t)$, $\eta(t)$ and $d(t)$ with state-feedback based (red) and NN-based (blue) ADAS assistance to varying driver behaviour for only train speed measurements

5.4.2.3 Fully functional ADAS (with both train and driver measurements)

In this scenario, we again consider that the driver advisory system with full functionality. Compared to previous scenario, ADAS will help the driver by adjusting the advisory

control signal $\eta(t)$, given by (5.10). Thus, the advisory control signal $\eta(t)$ depends on both, $G_{1,j}e(t_k)$ and $G_{2,j}\hat{d}(t_k)$. Thus the ADAS responds to the driver state change using both time-delayed train speed and driver state measurements. Fig. 5.18 gives speed $v(t)$ response of this scenario considering a varying driver behaviour $K(d(t))$. In order to simulate this scenario, we considered the NN parameters as $m_{1,1}, m_{1,2}, m_{2,1}, m_{2,2} = 0.5$ and $G_{1,1}, G_{1,2} = -0.5$ and $G_{2,1}, G_{2,2} = -1$ and obtained higher than $\bar{h} \sim 5min$ for $\gamma_1, \gamma_2 = 15$. Notice that the gains $G_{2,j}$ are non-zero. Thus $\eta(t)$ signal calculations use the estimated driver state. The following observations can be made from Fig. 5.18.

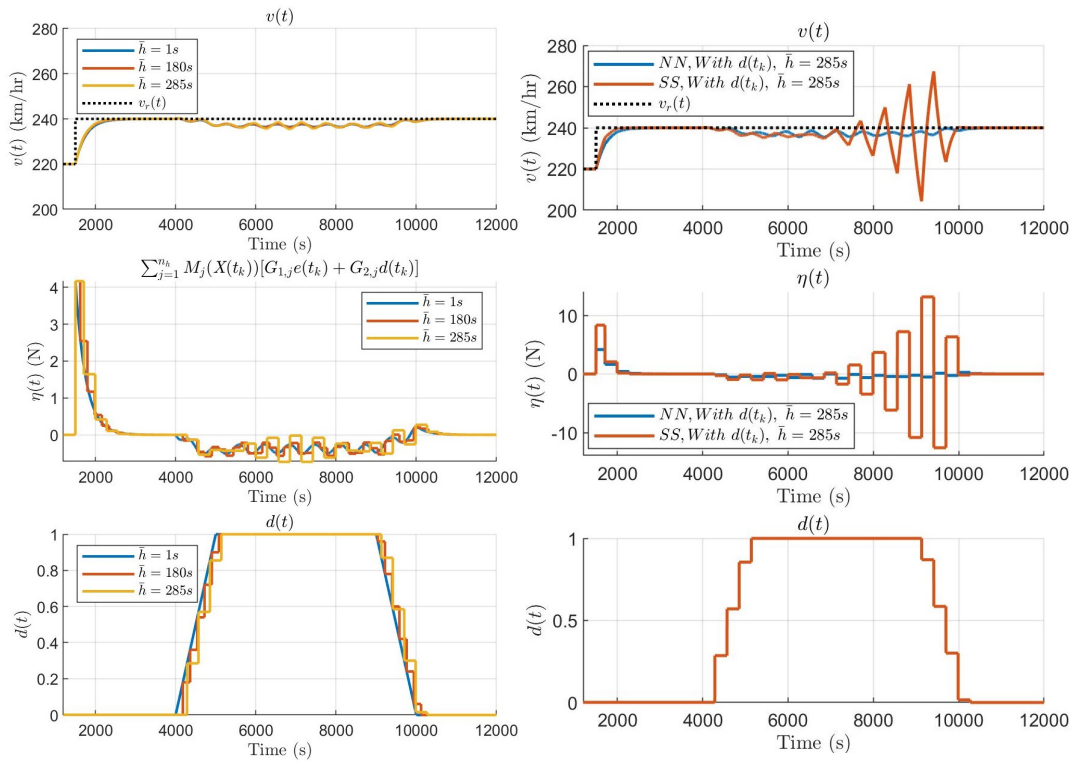


Figure 5.18: a) The response of $v(t)$, $\eta(t)$ and $d(t)$ with NN-based ADAS assistance to varying driver behaviour for both train speed and driver state measurements b) Comparison of the response of $v(t)$, $\eta(t)$ and $d(t)$ with state-feedback based (red) and NN-based (blue) ADAS assistance to varying driver behaviour for both train speed and driver state measurements

- Compared to previous scenario, when delay in train speed and driver state measurement increases, i.e. from $0s \rightarrow 180s \rightarrow 285s$, the train cruise control stability and the speed tracking performance are certainly achievable however with an steady state error. The steady state error is the acknowledgement of the information of driver state change with ADAS.

- Moreover, for this scenario, the maximum delay in driver and train state measurement until which stability can be guaranteed with a NN controller is $\bar{h} > 285s$ compared to $\bar{h} < 245s$ with a state-feedback controller. This is because the LMIs of Theorem 4.6 are solvable till this limit and provide the yellow plot with $\bar{h} \sim 285s$.
- Fig. 5.18 b) compares the speed $v(t)$ response of NN and state-feedback controller for this scenario at $\bar{h} \sim 285s$. The NN controller outperforms the state-feedback controller response even at the maximum delay of $\bar{h} \sim 285s$. The \bar{h} limit that satisfy LMIs of Theorem 4.9 for stability is larger than that of first abstraction.

5.5 3rd abstraction: Stability of non-linear Driver-Train system with neural-network based ADAS

In this section, we consider train, driver and ADAS model as a T-S non-linear system, a time-varying gain and a NN controller respectively.

5.5.1 System description

Compared to the previous modelling abstractions, for this approach, we considered the same driver and ADAS model. However, we considered a T-S model for representation of the train. Hence, we will only present train model.

Train model: We considered a single-point train dynamics model subject to rolling mechanical resistance and aerodynamic drag. However, we did not linearise the model for cruise motion. The single-point model is represented in T-S form as following:

$$\begin{aligned} \dot{x}(t) &= A(y(t))x(t) + Bu(t) - k_0, \\ y(t) &= Cx(t), \end{aligned} \tag{5.15}$$

where, $x(t) = v(t)$, $A(y(t)) = -k_1 - k_2y(t)$, $B = 1/m$, $C = 1$, $v(t)$ the train speed and k_0 , k_1 , k_2 are real coefficients. The train parameters are chosen as in the Table 5.1.

Now, as $y(t)$ is a measured state, we can use a polytopic description of $A(y(t))$ via T-S or quasi-LPV representation. Using the fact that $y(t) \in [\underline{y}, \bar{y}]$, the weighting functions $w_1(y(t)) = \frac{\bar{y}-y(t)}{\bar{y}-\underline{y}}$ and $w_2(y(t)) = 1 - w_1(y(t))$ trivially hold the convex sum property $\sum_{i=1}^2 w_i(y(t))$, $0 \leq w_i(y(t)) \leq 1$. Therefore, a T-S form of (5.15) has the following form:

$$\begin{aligned} \dot{x}(t) &= \sum_{i=1}^2 w_i(y(t))A_i x(t) + Bu(t) - k_0, \\ y(t) &= Cx(t), \end{aligned} \tag{5.16}$$

with, $A_1 = -(k_2\underline{y} + k_1)$ and $A_2 = -(k_2\bar{y} + k_1)$.

Closed-loop system: Considering $e(t) = x(t) - x_r(t)$ and $\dot{x}_r(t)$ negligible, the input vector of the neural-network to be $X(t_k) = [X_1(t_k) \ X_2(t_k)]^T = [e(t_k) \ \hat{d}(t_k)]^T$, then, the ADAS-Driver-Train closed-loop speed dynamics becomes,

$$\begin{aligned} \dot{e}(t) = & \sum_{j=1}^{n_h} M_j(X(t_k)) \sum_{i=1}^2 w_i(y(t)) \left[A_i e(t) + BK(d(t)) G_{1,j} e(t_k) \right. \\ & \left. + BK(d(t)) G_{2,j} (\hat{d}(t_k)) \right]. \end{aligned} \quad (5.17)$$

with $t_k \leq t < t_{k+1}$, $k \in \mathbb{N}$. Moreover, the sampling instants t_k , $k \in \mathbb{N}$ satisfy,

$$t_0 = 0, \ 0 < t_{k+1} - t_k \leq \bar{h}, \ \lim_{k \rightarrow \infty} t_k = \infty. \quad (5.18)$$

The objective is to find an estimate of the largest allowable sampling interval \bar{h} , (5.18), using Theorem 4.15, while guaranteeing exponential stability of the closed-loop system.

5.5.2 Simulation studies

In this subsection, we test the three scenarios to assess the usefulness of NN-based ADAS on a T-S form based train model to reduce tracking error in the presence of varying driver behaviour. Moreover in order to show robustness of stability we will also compare the speed response of T-S form based nonlinear train model with the speed response of linearised train model by considering a disturbance on train control as $u(t) + step(t)$.

Moreover in order to appreciate the importance of considering a delay in driver state, we will compare the speed response of partially functional and fully functional ADAS by considering a disturbance on train control as $u(t) + step(t)$.

5.5.2.1 Non functional ADAS

In this scenario, since there is no intervention of ADAS, the train speed response is similar to the scenario of last two sections. Thus, we skip to present these simulations.

5.5.2.2 Partially functional ADAS (with train measurements only)

In this scenario, we consider that a driver advisory system is present with partial functionality. Thus the ADAS helps the driver by providing the advisory control signal $\eta(t)$ based only on delayed train speed measurements, i.e. $\eta(t) = \sum_{j=1}^{n_h} M_j(X(t_k)) G_{1,j} e(t_k)$. Fig. 5.19 presents speed $v(t)$ response considering a varying driver behaviour $K(d(t))$. In order to simulate this scenario, we considered NN parameters similar to second scenario of the previous abstraction. The following observations can be made from Fig. 5.19.

- Similar to second scenario of the second abstraction, when delay in train speed measurement increases, i.e. from $0s \rightarrow 180s \rightarrow 285s$, the train cruise control stability is not compromised and the speed tracking performance is also achievable.
- Moreover, the comparison of speed $v(t)$ and advisory control $\eta(t)$ response of the second scenario of the two abstractions at $\bar{h} \sim 285s$ in Fig. 5.19 indicate that there is only a slight difference in control computation, i.e. during the acceleration phase. However, no big difference is visible during the cruise phase.

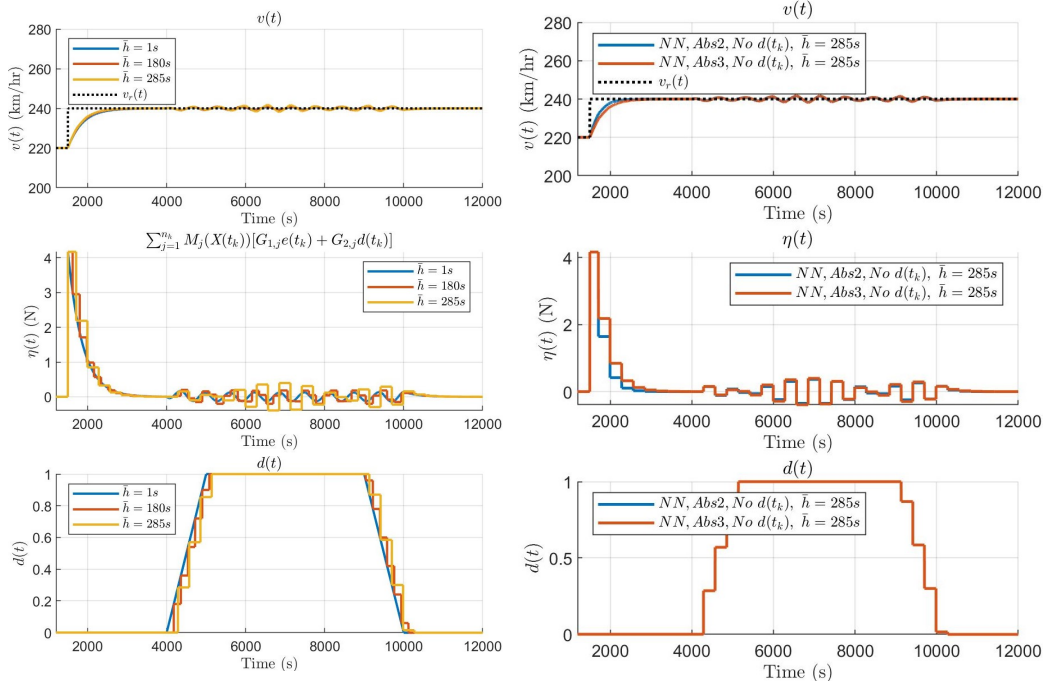


Figure 5.19: a) The response of $v(t)$, $\eta(t)$ and $d(t)$ with NN-based ADAS assistance to varying driver behaviour for only train speed measurements, b) Comparison of the response of $v(t)$, $\eta(t)$ and $d(t)$ with Abs3 NN-based (red) and Abs2 NN-based (blue) ADAS assistance to varying driver behaviour for only train speed measurements

Further, a simulation study with varying speed reference with a sinusoidal variation, $v_e = 2.4 \sin(\frac{t-1500-600}{300})$ if $2100s \leq t < 12000s$ to constant reference is considered to assess the impact of neglecting $\dot{x}_r(t)$ to derive closed-loop equation. Fig. 5.20 presents speed $v(t)$ response considering a varying driver behaviour $K(d(t))$ and a varying speed reference. The following observations can be made from Fig. 5.20.

- In spite of a varying reference, when delay in train speed measurement increases, i.e. from $0s \rightarrow 180s \rightarrow 285s$, the train cruise control stability is not compromised and the speed tracking performance is also achievable.

- Moreover, the comparison of speed $v(t)$ and advisory control $\eta(t)$ response of the second scenario of abstraction two and three at $\bar{h} \sim 285s$ in Fig. 5.20 for a varying speed reference indicate that the $\dot{v}_r(t)$ assumption does not impact stability.

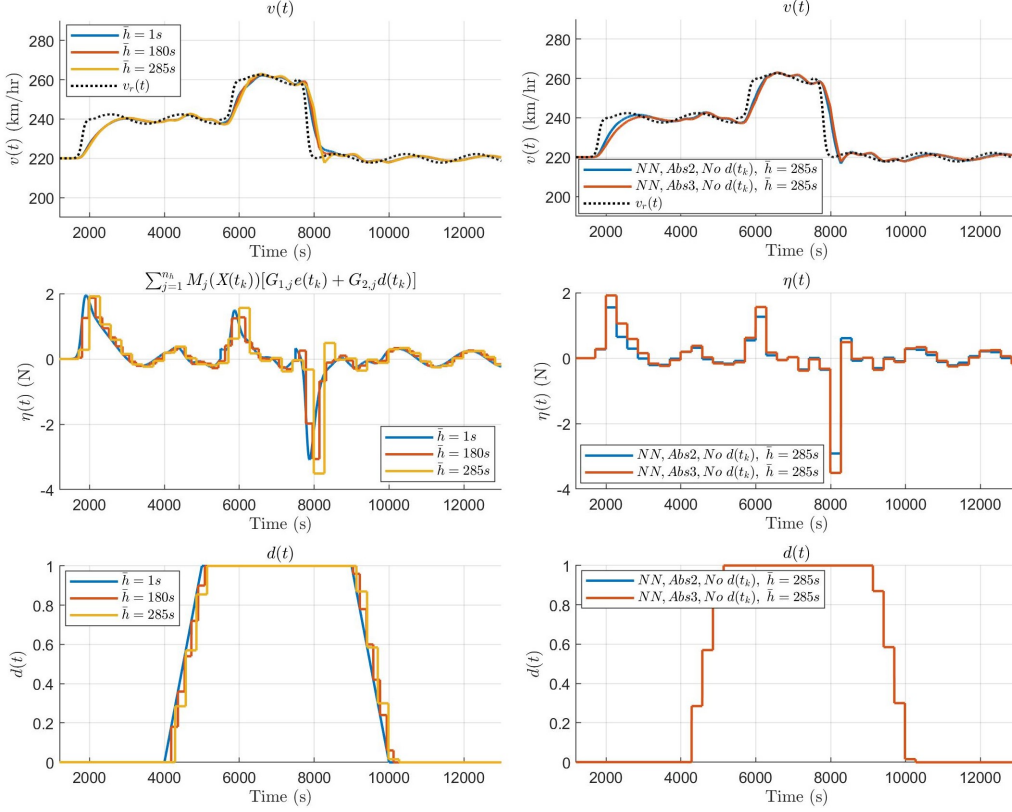


Figure 5.20: a) The response of $v(t)$, $\eta(t)$ and $d(t)$ with NN-based ADAS assistance to varying driver behaviour and varying speed reference, for only train speed measurements, b) Comparison of the response of $v(t)$, $\eta(t)$ and $d(t)$ with Abs3 NN-based (red) and Abs2 NN-based (blue) ADAS assistance to varying driver behaviour and varying speed reference for train speed measurements only

5.5.2.3 Fully functional ADAS (with both train and driver measurements)

In this scenario, we consider that the driver advisory system is present with full functionality. Thus, ADAS will help the driver by adjusting the advisory control signal $\eta(t)$, which depend on both $G_{1,j}e(t_k)$ and $G_{2,j}\hat{d}(t_k)$, i.e. time-delayed train speed and driver state measurements. Fig. 5.21 gives speed $v(t)$ response of this scenario considering a varying driver behaviour $K(d(t))$ and a varying speed reference. In order to simulate this scenario we considered the NN parameters similar to third scenario of the previous abstraction. The following observations can be made from Fig. 5.21.

- Similar to the third scenario of second abstraction, when delay in train speed and driver state measurement increases, i.e. from $0s \rightarrow 180s \rightarrow 285s$, the train cruise control stability and the speed tracking performance are again achievable however with an steady state error.
- Moreover, the comparison of speed $v(t)$ and advisory control $\eta(t)$ response of the third scenario of abstraction two and three at $\bar{h} \sim 285s$ in Fig. 5.21 for a varying speed reference indicate that the controller is also stable when ADAS has information about driver state.

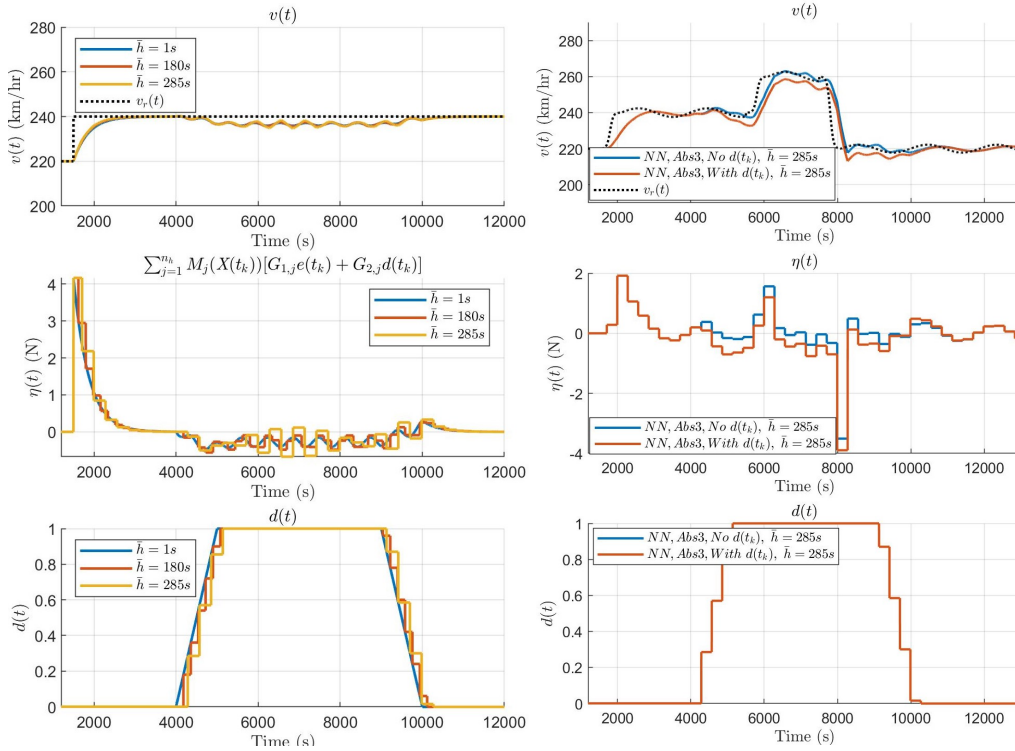


Figure 5.21: a) The response of $v(t)$, $\eta(t)$ and $d(t)$ with NN-based ADAS assistance to varying driver behaviour for both train speed and driver state measurements b) Comparison of the response of $v(t)$, $\eta(t)$ and $d(t)$ with Abs3 NN-based ADAS assistance to varying driver behaviour and varying speed reference for only train speed measurements (blue) and for both train speed and driver state measurements (red)

Next, we tested the robustness of the proposed controller by introducing a $step(t)$ disturbance to train control during varying driver behaviour as shown in Fig. 5.22. Fig. 5.23 presents speed $v(t)$ response considering varying driver behaviour $K(d(t))$ and a constant reference. The following observations can be made from Fig. 5.23.

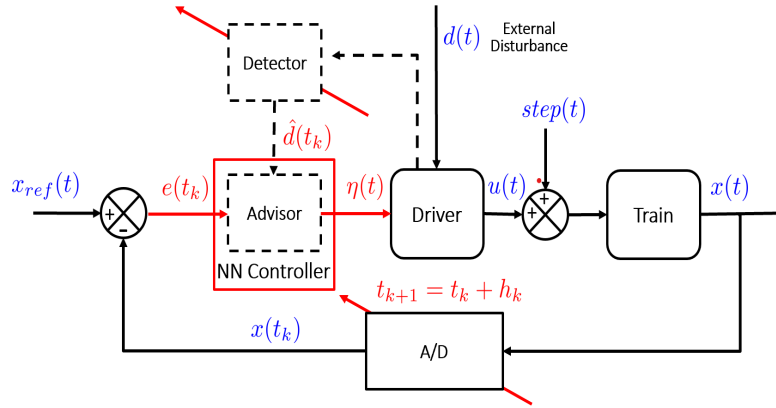


Figure 5.22: Closed-loop system schematic with $step(t)$ disturbance

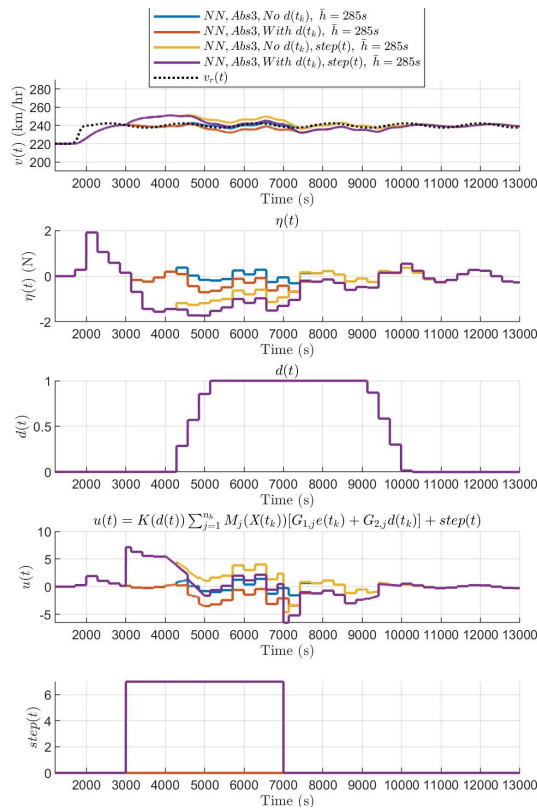


Figure 5.23: Comparison of the response of $v(t)$, $\eta(t)$ and $d(t)$ with Abs3 NN-based ADAS assistance to varying driver behaviour in the presence of only train state measurements (blue, yellow) and both train speed and driver state measurements (red, magenta) in the presence of a $step(t)$ disturbance (yellow, magenta)

The benefit of introducing $\hat{d}(t_k)$ in deriving stability conditions is visible when a *step*(t) disturbance is introduced. In spite of *step*(t) disturbance, fully functional ADAS (magenta) could achieve train cruise control stability with a better speed tracking performance.

5.6 Conclusion

In this chapter, we presented simulations to study stability of ADAS-Driver-Train closed-loop system in the presence of varying driver behaviour and time-delayed driver and train state measurements. For this purpose, we employed three modelling abstractions from the contribution chapter. For each abstraction, we considered three scenarios, *ADAS is not present*, *ADAS is present with partial functionality*, i.e. can access only time-delayed train state measurements and *ADAS is present with full functionality*, i.e. can access both time-delayed train and driver state measurements.

Our research concluded that a NN-based driver advisory system is viable compared to state-feedback based driver advisory system for all the three simulation scenarios while providing more design freedom, and potentially a better performance. It is evident from the simulation results of fully functional ADAS that the steady state response of the train speed has a steady state error, but remains stable. However, considering the fact that the activation functions of the NN adds a "lag" in the closed-loop, the maximum admissible delay is higher for NN-based fully functional ADAS. The admissible measurement delay were quantified using the results of contribution chapter, and conversely the theoretical results were also confirmed by the simulation results, both for stability and instability.

Moreover, when a disturbance appears at the train system level, a fully functional NN-based ADAS handled the disturbance better than a partially functional NN-based ADAS. This is because the discrepancy between the real driver state and the driver state as seen by the ADAS, will be matching at some point, which will improve the closed-loop performance, in spite of the mismatched estimation period due to the aperiodic sampling of driver state. Finally, we assessed the impact of the assumption of a "constant reference speed", used in the contribution chapter to derive stability conditions. Even though there was no theoretical result presented without the relaxation, the simulation results shown that this relaxation is possible, and this is a perspective improvement of our work.

General Conclusion

This PhD thesis was dedicated to achieve safety and performance guarantees of [ADAS](#) assistance to drivers for long journey railway transportation. For this purpose, an "approximate computing" based approach was considered, where sophisticated [ADAS](#) algorithms are approximated using offline learning based [NN](#), and then embedded in a stability assessment framework. Particularly, a stability analysis of [ADAS-Driver-Train](#) system in presence of delay in the driver and the train state measurement was conducted to ascertain performance guarantees. A particular attention was given to the context of varying driving behaviour. The main objective was to propose stability criteria that allows to find the maximum allowable delay before the closed-loop system loses stability. This means that even if the inputs to [ADAS](#) are missing due to corrupted measurements or delays, the global system remains stable under this maximum delay. Moreover, the introduced [ADAS](#) reach the first [GoA](#) and respects the principle of "atleast as good as" when replacing/extending existing driver interfaces.

In this work we have provided foundations to a novel approach to study stability of Driver-Train system by introducing [ADAS](#) model in the Driver-Train closed-loop system. We proposed three abstract models that approximate the train as a controlled system and [ADAS-Driver](#) as the controller. Further we considered time-delay approach based Lyapunov techniques for obtaining [LMI](#)-based stability conditions. Particularly, we considered time-dependent [LKF](#) technique because it can consider both slow and fast-varying delay properties and also gives the opportunity to estimate maximum time-delay for which the stability can be guaranteed. With the advantage to introduce time-delays in the stability conditions it was thus possible to estimate maximum delay in the driver and train state measurement in presence of varying driver behaviour.

Considering the aforementioned approach, we proposed three Theorems and also their corresponding delay search algorithms for the three abstract models to assess the maximum admissible delay in the driver and the train state measurements for each of the following three scenarios. The first scenario, used as a reference, non functional [ADAS](#), i.e. driver interacts with the train without any driver advisory signals. The second scenario considered partially functional [ADAS](#), i.e. driver interacts with the train via an [ADAS](#), however, driver advisory signals are based only on train state measurements. The third

scenario considers fully functional **ADAS**, i.e. driver interacts with the train via an **ADAS**, however, driver advisory signals are based on both driver and train state measurements. We studied the three scenarios for each abstract model and then compared the results of different scenarios for each abstraction and then of different abstractions.

Considering low complexity levels of the "to be approximated" system, the first two abstractions are proposed for a cruise driving context. The first abstraction considered a sampled-data **LTI** system to model the train cruise dynamics, a time-varying gain to model driver dynamics and a state-feedback controller to model the **ADAS** dynamics. In this context, a novel time-dependent **LKF** functional based on Wirtinger inequality was proposed to guarantee the \mathcal{L}_2 stability of the sampled-data **LTI** system. The stability proof used Jensen inequality to upper-bound the integral terms of **LKF** derivative and then used convex embedding approach to derive the **LMIs** for the estimation of the maximum allowable delay. The approach was illustrated by application to the **ADAS-Driver-Train** model for the aforementioned three scenarios. It was found that the maximum allowable delay for a fully functional state-feedback based **ADAS** was lower than that of partially functional **ADAS**, due to awareness of **ADAS** about exogenous perturbation on the driver state and limited capability of a state-feedback based **ADAS** to handle non-linearity.

Next, the second abstraction considered a sampled-data **LTI** system to model the train cruise dynamics, a time-varying gain to model driver dynamics and a **NN** controller to model the **ADAS** dynamics. In this context, a novel augmented time-dependent **LKF** functional was proposed to guarantee the \mathcal{L}_2 stability of the sampled-data **LTI** system. In order to increase even further the maximum allowable delay, the stability proof used affine Bessel-Legendre inequality than Jensen inequality to better upper-bound the integral terms of **LKF** derivative. Further, convex embedding approach was used to derive the **LMIs** for the estimation of the maximum allowable delay. The approach was then illustrated by application to the **ADAS-Driver-Train** model for the aforementioned three scenarios. A smooth and derivable *sigmoid* activation function was considered for a three layer feed-forward neural network to closely approximate non-linear **ADAS** and Driver-Train interaction. Moreover, it was found that the maximum allowable delay for a fully functional **NN**-based **ADAS** was higher than that of fully/partially functional state-feedback based **ADAS**.

Finally, third abstraction considered a **T-S** non-linear system to improve upon the train dynamics model, a time-varying gain to model driver dynamics and a similar **NN** controller to model the **ADAS** dynamics. In this context, a novel time-dependent **LKF** functional based on derivative of Wirtinger inequality was proposed to guarantee the exponential stability of the non-linear sampled-data system. The stability proof used Jensen inequality to upper-bound the integral terms of **LKF** derivative and then used convex embedding

approach to derive the LMIs for the estimation of the maximum allowable delay. The approach was then illustrated by application to the ADAS-Driver-Train model for the aforementioned three scenarios. In addition to constant reference, the simulation were also performed for varying speed reference to show the generality of the stability proof by this approach. Moreover, the robustness aspect with respect to exogenous disturbances at the train system level was introduced to show that a fully functional ADAS provided better performance than that of partially functional ADAS.

6.1 Perspectives

The implications of our results are twofold : First-of-all, the framework to assess stability of approximate computing solutions for advisory control via NN is usable to approximate and replace exogenous devices for embedded architectures. Secondly, the control-theoretic approach to assess stability of Human-Machine Systems, that suffer from modelling and measurement uncertainties is plausible. The proposed approaches are able to interpret these uncertainties quantitatively and use them for advisory controller design with guaranteed performance. This makes the certification process of ADAS easier by using advanced control techniques such as model-based control and neural-networks.

Another research direction would be to extend the results for other types of NN-based controller such as Recurrent Neural Networks, or more refined driver models or by considering Human-Machine shared control of transportation systems. In future, further improvements can be obtained by proposing detailed ADAS-Driver-Train dynamics modelling abstraction. For example, in addition to compensation behaviour, a driver model that considers both anticipation and delay in response time can be considered. For train, in addition to aerodynamic and mechanical drag, a more detailed model with energy source (electric/combustion), rail-wheel slip dynamics and even track topology can be considered.

In addition to detailed ADAS-Driver-Train models. the closed-loop stability conditions can be brought more close to reality by considering two different delays for driver and train state measurements. It is because, it is very likely that the sensor used for train speed measurement and that for driver state measurements may induce different maximum time-delay and that too at different delay-rates. Thus, it would be interesting to consider different delays in deriving two maximum delay dependent closed-loop stability conditions. Moreover, the simulation results shown that \mathcal{L}_2 stability proof of 2nd abstraction approach the exponential stability proof of the 3rd abstraction. It is likely due to stable train dynamics. Thus a relatively less stable train dynamic modelling could be considered. Lastly, an interesting direction of research could be to find alternative ways to resolve the issue pursued in this thesis, i.e. "how to embed ADAS compensation delays in the LMI".

Appendices

Some useful matrix properties

Theorem A.1 (Jensen's Inequality [Gu et al. 2003])

For any matrix $R \in S_{n_x}^{+*}$, scalar $r > 0$ and vector function $w : [0, r] \rightarrow \mathbb{R}^{n_x}$ such that the concerned inequalities are well defined, one has

$$\left(\int_0^r w(s) ds \right)^T R \left(\int_0^r w(s) ds \right) \leq r \left(\int_0^r w(s)^T R w(s) ds \right).$$

Theorem A.2 (Wirtinger's Inequality [Liu et al. 2010])

Given the space of functions $\phi : [a, b] \rightarrow \mathbb{R}^{n_x}$, which are absolutely continuous on $[a, b]$, have a finite $\lim_{\theta \rightarrow b^-} \phi(\theta)$ and have square integrable first-order derivatives is denoted by $W_{n_x}[a, b]$ with the norm, $\|\phi\|_{W_{n_x}[a, b]} = \max_{\theta \in [a, b]} \|\phi(\theta)\| + \left[\int_a^b \|\dot{\phi}(s)\|^2 ds \right]^{\frac{1}{2}}$. if we denote $W = W_{n_x}[-\bar{h}, 0)$ and $x_t(\theta) = x(t + \theta)$ with $\theta \in [-\bar{h}, 0]$ then,

Let $z \in W_n[a, b)$. assume that $z(a) = 0$. Then for any $n_x \times n_x$ -matrix $R > 0$. The following inequality holds;

$$\int_a^b z^T(\xi) R z(\xi) d\xi \leq \frac{4(b-a)^2}{\pi^2} \int_a^b \dot{z}^T(\xi) R \dot{z}(\xi) d\xi.$$

Theorem A.3 (Adapted from [Boyd et al. 1994])

Consider $x \in \mathbb{R}^{n_x}$, two matrices Γ_1 and Γ_2 in \mathbb{S}_{n_x} and two scalars $\lambda^- < \lambda^+$. The following statements are equivalent:

- (i) $\forall \lambda \in [\lambda^-, \lambda^+], x^T(\Gamma_1 + \lambda \Gamma_2)x \leq 0$
- (ii) $x^T(\Gamma_1 + \lambda^- \Gamma_2)x \leq 0$ and $x^T(\Gamma_1 + \lambda^+ \Gamma_2)x \leq 0$

Proof: Let $x \in \mathbb{R}^{n_x}$ and $\lambda \in [\lambda^-, \lambda^+]$. Remarking that $\Gamma_1 + \lambda \Gamma_2 = \frac{\lambda^+ - \lambda}{\lambda^+ - \lambda^-}(\Gamma_1 + \lambda^- \Gamma_2) + \frac{\lambda - \lambda^-}{\lambda^+ - \lambda^-}(\Gamma_1 + \lambda^+ \Gamma_2)$ achieves the proof since $\frac{\lambda^+ - \lambda}{\lambda^+ - \lambda^-}$ and $\frac{\lambda - \lambda^-}{\lambda^+ - \lambda^-}$ are positive.

Theorem A.4 (Affine Bessel-Legendre Inequality [Lee *et al.* 2018])

Let $x(s) \mid s \in [a, b] \rightarrow \mathbb{R}^{n_x}$ be a continuous function. Then, for a non-negative integer N , a positive integer c , an arbitrary vector $\zeta \in \mathbb{R}^{cn_x}$, $R \in \mathbb{S}_+^{n_x}$, and a matrix $F \in \mathbb{R}^{cn_x \times (N+1)n_x}$ with appropriate dimensions, the following inequality holds:

$$-\int_a^b \dot{x}^T(s) R \dot{x}(s) ds \leq (b-a) \zeta^T F R_N^{-1} F^T \zeta + \mathbf{He} \{ \zeta^T F \mathbb{L}(a, b) \}, \quad (\text{A.1})$$

where,

$$\begin{aligned} R_N &= \text{diag} \{ R, 3R, \dots, (2N+1)R \}, \\ \mathbb{L}(a, b) &= \text{col} \{ \mathbb{L}_0(a, b), \dots, \mathbb{L}_N(a, b) \}, \\ \mathbb{L}_k(a, b) &= \begin{cases} x(b) - x(a) & \text{if } k = 0 \\ x(b) - (-1)^k x(a) - \sum_{l=1}^k p_l^k \frac{l!}{(b-a)^l} \mathbb{L}_{l-1}(a, b) & \text{for } k \in \mathbb{N} \end{cases}, \\ p_l^k &= (-1)^{l+k} \binom{k}{l} \binom{k+l}{l}, \\ \mathbb{L}_l(a, b) &= \int_a^b \int_{s_1}^b \dots \int_{s_l}^b x(s_{l+1}) ds_{l+1} \dots ds_1. \end{aligned} \quad (\text{A.2})$$

Stability of sampled-data LTI systems

B.1 Basic stability concepts

In order to study stability of a sampled-data LTI system, it is imperative to understand what is stability of a system. Thus, we recall some fundamental concepts about system stability and the classical tools from [Fiter 2012].

B.1.1 Stability definition

A system is said to be stable, when, if the system state is punctually disturbed, the state stays close to an equilibrium position. Originally, stability is analysed for systems that are time-invariant and autonomous (i.e. for which there is no control or for a closed-loop system with a given control). Such systems are defined as follows:

Definition B.1: (Autonomous System) The following ordinary differential equation:

$$\dot{x}(t) = f(x(t)), \forall t \geq 0 \quad (\text{B.1})$$

with $f : \mathbb{R}^{n_x} \rightarrow \mathbb{R}^{n_x}$ Lipschitz¹ continuous, is said to be autonomous, if $f(x(t))$ does not depend explicitly on the free time variable, t . Further, x_e will be said to be an equilibrium point, if it represents a real solution of the equation $f(x(t)) = 0$. The quality of this equilibrium point can be ascertained based on the following definitions:

Definition B.2: [Khalil 2002] An equilibrium point x_e of the system (B.1) is

- stable (in the sense of Lyapunov), if $\forall \varepsilon > 0, \exists \delta = \delta(\varepsilon) > 0$ such that

$$\|x(0) - x_e\| < \delta \Rightarrow \|x(t) - x_e\| < \varepsilon, \forall t \geq 0;$$

¹Given two metric spaces (X, d_X) and (Y, d_Y) , where d_X denotes metric on the set X and d_Y denotes a metric on the set Y , a function $f : X \rightarrow Y$ is called Lipschitz continuous (or simply Lipschitz) if there exists real constant $K \geq 0$ such that for all $x_1, x_2 \in X$, $d_Y(f(x_1), f(x_2)) \leq K d_X(x_1, x_2)$.

- attractive if $\exists \rho > 0$ such that

$$\|x(0) - x_e\| < \rho \Rightarrow \lim_{t \rightarrow \infty} \|x(t) - x_e\| = 0;$$

- asymptotically stable, if it is stable and attractive;
- exponentially stable, if there exists scalars $\alpha, \beta, \delta > 0$ such that

$$\|x(0) - x_e\| < \delta \Rightarrow \lim_{t \rightarrow \infty} \|x(t) - x_e\| = \alpha \|x(0) - x_e\| e^{-\beta t}.$$

For such a scalar β , called (exponential) "decay rate", the equilibrium point is also said to be " β stable";

- globally asymptotically stable, if it is stable for $\forall x(0) \in \mathbb{R}^{n_x}$,

$$\lim_{t \rightarrow \infty} \|x(t) - x_e\| = 0$$

Note that, it is always possible to reformulate the problem as a stability analysis around $x_e = 0$, by using a translation of the origin. Therefore, the upcoming results and stability properties are written while taking $x_e = 0$ as the studied equilibrium point.

B.1.2 Lyapunov method

The most common stability tool is the Lyapunov stability approach. It is based on the fact that a system whose trajectory approaches origin, loses its energy. The Lyapunov approach makes use of a function $V : \mathbb{R}^{n_x} \rightarrow \mathbb{R}^+$, called "candidate Lyapunov function", which depends on the system's state and symbolises some sort of potential energy of the system, with respect to the origin. Very often, this function is chosen as a norm or a distance. The Lyapunov stability theory is described as follows [Khalil 2002].

Theorem B.3: Consider the autonomous system (B.1) with an isolated equilibrium point ($x_e = 0 \in \Omega \subseteq \mathbb{R}^{n_x}$, with Ω a neighbourhood of x_e). If there exists a locally Lipschitz function $V : \mathbb{R}^{n_x} \rightarrow \mathbb{R}^+$ with continuous partial derivatives and two class \mathcal{K} functions² α and β such that

$$\alpha(\|x\|) \leq V(x) \leq \beta(\|x\|), \quad \forall x \in \Omega,$$

then the origin $x_e = 0$ of the system is

- stable (in the sense of Lyapunov) if

$$\frac{dV(x)}{dt} \leq 0, \quad \forall x \in \Omega, \quad x \neq 0;$$

- asymptotically stable, if there exists a class \mathcal{K} function φ such that

$$\frac{dV(x)}{dt} \leq -\varphi(\|x\|), \quad \forall x \in \Omega, \quad x \neq 0;$$

²A class \mathcal{K} function is a function $\varphi : [0, a) \rightarrow [0, +\infty)$ that is strictly increasing, and such that $\varphi(0) = 0$.

- exponentially stable, if, moreover, there exist four scalars $\bar{\alpha}, \bar{\beta}, \gamma, p > 0$ such that

$$\alpha(\|x\|) = \bar{\alpha}\|x\|^p, \quad \beta(\|x\|) = \bar{\beta}\|x\|^p, \quad \varphi(\|x\|) = \gamma\|x\|.$$

In such a case, the equilibrium point x_e allows a decay rate equal to $\frac{\gamma}{p}$.

There also exist discrete-time version of the Lyapunov stability theory.

Theorem B.4: Consider the discrete-time autonomous system

$$x_{k+1} = f(x_k), \tag{B.2}$$

with an isolated equilibrium point ($x_e = 0 \in \Omega \subseteq \mathbb{R}^{n_x}$, with Ω a neighbourhood of x_e). If there exists a locally Lipschitz function $V : \mathbb{R}^{n_x} \rightarrow \mathbb{R}^+$ with continuous partial derivatives and two class \mathcal{K} functions α and β such that

$$\alpha(\|x\|) \leq V(x) \leq \beta(\|x\|), \quad \forall x \in \Omega,$$

then the origin $x_e = 0$ of the system is

- stable (in the sense of Lyapunov) if

$$\Delta V(x_k) \leq 0, \quad \forall x_k \in \Omega, \quad x_k \neq 0$$

where,

$$\begin{aligned} \Delta V(x_k) &= V(x_{k+1}) - V(x_k) \\ &= V(f(x_k)) - V(x_k) \end{aligned}$$

- asymptotically stable, if there exists a class \mathcal{K} function φ such that

$$\Delta V(x_k) \leq -\varphi(\|x_k\|), \quad \forall x_k \in \Omega, \quad x_k \neq 0;$$

- exponentially stable, if, moreover, there exist four scalars $\bar{\alpha}, \bar{\beta}, \gamma, p > 0$ such that

$$\alpha(\|x\|) = \bar{\alpha}\|x\|^p, \quad \beta(\|x\|) = \bar{\beta}\|x\|^p, \quad \varphi(\|x\|) = \gamma\|x\|.$$

Remark B.5: The local definitions of the above theorem is globally valid if the given functions are class \mathcal{K}_∞ functions³ and $\Omega = \mathbb{R}^{n_x}$.

The function $V : \mathbb{R}^{n_x} \rightarrow \mathbb{R}^+$ that verifies the property in the previous theorem is called the "Lyapunov function". In the case of linear systems, a system with a stable and a unique equilibrium point is often called a "stable system". Furthermore, if the system is not stable, we will say that it is "unstable".

³A class \mathcal{K}_∞ function is a class \mathcal{K} function such that $a = +\infty$ and $\lim_{t \rightarrow +\infty} \varphi(t) = \infty$.

B.1.3 Properties of LTI systems with sampled-data control

In order to study stability/stabilisation of a general system (linear/non-linear), broadly two approaches are used, i.e. either continuous or discrete-time approach. In the continuous-time approach, a continuous-time controller for a continuous-time system model is found by classical approaches [Khalil 2002], then the discrete-time controller is obtained by integrating the continuous-time controller solution over the interval $[t_k, t_{k+1})$. This approach, where continuous-time controller is discretized, is also called emulation.

Consequently, for the discrete-time approach, a discrete-time system model is derived first by integration (steps in (3.5) and (3.6)) and then a discrete-time controller is designed. In the literature, [Wittenmark *et al.* 1995], a large variety of discrete-time control design methodologies are available. An interesting property arise in the context of sampled-data LTI systems, about the equivalence of these approaches. The property concerns the equilibrium attractivity/asymptotic stability, and is formulated as follows:

Theorem B.6: (From [Fujioka 2009b]) For a given sampled-data LTI system (3.3) with bounded sampling intervals and a given initial state $x(0)$, the following conditions are equivalent:

1. $\lim_{t \rightarrow +\infty} x(t) = 0$,
2. $\lim_{k \rightarrow +\infty} x(t_k) = 0$.

This property means that the attractivity of the continuous-time system (3.3) is equivalent to attractivity of the discrete-time system (3.6). Therefore, it is possible to use either a continuous or a discrete-time approach to study the stability of LTI sampled-data systems.

B.2 Stability analysis under constant sampling

In this case (see Fig. B.1), the system's stability is usually analysed using the discrete-time LTI model of the system:

$$x_{k+1} = \Lambda(T)x_k. \quad (\text{B.3})$$

For a given sampling period T , the most common approach to analyse the stability (the so-called "Schur method") consists in studying the eigen values of the transition matrix $\Lambda(T)$. We call $\lambda_{max}(T)$ the eigen value of $\Lambda(T)$ with the largest modulus. We then have the following properties, [Åström & Wittenmark 1996].

Theorem B.7: The equilibrium $x_e = 0$ of (B.3) is

- Schur-stable (globally asymptotically stable) if and only if $\|\lambda_{max}(T)\| < 1$. In that case, $\Lambda(T)$ is called a Schur matrix;

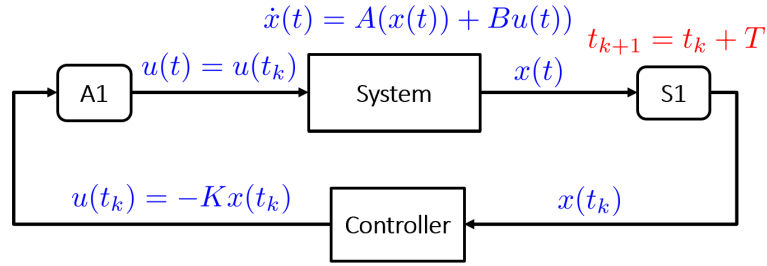


Figure B.1: Sampled-data system with constant sampling rate

- globally exponentially stable with decay-rate $\alpha > 0$ if and only if $\|\lambda_{max}(T)\| \leq e^{-\alpha T}$.

Equivalent LMI stability conditions can also be obtained using the Lyapunov stability theory for discrete-time LTI model of the system.

Theorem B.8: The considered LTI system (B.3) is

- stable (globally) if and only if there exists a matrix $P \in S_{n_x}^{+*}$ such that

$$\Lambda(T)^T P \Lambda(T) - P \preceq 0;$$

- Schur-stable (globally asymptotically stable) if and only if there exists a matrix $P \in S_{n_x}^{+*}$ such that

$$\Lambda(T)^T P \Lambda(T) - P \prec 0;$$

- exponentially stable (globally) with a decay rate α if and only if there exists a matrix $P \in S_{n_x}^{+*}$ such that

$$\Lambda(T)^T P \Lambda(T) - e^{-\alpha T} P \preceq 0.$$

B.3 Stability analysis under time-varying sampling

In this case, where, time-varying sampling arise due to delay in sensor measurement, such systems can be represented by the block diagram in Fig. B.2.

B.3.1 Difficulties and challenges

From control theoretic point of view, these variations in the sampling interval bring up new challenges since they may have a destabilising effect if they are not properly taken into account [Wittenmark *et al.* 1995], [Li *et al.* 2010]. Consider for example the sampled-data

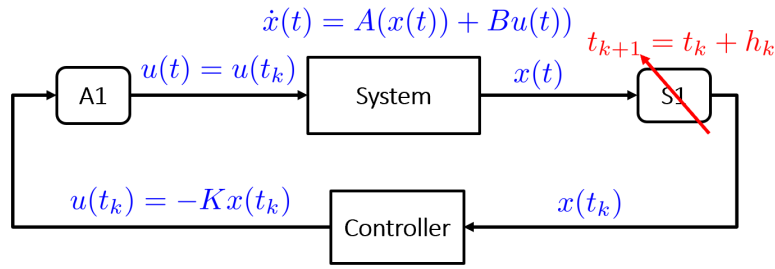
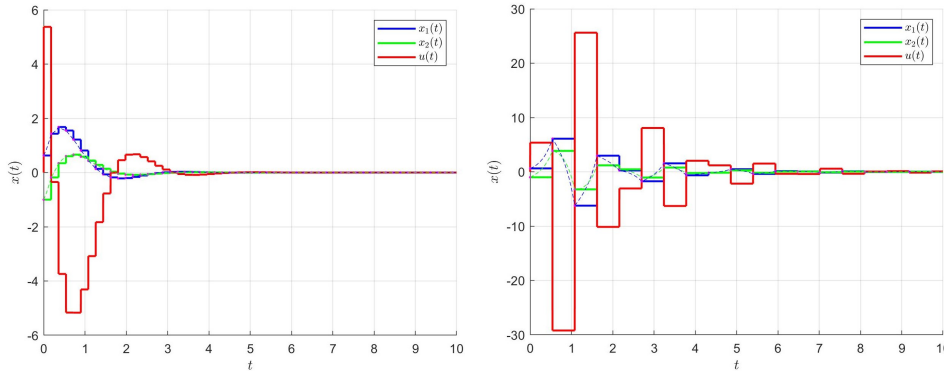


Figure B.2: Sampled-data system with time-varying sampling rate

LTI system [Zhang *et al.* 2001]:

$$\begin{aligned} \dot{x}(t) &= \begin{bmatrix} 1 & 3 \\ 2 & 1 \end{bmatrix} x(t) + \begin{bmatrix} 1 \\ 0.6 \end{bmatrix} u(t), \quad \forall t > 0, \\ u(t) &= - \begin{bmatrix} 1 & 6 \end{bmatrix} x(t_k), \quad \forall t \in [t_k, t_{k+1}), \quad k \in \mathbb{N}. \end{aligned} \quad (\text{B.4})$$

In the case of a constant sampling rate, using the stability conditions from Theorem 2.9, one can find that the origin of the system is Schur-stable if $T \in [0s, T_{const}^{max} = 0.5937s]$, and unstable for $T \in [T_{const}^{max}, +\infty]$. The system's evolution for constant sampling rate $T_1 = 0.18s$ and $T_2 = 0.54s$ is illustrated by Fig. B.3.

Figure B.3: Constant sampling rate with $T_1 = 0.18s$ and $T_2 = 0.54s$ - Stable

When the sampling interval is constant, the Schur property of $\Lambda(T)$ represents a necessary condition for stability of the sampled-data LTI system (B.4). However, it is not a sufficient one. When we sample using a fixed sequence of sampling intervals $T_1 \rightarrow T_2 \rightarrow T_1 \rightarrow T_2 \rightarrow \dots$, the system becomes unstable, Fig. B.4.

This is due to the fact that the Schur property of matrices is not preserved under matrix product (i.e. the product of two Schur matrices is not necessarily Schur). In this case, the discrete-time equivalent system over two sampling instants can be written as,

$$x_{k+2} = \Lambda(T_2)\Lambda(T_1)x_k, \quad \forall k \in 2\mathbb{N}$$

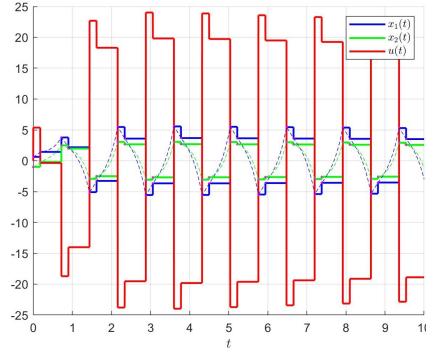


Figure B.4: Variable sampling $T_1 = 0.18s \rightarrow T_2 = 0.54s \rightarrow T_1 \rightarrow T_2 \rightarrow \dots$ - unstable

which can be rewritten as, $x_{l+1} = \Lambda(T_1, T_2)x_l, \forall l \in \mathbb{N}$,

with l representing $2k^{\text{th}}$ sampling, and the transition matrix,

$$\Lambda(T_1, T_2) \equiv \Lambda(T_2)\Lambda(T_1) = \begin{bmatrix} 0.8069 & -3.2721 \\ 0.6133 & -2.1125 \end{bmatrix},$$

over two sampling intervals T_1 and T_2 , which is not Schur in this example. In addition to existence of unstable sampling sequences made of stable sampling intervals⁴, one can also find cases where there exist stable sampling sequences made of stable/unstable or even unstable/unstable sampling sequences.

Let us now consider the following sampled-data LTI system, [Gu *et al.* 2003],

$$\begin{aligned} \dot{x}(t) &= \begin{bmatrix} 0 & 1 \\ -2 & 0.1 \end{bmatrix} x(t) + \begin{bmatrix} 0 \\ 1 \end{bmatrix} u(t), \forall t > 0, \\ u(t) &= - \begin{bmatrix} -1 & 0 \end{bmatrix} x(t_k), \forall t \in [t_k, t_{k+1}), k \in \mathbb{N}. \end{aligned} \quad (\text{B.5})$$

Assume that the sampling is restricted to the set $T \in [T_1, T_2]$ with $T_1 = 2.126s$ and $T_2 = 3.950s$. For constant sampling interval values T_1 and T_2 , the sampled-data LTI system (B.5) behaviour is unstable with both the samplings. This is because, individually, for these values, system's transition matrix $\Lambda(T)$ is not a Schur matrix. However, it can be seen in Fig. B.5, the system's transition matrix $\Lambda(T_1, T_2)$ is Schur-stable under the periodic sampling $T_1 \rightarrow T_2 \rightarrow T_1 \rightarrow T_2 \rightarrow \dots$.

According to previous observation, it is clear that the existing stability tools for sampled-data LTI systems with constant sampling will not provide any guarantee of stability for sampled-data LTI systems with unknown time-varying sampling that arises in real-time control conditions.

⁴By "stable sampling interval", we mean that the transition matrix of associated sampling interval is Schur.

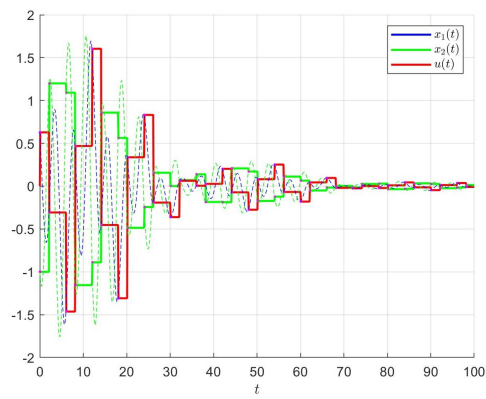


Figure B.5: Variable sampling $T_1 = 2.126s \rightarrow T_2 = 3.950s \rightarrow T_1 \rightarrow T_2 \rightarrow \dots$ - stable

Numerical example: Stability of non-linear sampled-data system with neural-network control

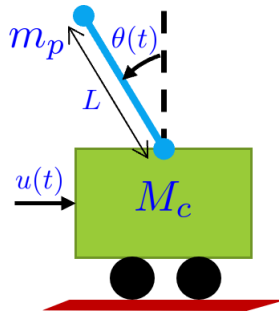


Figure C.1: Schematic of an inverted pendulum

In this section, a sampled-data TLFCFNN-based controller is shown to stabilize an inverted pendulum on a moving cart (Fig. C.1). The dynamics of the inverted pendulum is described by the equation,

$$\ddot{\theta}(t) = \frac{g \sin(\theta(t)) - am_p L \dot{\theta}(t)^2 \frac{\sin(2\theta(t))}{2} - a \cos(\theta(t))u(t)}{\frac{4L}{3} - am_p L \cos(\theta(t))^2},$$

where, $\theta(t)$ is the angular displacement of the pendulum, $g = 9.8 \text{ m/s}^2$ is the acceleration due to gravity, $m_p \in [m_{pmin}, m_{pmax}] = [2, 5]$ Kg is the mass of the pendulum, $M_c \in [M_{cmin}, M_{cmax}] = [30, 35]$ Kg is the mass of the cart, $2L = 1\text{m}$ is the length of the pendulum, $u(t)$ is the force applied to the cart, and $a = 1/(m_p + M_c)$, with m_p and M_c being parameter uncertainties. By choosing,

$$x(t) = [x_1(t) \ x_2(t)]^T = [\theta(t) \ \dot{\theta}(t)]^T,$$

and considering $x_1(t) \in [x_{1min}, x_{1max}] = [-\pi/3, \pi/3]$ and $x_2(t) \in [x_{2min}, x_{2max}] = [-5, 5]$ as in [Wu *et al.* 2014b], the non-linear motion of an inverted pendulum can be represented

by a T-S model,

$$\dot{x}(t) = \sum_{i=1}^p w_i(x(t))(A_i x(t) + B_i u(t)),$$

with the parameters, A_i , B_i and $w_i(x(t))$ of the system as,

$$A_1 = A_2 = \begin{bmatrix} 0 & 1 \\ f_{1min} & 0 \end{bmatrix}, A_3 = A_4 = \begin{bmatrix} 0 & 1 \\ f_{1max} & 0 \end{bmatrix},$$

$$B_1 = B_3 = \begin{bmatrix} 0 \\ f_{2min} \end{bmatrix}, B_2 = B_4 = \begin{bmatrix} 0 \\ f_{2max} \end{bmatrix},$$

$$w_i(x(t)) = \frac{\mu_i(f_1(x(t))).v_i(f_2(x(t)))}{\sum_{j=1}^4 (\mu_i(f_1(x(t))).v_i(f_2(x(t))))},$$

with, $f_{1min} = 11.3533$, $f_{1max} = 16.4640$, $f_{2min} = -0.0192$, $f_{2max} = -0.0492$ and

$$\mu_j(f_1(x(t))) = \frac{-f_1(x(t)) + f_{1max}}{f_{1max} - f_{1min}} \text{ for } j = 1, 2,$$

$$\mu_j(f_1(x(t))) = 1 - \mu_1(f_1(x(t))) \text{ for } j = 3, 4,$$

$$v_j(f_2(x(t))) = \frac{-f_2(x(t)) + f_{2max}}{f_{2max} - f_{2min}} \text{ for } j = 1, 3,$$

$$v_j(f_2(x(t))) = 1 - v_1(f_2(x(t))) \text{ for } j = 2, 4,$$

$$f_1(x(t)) = \frac{g - am_p L x_2(t)^2 \cos(x_1(t)) \sin(x_1(t))}{\frac{4L}{3} - am_p L \cos(x_1(t))^2} \frac{\sin(x_1(t))}{x_1(t)},$$

$$f_2(x(t)) = -\frac{a \cos(x_1(t))}{\frac{4L}{3} - am_p L \cos(x_1(t))^2}.$$

Further, for this example, we considered a sampled-data TLFCFFNN-based controller with four hidden nodes to control the inverted pendulum. The sampled-data TLFCFFNN-based controller is given by

$$u(t) = \sum_{l=1}^4 M_l(x(t_k)) G_l x(t_k), \quad \forall t_k \leq t < t_{k+1}, \quad (\text{C.1})$$

where, $M_l(x(t_k))$ is defined in (4.47), and

$$t_f \left(\sum_{i=1}^2 m_{j,i} x_i(t_k) + b_j \right) = \frac{1}{1 + \exp \left(- \sum_{i=1}^2 m_{j,i} x_i(t_k) - b_j \right)}.$$

Our aim is to find the largest sampling interval \bar{h} upto which closed-loop system stability is guaranteed. For this aim, we considered the following stabilizing connection

weights G_j , $\forall j \in \{1, \dots, 4\}$,

$$G_1 = [1790.3422 \quad 471.7552]$$

$$G_2 = [1790.3904 \quad 471.7757]$$

$$G_3 = [1790.1572 \quad 471.6711]$$

$$G_4 = [1790.1696 \quad 471.6766],$$

and the following parameters (as given in [Wu *et al.* 2014b]),

$$m_{1,1} = -0.0591, \quad m_{1,2} = 0.5511$$

$$m_{2,1} = -0.9863, \quad m_{2,2} = 0.5118$$

$$m_{3,1} = 0.3058, \quad m_{3,2} = 0.1582$$

$$m_{4,1} = -0.6254, \quad m_{4,2} = -0.7569$$

$$b_1 = -0.2765, \quad b_2 = -0.3234$$

$$b_3 = -0.7899, \quad b_4 = 0.4423$$

$$m_p = 2kg, \quad M_c = 30kg.$$

The combination of decay-rate λ and the largest sampling interval \bar{h} that satisfy Theorem 4.15 and preserves the exponential stability of the closed-loop system are listed in Table C.1.

Table C.1: Maximum upper bound \bar{h} V/S decay-rate λ

| λ | 0.1 | 0.3 | 0.5 | 0.7 | 0.9 |
|--------------|-------|-------|-------|-------|-------|
| Theorem 3.13 | 0.250 | 0.227 | 0.205 | 0.180 | 0.152 |

When the decay-rate λ is fixed to 0.15, the maximum allowable sampling interval obtained by [Wu *et al.* 2014b] is 0.035. It can be found in Table C.1 that Theorem 4.15 gives larger upper bound of the sampling interval, h_k as 0.244s.

Supposing the initial condition $x(0) = [\frac{\pi}{5} \quad -1]^T$ and the maximum sampling interval \bar{h} as 0.244s, the system responses are as shown in Fig. C.2. The non-linear system is exponentially stable for equilibrium point $x_e = [0 \ 0]^T$ for $\bar{h} = 0.244s$.

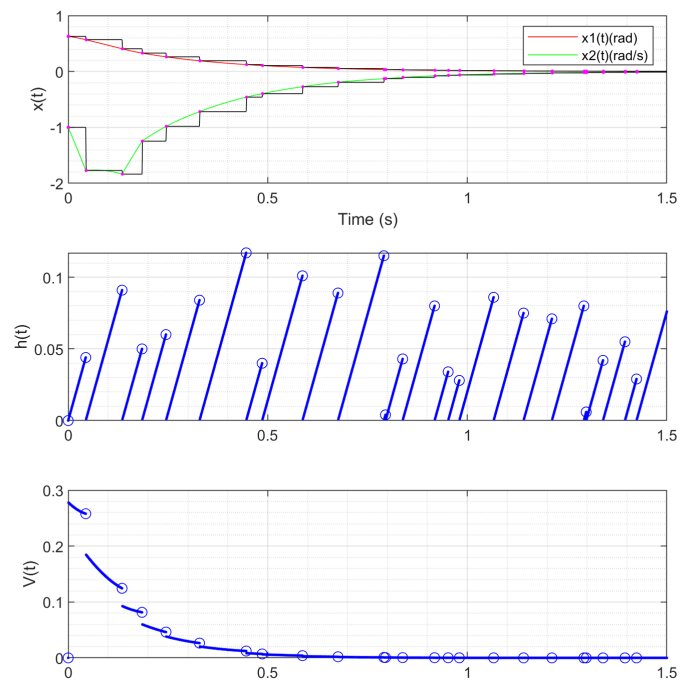


Figure C.2: $x(t)$, $h(t)$, $V(t)$ variation

Bibliography

- [Abichou *et al.* 2015] B. Abichou, D. Berdjag, P. Polet and F. Vanderhaegen. *Human operator's vigilance monitoring using non-intrusive sensors*. 11th Berliner Werkstatt Mensch-Maschine-Systeme, 2015. (Cited on page 41.)
- [Abuali & Abouzeid 2016] N. Abuali and H. Abouzeid. *Driver Behaviour Modelling: Developments and Future Directions*. International Journal of Vehicular Technology, vol. 2016, pages 1–12, Jan 2016. (Cited on page 46.)
- [Ahmadi & Parrilo 2008] A. A. Ahmadi and P. A. Parrilo. *Non-monotonic Lyapunov Functions for Stability of Discrete Time Nonlinear and Switched Systems*. IEEE Conference on Decision and Control, 2008. (Cited on page 66.)
- [Aigner & McCarraghar 1996] P. Aigner and B. McCarraghar. *Human Integration into Control Systems: Discrete Event Theory and Experiments*. World Automation Congress, May 1996. (Cited on page 50.)
- [Akin *et al.* 2008] M. Akin, M. Kurt, N. Sezgin and M. Bayram. *Estimating Vigilance Level by Using EEG and EMG Signals*. Neural Computing and Applications, vol. 17, pages 227–236, 06 2008. (Cited on page 39.)
- [Albrecht *et al.* 2016] A. R. Albrecht, P. G. Howlett, P. J. Pudney, X. T. Vu and P. Zhou. *The Key Principles of Optimal Train Control — Part 2: Existence of an Optimal Strategy, The Local Energy Minimization Principle, Uniqueness, Computational Techniques*. Transportation Research Part B - Methodological, vol. 94, pages 509–538, 2016. (Cited on page 21.)
- [Ali & Abouzeid 2016] N. A. Ali and H. Abouzeid. *Driver Behavior Modeling: Developments and Future Directions*. International Journal of Vehicular Technology, vol. 2016, pages 1–12, Jan 2016. (Cited on page 53.)
- [Ariba & Gouaisbaut 2009] Y. Ariba and F. Gouaisbaut. *An Augmented Model for Robust Stability Analysis of Time-varying Delay Systems*. International Journal of Control, vol. 82, no. 9, pages 1616–1626, 2009. (Cited on page 83.)
- [Atamturk & Savelsbergh 2005] A. Atamturk and M. W. P. Savelsbergh. *Integer Programming Software Systems*. Annals of Open Research, vol. 140, pages 67–124, 2005. (Cited on page 21.)

- [Badamchizadeh *et al.* 2010] M. A. Badamchizadeh, K. Sohrab and T. Mohammadali. *Driver's Behaviour Modelling Using Fuzzy Logic*. Mathematical Problems in Engineering, vol. 2010, Jul 2010. (Cited on page 54.)
- [Balasubramanian & Adalarasu 2007] V. Balasubramanian and K. Adalarasu. *EMG-based Analysis of change in Muscle Activity during Simulated Driving*. Journal of Bodywork and Movement Therapies, vol. 11, no. 2, pages 151–158, 2007. (Cited on page 39.)
- [Barbalat 1959] I. Barbalat. *Systemes d'équations différentielles d'oscillations non linéaires*. Rev. Math. Pures Appl, vol. 4, no. 2, pages 267–270, 1959. (Cited on page 80.)
- [Bekiaris & Amditis 2001] D. Bekiaris and A. Amditis. *Advanced Driver Monitoring: The AWAKE Project*. pages 1–9, 2001. (Cited on page 40.)
- [Berdjag *et al.* 2014] D. Berdjag, F. Vanderhaegen, A. Shumsky and A. Zhirabok. *Unexpected Situations Diagnosis: A Model-based Approach for Human Machine Systems*. IFAC Proceedings Volumes, vol. 47, no. 3, pages 3545–3550, 2014. 19th IFAC World Congress. (Cited on page 51.)
- [Berdjag *et al.* 2015] D. Berdjag, F. Vanderhaegen, A. Shumsky and A. Zhirabok. *Abnormal Operation Diagnosis in Human-Machine Systems*. pages 1–6, 2015. (Cited on page 51.)
- [Bergasa *et al.* 2006] L. Bergasa, J. Nuevo, M. A. Sotelo, R. Barea and M. Guillén. *Real Time System for Monitoring Driver Vigilance*. IEEE Transactions on Intelligent Transportation Systems, vol. 7, pages 63–77, 01 2006. (Cited on page 39.)
- [Bienfait *et al.* 2012] B. Bienfait, P. Zeotardt and B. Barnard. *Automatic Train Operation: The mandatory Improvement for ETCS Application*. Sep 2012. (Cited on page 30.)
- [Bing *et al.* 2009] G. Bing, D. Hairong and Z. Yanxin. *Speed Adjustment Braking of Automatic Train Operation System Based on Fuzzy-PID Switching Control*. In International Conference on Fuzzy Systems and Knowledge Discovery, volume 3, pages 577–580, 2009. (Cited on page 25.)
- [Bornard 2012] J. C. Bornard. *Développement D'un Modèle du Conducteur Automobile : De La Modélisation Cognitive à La Simulation Numérique*. Nov 2012. (Cited on page 52.)

- [Boussemart 2013] Y. Boussemart. *Predictive Models of Procedural Human Supervisory Control Behaviour*. Jul 2013. (Cited on page 54.)
- [Boyd *et al.* 1994] S. Boyd, L. E. Ghaoui, E. Feron and V. Balakrishnan. Linear matrix inequalities in system and control theory. Society for Industrial and Applied Mathematics, 1994. (Cited on page 155.)
- [Briat 2011] C. Briat. *Convergence and Equivalence Results for the Jensen's Inequality—Application to Time-Delay and Sampled-Data Systems*. IEEE Transactions on Automatic Control, vol. 56, no. 7, pages 1660–1665, 2011. (Cited on page 76.)
- [Briat 2015] C. Briat. *Linear Parameter-Varying and Time-Delay Systems*. pages 165–242, Sept 2015. (Cited on page 70.)
- [Buntins *et al.* 2013] M. Buntins, J. W. Schicke, F. Eggert and U. Goltz. *Hybrid Automata as a Modelling Approach in the Behavioural Sciences*. Electronic Notes in Theoretical Computer Science, vol. 297, pages 47–59, 2013. 1st workshop on Hybrid Autonomous Systems. (Cited on page 51.)
- [Cabon *et al.* 1993] P. Cabon, A. Coblenz, R. Mollard and J. Fouillot. *Human Vigilance in Railway and Long Haul Flight Operation*. Ergonomics, vol. 36, pages 1019–33, 10 1993. (Cited on pages 37 and 41.)
- [Calderaro *et al.* 2014] V. Calderaro, V. Galdi, G. Graber, A. Piccolo and D. Cogliano. *An Algorithm to Optimize Speed Profiles of the Metro Vehicles for Minimizing Energy Consumption*. In 2014 International Symposium on Power Electronics, Electrical Drives, Automation and Motion, pages 813–819, Jun 2014. (Cited on page 21.)
- [Cao *et al.* 2019] Y. Cao, L. Ma and Y. Zhang. *Application of Fuzzy Predictive Control Technology in Automatic Train Operation*. Cluster Computing, vol. 22, 11 2019. (Cited on page 26.)
- [Chang & Sim 1997] C. S. Chang and S. S. Sim. *Optimising Train Movements through Coast Control using Genetic Algorithms*. IEE Proceedings Electric Power Applications, vol. 144, no. 1, pages 65–73, Jan 1997. (Cited on page 21.)
- [Chen & Francis 1991] T. Chen and B. Francis. Optimal Sampled Data Control Systems. Springer, 1991. (Cited on page 66.)
- [Chen *et al.* 2017a] J. Chen, S. Xu, B. Zhang and G. Liu. *A Note on Relationship Between Two Classes of Integral Inequalities*. IEEE Transactions on Automatic Control, vol. 62, no. 8, pages 4044–4049, 2017. (Cited on page 82.)

- [Chen *et al.* 2017b] Z. Chen, Z. Li and C. L. P. Chen. *Disturbance Observer-Based Fuzzy Control of Uncertain MIMO Mechanical Systems With Input Nonlinearities and its Application to Robotic Exoskeleton*. IEEE Transactions on Cybernetics, vol. 47, no. 4, pages 984–994, 2017. (Cited on page 110.)
- [Chen *et al.* 2019] H. Chen, Z. Xiong and Y. Ji. *Iterative Learning Control for Automatic Train Operation with Discrete Gears*. In 8th IEEE Data Driven Control and Learning Systems Conference, pages 1284–1289, May 2019. (Cited on page 27.)
- [Cheng *et al.* 2012] B. Cheng, W. Zhang, Y. Lin, R. Feng and X. Zhang. *Driver Drowsiness Detection Based on Multi Source Information*. Human Factors and Ergonomics in Manufacturing and Service Industries, vol. 22, 09 2012. (Cited on page 41.)
- [Chiddarwar & Babu 2011] S. Chiddarwar and N. R. Babu. *Neural Network Based Method for Estimation of Robot Trajectory Control Parameters*. International Journal of Control and Automation, 2011. (Cited on page 88.)
- [Choi *et al.* 2017] H. D. Choi, C. K. Ahn, P. Shi, L. Wu and M. T. Lim. *Dynamic Output-Feedback Dissipative Control for T-S Fuzzy Systems With Time-Varying Input Delay and Output Constraints*. IEEE Transactions on Fuzzy Systems, vol. 25, no. 3, pages 511–526, 2017. (Cited on page 110.)
- [Chou & Xia 2007] M. Chou and X. Xia. *Optimal Cruise Control of Heavy Haul Trains Equipped with Electronically Controlled Pneumatic Brake Systems*. Control Engineering Practice, vol. 15, no. 5, pages 511–519, 2007. (Cited on page 29.)
- [Chou *et al.* 2007] M. Chou, X. Xia and C. Kayser. *Modelling and Model Validation of Heavy Haul Trains Equipped with Electronically Controlled Pneumatic Brake Systems*. Control Engineering Practice, vol. 15, no. 4, pages 501–509, 2007. (Cited on page 24.)
- [Chouvarda *et al.* 2007] I. Chouvarda, C. Papadelis, P. Bamidis, D. Koufogiannis, E. Bekiaris and N. Maglaveras. *Non-Linear Analysis for the Sleepy Drivers Problem*. Studies in Health Technology and Informatics, vol. 129, pages 1294–8, Feb 2007. (Cited on page 39.)
- [Cloosterman *et al.* 2010] M. B. G. Cloosterman, L. Hetel, N. V. D. Wouw, W. P. M. H. Heemels, J. Daafouz and H. Nijmeijer. *Controller Synthesis for Networked Control Systems*. Automatica, vol. 46, no. 10, pages 1584–1594, 2010. (Cited on pages 72 and 73.)

- [Cong & Liang 2009] S. Cong and Y. Liang. *PID-Like Neural Network Nonlinear Adaptive Control for Uncertain Multivariable Motion Control Systems*. IEEE Transactions on Industrial Electronics, vol. 56, no. 10, pages 3872–3879, 2009. (Cited on page 89.)
- [Craig *et al.* 2006] A. Craig, Y. Tran, N. Wijesuriya and P. Boord. *A Controlled Investigation into the Psychological Determinants of Fatigue*. Biological Psychology, vol. 72, pages 78–87, 2006. (Cited on page 40.)
- [Critchley *et al.* 2000] H. Critchley, R. Elliott, C. Mathias and R. Dolan. *Neural Activity relating to Generation and Representation of Galvanic Skin Conductance Responses: A Functional Magnetic Resonance Imaging Study*. The Journal of Neuroscience, vol. 20, pages 3033–40, May 2000. (Cited on page 39.)
- [Dambrine 1995] M. Dambrine. *Contribution a l’etude de la stabilite de systeme a retard*. PhD Thesis, University of Lille, Villeneuve d’Ascq, France, 1995. (Cited on page 69.)
- [Damousis & Tzovaras 2008] Y. Damousis and D. Tzovaras. *Fuzzy Fusion of Eyelid activity Indicators for Hypovigilance related Accident Prediction*. IEEE Transactions on Intelligent Transportation Systems, vol. 9, pages 491–500, 10 2008. (Cited on page 39.)
- [Degani 1996] A. Degani. *Modeling Human-Machine Systems :On Modes, Error, and Patterns of Interaction*. 1996. (Cited on page 52.)
- [Delice & Ertugrul 2007] I. Delice and S. Ertugrul. *Intelligent Modelling of Human Driver: A Survey*. pages 648–651, Jul 2007. (Cited on page 54.)
- [Dominguez *et al.* 2012] M. Dominguez, A. F. Cardador, A. P. Cucala and R. R. Pecharroman. *Energy Savings in Metropolitan Railway Substations through Regenerative Energy Recovery and Optimal Design of ATO Speed Profiles*. IEEE Transactions on Automation Science and Engineering, vol. 9, no. 3, pages 496–504, Jul 2012. (Cited on page 21.)
- [Dong *et al.* 2010] H. Dong, B. Ning, B. Cai and Z. Hou. *Automatic Train Control System Development and Simulation for High Speed Railways*. IEEE Circuits and Systems Magazine, vol. 10, no. 2, pages 6–18, 2010. (Cited on page 28.)
- [Dong *et al.* 2013] H. R. Dong, S. G. Gao, B. Ning and L. Li. *Extended Fuzzy Logic Controller for High Speed Train*. Neural Computing and Applications, vol. 22, no. 2, pages 321–328, Feb 2013. (Cited on page 26.)

- [Dong *et al.* 2018] H. Dong, H. Zhu and S. Gao. *An Approach for Energy Efficient and Punctual Train Operation via Driver Advisory System*. IEEE Intelligent Transportation Systems Magazine, vol. 10, no. 3, pages 57–67, 2018. (Cited on page 42.)
- [Donges 1978] E. Donges. *A Two-Level Model of Driver Steering Behaviour*. Human Factors, vol. 20, no. 6, pages 691–707, 1978. (Cited on page 47.)
- [Donkers *et al.* 2011] M. C. F. Donkers, W. P. M. H. Heemels, N. V. D. Wouw and L. Hetel. *Stability Analysis of Networked Control Systems using a Switched Linear Systems Approach*. IEEE Transactions on Automatic Control, vol. 56, no. 9, pages 2101–2115, Sep 2011. (Cited on pages 68, 73 and 90.)
- [Dore 1998] D. M. Dore. *The Pro-Active Automatic Warning System (PAWS)*. 1998. (Cited on page 34.)
- [Driver 1977] R. D. Driver. *Ordinary and Delay Differential Equations*. Applied Mathematical Sciences, Springer, vol. 463, 1977. (Cited on page 72.)
- [Engstrm & Monk 2013] J. Engstrm and C. A. Monk. *A Conceptual Framework and Taxonomy for Understanding and Categorizing Driver Inattention*. 2013. (Cited on page 36.)
- [Ersal *et al.* 2010] T. Ersal, H. J. A. Fuller, O. Tsimhoni, J. L. Stein and H. K. Fathy. *Model based Analysis and Classification of Driver Distraction under Secondary Tasks*. IEEE Transactions on Intelligent Transportation Systems, vol. 11, no. 3, pages 692–701, Sep 2010. (Cited on page 40.)
- [Ertugrul 2008] S. Ertugrul. *Predictive Modelling of Human Operators using Parametric and Neuro Fuzzy Models by Means of Computer Based Identification Experiment*. Engineering Applications of Artificial Intelligence, vol. 21, no. 2, pages 259–268, 2008. (Cited on page 55.)
- [Eskandarian & Mortazavi 2007] A. Eskandarian and A. Mortazavi. *Evaluation of a Smart Algorithm for Commercial Vehicle Driver Drowsiness Detection*. In IEEE Intelligent Vehicles Symposium, pages 553–559, Jun 2007. (Cited on pages 40 and 41.)
- [EU 2018] EU. *Automation in Transport: How does it affect the labour force?* Conference on the Impact of Automation in Transport, 2018. (Cited on page 18.)
- [Faieghi *et al.* 2014] M. Faieghi, A. Jalali and S. K. M. Mashhadi. *Robust Adaptive Cruise Control of High Speed Trains*. ISA Transactions, vol. 53, no. 2, pages 533–541, 2014. (Cited on page 29.)

- [Fan *et al.* 2007] X. Fan, B. Yin and Y. Sun. *Yawning Detection for Monitoring Driver Fatigue*. In International Conference on Machine Learning and Cybernetics, volume 2, pages 664–668, Aug 2007. (Cited on page 39.)
- [Fan *et al.* 2010] X. Fan, Y. Sun, B. Yin and X. Guo. *Gabor based Dynamic Representation for Human Fatigue Monitoring in Facial Image Sequences*. Pattern Recognition Letters, vol. 31, no. 3, pages 234–243, 2010. (Cited on page 39.)
- [Farid *et al.* 2006] M. N. Farid, M. Kopf, H. Bubb and A. E. Essaili. *Methods to Develop a Driver Observation System used in an Active Safety System*. Vdi Berichte, vol. 1960, Jan 2006. (Cited on page 40.)
- [Filtness & Naweed 2017] A.J. Filtness and A. Naweed. *Causes, Consequences and Countermeasures to Driver Fatigue in the Rail Industry: The Train Driver Perspective*. Applied Ergonomics, vol. 60, pages 12–21, 2017. (Cited on pages 36 and 42.)
- [Fiter *et al.* 2012] C. Fiter, L. Hetel, W. Perruquetti and J. P. Richard. *A State Dependent Sampling for Linear State Feedback*. Automatica, vol. 48, no. 8, pages 1860–1867, 2012. (Cited on page 73.)
- [Fiter *et al.* 2015] C. Fiter, L. Hetel, W. Perruquetti and J. P. Richard. *A Robust Stability Framework for LTI systems with Time Varying Sampling*. Automatica, vol. 54, pages 56–64, 2015. (Cited on pages 73 and 90.)
- [Fiter 2012] C. Fiter. *Contribution to the Control of Systems with Time-Varying and State-Dependent Sampling*. Ecole Centrale Lille, PhD Thesis, 2012. (Cited on pages 60 and 157.)
- [Fletcher *et al.* 2005] L. Fletcher, L. Petersson and A. Zelinsky. *Road Scene Monotony Detection in a Fatigue Management Driver Assistance System*. In IEEE Intelligent Vehicles Symposium, pages 484–489, Jun 2005. (Cited on page 36.)
- [Fridman & Shaked 2002] E. Fridman and U. Shaked. *A Descriptor System Approach to H_∞ Control of Linear Time-delay Systems*. IEEE Transactions on Automatic Control, vol. 47, no. 2, pages 253–270, 2002. (Cited on page 75.)
- [Fridman & Shaked 2003a] E. Fridman and U. Shaked. *Delay Dependent Stability and H_∞ Control: Constant and Time Varying Delays*. International Journal of Control, vol. 76, no. 1, pages 48–60, 2003. (Cited on pages 75, 76 and 77.)
- [Fridman & Shaked 2003b] E. Fridman and U. Shaked. *Special Issue on Time Delay Systems*. International Journal of Robust and Nonlinear Control, vol. 13, no. 9, pages 791–792, 2003. (Cited on page 69.)

- [Fridman & Shaked 2005] E. Fridman and U. Shaked. *Stability and Guaranteed Cost Control of Uncertain Discrete Delay Systems*. International Journal of Control, vol. 78, no. 4, pages 235–246, 2005. (Cited on page 71.)
- [Fridman & Shaked 2006] E. Fridman and U. Shaked. *Input–output Approach to Stability and L2-gain Analysis of Systems with Time-varying Delays*. Systems and Control Letters, vol. 55, no. 12, pages 1041–1053, 2006. (Cited on page 75.)
- [Fridman *et al.* 2004] E. Fridman, A. Seuret and J. P. Richard. *Robust Sampled Data Stabilization of Linear Systems: An Input Delay Approach*. Automatica, vol. 40, no. 8, pages 1441–1446, 2004. (Cited on pages 74, 78 and 80.)
- [Fridman 2001] E. Fridman. *New Lyapunov–Krasovskii Functionals for Stability of Linear Retarded and Neutral Type Systems*. Systems and Control Letters, vol. 43, no. 4, pages 309–319, 2001. (Cited on page 75.)
- [Fridman 2006] E. Fridman. *Stability of Systems with Uncertain Delays: A New "Complete" Lyapunov–Krasovskii Functional*. IEEE Transactions on Automatic Control, vol. 51, no. 5, pages 885–890, 2006. (Cited on page 71.)
- [Fridman 2010] E. Fridman. *A Refined Input Delay Approach to Sampled Data Control*. Automatica, vol. 46, no. 2, pages 421–427, 2010. (Cited on pages 74, 78, 92, 93, 94, 97, 107, 113 and 118.)
- [Fridman 2014a] E. Fridman. Introduction to time delay systems: Analysis and control, pages 1–362. 01 2014. (Cited on page 83.)
- [Fridman 2014b] E. Fridman. *Tutorial on Lyapunov-based Methods for Time-delay Systems*. European Journal of Control, vol. 20, no. 6, pages 271–283, 2014. (Cited on page 74.)
- [Friedrichs & Yang 2010] F. Friedrichs and B. Yang. *Camera based Drowsiness Reference for Driver State Classification under Real Driving Conditions*. In IEEE Intelligent Vehicles Symposium, pages 101–106, June 2010. (Cited on pages 39 and 41.)
- [Fujioka 2009a] H. Fujioka. *A Discrete Time Approach to Stability Analysis of Systems With Aperiodic Sample and Hold Devices*. IEEE Transactions on Automatic Control, vol. 54, no. 10, pages 2440–2445, Oct 2009. (Cited on pages 72 and 90.)
- [Fujioka 2009b] H. Fujioka. *Stability Analysis of Systems with Aperiodic Sample and Hold Devices*. Automatica, vol. 45, no. 3, pages 771–775, 2009. (Cited on pages 90 and 160.)

- [Furugori *et al.* 2005] S. Furugori, N. Yoshizawa, C. Iname and Y. Miura. *Estimation of Driver Fatigue by Pressure Distribution on Seat in Long Term Driving*. Review of Automotive Engineering, vol. 26, pages 053–058, 2005. (Cited on page 40.)
- [Gao *et al.* 2013] S. Gao, H. Dong, Y. Chen, B. Ning, G. Chen and X. Yang. *Approximation Based Robust Adaptive Automatic Train Control: An Approach for Actuator Saturation*. IEEE Transactions on Intelligent Transportation Systems, vol. 14, pages 1733–1742, Dec 2013. (Cited on page 28.)
- [George 2008] G. R. George. *New Methods of Mathematical Modelling of Human Behaviour in the Manual Tracking Task*. 2008. (Cited on page 55.)
- [Gibson 1979] J. J. Gibson. *The ecological approach to visual perception*. Houghton Mifflin, Boston, 1979. (Cited on page 33.)
- [Gielen *et al.* 2010] R. H. Gielen, S. Oлару, M. Lazar, W. P. M. H. Heemels, N. V. D. Wouw and S. I. Niculescu. *On Polytopic Inclusions as a Modeling Framework for Systems with Time Varying Delays*. Automatica, vol. 46, no. 3, pages 615–619, 2010. (Cited on pages 72 and 73.)
- [Gindele *et al.* 2010] T. Gindele, S. Brechtel and R. Dillmann. *A Probabilistic Model for Estimating Driver Behaviours and Vehicle Trajectories in Traffic Environments*. In IEEE Conference on Intelligent Transportation Systems, pages 1625–1631, 2010. (Cited on page 54.)
- [Gingrich *et al.* 1992] C. G. Gingrich, D. R. Kuespert and T. J. McAvoy. *Modeling Human Operators using Neural Networks*. ISA Transactions, vol. 31, no. 3, pages 81–90, 1992. (Cited on pages 54 and 88.)
- [Goebel *et al.* 2012] R. Goebel, R. Sanfelice and A. Teel. *Hybrid Dynamical Systems: Modeling, Stability, and Robustness*. IEEE Control Systems Magazine, vol. 2, no. 2, Mar 2012. (Cited on page 73.)
- [Gordon 2009] T. J. Gordon. *Nonlinear Crossover Model of Vehicle Directional Control*. In American Control Conference, pages 451–456, 2009. (Cited on page 48.)
- [Gouaisbaut & Peaucelle 2006a] F. Gouaisbaut and D. Peaucelle. *Delay-dependent Robust Stability Of Time Delay Systems*. IFAC Symposium on Robust Control Design, vol. 39, no. 9, pages 453–458, 2006. (Cited on page 75.)
- [Gouaisbaut & Peaucelle 2006b] F. Gouaisbaut and D. Peaucelle. *Delay-Dependent Stability Analysis Of Linear Time Delay Systems*. IFAC Proceedings Volumes, vol. 39,

- no. 10, pages 54–59, 2006. IFAC Workshop on Time Delay Systems. (Cited on page 76.)
- [Gruber & Bayoumi 1982] P. Gruber and M. Bayoumi. *Suboptimal Control Strategies for Multilocomotive Powered Trains*. IEEE Transactions on Automatic Control, vol. 27, no. 3, pages 536–546, Jun 1982. (Cited on pages 23 and 28.)
- [Gu *et al.* 2003] K. Gu, J. Chen and V. L. Kharitonov. Stability of time delay systems. Springer, 2003. (Cited on pages 69, 71, 74, 76, 96, 117, 155 and 163.)
- [Gu 1997] K. Gu. *Discretized LMI Set in the Stability Problem of Linear Uncertain Time-Delay Systems*. International Journal of Control, vol. 68, no. 4, pages 923–934, 1997. (Cited on page 71.)
- [Guo & Ahn 2020] X. Guo and C. K. Ahn. *Adaptive Fault-Tolerant Pseudo-PID Sliding-Mode Control for High-Speed Train With Integral Quadratic Constraints and Actuator Saturation*. IEEE Transactions on Intelligent Transportation Systems, pages 1–11, 2020. (Cited on page 25.)
- [Gyurkovics 2015] E. Gyurkovics. *A Note on Wirtinger-type Integral Inequalities for Time-delay Systems*. Automatica, vol. 61, pages 44–46, 2015. (Cited on page 80.)
- [H. & Michel 2000] B. H. and A. N. Michel. *Stability Analysis of Digital Feedback Control Systems with Time-varying Sampling Periods*. Automatica, vol. 36, no. 6, pages 897–905, 2000. (Cited on pages 83 and 84.)
- [Hamilton & Clarke 2005] W. I. Hamilton and T. Clarke. *Driver Performance Modelling and Its Practical Application to Railway Safety*. Applied Ergonomics, vol. 36, no. 6, pages 661–670, 2005. (Cited on page 53.)
- [Hardy *et al.* 1934] G. H. Hardy, J. E. Littlewood and G. Polyakova. *Inequalities*. The Mathematical Gazette, vol. 18, no. 231, page 341–343, 1934. (Cited on pages 80 and 94.)
- [He *et al.* 2005] Y. He, Q. G. Wang, C. Lin and M. Wu. *Augmented Lyapunov Functional and Delay-dependent Stability Criteria for Neutral Systems*. International Journal of Robust and Nonlinear Control, vol. 15, no. 18, pages 923–933, 2005. (Cited on page 82.)
- [He *et al.* 2007] Y. He, Q. G. Wang, C. L. and M. Wu. *Delay-range-dependent Stability for Systems with Time-varying Delay*. Automatica, vol. 43, no. 2, pages 371–376, 2007. (Cited on pages 77 and 83.)

- [Heemels *et al.* 2010] W. P. M. H. Heemels, A. R. Teel, N. van de Wouw and D. Nešić. *Networked Control Systems With Communication Constraints: Tradeoffs Between Transmission Intervals, Delays and Performance*. IEEE Transactions on Automatic Control, vol. 55, no. 8, pages 1781–1796, 2010. (Cited on page 61.)
- [Hetel *et al.* 2006] L. Hetel, J. Daafouz and C. Iung. *Stabilization of Arbitrary Switched Linear Systems With Unknown Time Varying Delays*. IEEE Transactions on Automatic Control, vol. 51, no. 10, pages 1668–1674, Oct 2006. (Cited on pages 72, 73 and 90.)
- [Hetel *et al.* 2007a] L. Hetel, J. Daafouz and C. Iung. *LMI Control Design for a Class of Exponential Uncertain Systems with Application to Network Controlled Switched Systems*. In American Control Conference, pages 1401–1406, 2007. (Cited on page 73.)
- [Hetel *et al.* 2007b] L. Hetel, J. Daafouz and C. Iung. *LMI Control Design for a Class of Exponential Uncertain Systems with Application to Network Controlled Switched Systems*. In American Control Conference, pages 1401–1406, July 2007. (Cited on page 90.)
- [Hetel *et al.* 2011] L. Hetel, A. Kruszewski, W. Perruquetti and J. P. Richard. *Discrete and Intersample Analysis of Systems With Aperiodic Sampling*. IEEE Transactions on Automatic Control, vol. 56, pages 1696–1701, Aug 2011. (Cited on pages 66, 73 and 90.)
- [Hetel *et al.* 2017] L. Hetel, C. Fiter, H. Omran, A. Seuret, E. Fridman, J. P. Richard and S. I. Niculescu. *Recent Developments on the Stability of Systems with Aperiodic Sampling: An Overview*. Automatica, vol. 76, pages 309–335, 2017. (Cited on pages 60, 64 and 67.)
- [Hollnagel 1998] E. Hollnagel. Cognitive reliability and error analysis method. Elsevier, 1998. (Cited on page 33.)
- [Hou *et al.* 1997] L. Hou, A. Michel and H. Ye. *Some Qualitative Properties of Sampled-data Control Systems*. IEEE Transactions on Automatic Control, vol. 42, pages 1721–1725, 1997. (Cited on page 83.)
- [Howlett *et al.* 1994] P. Howlett, I. P. Milroy and P. J. Pudney. *Energy Efficient Train Control*. Control Engineering Practice, vol. 2, no. 2, pages 193–200, 1994. (Cited on page 21.)

- [Howlett *et al.* 2009] P. Howlett, P. Pudney and X. Vu. *Local Energy Minimization in Optimal Train Control*. *Automatica*, vol. 45, no. 11, pages 2692–2698, 2009. (Cited on page 21.)
- [Howlett 1996] P. Howlett. *Optimal Strategies for the Control of a Train*. *Automatica*, vol. 32, no. 4, pages 519–532, 1996. (Cited on page 28.)
- [Howlett 2000] P. Howlett. *The Optimal Control of a Train*. *Annals of Operations Research*, vol. 98, pages 65–87, 12 2000. (Cited on page 21.)
- [Hu & Zheng 2009] S. Hu and G. Zheng. *Driver Drowsiness detection with Eyelid related parameters by Support Vector Machine*. *Expert Systems with Applications*, vol. 36, no. 4, pages 7651–7658, 2009. (Cited on page 39.)
- [Hu *et al.* 2009] S. Hu, R. L. Bowlds, Y. Gu and X. Yu. *Pulse Wave Sensor for Non-Intrusive Driver's Drowsiness Detection*. In *IEEE Engineering in Medicine and Biology Society*, pages 2312–2315, Sep 2009. (Cited on page 38.)
- [Hu *et al.* 2018] S. Hu, D. Yue, X. Xie, Y. Ma and X. Yin. *Stabilization of Neural Network based Control Systems via Event-Triggered Control With Nonperiodic Sampled Data*. *IEEE Transactions on Neural Networks and Learning Systems*, vol. 29, no. 3, pages 573–585, Mar 2018. (Cited on page 120.)
- [Huang *et al.* 2019] D. Huang, Y. Chen, D. Meng and P. Sun. *Adaptive Iterative Learning Control for High-Speed Train: A Multi-Agent Approach*. *IEEE Transactions on Systems, Man, and Cybernetics: Systems*, pages 1–11, 2019. (Cited on page 27.)
- [Hutchins 1995] E. Hutchins. *Cognition in the wild*. MIT Press, CAE, 1995. (Cited on page 33.)
- [IEC62290-1 2014] IEC62290-1. *Railway Applications: Urban Guided Transport Management and Control Systems*. International Electro Technical Commission, 2014. (Cited on page 18.)
- [Ingre *et al.* 2006] M. Ingre, T. Åkerstedt, B. Peters, A. Anind and G. Kecklund. *Subjective Sleepiness, Simulated Driving Performance and Blink Duration: Examining Individual Differences*. *Journal of Sleep Research*, vol. 15, no. 1, pages 47–53, 2006. (Cited on page 40.)
- [IRJ 2018] IRJ. *Automatic Train Operation takes to the Main Line*. *International Rail Journal*, 2018. (Cited on page 18.)

- [Jain *et al.* 2019] A. K. Jain, C. Fiter, D. Berdjag, P. Polet and R. Béarée. *Approximate Computing Control Approaches Using Recurrent Neural Networks*. In JN-JDMACS, pages 1–4. GDRMACS, 2019. (Cited on page 89.)
- [Jiang & Seuret 2010] W. Jiang and A. Seuret. *Improved Stability Analysis of Networked Control Systems under Asynchronous Sampling and Input Delay*. IFAC Proceedings Volumes, vol. 43, no. 19, pages 79–84, 2010. (Cited on page 94.)
- [Jiang *et al.* 2010] W. Jiang, A. Kruszewski, E. Fridman and J. P. Richard. *Delay Dependent Stability Analysis of Interval Time Delay Systems*. IFAC Proceedings Volumes, vol. 43, no. 2, pages 313–318, 2010. (Cited on page 94.)
- [Kaida *et al.* 2006] K. Kaida, M. Takahashi, T. Åkerstedt, A. Nakata, Y. Otsuka, T. Haratani and K. Fukasawa. *Validation of the Karolinska Sleepiness Scale against Performance and EEG Variables*. Clinical Neurophysiology, vol. 117, no. 7, pages 1574–1581, 2006. (Cited on page 40.)
- [Kamen & Khargonekar 1984] E. Kamen and P. Khargonekar. *On the Control of Linear Systems Whose Coefficients are Functions of Parameters*. IEEE Transactions on Automatic Control, vol. 29, no. 1, pages 25–33, 1984. (Cited on page 65.)
- [Kao & Lincoln 2004] C. Y. Kao and B. Lincoln. *Simple Stability Criteria for Systems with Time Varying Delays*. Automatica, vol. 40, no. 8, pages 1429–1434, 2004. (Cited on page 90.)
- [Kao & Rantzer 2007] C. Y. Kao and A. Rantzer. *Stability Analysis of Systems with Uncertain Time Varying Delays*. Automatica, vol. 43, no. 6, pages 959–970, 2007. (Cited on page 90.)
- [Karafyllis & Kravaris 2009] I. Karafyllis and C. Kravaris. *Global Stability results for Systems under Sampled Data Control*. International Journal of Robust and Nonlinear Control, vol. 19, no. 10, pages 1105–1128, 2009. (Cited on page 68.)
- [Katsis *et al.* 2004] C. Katsis, N. Ntouvas, C. Bafas and D. Fotiadis. *Assessment of Muscle Fatigue during Driving using Surface EMG*. Jan 2004. (Cited on page 39.)
- [Ke *et al.* 2011] B. R. Ke, C. L. Lin and C. W. Lai. *Optimization of Train Speed Trajectory and Control for Mass Rapid Transit Systems*. Control Engineering Practice, vol. 19, no. 7, pages 675–687, 2011. (Cited on pages 21 and 26.)
- [Khalil 2002] H. K. Khalil. *Nonlinear Systems*. Prentice-Hall, Upper Saddle River, NJ, 2002. (Cited on pages 84, 157, 158 and 160.)

- [Kharitonov & Niculescu 2003] V. L. Kharitonov and S. Niculescu. *On the Stability of Linear Systems with Uncertain Delay*. IEEE Transactions on Automatic Control, vol. 48, no. 1, pages 127–132, 2003. (Cited on page 74.)
- [Kharitonov & Zhabko 2003] V. L. Kharitonov and A. P. Zhabko. *Lyapunov–Krasovskii Approach to the Robust Stability Analysis of Time-Delay Systems*. Automatica, vol. 39, no. 1, pages 15–20, 2003. (Cited on page 71.)
- [Khmelnitsky 2000] E. Khmelnitsky. *On an Optimal Control Problem of Train Operation*. IEEE Transactions on Automatic Control, vol. 45, no. 7, pages 1257–1266, July 2000. (Cited on pages 21 and 28.)
- [Khodayari *et al.* 2012] A. Khodayari, A. Ghaffari, R. Kazemi and R. Braunstingl. *A Modified Car-Following Model Based on a Neural Network Model of the Human Driver Effects*. IEEE Transactions on Systems, Man, and Cybernetics - Part A: Systems and Humans, vol. 42, no. 6, pages 1440–1449, 2012. (Cited on page 88.)
- [Khushaba *et al.* 2011] R. N. Khushaba, S. Kodagoda, S. Lal and G. Dissanayake. *Intelligent Driver Drowsiness Detection System using Uncorrelated Fuzzy Locality Preserving Analysis*. In 2011 IEEE International Conference on Intelligent Robots and Systems, pages 4608–4614, Sep 2011. (Cited on page 41.)
- [Kiencke *et al.* 1999] U. Kiencke, R. Majjad and S. Kramer. *Modelling and Performance Analysis of a Hybrid Driver Model*. Control Engineering Practice, vol. 7, no. 8, pages 985–991, 1999. (Cited on page 51.)
- [Kim & Chien 2011] K. Kim and S. I. Chien. *Optimal Train Operation for Minimum Energy Consumption Considering Track Alignment, Speed Limit, and Schedule Adherence*. Journal of Transportation Engineering, vol. 137, pages 665–674, 09 2011. (Cited on page 21.)
- [Kim *et al.* 2005] J. H. Kim, S. Okuma, Y. W. Kim, D. H. Hwang, M. H. Kim and D. H. Kim. *Modelling of Human Driving Behaviour Based on Piece wise Linear Model*. pages 25–30, Feb 2005. (Cited on page 51.)
- [Kim *et al.* 2010] N. Kim, L. Rothrock, J. Joo and R. A. Wysk. *An Affordance-based Formalism for Modelling Human-Involvement in Complex Systems for Prospective Control*. In Winter Simulation Conference, pages 811–823, 2010. (Cited on pages 50 and 51.)
- [Ko *et al.* 2004] H. Ko, T. Koseki and M. Miyatake. *Application of Dynamic Programming to Optimization of Running Profile of a Train*. 05 2004. (Cited on page 21.)

- [Kolmanovskii & Myshkis 1992] V. Kolmanovskii and A. Myshkis. Applied theory of functional differential equations, volume 85. Springer Science and Business Media, 1992. (Cited on page 79.)
- [Kolmanovskii & Myshkis 1999] V. Kolmanovskii and A. Myshkis. *Introduction to the Theory and Applications of Functional Differential Equations*. Mathematics and Its Application, Springer, vol. 463, 1999. (Cited on page 72.)
- [Kolmanovskii & Richard 1999] V. B. Kolmanovskii and J. Richard. *Stability of Some Linear Systems with Delays*. IEEE Transactions on Automatic Control, vol. 44, no. 5, pages 984–989, 1999. (Cited on pages 74 and 75.)
- [Kolmanovskii & Shaikhet 1996] V. Kolmanovskii and L. E. Shaikhet. *Control of Systems with After Affect*. Translations of Mathematical Monographs, American Mathematical Society, vol. 157, 1996. (Cited on page 71.)
- [Kolmanovskii *et al.* 1998] V. Kolmanovskii, J. Richard and A. P. Tchangan. *Some Model Transformation for the Stability Study of Linear Systems With Delay*. IFAC Proceedings Volumes, vol. 31, pages 63–68, 1998. (Cited on page 75.)
- [Kosinski 2008] R. J. Kosinski. *A Literature Review on Reaction Time*. Online, Available: <http://biae.clemson.edu/bpc/bp/Lab/110/reaction.html>, Sept 2008. (Cited on page 37.)
- [Krajewski *et al.* 2017] J. Krajewski, D. Sommer, U. Trutschel, D. Edwards and M. Golz. *Steering Wheel Behavior based Estimation of Fatigue*. pages 118–124, Oct 2017. (Cited on page 40.)
- [Krasovskii 1963] N. N. Krasovskii. *Stability Of Motion: Applications Of Lyapunov's Second Method To Differential Systems And Equations With Delay*. Stanford University Press, 1963. (Cited on page 70.)
- [Kuefler *et al.* 2017] A. Kuefler, J. Morton, T. Wheeler and M. Kochenderfer. *Imitating Driver Behavior with Generative Adversarial Networks*. In IEEE Intelligent Vehicles Symposium, pages 204–211, 2017. (Cited on page 88.)
- [Ladelfa *et al.* 2019] S. Ladelfa, S. Enjalbert, P. Polet and F. Vanderhaegen. *Design of a Cooperative Eco Driving Rail Control System: An Experimental Study*. Cognition, Technology and Work, 12 2019. (Cited on page 43.)
- [Lam & Leung 2006] H. K. Lam and F. H. F. Leung. *Design and Stabilization of Sampled Data Neural Network based Control Systems*. IEEE Transactions on Systems, Man,

- and Cybernetics, Part B, vol. 36, no. 5, pages 995–1005, Oct 2006. (Cited on page 137.)
- [Lam *et al.* 2000] H. K. Lam, F. H. F. Leung and P. K. S. Tam. *Stable and Robust Fuzzy Control for Uncertain Nonlinear Systems*. IEEE Transactions on Systems, Man, and Cybernetics - Part A: Systems and Humans, vol. 30, no. 6, pages 825–840, 2000. (Cited on page 110.)
- [Lauffenburger 2002] J. P. Lauffenburger. *Contribution a La Surveillance Temps-Reel du Systeme Conducteur Vehicule Environnement : Elaboration D'un Systeme Intelligent D'aide a La Conduite*. December 2002. (Cited on page 50.)
- [Leander *et al.* 2013] P. Leander, T. Liden, M. Joborn and T. Nordmark. *Implications on Capacity and Energy by Introduction of a Driver Advisory System*. Proceedings of International Heavy Haul Conference, 2013. (Cited on page 42.)
- [Lee & Chung 2012] B. G. Lee and W. Y. Chung. *Driver Alertness Monitoring using Fusion of Facial Features and Bio Signals*. IEEE Sensors Journal, vol. 12, pages 2416–2422, 07 2012. (Cited on page 41.)
- [Lee & Kwon 2002] Y. S. Lee and W. H. Kwon. *Delay-dependent Robust Stabilization Of Uncertain Discrete-Time State-Delayed Systems*. IFAC Proceedings Volumes, vol. 35, no. 1, pages 261–266, 2002. IFAC World Congress. (Cited on page 78.)
- [Lee *et al.* 2014] T. H. Lee, J. H. Park, H. Y. Jung, O. M. Kwon and S. M. Lee. *Improved Results on Stability of Time-delay Systems using Wirtinger-based Inequality*. IFAC World Congress, vol. 47, no. 3, pages 6826–6830, 2014. (Cited on page 80.)
- [Lee *et al.* 2018] S. Y. Lee, W. I. Lee and P. Park. *Orthogonal-polynomials-based Integral Inequality and its Applications to Systems with Additive time-varying Delays*. Journal of the Franklin Institute, vol. 355, no. 1, pages 421–435, 2018. (Cited on pages 82, 107 and 156.)
- [Li & Lo 2014] X. Li and H. K. Lo. *An Energy Efficient Scheduling and Speed Control Approach for Metro Rail Operations*. Transportation Research Part B: Methodological, vol. 64, pages 73–89, 2014. (Cited on page 21.)
- [Li & Souza 1997] X. Li and C. E. D. Souza. *Criteria for Robust Stability and Stabilization of Uncertain Linear Systems with State Delay*. Automatica, vol. 33, no. 9, pages 1657–1662, 1997. (Cited on page 74.)

- [Li *et al.* 2010] X. G. Li, A. Çela, S. I. Niculescu and A. Reama. *Some Problems in the Stability of Networked Control Systems with Periodic Scheduling*. International Journal of Control, vol. 83, no. 5, pages 996–1008, 2010. (Cited on pages 67 and 161.)
- [Li *et al.* 2014] S. Li, L. Yang, K. Li and Z. Gao. *Robust Sampled Data Cruise Control Scheduling of High Speed Train*. Transportation Research Part C: Emerging Technologies, vol. 46, pages 274–283, 2014. (Cited on page 30.)
- [Li *et al.* 2015] S. Li, L. Yang and K. P. Li. *Robust Output Feedback Cruise Control for High Speed Train Movement with Uncertain Parameters*. Chinese Physics B, vol. 24, Jan 2015. (Cited on page 29.)
- [Li *et al.* 2016] S. Li, L. Yang, Z. Gao and K. Li. *Optimal Guaranteed Cost Cruise Control for High Speed Train Movement*. IEEE Transactions on Intelligent Transportation Systems, vol. 17, no. 10, pages 2879–2887, Oct 2016. (Cited on page 30.)
- [Li *et al.* 2018] Z. Li, L. Chen, C. Roberts and N. Zhao. *Dynamic Trajectory Optimization Design for Railway Driver Advisory System*. IEEE Intelligent Transportation Systems Magazine, vol. 10, no. 1, pages 121–132, 2018. (Cited on page 43.)
- [Li *et al.* 2019] Z. Li, T. Tang and C. Gao. *Long Short-Term Memory Neural Network Applied to Train Dynamic Model and Speed Prediction*. Algorithms, vol. 12, page 173, Aug 2019. (Cited on page 88.)
- [Lin *et al.* 2005] Y. Lin, P. Tang, W. Zhang and Q. Yu. *Artificial Neural Network Modelling of Driver Handling Behaviour in a Driver-Vehicle-Environment System*. International Journal of Vehicle Design, vol. 37, pages 24–45, 2005. (Cited on page 88.)
- [Lin *et al.* 2006a] C. Lin, Q. G. Wang and T. H. Lee. *A Less Conservative Robust Stability test for Linear Uncertain Time-delay Systems*. IEEE Transactions on Automatic Control, vol. 51, no. 1, pages 87–91, 2006. (Cited on page 82.)
- [Lin *et al.* 2006b] C. T. Lin, R. C. Wu, S. F. Liang, W. H. Chao, Y. J. Chen and T. P. Jung. *EEG-based Drowsiness Estimation for Safety Driving using Independent Component Analysis*. IEEE Transactions on Circuits and Systems, vol. 52, pages 2726–2738, Jan 2006. (Cited on page 39.)
- [Lin *et al.* 2008] C. Lin, Y. Chen, T. Huang, T. Chiu, L. Ko, S. Liang, H. Hsieh, S. Hsu and J. Duann. *Development of Wireless Brain Computer Interface with Embedded*

- Multitask Scheduling and its Application on Real-Time Driver's Drowsiness Detection and Warning*. IEEE Transactions on Biomedical Engineering, vol. 55, no. 5, pages 1582–1591, May 2008. (Cited on page 39.)
- [Linderoth & Ralphs 2005] J. Linderoth and T. Ralphs. *Noncommercial Software for Mixed-Integer Linear Programming*. Integer Programming: Theory and Practice, 09 2005. (Cited on page 21.)
- [Liu & Fridman 2012] K. Liu and E. Fridman. *Wirtinger Inequality and Lyapunov based Sampled Data Stabilization*. Automatica, vol. 48, no. 1, pages 102–108, 2012. (Cited on pages 80 and 81.)
- [Liu & Golovitcher 2003] R. Liu and I. M. Golovitcher. *Energy Efficient Operation of Rail Vehicles*. Transportation Research Part A: Policy and Practice, vol. 37, no. 10, pages 917–932, Dec 2003. (Cited on pages 21 and 28.)
- [Liu & Wu 2006] Y. Liu and Z. Wu. *Multitasking Driver Cognitive Behaviour Modelling*. In 3rd International IEEE Conference Intelligent Systems, pages 52–57, 2006. (Cited on page 52.)
- [Liu *et al.* 2010] K. Liu, V. Suplin and E. Fridman. *Stability of Linear Systems with General Sawtooth Delay*. IMA Journal of Mathematical Control and Information, vol. 27, no. 4, pages 419–436, 2010. (Cited on pages 80, 95, 116 and 155.)
- [Liu *et al.* 2013] Y. Liu, S. Tong and C. L. P. Chen. *Adaptive Fuzzy Control via Observer Design for Uncertain Nonlinear Systems With Unmodelled Dynamics*. IEEE Transactions on Fuzzy Systems, vol. 21, no. 2, pages 275–288, 2013. (Cited on page 110.)
- [Liu *et al.* 2015] S. Liu, F. Cao, J. Xun and Y. Wang. *Energy Efficient Operation of Single Train Based on the Control Strategy of ATO*. In IEEE International Conference on Intelligent Transportation Systems, pages 2580–2586, Sep 2015. (Cited on page 21.)
- [Liu *et al.* 2017] W. Liu, Z. Wang, X. Liu, N. Zeng, Y. Liu and F. E. Alsaadi. *A Survey of Deep Neural Network Architectures and their Applications*. Neurocomputing, vol. 234, pages 11–26, 2017. (Cited on page 89.)
- [Liu *et al.* 2019] K. Liu, A. Selivanov and E. Fridman. *Survey on Time-Delay Approach to Networked Control*. Annual Reviews in Control, vol. 48, pages 57–79, 2019. (Cited on pages 60 and 67.)
- [Louisell 1999] J. Louisell. *New Examples of Quenching in Delay Differential Equations having Time-varying Delay*. IEEE European Control Conference, 1999. (Cited on page 78.)

- [Lu *et al.* 2013] S. Lu, S. Hillmansen, T. K. Ho and C. Roberts. *Single Train Trajectory Optimization*. IEEE Transactions on Intelligent Transportation Systems, vol. 14, no. 2, pages 743–750, Jun 2013. (Cited on page 21.)
- [Macadam 2003] C. Macadam. *Understanding and Modelling the Human Driver*. Vehicle System Dynamics, vol. 40, pages 101–134, Sep 2003. (Cited on page 47.)
- [Maeda *et al.* 1989] T. Maeda, M. Kinoshita, H. Kajiyama and K. Tanemoto. *Aerodynamic Drag of Shinkansen Electric Cars*. Railway Technical Research Institute, Quaterly Reports, vol. 30, no. 1, 1989. (Cited on page 131.)
- [Marino *et al.* 2013] R. Marino, S. Scalzi, P. Tomei and C. M. Verrelli. *Fault Tolerant Cruise Control of Electric Vehicles with Induction Motors*. Control Engineering Practice, vol. 21, pages 860–869, 2013. (Cited on page 29.)
- [Mars & Chevrel 2017] F. Mars and P. Chevrel. *Modelling Human Control of Steering for the Design of Advanced Driver Assistance Systems*. Annual Reviews in Control, vol. 44, pages 292–302, 2017. (Cited on page 49.)
- [Martinez *et al.* 2018] C. M. Martinez, M. Heucke, F. Wang, B. Gao and D. Cao. *Driving Style Recognition for Intelligent Vehicle Control and Advanced Driver Assistance: A Survey*. IEEE Transactions on Intelligent Transportation Systems, vol. 19, no. 3, pages 666–676, 2018. (Cited on page 38.)
- [Mcclanachan & Cole 2012] M. Mcclanachan and C. Cole. *Current Train Control Optimization Methods with a view for Application in Heavy Haul Railways*. Institution of Mechanical Engineers, Part F: Journal of Rail and Rapid Transit, vol. 226, no. 1, pages 36–47, 2012. (Cited on page 22.)
- [McLeod *et al.* 2005] R. W. McLeod, G. H. Walker and N. Moray. *Analysing and Modelling Train Driver Performance*. Applied Ergonomics, vol. 36, no. 6, pages 671–680, 2005. Special Issue: Rail Human Factors. (Cited on pages 32, 34 and 53.)
- [McRuer & Jex 1967] D. T. McRuer and H. R. Jex. *A Review of Quasi-Linear Pilot Models*. IEEE Transactions on Human Factors in Electronics, vol. 8, no. 3, pages 231–249, 1967. (Cited on pages 45 and 47.)
- [Mcruer & Krendel 1962] D. T. Mcruer and E. S. Krendel. *The Man-Machine System Concept*. IRE, vol. 50, no. 5, pages 1117–1123, 1962. (Cited on page 47.)
- [Mcruer 1980] D. Mcruer. *Human Dynamics in Man Machine Systems*. Automatica, vol. 16, no. 3, pages 237–253, 1980. (Cited on page 47.)

- [Michon 1985] J. A. Michon. A critical view of driver behaviour models: What do we know, what should we do?, pages 485–524. Springer, 1985. (Cited on page 52.)
- [Mikami *et al.* 2010] K. Mikami, H. Okuda, S. Taguchi, Y. Tazaki and T. Suzuki. *Model Predictive Assisting Control of Vehicle Following Task based on Driver Model*. In IEEE International Conference on Control Applications, pages 890–895, 2010. (Cited on page 51.)
- [Mikheev *et al.* 1988] Y. Mikheev, V. Sobolev and E. Fridman. *Asymptotic Analysis of Digital Control Systems*. vol. 49, no. 9, pages 1175–1180, 1988. (Cited on pages 67 and 68.)
- [Mirkin 2007] L. Mirkin. *Some remarks on the use of Time Varying Delay to Model Sample and Hold Circuits*. IEEE Transactions on Automatic Control, vol. 52, no. 6, pages 1109–1112, Jun 2007. (Cited on page 90.)
- [Miyatake & Ko 2010] M. Miyatake and H. Ko. *Optimization of Train Speed Profile for Minimum Energy Consumption*. IEEJ Transactions on Electrical and Electronic Engineering, vol. 5, no. 3, pages 263–269, 2010. (Cited on page 21.)
- [Miyatake & Matsuda 2009] M. Miyatake and K. Matsuda. *Energy Saving Speed and Charge Discharge Control of a Railway Vehicle with On-board Energy Storage by means of an Optimization Model*. IEEJ Transactions on Electrical and Electronic Engineering, vol. 4, no. 6, pages 771–778, 2009. (Cited on page 21.)
- [Mounier & Rudolph 2003] H. Mounier and J. Rudolph. *Time-Delay Systems*. Encyclopedia of Life and Support Systems, Jan 2003. (Cited on page 69.)
- [Mulder *et al.* 2018] M. Mulder, D. M. Pool, D. A. Abbink, E. R. Boer, P. M. T. Zaal, F. M. Drop, K. v. d. El and M. M. V. Paassen. *Manual Control Cybernetics: State-of-the-Art and Current Trends*. IEEE International Transactions on Human-Machine Systems, vol. 18, no. 5, October 2018. (Cited on page 48.)
- [Naghshtabrizi *et al.* 2007] P. Naghshtabrizi, J. P. Hespanha and A. R. Teel. *Stability of Delay Impulsive Systems with Application to Networked Control Systems*. In American Control Conference, pages 4899–4904, 2007. (Cited on page 67.)
- [Naghshtabrizi *et al.* 2008] P. Naghshtabrizi, J. P. Hespanha and A. R. Teel. *Exponential Stability of Impulsive Systems with Application to Uncertain Sampled Data Systems*. Systems & Control Letters, vol. 57, no. 5, pages 378–385, 2008. (Cited on pages 74, 78 and 94.)

- [Nechyba & Xu 1994] M. Nechyba and Y. Xu. *Neural Network Approach to Control System Identification with Variable Activation Functions*. IEEE International Symposium on Intelligent Control, pages 358–363, 1994. (Cited on page 89.)
- [Niculescu 2001a] S. I. Niculescu. Delay effects on stability - a robust control approach, volume 269 of *Lecture Notes in Control and Information Sciences*. January 2001. (Cited on page 71.)
- [Niculescu 2001b] S. I. Niculescu. *On Delay-dependent Stability in Neutral Systems*. In American Control Conference, volume 5, pages 3384–3388, June 2001. (Cited on page 75.)
- [Nilsson 1998] J. Nilsson. *Real-Time Control Systems with Delays*. Lund Institute of Technology, PhD Thesis, 1998. (Cited on page 67.)
- [Niu *et al.* 2018] B. Niu, C. K. Ahn, H. Li and M. Liu. *Adaptive Control for Stochastic Switched Nonlower Triangular Nonlinear Systems and Its Application to a One-Link Manipulator*. IEEE Transactions on Systems, Man, and Cybernetics: Systems, vol. 48, no. 10, pages 1701–1714, 2018. (Cited on page 110.)
- [Nwankpa *et al.* 2018] C. Nwankpa, W. Ijomah, A. Gachagan and S. Marshall. *Activation Functions: Comparison of trends in Practice and Research for Deep Learning*. arXiv: 1811.03378, 2018. (Cited on page 137.)
- [Okamoto & Tsiotras 2019] K. Okamoto and P. Tsiotras. *Data Driven Human Driver Lateral Control Models for Developing Haptic Shared Control Advanced Driver Assist Systems*. Robotics and Autonomous Systems, vol. 114, pages 155–171, 2019. (Cited on pages 55 and 88.)
- [Olabiyi *et al.* 2017] O. Olabiyi, E. Martinson, V. Chintalapudi and R. Guo. *Driver Action Prediction Using Deep (Bidirectional) Recurrent Neural Network*. arXiv, Jun 2017. (Cited on pages 54 and 88.)
- [Olaru & Niculescu 2008] S. Olaru and S. I. Niculescu. *Predictive Control for Linear Systems with Delayed Input Subject to Constraints*. IFAC Proceedings Volumes, vol. 41, no. 2, pages 11208–11213, 2008. IFAC World Congress. (Cited on page 73.)
- [Orazio *et al.* 2007] T. D. Orazio, M. Leo, C. Guaragnella and A. Distante. *A Visual approach for Driver Inattention Detection*. Pattern Recognition, vol. 40, no. 8, pages 2341–2355, 2007. Special Issue on Visual Information Processing. (Cited on page 39.)

- [Oshima *et al.* 1988] H. Oshima, S. Yasunobu and S. Sekino. *Automatic Train Operation System based on Predictive Fuzzy Control*. In International Workshop on Artificial Intelligence for Industrial Applications, pages 485–489, May 1988. (Cited on page 26.)
- [Oza 1999] N. Oza. *Probabilistic Models of Driver Behaviour*. 1999. (Cited on page 54.)
- [Papachristodoulou *et al.* 2007] A. Papachristodoulou, M. M. Peet and S. I. Niculescu. *Stability Analysis of Linear Systems with Time-varying Delays: Delay Uncertainty and Quenching*. pages 2117–2122, 2007. (Cited on page 78.)
- [Park & Ko 2007] P. Park and J. W. Ko. *Stability and Robust stability for Systems with a Time Varying Delay*. *Automatica*, vol. 43, no. 10, pages 1855–1858, 2007. (Cited on page 78.)
- [Park & Park 2018] J. Park and P. Park. *Stability Analysis for Systems with Time-varying Delay via Orthogonal-polynomial-based Integral Inequality*. *IFAC-PapersOnLine*, vol. 51, no. 14, pages 277–281, 2018. (Cited on page 105.)
- [Park *et al.* 2011a] M. J. Park, O. M. Kwon, J. H. Park and S. M. Lee. *A New Augmented Lyapunov–Krasovskii Functional Approach for Stability of Linear Systems with Time-varying Delays*. *Applied Mathematics and Computation*, vol. 217, no. 17, pages 7197–7209, 2011. (Cited on page 83.)
- [Park *et al.* 2011b] P. Park, J. W. Ko and C. Jeong. *Reciprocally Convex Approach to Stability of Systems with Time-varying Delays*. *Automatica*, vol. 47, pages 235–238, 2011. (Cited on pages 77, 78 and 83.)
- [Park *et al.* 2015a] M. Park, O. Kwon, J. H. Park, S. Lee and E. Cha. *Stability of Time-delay Systems via Wirtinger-based Double Integral Inequality*. *Automatica*, vol. 55, pages 204–208, 2015. (Cited on page 81.)
- [Park *et al.* 2015b] P. Park, W. I. Lee and S. Y. Lee. *Auxiliary Function-based Integral Inequalities for Quadratic Functions and Their Applications to Time-delay Systems*. *Journal of the Franklin Institute*, vol. 352, no. 4, pages 1378–1396, 2015. (Cited on pages 81 and 100.)
- [Park 1999] P. Park. *A Delay-dependent Stability Criterion For Systems with Uncertain Time-invariant Delays*. *IEEE Transactions on Automatic Control*, vol. 44, no. 4, pages 876–877, 1999. (Cited on page 74.)

- [Pentland & Liu 1999] A. Pentland and Andrew Liu. *Modeling and Prediction of Human Behavior*. Neural Computation, vol. 11, pages 229–242, 1999. (Cited on page 55.)
- [Phillips *et al.* 2017] D. J. Phillips, T. A. Wheeler and M. J. Kochenderfer. *Generalizable Intention Prediction of Human Drivers at Intersections*. In IEEE Intelligent Vehicles Symposium, pages 1665–1670, 2017. (Cited on page 88.)
- [Picot *et al.* 2012] A. Picot, S. Charbonnier and A. Caplier. *Online Detection of Drowsiness using Brain and Visual Information*. IEEE Transactions on Systems, Man, and Cybernetics - Part A: Systems and Humans, vol. 42, no. 3, pages 764–775, May 2012. (Cited on page 41.)
- [Precup *et al.* 2010] R. Precup, M. L. Tomescu, E. M. Petriu, S. Preitl, J. Fodor and D. Bărbulescu. *Stability Analysis of a Class of MIMO Fuzzy Control Systems*. In International Conference on Fuzzy Systems, pages 1–6, 2010. (Cited on page 110.)
- [Qian *et al.* 2010] H. Qian, Y. Ou, X. Wu, M. Xiaoning and X. Yangsheng. *Support Vector Machine for Behaviour-Based Driver Identification System*. Journal of Robotics, vol. 2010, Apr 2010. (Cited on page 55.)
- [Raats *et al.* 2020] K. Raats, V. Fors and S. Pink. *Trusting Autonomous Vehicles: An Interdisciplinary Approach*. Transportation Research Interdisciplinary Perspectives, vol. 7, page 100201, 2020. (Cited on page 36.)
- [Rachedi *et al.* 2013] N. D. Rachedi, D. Berdjag and F. Vanderhaegen. *Operator Behavior Modeling: Unexpected Situations Management*. 12th IFAC Symposium on Analysis, Design, and Evaluation of Human-Machine Systems, vol. 46, no. 15, pages 381–386, 2013. (Cited on page 51.)
- [Rachedi 2015] N. D. E. Rachedi. *Modelling and Monitoring of Human-Machine Systems: Application to Railway Driving*. PhD Thesis, pages 42–43, 2015. (Cited on pages 32, 40 and 49.)
- [Ramadge & Wonham 1989] P. J. G. Ramadge and W. M. Wonham. *The Control of Discrete Event Systems*. IEEE, vol. 77, no. 1, pages 81–98, 1989. (Cited on page 50.)
- [Rasmussen *et al.* 1994] J. Rasmussen, A. M. Pejtersen and L. Goodstein. *Cognitive Engineering: Concepts and Applications*. 1994. (Cited on page 33.)
- [Rasmussen 1983] J. Rasmussen. *Skills, Rules, and Knowledge; Signals, Signs, and Symbols, and other Distinctions in Human Performance Models*. IEEE Transactions

- on Systems, Man, and Cybernetics, vol. 13, no. 3, pages 257–266, 1983. (Cited on page 52.)
- [Razumikhin 1956] B. S. Razumikhin. *On the Stability of Systems with Delay*. *Prikladnaya Matematika i Mekhanika*, vol. 20, no. 4, pages 500–512, 1956. (Cited on page 70.)
- [Richard 2003] J. P. Richard. *Time-delay Systems: An Overview Of Some Recent Advances And Open Problems*. *Automatica*, vol. 39, no. 10, pages 1667–1694, 2003. (Cited on page 69.)
- [Robert *et al.* 2010] D. Robert, O. Sename and D. Simon. *An H_∞ LPV Design for Sampling Varying Controllers: Experimentation With a T-Inverted Pendulum*. *IEEE Transactions on Control Systems Technology*, vol. 18, no. 3, pages 741–749, 2010. (Cited on page 67.)
- [Rochard & Schmid 2000] B. P. Rochard and F. Schmid. *A Review of Methods to Measure and Calculate Train Resistances*. *Proceedings of the Institution of Mechanical Engineers, Part F: Journal of Rail and Rapid Transit*, vol. 214, no. 4, pages 185–199, 2000. (Cited on page 23.)
- [Rodrigo *et al.* 2013] E. Rodrigo, S. Tapia, J. Mera and M. Soler. *Optimizing Electric Rail Energy Consumption using the Lagrange Multiplier Technique*. *Journal of Transportation Engineering*, vol. 139, pages 321–329, Mar 2013. (Cited on page 21.)
- [Sahoo & Narayanan 2018] A. Sahoo and V. Narayanan. *Event-based Near Optimal Sampling and Tracking Control of Nonlinear Systems*. In *IEEE Conference on Decision and Control*, pages 55–60, 2018. (Cited on page 89.)
- [Sahoo *et al.* 2016] A. Sahoo, H. Xu and S. Jagannathan. *Neural Network based Event Triggered State Feedback Control of Nonlinear Continuous Time Systems*. *IEEE Transactions on Neural Networks and Learning Systems*, vol. 27, no. 3, pages 497–509, Mar 2016. (Cited on page 103.)
- [Saleh *et al.* 2013] L. Saleh, P. Chevrel, F. Claveau, J. F. Lafay and F. Mars. *Shared Steering Control Between a Driver and an Automation: Stability in the Presence of Driver Behavior Uncertainty*. *IEEE International Transactions on Intelligent Transportation Systems*, June 2013. (Cited on page 47.)
- [Sarter & Woods 1998] N. Sarter and D. Woods. *Team Play with a Powerful and Independent Agent: Operational Experiences and Automation Surprises on the Airbus A-320*. *Human factors*, vol. 39, pages 553–69, Jan 1998. (Cited on page 33.)

- [Sathyanarayana *et al.* 2008] A. Sathyanarayana, P. Boyraz and J. H. L. Hansen. *Driver Behaviour Analysis and Route Recognition by Hidden Markov Models*. In IEEE International Conference on Vehicular Electronics and Safety, pages 276–281, 2008. (Cited on page 55.)
- [Sayed & Eskandarian 2001] R. Sayed and A. Eskandarian. *Unobtrusive Drowsiness Detection by Neural Network Learning of Driver Steering*. Institution of Mechanical Engineers, Part D: Journal of Automobile Engineering, vol. 215, no. 9, pages 969–975, 2001. (Cited on page 40.)
- [Scheepmaker *et al.* 2017] G. M. Scheepmaker, R. M. P. Goverde and L. G. Kroon. *Review of energy-efficient train control and timetabling*. European Journal of Operational Research, vol. 257, no. 2, pages 355–376, 2017. (Cited on page 25.)
- [Schleicher *et al.* 2008] R. Schleicher, N. Galley, S. Briest and L. Galley. *Blinks and Saccades as Indicators of Fatigue in Sleepiness Warnings: Looking Tired*. Ergonomics, vol. 51, no. 7, pages 982–1010, 2008. (Cited on page 37.)
- [Schwarze *et al.* 2013] A. Schwarze, M. Buntins, J. S. Uffmann, U. Goltz and F. Eggert. *Modelling Driving Behaviour using Hybrid Automata*. IET Intelligent Transport Systems, vol. 7, no. 2, pages 251–256, 2013. (Cited on page 52.)
- [Sekizawa *et al.* 2007] S. Sekizawa, S. Inagaki, T. Suzuki, S. Hayakawa, N. Tsuchida, T. Tsuda and H. Fujinami. *Modelling and Recognition of Driving Behaviour Based on Stochastic Switched ARX Model*. IEEE Transactions on Intelligent Transportation Systems, vol. 8, no. 4, pages 593–606, 2007. (Cited on page 51.)
- [Selivanov & Fridman 2016] A. Selivanov and E. Fridman. *Observer-based Input-to-state Stabilization of Networked Control Systems with Large Uncertain Delays*. Automatica, vol. 74, pages 63–70, 2016. (Cited on page 81.)
- [Senaratne *et al.* 2007] R. Senaratne, D. Hardy, B. Vanderaa and S. Halgamuge. *Driver Fatigue detection by Fusing Multiple Cues*. pages 801–809, 06 2007. (Cited on page 39.)
- [Sentouh *et al.* 2009] C. Sentouh, P. Chevrel, F. Mars and F. Claveau. *A Sensorimotor Driver Model for Steering Control*. IEEE International Transactions on Systems Man and Cybernetics, October 2009. (Cited on page 47.)
- [Seuret & Gouaisbaut 2013] A. Seuret and F. Gouaisbaut. *Wirtinger-based Integral Inequality: Application to Time-delay Systems*. Automatica, vol. 49, no. 9, pages 2860–2866, 2013. (Cited on pages 76, 80 and 100.)

- [Seuret & Gouaisbaut 2014] A. Seuret and F. Gouaisbaut. *Complete Quadratic Lyapunov Functionals using Bessel-Legendre Inequality*. In IEEE European Control Conference, pages 448–453, 2014. (Cited on page 81.)
- [Seuret & Gouaisbaut 2015] A. Seuret and F. Gouaisbaut. *Hierarchy of LMI Conditions for the Stability Analysis of Time-delay Systems*. Systems & Control Letters, vol. 81, pages 1–7, 2015. (Cited on page 81.)
- [Seuret & Gouaisbaut 2018] A. Seuret and F. Gouaisbaut. *Stability of Linear Systems With Time-Varying Delays Using Bessel–Legendre Inequalities*. IEEE Transactions on Automatic Control, vol. 63, no. 1, pages 225–232, 2018. (Cited on pages 83 and 100.)
- [Seuret *et al.* 2013] A. Seuret, F. Gouaisbaut and E. Fridman. *Stability of Systems with Fast-varying Delay Using Improved Wirtinger’s Inequality*. IEEE Conference on Decision and Control, page 6, 2013. (Cited on page 83.)
- [Seuret *et al.* 2018] A. Seuret, K. Liu and F. Gouaisbaut. *Generalized Reciprocally Convex Combination Lemmas and Its Application to Time-delay Systems*. Automatica, vol. 95, pages 488–493, 2018. (Cited on page 78.)
- [Seuret 2009] A. Seuret. *Stability Analysis for Sampled Data Systems with a Time Varying Period*. In IEEE Conference on Decision and Control (CDC), pages 8130–8135, 2009. (Cited on page 74.)
- [Seuret 2012] A. Seuret. *A Novel Stability Analysis of Linear Systems under Asynchronous Samplings*. Automatica, vol. 48, no. 1, pages 177–182, 2012. (Cited on pages 74 and 94.)
- [Shao & Han 2012] H. Shao and Q. L. Han. *Less Conservative Delay-dependent Stability Criteria for Linear Systems with Interval Time-varying Delays*. International Journal of Systems Science, vol. 43, no. 5, pages 894–902, 2012. (Cited on page 83.)
- [Shao 2009] H. Shao. *New Delay-dependent Stability Criteria for Systems with Interval Delay*. Automatica, vol. 45, no. 3, pages 744–749, 2009. (Cited on page 83.)
- [Shaw 1993] I. S. Shaw. *Fuzzy Model of a Human Control Operator in a Compensatory Tracking Loop*. International Journal of Man Machine Studies, vol. 39, no. 2, pages 305–332, 1993. (Cited on page 54.)
- [Shen *et al.* 2008] K. Q. Shen, X. P. Li, C. J. Ong, S. Y. Shao and E. Smith. *EEG-based Mental Fatigue measurement using Multi Class Support Vector Machines with*

- Confidence Estimate*. Clinical Neurophysiology, vol. 119, no. 7, pages 1524–1533, 2008. (Cited on page 39.)
- [Sicre *et al.* 2012] C. Sicre, A. P. Cucala, A. Fernández and P. Lukaszewicz. *Modelling and Optimizing Energy Efficient Manual Driving on High Speed Lines*. IEEJ Transactions on Electrical and Electronic Engineering, vol. 7, no. 6, pages 633–640, 2012. (Cited on page 21.)
- [Sikander & Anwar 2019] G. Sikander and S. Anwar. *Driver Fatigue Detection Systems: A Review*. IEEE Transactions on Intelligent Transportation Systems, vol. 20, no. 6, pages 2339–2352, Jun 2019. (Cited on page 38.)
- [Simon *et al.* 2017] D. Simon, A. Seuret and O. Sename. *Real-time Control Systems: Feedback, Scheduling and Robustness*. International Journal of Systems Science, vol. 48, pages 1–11, 04 2017. (Cited on page 67.)
- [Singh *et al.* 2009] S. Singh, H. Tu, W. Donat, K. Pattipati and P. Willett. *Anomaly Detection via Feature-Aided Tracking and Hidden Markov Models*. IEEE Transactions on Systems, Man, and Cybernetics - Part A: Systems and Humans, vol. 39, no. 1, pages 144–159, 2009. (Cited on page 53.)
- [Sivashankar & Khargonekar 1994] N. Sivashankar and P. P. Khargonekar. *Characterization of the \mathcal{L}_2 -Induced Norm for Linear Systems with Jumps with Applications to Sampled-Data Systems*. SIAM Journal on Control and Optimization, vol. 32, no. 4, pages 1128–1150, 1994. (Cited on page 67.)
- [Skaf & Boyd 2009] J. Skaf and S. Boyd. *Analysis and Synthesis of State Feedback Controllers With Timing Jitter*. IEEE Transactions on Automatic Control, vol. 54, no. 3, pages 652–657, Mar 2009. (Cited on pages 66, 73 and 90.)
- [Song & Song 2011] Q. Song and Y. Song. *Data Based Fault Tolerant Control of High Speed Trains With Traction/Braking Notch Nonlinearities and Actuator Failures*. IEEE Transactions on Neural Networks, vol. 22, no. 12, pages 2250–2261, Dec 2011. (Cited on page 27.)
- [Song *et al.* 2011a] Q. Song, Y. Song and W. C. Cai. *Adaptive Backstepping Control of Train Systems with Traction/Braking Dynamics and Uncertain Resistive Forces*. Vehicle System Dynamics, vol. 49, pages 1441–1454, 09 2011. (Cited on page 29.)
- [Song *et al.* 2011b] Q. Song, Y. Song, T. Tang and B. Ning. *Computationally Inexpensive Tracking Control of High-Speed Trains With Traction/Braking Saturation*. IEEE

- Transactions on Intelligent Transportation Systems, vol. 12, no. 4, pages 1116–1125, Dec 2011. (Cited on page 29.)
- [Su *et al.* 2013] S. Su, X. Li, T. Tang and Z. Gao. *A Subway Train Timetable Optimization Approach Based on Energy Efficient Operation Strategy*. IEEE Transactions on Intelligent Transportation Systems, vol. 14, no. 2, pages 883–893, Jun 2013. (Cited on page 21.)
- [Su *et al.* 2015] S. Su, T. Tang and C. Roberts. *A Cooperative Train Control Model for Energy Saving*. IEEE Transactions on Intelligent Transportation Systems, vol. 16, no. 2, pages 622–631, Apr 2015. (Cited on page 28.)
- [Sultan *et al.* 2013] S. A. Sultan, A. H. A. Bayatti and H. Zedan. *Context Aware Driver Behaviour Detection System in Intelligent Transportation Systems*. IEEE Transactions on Vehicular Technology, vol. 62, no. 9, pages 4264–4275, Nov 2013. (Cited on page 41.)
- [Sun *et al.* 2007] X. Sun, L. Xu and J. Yang. *Driver Fatigue Alarm based on Eye Detection and Gaze Estimation*. International Symposium on Multispectral Image Processing and Pattern Recognition, pages 278–283, 2007. (Cited on page 39.)
- [Sun *et al.* 2015] W. Sun, X. Zhang, S. Peeta, X. He, Y. Li and S. Zhu. *A Self Adaptive Dynamic Recognition Model for Fatigue Driving based on Multi Source Information and Two Levels of Fusion*. Sensors, vol. 15, pages 24191–24213, 2015. (Cited on page 41.)
- [Suplin *et al.* 2005] V. Suplin, E. Fridman and U. Shaked. *A Projection Approach to H_∞ Control of Time-delay Systems*. volume 5, pages 4548–4553, 01 2005. (Cited on page 75.)
- [Suplin *et al.* 2007] V. Suplin, E. Fridman and U. Shaked. *Sampled-data H_∞ Control and Filtering: Nonuniform Uncertain Sampling*. Automatica, vol. 43, no. 6, pages 1072–1083, 2007. (Cited on page 75.)
- [Suzuki *et al.* 2006] M. Suzuki, N. Yamamoto, O. Yamamoto, T. Nakano and S. Yamamoto. *Measurement of Driver's Consciousness by Image Processing - A Method for Presuming Driver's Drowsiness by Eye Blinks coping with Individual Differences*. In IEEE International Conference on Systems, Man and Cybernetics, volume 4, pages 2891–2896, Oct 2006. (Cited on page 39.)
- [Svensson 2004] U. Svensson. *Blink Behaviour based Drowsiness Detection : Method Development and Validation*. Jan 2004. (Cited on page 40.)

- [Takagi & Sugeno 1985] T. Takagi and M. Sugeno. *Fuzzy Identification of Systems and its Applications to Modelling and Control*. IEEE Transactions on Systems, Man, and Cybernetics, vol. 15, no. 1, pages 116–132, Jan 1985. (Cited on pages 110 and 111.)
- [Takei & Furukawa 2005] Y. Takei and Y. Furukawa. *Estimate of Driver's Fatigue through Steering Motion*. In IEEE International Conference on Systems, Man and Cybernetics, volume 2, pages 1765–1770, Oct 2005. (Cited on page 40.)
- [Thiruvengada & Rothrock 2007] H. Thiruvengada and L. Rothrock. *Affordance-based Computational Model of Driver Behaviour on Highway Systems: A Colored Petri Net approach*. In IEEE International Conference on Systems, Man and Cybernetics, pages 888–893, 2007. (Cited on page 50.)
- [Torkkola *et al.* 2004] K. Torkkola, N. Massey and C. Wood. *Driver Inattention Detection through Intelligent Analysis of readily available Sensors*. In IEEE Conference on Intelligent Transportation Systems, pages 326–331, Oct 2004. (Cited on page 40.)
- [Tustin 1947] A. Tustin. *The Nature of the Operator's Response in Manual Control, and Its Implications for Controller Design*. Journal of the Institution of Electrical Engineers - Part I: General, vol. 94, no. 83, pages 532–533, 1947. (Cited on pages 46 and 47.)
- [UITP 2018] UITP. *World Report on Metro Automation*. Statics Brief Publication, 2018. (Cited on page 18.)
- [UPHF 2014] LAMIH UPHF CNRS UMR 8201. *PSCHITT Platform*, 2014. (Cited on page 44.)
- [Vrkalovic *et al.* 2017] S. Vrkalovic, T. A. Teban and L. D. Borlea. *Stable Takagi-Sugeno Fuzzy Control Designed by Optimization*. International Journal of Artificial Intelligence, vol. 15, pages 17–29, Jan 2017. (Cited on page 110.)
- [Vural *et al.* 2007] E. Vural, M. Cetin, A. Ercil, G. Littlewort and J. Movellan. *Drowsy Driver Detection through Facial Movement Analysis*. pages 6–18, 11 2007. (Cited on page 39.)
- [Wakita *et al.* 2005] T. Wakita, K. Ozawa, C. Miyajima, K. Igarashi, K. Itou, K. Takeda and F. Itakura. *Driver Identification using Driving Behavior Signals*. volume E89D, pages 396–401, 10 2005. (Cited on page 40.)

- [Wang & Goverde 2016] P. Wang and R. M. P. Goverde. *Multiple Phase Train Trajectory Optimization with Signalling and Operational Constraints*. Transportation Research Part C: Emerging Technologies, vol. 69, pages 255–275, 2016. (Cited on page 21.)
- [Wang & Tang 2017] X. Wang and T. Tang. *Optimal Operation of High Speed Train based on Fuzzy Model Predictive Control*. Advances in Mechanical Engineering, vol. 9, no. 3, pages 1–1, 2017. (Cited on page 26.)
- [Wang *et al.* 2004] R. Wang, G. Lie, T. Bingliang and J. Lisheng. *Monitoring Mouth Movement for Driver Fatigue or Distraction with One Camera*. In 7th International IEEE Conference on Intelligent Transportation Systems, pages 314–319, Oct 2004. (Cited on page 39.)
- [Wang *et al.* 2013a] J. Wang, L. Zhang, D. Zhang and K. Li. *An Adaptive Longitudinal Driving Assistance System based on Driver Characteristics*. IEEE Transactions on Intelligent Transportation Systems, vol. 14, pages 1–12, 03 2013. (Cited on page 43.)
- [Wang *et al.* 2013b] Y. Wang, B. D. Schutter, T. Boom and B. Ning. *Optimal Trajectory Planning for Trains – A Pseudospectral Method and a Mixed Integer Linear Programming Approach*. Transportation Research Part C: Emerging Technologies, vol. 29, pages 97–114, 2013. (Cited on page 21.)
- [Wang *et al.* 2016] N. Wang, M. J. Er, J. Sun and Y. Liu. *Adaptive Robust Online Constructive Fuzzy Control of a Complex Surface Vehicle System*. IEEE Transactions on Cybernetics, vol. 46, no. 7, pages 1511–1523, 2016. (Cited on page 110.)
- [Wang *et al.* 2018] N. Wang, S. Su, J. Yin, Z. Zheng and M. J. Er. *Global Asymptotic Model-Free Trajectory-Independent Tracking Control of an Uncertain Marine Vehicle: An Adaptive Universe-Based Fuzzy Control Approach*. IEEE Transactions on Fuzzy Systems, vol. 26, no. 3, pages 1613–1625, 2018. (Cited on page 110.)
- [Wang *et al.* 2019a] X. Wang, S. Li and T. Tang. *Periodically Intermittent Cruise Control of Heavy Haul Train with Uncertain Parameters*. Journal of the Franklin Institute, vol. 356, no. 13, pages 6989–7008, 2019. (Cited on page 35.)
- [Wang *et al.* 2019b] X. Wang, S. Li and T. Tang. *Robust Optimal Predictive Control of Heavy Haul Train under Imperfect Communication*. ISA Transactions, vol. 91, pages 52–65, 2019. (Cited on page 30.)

- [Wang *et al.* 2019c] X. Wang, S. Li, T. Tang, X. Wang and J. Xun. *Intelligent Operation of Heavy Haul Train with Data Imbalance: A Machine Learning Method*. Knowledge Based Systems, vol. 163, pages 36–50, 2019. (Cited on pages 27 and 88.)
- [Wei *et al.* 2013] H. Wei, W. Ross, S. Varisco, P. Krief and S. Ferrari. *Modelling of Human Driver Behaviour via Receding Horizon and Artificial Neural Network Controllers*. IEEE Conference on Decision and Control, pages 6778–6785, 2013. (Cited on page 88.)
- [Wei *et al.* 2018] Y. Wei, J. Qiu and H. R. Karimi. *Fuzzy-Affine-Model-Based Memory Filter Design of Nonlinear Systems With Time-Varying Delay*. IEEE Transactions on Fuzzy Systems, vol. 26, no. 2, pages 504–517, 2018. (Cited on page 110.)
- [Wilson 2020] A. Wilson. *World’s Fastest Driverless Bullet Train Launches in China*. <https://www.theguardian.com/travel/2020/jan/09/worlds-fastest-driverless-automated-bullet-train-launches-beijing-china-olympics>, Jan 2020. (Cited on page 19.)
- [Wittenmark *et al.* 1995] B. Wittenmark, J. Nilsson and M. Torngren. *Timing Problems in Real-Time Control Systems*. In American Control Conference, volume 3, pages 2000–2004, 1995. (Cited on pages 67, 160 and 161.)
- [Wong & Ho 2004] K. K. Wong and T. K. Ho. *Coast Control for Mass Rapid Transit Railways with Searching Methods*. IEE Electric Power Applications, vol. 151, no. 3, pages 365–376, May 2004. (Cited on page 21.)
- [Woodworth & Shlosberg 1954] R. Woodworth and H. Shlosberg. *Experimental psychology*. Holt, Rinehart, and Winston, Newyork, 1954. (Cited on page 46.)
- [Wouw *et al.* 2010] N. V. D. Wouw, P. Naghshtabrizi, M. B. G. Cloosterman and J. P. Hespanha. *Tracking Control for Sampled Data Systems with Uncertain Time Varying Sampling Intervals and Delays*. International Journal of Robust and Nonlinear Control, vol. 20, no. 4, pages 387–411, 2010. (Cited on pages 73 and 90.)
- [Wu *et al.* 2011] N. Wu, F. Chu, S. Mammar and M. Zhou. *Petri Net Modelling of the Cooperation Behaviour of a Driver and a Copilot in an Advanced Driving Assistance System*. IEEE Transactions on Intelligent Transportation Systems, vol. 12, no. 4, pages 977–989, 2011. (Cited on pages 50 and 51.)
- [Wu *et al.* 2014a] H. Wu, W. Su and Z. Liu. *PID controllers: Design and Tuning Methods*. In IEEE Conference on Industrial Electronics and Applications, pages 808–813, 2014. (Cited on page 25.)

- [Wu *et al.* 2014b] Z. G. Wu, P. Shi, H. Su and J. Chu. *Exponential Stabilization for Sampled Data Neural Network Based Control Systems*. IEEE Transactions on Neural Networks and Learning Systems, vol. 25, no. 12, pages 2180–2190, 2014. (Cited on pages 165 and 167.)
- [Xiang *et al.* 2015] X. Xiang, K. Zhou, W. B. Zhang, W. Qin and Q. Mao. *A Closed Loop Speed Advisory Model with Driver Behavior Adaptability for Eco Driving*. IEEE Transactions on Intelligent Transportation Systems, vol. 16, pages 1–12, 07 2015. (Cited on page 43.)
- [Xiangxian *et al.* 2010] C. Xiangxian, Z. Yue and H. Hai. *Train Speed Control Algorithm Based on PID Controller and Single-Neuron PID Controller*. In WRI Global Congress on Intelligent Systems, volume 1, pages 107–110, 2010. (Cited on page 25.)
- [Xing *et al.* 2018a] Y. Xing, C. Lv, D. Cao, H. Wang and Y. Zhao. *Driver Workload Estimation using a Novel Hybrid Method of Error Reduction Ratio Causality and Support Vector Machine*. Measurement, vol. 114, page 390–397, Jan 2018. (Cited on page 38.)
- [Xing *et al.* 2018b] Y. Xing, C. Lv, D. Cao, H. Wang and Y. Zhao. *Identification and Analysis of Driver postures for Invehicle Driving Activities and Secondary Tasks Recognition*. IEEE Transactions Computational Social System, vol. 5, no. 1, page 95–108, Mar 2018. (Cited on page 38.)
- [Yan *et al.* 2018] R. Yan, C. Wu and Y. Wang. *Exploration and Evaluation of Individual Difference to Driving Fatigue for High-speed Railway: A Parametric SVM Model based on Multidimensional Visual Cue*. IET Intelligent Transport Systems, vol. 12, no. 6, pages 504–512, 2018. (Cited on page 35.)
- [Yang & Sun 2001] C. D. Yang and Y. P. Sun. *Mixed H_2/H_∞ cruise controller design for high speed train*. International Journal of Control, vol. 74, no. 9, pages 905–920, jun 2001. (Cited on page 29.)
- [Yang *et al.* 2009] J. H. Yang, Z. Mao, L. Tijerina, T. Pilutti, J. F. Coughlin and E. Feron. *Detection of Driver Fatigue caused by Sleep Deprivation*. IEEE Transactions on Systems, Man, and Cybernetics - Part A: Systems and Humans, vol. 39, no. 4, pages 694–705, Jul 2009. (Cited on page 40.)
- [Yang *et al.* 2010] G. Yang, Y. Lin and P. Bhattacharya. *A Driver Fatigue Recognition Model based on Information Fusion and Dynamic Bayesian Network*. Information

- Sciences, vol. 180, no. 10, pages 1942–1954, 2010. Special Issue on Intelligent Distributed Information Systems. (Cited on page 41.)
- [Yang *et al.* 2013] L. Yang, T. Lidén and P. Leander. *Achieving Energy Efficiency and On-Time Performance with Driver Advisory Systems*. IEEE International Conference on Intelligent Rail Transportation Proceedings, pages 13–18, Aug 2013. (Cited on pages 42 and 43.)
- [Yang *et al.* 2016] X. Yang, X. Li, B. Ning and T. Tang. *A Survey on Energy-Efficient Train Operation for Urban Rail Transit*. IEEE Transactions on Intelligent Transportation Systems, vol. 17, no. 1, pages 2–13, Jan 2016. (Cited on page 20.)
- [Yang *et al.* 2017] C. Yang, T. Teng, B. Xu, Z. Li, J. Na and C. Y. Su. *Global Adaptive Tracking Control of Robot Manipulators using Neural Networks with Finite-time Learning Convergence*. International Journal of Control, Automation and Systems, vol. 15, Jul 2017. (Cited on page 89.)
- [Yao *et al.* 2019] X. Yao, J. H. Park, H. Dong, L. Guo and X. Lin. *Robust Adaptive Non Singular Terminal Sliding Mode Control for Automatic Train Operation*. IEEE Transactions on Systems, Man, and Cybernetics: Systems, vol. 49, no. 12, pages 2406–2415, Dec 2019. (Cited on page 28.)
- [Yasunobu *et al.* 1983] S. Yasunobu, S. Miyamoto and H. Ihara. *Fuzzy Control for Automatic Train Operation System*. In *Fuzzy Sets for Intelligent Systems*, pages 348–354. 1983. (Cited on page 26.)
- [Yeo *et al.* 2009] M. Yeo, X. Li, K. Shen and E. W. Smith. *Can SVM be used for Automatic EEG Detection of Drowsiness during Car Driving?* Safety Science, vol. 47, pages 115–124, 01 2009. (Cited on page 39.)
- [Yin *et al.* 2014] J. Yin, D. Chen and L. Li. *Intelligent Train Operation Algorithms for Subway by Expert System and Reinforcement Learning*. IEEE Transactions on Intelligent Transportation Systems, vol. 15, no. 6, pages 2561–2571, Dec 2014. (Cited on pages 27 and 88.)
- [Yin *et al.* 2016] J. Yin, D. Chen and Y. Li. *Smart Train Operation Algorithms based on Expert Knowledge and Ensemble Cart for the Electric Locomotive*. Knowledge Based Systems, vol. 92, pages 78–91, 2016. (Cited on page 27.)
- [Yin *et al.* 2017] J. Yin, T. Tang, L. Yang, J. Xun, Y. Huang and Z. Gao. *Research and Development of Automatic Train Operation for Railway Transportation Systems:*

- A survey*. Transportation Research Part C: Emerging Technologies, vol. 85, pages 548–572, 2017. (Cited on pages 11 and 17.)
- [Yin *et al.* 2019] J. Yin, S. Su, J. Xun, T. Tang and R. Liu. *Data Driven Approaches for Modelling Train Control Models: Comparison and Case Studies*. ISA Transactions, vol. 98, Aug 2019. (Cited on pages 26 and 88.)
- [Zadeh 1965] L. A. Zadeh. *Fuzzy sets*. Information and Control, vol. 8, no. 3, pages 338–353, 1965. (Cited on page 26.)
- [Zames 1966] G. Zames. *On the Input-Output Stability of Time-Varying Nonlinear Feedback Systems Part one: Conditions Derived Using Concepts of Loop Gain, Conicity, and Positivity*. IEEE Transactions on Automatic Control, vol. 11, no. 2, pages 228–238, 1966. (Cited on page 67.)
- [Zeng *et al.* 2015] H. B. Zeng, Y. He, M. Wu and J. She. *Free-matrix-based Integral Inequality for Stability Analysis of Systems with Time-varying Delay*. IEEE Transactions on Automatic Control, vol. 60, no. 10, pages 2768–2772, 2015. (Cited on page 80.)
- [Zhang & Zhuan 2014] L. Zhang and X. Zhuan. *Optimal Operation of Heavy Haul Trains Equipped with Electronically Controlled Pneumatic Brake Systems using Model Predictive Control Methodology*. IEEE Transactions on Control Systems Technology, vol. 22, no. 1, pages 13–22, Jan 2014. (Cited on page 29.)
- [Zhang & Zhuan 2015] L. Zhang and X. Zhuan. *Development of an Optimal Operation Approach in the MPC Framework for Heavy-Haul Trains*. IEEE Transactions on Intelligent Transportation Systems, vol. 16, no. 3, pages 1391–1400, Jun 2015. (Cited on page 29.)
- [Zhang *et al.* 2001] W. Zhang, M. S. Branicky and S. M. Phillips. *Stability of Networked Control Systems*. IEEE Control Systems Magazine, vol. 21, no. 1, pages 84–99, 2001. (Cited on pages 60, 62, 66, 67 and 162.)
- [Zhang *et al.* 2005] Z. Zhang, F. Vanderhaegen and P. Millot. *Prediction of Human Behaviour Using Artificial Neural Networks*. volume 3930, pages 770–779, 01 2005. (Cited on page 88.)
- [Zhang *et al.* 2006] Z. Zhang, F. Vanderhaegen and P. Millot. *Prediction of Human Behaviour Using Artificial Neural Networks*. In Advances in Machine Learning and Cybernetics, pages 770–779. Springer, 2006. (Cited on page 54.)

- [Zhang *et al.* 2016a] C. K. Zhang, Y. He, L. Jiang, M. Wu and H. B. Zeng. *Stability Analysis of Systems with Time-varying Delay via Relaxed Integral Inequalities*. *Systems and Control Letters*, vol. 92, pages 52–61, 2016. (Cited on page 78.)
- [Zhang *et al.* 2016b] H. Y. Zhang, Y. Liang, X. J. Ban and F. Wu. *Dynamic Output Feedback Control for Continuous-Time T-S Fuzzy Systems Using Fuzzy Lyapunov Functions*. *IEEE Transactions on Fuzzy Systems*, vol. 20, pages 86–91, Nov 2016. (Cited on page 111.)
- [Zhang *et al.* 2016c] X. Zhang, Q. Han and X. Yu. *Survey on Recent Advances in Networked Control Systems*. *IEEE Transactions on Industrial Informatics*, vol. 12, no. 5, pages 1740–1752, 2016. (Cited on pages 60 and 61.)
- [Zhang *et al.* 2017a] C. K. Zhang, Y. He, L. Jiang and M. Wu. *Notes on Stability of Time-Delay Systems: Bounding Inequalities and Augmented Lyapunov-Krasovskii Functionals*. *IEEE Transactions on Automatic Control*, vol. 62, pages 5331–5336, 10 2017. (Cited on pages 82 and 100.)
- [Zhang *et al.* 2017b] C. K. Zhang, Y. He, L. Jiang, M. Wu and Q. G. Wang. *An Extended Reciprocally Convex Matrix Inequality for Stability Analysis of Systems with Time-varying Delay*. *Automatica*, vol. 85, pages 481–485, 2017. (Cited on page 78.)
- [Zhang *et al.* 2017c] X. M. Zhang, Q. L. Han, A. Seuret and F. Gouaisbaut. *An Improved Reciprocally Convex Inequality and an augmented Lyapunov-Krasovskii Functional for Stability of Linear Systems with Time-varying delay*. *Automatica*, vol. 84, pages 221–226, 2017. (Cited on page 82.)
- [Zhang *et al.* 2018a] X. Zhang, Q. Han and Z. Zeng. *Hierarchical Type Stability Criteria for Delayed Neural Networks via Canonical Bessel-Legendre Inequalities*. *IEEE Transactions on Cybernetics*, vol. 48, no. 5, pages 1660–1671, 2018. (Cited on pages 82, 83 and 100.)
- [Zhang *et al.* 2018b] X. M. Zhang, Q. L. Han, X. Ge and D. Ding. *An Overview of Recent Developments in Lyapunov-Krasovskii Functionals and Stability Criteria for Recurrent Neural Networks with Time Varying Delays*. *Neurocomputing*, vol. 313, pages 392–401, 2018. (Cited on page 81.)
- [Zhang *et al.* 2018c] X. M. Zhang, Q. L. Han, A. Seuret, F. Gouaisbaut and Y. He. *Overview of Recent Advances in Stability of Linear Systems with Time-varying Delays*. *IET Control Theory & Applications*, vol. 13, no. 1, pages 1–16, 2018. (Cited on page 107.)

- [Zhao *et al.* 2014] X. Zhao, L. Zhang, P. Shi and H. R. Karimi. *Novel Stability Criteria for T-S Fuzzy Systems*. IEEE Transactions on Fuzzy Systems, vol. 22, no. 2, pages 313–323, 2014. (Cited on page 110.)
- [Zhao *et al.* 2017] Y. Zhao, L. Gorne, I. M. Yuen, D. Cao, M. Sullman, D. Auger, C. Lv, H. Wang, R. Matthias, L. Skrypchuk and A. Mouzakitis. *An Orientation Sensor-Based Head Tracking System for Driver Behaviour Monitoring*. Sensors, vol. 17, no. 11, page 2692, 2017. (Cited on page 38.)
- [Zhong *et al.* 2007] Y. J. Zhong, L. P. Du, K. Zhang and X. H. Sun. *Localized Energy study for Analyzing Driver Fatigue State based on Wavelet Analysis*. In International Conference on Wavelet Analysis and Pattern Recognition, volume 4, pages 1843–1846, Nov 2007. (Cited on page 40.)
- [Zhong *et al.* 2013] X. Zhong, H. He and D. V. Prokhorov. *Robust Controller Design of Continuous-time Nonlinear System using Neural Network*. In International Joint Conference on Neural Networks, pages 1–8, 2013. (Cited on page 89.)
- [Zhong 2006] Q. C. Zhong. *Robust Control of Time-Delay Systems*. Robust Control of Time-delay Systems, Springer, Jan 2006. (Cited on page 69.)
- [Zhou *et al.* 1996] K. Zhou, J. C. Doyle and K. Glover. *Robust and optimal control*. Prentice Hall, USA, 1996. (Cited on page 67.)
- [Zhu *et al.* 2014] X. Zhu, W. Zheng, B. Lu, X. Chen, S. Chen and C. Wang. *EOG-based Drowsiness Detection using Convolutional Neural Networks*. In International Joint Conference on Neural Networks, pages 128–134, 2014. (Cited on page 39.)
- [Zhu *et al.* 2016] H. Zhu, X. Sun, L. Chen, S. Gao and H. Dong. *Analysis and Design of Driver Advisory System for Energy Efficient Train Operation with Real Time Information*. IEEE International Conference on Intelligent Rail Transportation, pages 99–104, Aug 2016. (Cited on pages 15 and 43.)
- [Zhu *et al.* 2018] H. Zhu, S. Gao and H. Dong. *Improving Train Driving Performance under Disturbances by Intelligent Driver Advisory System*. In International Conference on Intelligent Rail Transportation, pages 1–5, Dec 2018. (Cited on page 43.)
- [Zhuan & Xia 2006] X. Zhuan and X. Xia. *Cruise Control Scheduling of Heavy Haul Trains*. IEEE Transactions on Control Systems Technology, vol. 14, no. 4, pages 757–766, July 2006. (Cited on page 29.)

- [Zhuan & Xia 2008] X. Zhuan and X. Xia. *Speed Regulation with Measured Output Feedback in the Control of Heavy Haul Trains*. Automatica, vol. 44, no. 1, pages 242–247, 2008. (Cited on page 29.)
- [Zyla & Skotniczny 1996] M. K. Zyla and K. P. Skotniczny. *Subjective Fatigue Symptoms among Computer Systems Operators in Poland*. Applied Ergonomics, vol. 27, no. 3, page 217–220, 1996. (Cited on page 37.)
- [Zyner *et al.* 2018] A. Zyner, S. Worrall and E. Nebot. *A Recurrent Neural Network Solution for Predicting Driver Intention at Unsignalized Intersections*. IEEE Robotics and Automation Letters, vol. 3, no. 3, pages 1759–1764, 2018. (Cited on page 88.)
- [Åström & Wittenmark 1996] K. J. Åström and B. Wittenmark. *Computer Controlled Systems: Theory and Design*. Prentice-Hall, 1996. (Cited on pages 66 and 160.)

Étude de la Stabilité du Système Conducteur-Véhicule sous des Mesures d'échantillonnage apériodiques

Résumé: Les trains à grande vitesse ont une exigence de sécurité de conduite importante par rapport aux autres transports publics en raison de leur vitesse plus élevée et de la demande croissante du public. Cependant, la particularité de la conduite des trains conduit souvent à des conducteurs sensibles à la fatigue. Dans ce contexte, la dernière décennie a vu l'adoption généralisée de **ADAS** dans l'industrie du transport ferroviaire, en particulier le système de détection de la fatigue des conducteurs.

ADAS est destiné à aider les conducteurs de train. Le planificateur de trajectoire dans **ADAS** guide le conducteur pour maintenir un niveau de vitesse (v) et d'accélération (a) pour aller de la station A à la station B, en tenant compte de divers facteurs comme la consommation de carburant, le terrain de la route, le trafic et aussi le l'état du conducteur à partir du système de détection de fatigue du conducteur. Cependant, parfois en raison de mauvaises conditions d'éclairage/mauvaise position du conducteur/capteur défectueux, les informations précises sur le train et l'état du conducteur peuvent être retardées.

L'indisponibilité apériodique du conducteur et de l'état du train au système **ADAS** soulève des inquiétudes quant à la stabilité et la sécurité de la dynamique du train. Par conséquent, la prise en compte de l'incertitude dans l'état du conducteur et du train lors de l'analyse de la stabilité du train devient essentielle. À cette fin, une approche basée sur un modèle est utilisée pour approximer l'interaction **ADAS**-conducteur-train et prouver la stabilité du système de contrôle de train consultatif du conducteur.

Pour l'étude de stabilité, le système constitué de Driver-Train en boucle ouverte est considéré comme un système de données échantillonnées et **ADAS** comme un contrôleur. En outre, l'approche du retard d'entrée est utilisée pour transformer le système de données échantillonnées en un système de retard variable dans le temps. De plus, des fonctionnelles de Lyapunov dépendantes du temps et des arguments de convexification sont utilisés pour dériver des critères de stabilité en termes de conditions **LMI**. Le critère permet d'estimer le délai maximal admissible dans la mesure de l'état du conducteur et du train pour garantir la stabilité de la dynamique du train.

Mots-clés: Système conducteur-train, système commandé par réseau, système échantillonné, système à retard, échantillonnage variable, stabilité, inégalité matricielle linéaire.

Investigating Stability of Driver-Vehicle System under Aperiodic Sampling Measurements

Abstract: High-speed rails have a significant driving safety requirement than other public transport because of faster speed and an increasing public demand. However, the particularity of train driving often leads to driver's susceptible to fatigue. Under this consideration, last decade has seen widespread adoption of [ADAS](#) in rail-based transportation industry, specifically driver fatigue detection system.

[ADAS](#) is meant to help the train drivers. The trajectory planner in [ADAS](#) guides the driver to maintain a level of velocity (v) and acceleration (a) to go from station A to station B, by considering various factors as fuel efficiency, road terrain, traffic and also the state of the driver from the driver fatigue detection system. However, sometimes due to bad lighting conditions/ bad driver position/ faulty sensor, the accurate information about the train and the driver state may be delayed.

The aperiodic unavailability of the driver and the train state to the [ADAS](#) system raises concern about the train dynamics stability and safety. Therefore, consideration of uncertainty in driver's and train's state during train stability analysis becomes essential. For this purpose, a model-based approach is employed to approximate [ADAS](#)-Driver-Train interaction and prove stability of driver advisory train control system.

For the stability study, the system consisting of Driver-Train in open-loop is considered as a sampled-data system and [ADAS](#) as a controller. Further, the input-delay approach is used to transform the sampled-data system to time-varying delay system. Further, time-dependent Lyapunov functionals and convexification arguments are used to derive stability criteria in terms of [LMI](#) conditions. The criteria allows to estimate the maximum allowable delay in driver and train state measurement to guarantee train dynamics stability.

Keywords: Driver-Train system, network control system, sampled-data system, time-delay system, time-varying sampling, stability, linear matrix inequality.
